Development of a Novel *In Vitro* Approach to Study the Transmission of Airborne Disease

by

Mara Otero Fernández

A dissertation submitted to the University of Bristol in accordance with the requirements of the degree of Doctor of Philosophy in the School of Chemistry, Faculty of Science.

February 2021

54,000 words

Abstract

Emerging outbreaks of airborne pathogenic infections worldwide, such as the current Severe Acute Respiratory Syndrome Coronavirus 2 (SARS-CoV-2) pandemic, have raised the urgency to explain the parameters affecting the survival of airborne microbes in order to develop effective infection control strategies. Conventional techniques for investigating bioaerosol survival *in vitro* have systemic limitations that prevent the accurate representation of conditions that these particles would experience in the natural environment. Therefore, some basic questions about the fundamental mechanisms influencing the airborne transmission of disease remain unknown.

This thesis describes a laboratory-based approach to explore the synergistic interactions between the physicochemical and biological processes that impact the survival of airborne microorganisms. This novel experimental strategy combines two complementary techniques for probing aerosol particles directly: the CK-EDB (Comparative Kinetics Electrodynamic Balance) and CELEBS (Controlled Electrodynamic Levitation and Extraction of Bio-aerosol onto a Substrate) technologies. Both are based on the electrodynamic levitation of charged droplets and utilize droplet-on-demand dispensers to produce droplets with high monodisperse size distribution. By using the CK-EDB, it is possible to measure the changes in the physicochemical properties of the bioaerosol droplets during and after evaporation with the aim to ultimately interrelate this information to the biological decay responses measured by the CELEBS system.

Therefore, the presented methodology provides a detailed understanding of the processes taking place from aerosol droplet generation through to equilibration and biological decay in the environment, elucidating decay mechanisms not previously described. The impact of evaporation kinetics, solute hygroscopicity and concentration, particle morphology, evaporative cooling, surface enrichment and equilibrium particle size on the airborne survival of microorganisms are reported, using *Escherichia coli* (MRE-162) as a benchmark microorganism. This new approach can enable direct studies at the interface between aerobiology, atmospheric chemistry, and aerosol physics to determine the main mechanisms of death of airborne pathogens under the unique microphysical properties of the aerosol droplets.

Acknowledgements

First, thanks to my supervisor, Professor Jonathan Reid, for giving me the opportunity to be part of his research group. I am sincerely grateful for your support and encouragement over the years and all the given opportunities to become a more experienced scientist. My thanks go also to my co-supervisor, Dr Allen Haddrell, whose guidance has been exceptional. Thanks for your endless patience, humour and for creating a work atmosphere where everybody feels excited to be part of. Having you as a supervisor made my PhD a very enjoyable experience. I am also thankful for the opportunity I had to work with Dr Richard J. Thomas from DSTL. Your input in my project has been profound. I'll be forever grateful for your guidance, kindness, and hilarious comments during the many hours we shared in the lab. To all the brainiac BARC crew, past and current members, you have provided me with the most stimulating work environment anyone could ask for. Particularly, I'd like to thank Lilly, Flo, Stephen, Lara, Rose, Nat, Malcolm, Dan and my humorous padawan Henry, for all your help, useful discussions, and the good pre-pandemic old times. To the Post-Doc members through the years: Antonio, Justice, Jim, Rachael and Bryan, thanks for all your guidance on my project.

Outside of the department, I want to thank my sweet immigrants' family who always made me feel at home: Camilo, Lucia, Pablo, Juan and Ramon. Thanks also to the NCAS gang, for all the bounding, banter, unbelievable scenes, and the China trip. Especially to Mike, who ensured I made it back! A huge thanks to my friends in Spain, the loves of my life: Fras, Cris, Sonia, Andrea, Yoryi, Isma, Esther, Chochy, Rocio, Las Lauras, Terry, Alba, Guiño, Dal and Bruno. Thanks for your visits, the Skype calls and for always being there. I miss you every day!

Petros, thank you for all your support, love and infinite laughter throughout our many years together in the UK. Thanks for being constantly teaching me the Greek way of life which changed me lots. What an epiphany! Thank you so much for everything, this wouldn't have been possible without you.

Finalmente, gracias mamá y papá, por darme todo lo que vosotros no pudisteis tener sin esperar nunca nada a cambio. Gracias por confíar siempre en mi, por vuestro apoyo inagotable y por enviarme "pedaciños da Terra" cada vez que imperaba la morriña. Papá, se alguén me inspirou a seguir sempre aprendendo, especialmente no campo científico, fuches ti.

Author’s Declaration

I declare that the work in this dissertation was carried out in accordance with the requirements of the University's *Regulations and Code of Practice for Research Degree Programmes* and that it has not been submitted for any other academic award. Except where indicated by specific reference in the text, the work is the candidate's own work. Work done in collaboration with, or with the assistance of, others, is indicated as such. Any views expressed in the dissertation are those of the author

Signed……. Date…….

Table of Contents

List of Figures

List of Tables

List of Symbols and Abbreviations

Symbols

a_w - Water activity
A - Correction for Stefan flow
C - Culturable concentration
D - Diffusion coefficient
H - Henry's law constant I
I - Mass flux k
k - Evaporation rate K
K - Thermal conductivity
L - Latent heat of vaporisation
M - Molecular mass
n – refractive index
r - radius
R_i - Molar refraction of i
T - Temperature
V - Voltage
x_i - Mole fraction of i

Greek Alphabet Symbols

β_M - Transitional correction factor for mass transfer βT

β_T - Transitional correction factor for heat transfer

λ - Wavelength

ϑ - Angle

p - Density

p_s - Melt density of solute

p_w - Density of water

φ_s - Mass fraction of solute

Subscript

i - Property of one component

s - Property of pure component

w- Property of water

N - sum of components

∞ - gas-phase property

Fundamental Constants

R - Molar gas constant

Acronyms

AC - Alternating current

CELEBS - Controlled Electrodynamic Levitation and Extraction of Bioaerosol onto a Substrate

CCD - Charged coupled device

CFU- Colony-forming unit

CK-EDB - Comparative kinetics electrodynamic balance

DC - Direct Current

DoD - Droplet on demand

E-AIM - Extended Aerosol Inorganic Model

EDB - Electrodynamic balance

LB - Luria-Bertani

MHV – Mouse Hepatitis Virus

MFS- Mass fraction of solute

MODE- Millikan's oil drop experiment

OD - Optical density

Pe - Péclet Number

PBS - Phosphate buffer saline

PDF - Probability distribution function

PFU - Plaque-forming units

RH - Relative Humidity

RI - Refractive index

SARS-CoV-2 - Severe Acute Respiratory Syndrome Coronavirus 2

Sh - Sherwood number

SEM - Scanning Electron Microscopy

SOA - Secondary Organic Aerosol

UV- Ultraviolet

Chapter 1

Introduction

As of January 1st, 2021, near 2 million deaths have been confirmed due to the novel coronavirus pandemic which emerged in China in late 2019. Originally, direct and respiratory droplet transmission had been indicated as the main transmission pathways. However, there is now a growing scientific consensus that the airborne transmission of Severe Acute Respiratory Syndrome Coronavirus 2 (SARS-CoV-2) (via aerosols) can play a more significant role than initially considered, presenting enormous challenges for effective control over transmission and spread.[1–8] Therefore, knowledge of the fundamental mechanisms that define the transmission of airborne pathogens is critical to limit the risk of infection and develop mitigation strategies to prevent the spread of disease.

The dynamics involved in the airborne transmission of disease concerning human, animal or plant health relies on the ability of pathogens to survive aerosol transport and, subsequently, cause infection when interacting with a host. The length of time airborne microorganisms remain infectious in the aerosol phase is a function of a wide range of variables (e.g. atmospheric, microbiological, compositional, etc.) that affect their viability/infectivity[9] and, therefore, have the potential to impact the dissemination of the disease outbreak.

The presented thesis reports the development and utilisation of a new approach to probe the fundamental mechanisms that define the transmission of airborne pathogens. The work presented in here includes experimental measurements of mass and heat transfer from liquid aerosol droplets combined with airborne survival data under a wide range of environmental conditions, droplet compositions and microbiological conditions, to demonstrate the importance of understanding the complex interrelationship between aerosol microphysics and bioaerosol survival. Specifically, our data consists of the correlation of a wide range of

physicochemical properties (e.g. evaporation dynamics, hygroscopicity, droplet morphology, compositional changes, etc) with airborne viability decay to measure the impact of aerosol microphysics on airborne bacterial survival. The approach developed, named TAMBAS (tandem approach for microphysical and biological assessment of airborne microorganism survival), was used allowing the determination of the main mechanisms of death of microorganism under the unique microphysical properties of the aerosol droplets.[10] As a proof of concept, *Escherichia Coli (E. coli)* MRE-162 was primarily selected as the microorganisms of choice due to its safely use in a non-containment environment as it has been previously utilized with different systems in bioaerosol studies which makes it a suitable benchmarking organism. Additionally, *E. coli* MRE-162 was also chosen as a representative bioaerosol due to its high persistence in hotspots for bioaerosol generation, such as toilets, water waste treatment plants, and polluted rivers where a severe risk of infection for humans via the airborne route is presented.[11] This thesis aims to describe a novel framework to predict the survival of airborne pathogens as a function of fundamental mechanisms characterized by a range of biological, microphysical, environmental and aerosol-generation processes allowing us to better understand the transmission of airborne infection.

The present chapter focuses on the general motivation for studying the bioaerosol survival in the context of airborne disease outbreaks, introducing some relevant facts from previous and the current SARS-CoV-2 pandemic, before describing the key mechanisms and bioaerosol properties behind the spread of airborne transmission of disease which leads to the different types of control measurements. Moreover, a summary of the conventional techniques for conducting measurements of bioaerosol viability is also presented.

1.1 An Overview of Bioaerosols

Bioaerosols are a suspension of airborne particles emitted directly from the biosphere into the atmosphere which represent a quarter of the total atmospheric aerosols.[12] These airborne particles are composed of different biological units and structures, including living or dead organisms (e.g. bacteria, viruses, algae), dispersal units (e.g. pollen, fungal spores) and fragments of plants, animal matter and other microorganisms (e.g. plant debris, brochosomes and endotoxins).[13] The term primary biological aerosol (PBA) refers to airborne particles emitted from a biological source whereas secondary bioaerosols are the result of atmospheric oxidation and condensation of gaseous volatile organic compounds emitted from a biological source.[14] Bioaerosol particles can be released into the atmosphere from natural (e.g. sea-sprays) or anthropogenic (e.g. agricultural practices) sources, both actively (e.g. viruses emitted by sneezing) or passively (e.g. wind-driven pollen emissions). The composition and concentration of microorganisms in bioaerosol particles depend on the source and the dispersion in the air while they are airborne, which will be affected by their physical properties and the environmental parameters that they encounter in the air until deposition.[15]

Primary bioaerosol particles can cover a broad range of sizes from nanometers up to about hundreds of micrometres as shown in Figure 1-1. Large bioaerosol particles (> 1μm diameter) belong to the coarse mode and have a short lifetime in the atmosphere due to their rapid sedimentation, while small bioaerosol particles are found in the nucleation and accumulation modes (from 0.001 to 1 μm) and remain airborne for extended periods. Particle size is an important factor that determines not only the particle's lifetime in the atmosphere but also their deposition in the respiratory tract,[16] the survival of microbes enclosed in aerosol particles,[17] as well as the likelihood of a biological particle to become and remain airborne.[12]

The role of bioaerosols is especially important in human health, atmospheric and ecological impacts.[15] This thesis focuses on bioaerosols containing only viable (capable of living) microbes and the interrelationship between environmental, microbiological and compositional factors governing their survival that are associated with the spread of airborne infectious respiratory diseases.

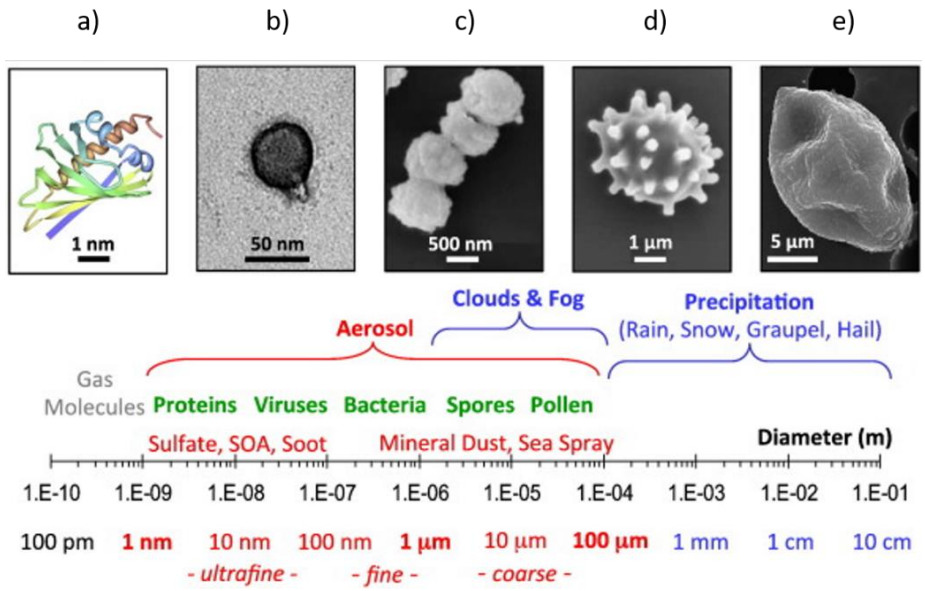

Figure 1-1. Scale describing the size ranges of different biological units and bioaerosols with exemplary insets images: (a) protein, (b) virus, (c) bacteria, (d) fungal spores, and (e) pollen. This figure was reprinted with permission from Refs.[13].

1.2 Aerobiology: The Study of Airborne Biological Particles

The study of airborne microorganisms was first reported in 1833 when mould spores were detected by Charles Darwin in air samples taken on the Cape Verde Islands.[15] Later in 1859, Pasteur demonstrated the presence of airborne microbes that can contaminate and cause disease by conducting his swan-necked vessels experiment (Figure 1-2). This essay was based on the use of the long, twisted neck flasks to allow the entrance of air within the vessel but prevent the introduction of any dust particle-containing microorganisms which would remain in the twists of the flasks' necks. Thus, he correctly proved that the sterile broth contained inside the vessels would remain sterile as long as the broth was not in contact with the atmospheric dust particles containing airborne microbes which were trapped in the neck of the vessels, even if allowing air inside the flasks. In 1861, his paper "*Memoir on the organized bodies which exist in the atmosphere*" was published, irrefutably disproving the ancient theory of spontaneous generation.[14,18]

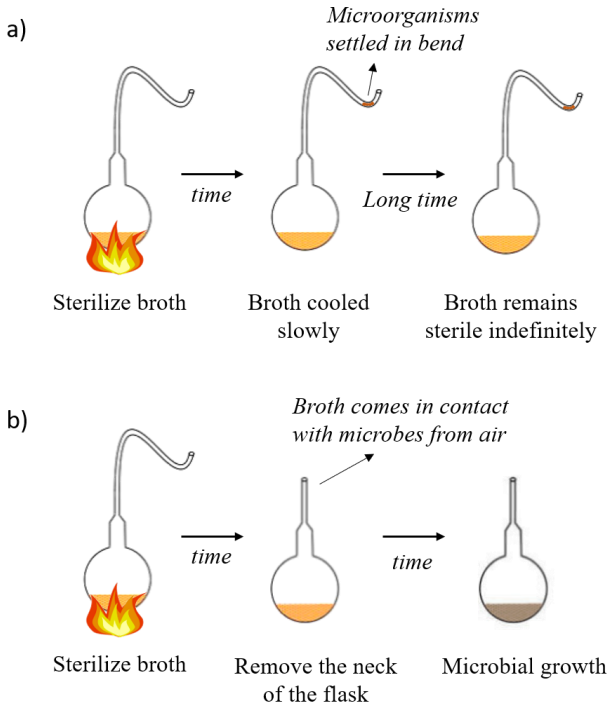

Figure 1-2. Schematic of the swan neck experiment of Louis Pasteur in 1859. (a) the unique swan neck of the flask allows air in but prevents airborne microbes to enter in contact with the sterile broth, therefore no contamination occurs. (b) the neck of the flask is removed, and the sterile broth becomes contaminated.

Biological aerosol particles play important roles in human health, epidemiology, ecology, agriculture, biosecurity, climate, and even atmospheric processes, to mention a few.[15] For example, microbial aerosols may result in plant, animal, and human diseases, the exacerbation of allergies and the colonisation of new habitats. However, despite these important effects, the bioaerosol field is still understudied in comparison to other fields in aerosol science and little is known about their composition, abundance and reactivity which are not yet well characterized and understood.[13,18] Fortunately, in recent decades, there has been an increased interest in bioaerosol research due to recurrent cases of new airborne pathogenic outbreaks such as SARS in 2003, H1N1 in 2009 and the on-going SARS-CoV-2 worldwide pandemic. Moreover, the development of more advance instrumentation allowed the interdisciplinary approach necessary to understand the heterogeneity of these biological airborne particles.[19] Therefore, a multidisciplinary collaboration across a wide variety of scientific fields started to emerge to tackle fundamental questions concerning the influence of bioaerosol in climate and

atmospheric processes as well as to develop an improved understanding of their impacts in human health by disentangling their main mechanisms of transport and innactivation.[14,15]

Nowadays, aerobiology is a developing field of scientific research that brings together a large group of biological, physical and medical science disciplines, impacting applied sciences such as epidemiology, air quality, microbiology, physics, climate, engineering and immunology. The SARS-CoV-2 pandemic has highlighted the present limitations in the field and the importance of developing a better understanding to improve measures for effective infection control.

1.3 A Brief History of Pandemics

Throughout history, infectious diseases have deeply moulded our societies and cultures, determined the outcome of wars and even eradicated entire populations. However, they also defined the very basic principles of modern medicine, public health, political systems and even economy.[20] Interestingly, although the most well-known plagues are those referred to in the Old Testament and the Qur'an, the greatest catastrophe in the entire history of humanity was the outbreak of the Black Death, which led to the death of one-third of the entire world's population.[21,22]

Table 1-1 outlines the deadliest airborne pandemic outbreaks across history, from the earliest recorded Athenian Plague, occurred in 430-26 B.C, to the current SARS-CoV-2 pandemic. It is important to note that all the pathogens involved in the most lethal pandemics throughout history are airborne and only the HIV/AIDS, yellow fever and the Cholera pandemics were excluded from this list due to different modes of transmission.

Table 1-1. List of the main pandemics in history (including both viral and bacterial pathogens) transmitted via the airborne route (large and aerosol droplets). Note that some of the estimated death tolls are subject to debate based on new evidence.

Disease Name	Period	Disease-Causing Pathogen	Death Toll
Athenian Plague	430-426 B.C.	Unsure	100000
Antonine Plague	165-180	Variola or measles virus	5M
Japanese Smallpox Epidemic	735-737	Variola major virus	1M
Plague of Justinian	541-542	*Yersinia pestis* bacteria	30-50M
Black Death	1347-1353	*Yersinia pestis* bacteria	200M
New World Smallpox	1520-1980	Variola major virus	56M
Great Plague of London	1665	*Yersinia pestis* bacteria	100000
Italian Plague	1629-1631	*Yersinia pestis* bacteria	1M
Third Plague	1885	*Yersinia pestis* bacteria	12M
Russian Flu	1889-1890	H2N2 virus	1M
Spanish Flu	1918-1919	H1N1 virus	40-50 M
Asian Flu	1957-1958	H2N2 virus	1.1 M
Hong Kong Flu	1968-1970	H3N2 virus	1M
Swine Flu	2009-2010	H1N1 virus	200000
SARS	2002-2003	Coronavirus	770
MERS	2015-Present	Coronavirus	850
SARS-CoV-2	2019-Present	Coronavirus	2.2 M

Briefly, the second-largest outbreak of the Bubonic plague is referred to as the Black Death. It began in China in 1347 and quickly spread across Europe, entering the continent through Sicily in 1347. With a mortality rate of 70%, this disease killed more than 200 million people, usually within the first 8 days of showing symptoms. Against the common believe about the Black Death being a bubonic plague, scientists working at Public Health England in Porton Down argued that the associated high number of deaths together with its fast pace of infection across Europe are more characteristic of airborne transmission. [23,24] The effects of such as large-scale catastrophe influenced wars, economic systems and even all forms of art across in Europe during this period.[21]

Although smallpox is related to the Athenian plague occurring in 430 B.C, a relevant outbreak of smallpox emerged with the arrival of European in the New World in 1520, killing 90% of the Native Americans and 400,000 Europeans each year, reporting a mortality rate of approximately 30%.[25] Most of the infected cases of smallpox were fatal, death occurring within 10-16 days after onset of symptoms, being especially devastating in previously isolated populations, and thus, helping the big empires to pave the way of colonization.[26]

The overall historic death toll of smallpox is so large that it is often compared to the Black Death. Smallpox has had a major impact on the global history of medicine for several reasons: the smallpox vaccine, developed at the end of the 18th century by the British surgeon, Edward Jenner,[27] was the first vaccine developed in history which remarkably increased the life expectancy over that period.[28] Although being an endemic disease, it is the only human disease that has been completely eradicated.[26]

During the 17th and 18th centuries, several outbreaks of Great Plagues regularly emerged across Europe. The flu of 1918 or Spanish flu represents the deadliest pandemic of the entire 20th century with approximately 50 million deaths worldwide, reporting a mortality rate of 2.5%, especially high among young and healthy individuals.[29] The spread of this virus was intensified by the movements of troops during World War I. The name of "Spanish" flu arose from the fact that the Spanish newspapers (which were not censored to the extent they were in other countries) reported the Spanish king fell seriously ill with this virus. However, the true country of origin for this outbreak remains unknown.[30,31]

Recently, on March 11 2019, the Wealth Organization (WHO) officially declared the current state of a pandemic caused by SARS-CoV-2. The lack of information about this new disease and the fact that the data is still being generated, restrict current estimations of the overall impact of this disease. SARS-CoV-2 has been reported to be more infectious and have a higher fatality rate than influenza (~1%), especially affecting older adults (>65 years).[32]

Importantly, a trend showing a progressive reduction in the mortality rate of these pandemics is consistent over time due to the advances in medicine and healthcare sciences. The presented timeline of historical pandemics (Table 1-1), allows us to envision the devastating impact of having experienced an exponentially worse infectious pathogen than SARS-CoV-2 without the benefits of modern sciences and healthcare systems.

1.4 The Dynamics of Disease Transmission

1.4.1 Expiratory Events and Other Aerosol Generating Procedures

Bioaerosol particles are emitted into the natural environment throughout several generation mechanisms usually classified into two groups: anthropogenic (e.g. from sneezing, coughing, compost facilities) or natural (e.g. from waters, mechanical wind, active release).[33]

Violent expiratory events such as coughing and sneezing play a critical role in the dissemination of respiratory infectious diseases such as SARS-CoV-2,[6] so much so that the slogan "Coughs and Sneezes Spread Diseases" was coined in the USA during the 1918 flu.[34] Extensive research before and during the current pandemic has been focused on the characterisation of this type of respiratory processes to improve the physical understanding of these airborne transmission mechanisms.[34–38] Observations indicate that coughs and sneezes are generated from a high-momentum, multiphase, buoyant cloud that produces the fragmentation of the respiratory tract fluid into microdroplets.[35] Thus, the physical properties of this "puff cloud" dictate the range of dispersal of pathogens, reporting significant larger distances (i.e. up to 8 m for a sneeze and 6 m for a cough) than the conventionally accepted 1-2 m for the deposition of large droplets.[37] Other exhalation mechanisms such as speaking and breathing are also reported to generate significant amounts of bioaerosols. The experimental data from these studies has shown that vocalization increases the generated particle concentrations by one order of magnitude and the mean particle size. Furthermore, a recent study has characterized the size distributions and concentrations of aerosols generated from different types of vocalization procedures (i.e. singing, speaking and breathing). Interestingly, the effect of volume is reported to have a more significant impact on aerosol production than the type of vocalization itself, increasing aerosol concentrations more than an order of magnitude depending on the examined volume range.[39–41] Besides, aerosols generated while breathing produced smaller particles than those generated by speaking and singing, which generated similar particle size distributions and whose concentrations proportionally increased with the loudness.[40]

An aerosolization mechanism that has received little attention is the emission of pathogen-containing droplets from toilets. Bourouiba *et al.*[42] reported the characterisation of the fluid dynamics governing droplet generation during toilet flushing events employing high-speed

recordings. The flow visualization reported significant quantities of large and small droplets generated as a result of fluid fragmentation induced during toilet flushing. These findings agree with previous studies reporting small droplets suspended in the air containing *C. difficile* spores, among other pathogens, even an hour after flushing.[43,44] Interestingly, Bourouiba *et al*. also found that the generated aerosol concentrations dramatically increased with the use of high-pressure flushes and cleaning products commonly used in hospitals, therefore, aggravating the spread of bioaerosol particles in these settings.[42] These findings pose an important concern in North America due to the lack of lids in hospital toilets.

One of the most relevant mechanisms of bioaerosol generation is bursting bubbles on watery surfaces (e.g. oceans, fresh water bodies, rain puddles, water treatment plants). It has been estimated that a total of 10^{19} bubbles are naturally emitted every second from the Earth's oceans and seas, being produced during wave breaking or rainfall impacts.[45] These generated droplets carry what the waters contains, including microorganisms, salts and organic materials. As they burst, each bubble can emit hundreds of droplets. The important factors governing the concentration of droplets emitted when bursting bubbles are the ageing and the thickness of the bubble. Thus, older bubbles, being thinner, generate more, smaller and faster-moving droplets than do younger, thicker bubbles.[45] Moreover, the presence of bacteria can also stabilise bubbles, increasing their lifetimes by producing secretions that may impact the concentration, composition, ejection speed and size of the droplets generated by orders of magnitude, producing a similar effect to that of adding surfactant molecules to liquid films.[45,46] Similarly to bursting bubbles, the generation of bioaerosols via splashes from wet surfaces (e.g. rainfall impacting on plant leaves, soil, etc) remains especially important for pathogens transmission from plant to plant (e.g. crop systems) which presents an important threat to the global food industry.[47–49]

Importantly, aerosol-containing microorganisms are easily dispersed in high populated areas associated with agriculture and livestock practices as well as vulnerable indoor environments such as healthcare facilities with ventilation or heating systems, leading to important health, economic and social consequences.[50] Therefore, the information provided by these type of studies, such as the effect of loudness on the generated concentrations of aerosols, should be thoughtfully taken into consideration to develop effective public health guidelines.

1.4.2 Size Distribution

The distributions of bioaerosol particle size are crucial to understand airborne disease transmission since they determine how far the droplets can travel, how many microorganisms a droplet can contain (which would determine the infectious dose), and the site of deposition in the respiratory tract after inhalation (which also dictates the pathogenicity).[37,51] Thus, small particles (1-5μm in diameter) experience the highest retention in the alveolar region producing an acute infection, while bigger particles (>5μm) are more likely to be deposited in the upper respiratory tract and can be more easily removed by mucociliary action or sneezing.[16] The probability of infection will also be influenced by the tropism of microbe receptors in the different regions of the respitaroty system.

Despite the importance of particle size distributions for evaluating the risk of infection, discrepancies related to the size distribution of both coughs and sneezes persist. A series of techniques have been used over the years to measure droplet size distributions of expiratory droplets, including glass slides,[52] optical counters,[53] laser diffraction,[54] aerodynamic particle sizers,[55] scanning mobility droplet sizer [56] and interferometric Mie imaging.[56] However, the reported droplet sizes have significant uncertainties due to the measurement challenges associated with the dynamic nature of aerosol droplets, the difficulty of time-zero measurements, the continually evolving local conditions and the low concentrations.[36,55] Measurements published by Johson *et al*. [55] reported multimodal distributions associated with the particle size distributions of coughs and speech. The different modes have been associated with distinct processes of droplet generation occurring in different regions of the respiratory tract (lower respiratory tract, larynx region and upper respiratory tract including the oral cavity).[55]

The size of microorganisms spans the nanometre and micrometre scales (e.g. SARS-COV-2 is ~0.12 μm and *E. coli* bacteria is ~1.5 μm).[57] However, microbes are never emitted in the atmosphere by themselves but may be accompanied by fluids, solutes and/or solid materials during aerosol transport before eventually settling out. Therefore, the droplet composition is an important factor governing the particle size distribution, both interconnected at the same time with the ambient RH.[10]

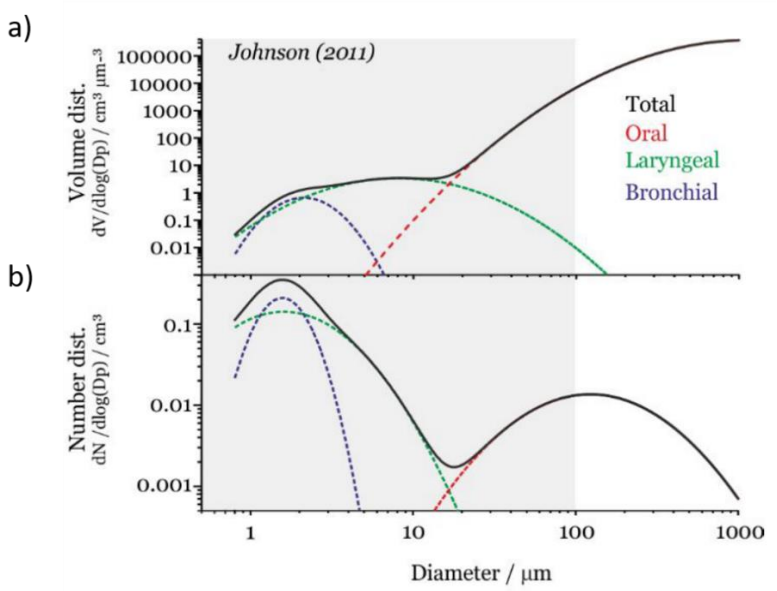

Figure 1-3. Droplet distribution for respiratory fluids (cough) from Johnson et at (2011). [55] **This figure was reprinted with permission from Refs. 56.**

In terms of the spread of infection, the absolute dose is key. Consider the size distribution of respiratory droplets (Figure 1-3b). While the vast majority of the droplet numbers reside in the smallest size regime, the largest volume (e.g. microbe dose), resides in the larger size fraction (Figure 1-3a). Thus, in order to understand and predict the spread of disease vias the aerosol/droplet phase, many aspects of aerosol science must be considered simultaneously.

1.4.3 Modes of Transmission: Direct, Indirect and Airborne

Acute respiratory infections lead to most of 7% of total fatalities worldwide associated with lower respiratory tract infections mostly in low-income countries.[58] Understanding the different routes of transmission is critical for implementing effective public health measures. There are four main transmission routes for respiratory pathogens, [59,60] including:

- Direct contact, which requires person-to-person contact (e.g. shaking hands) to transfer the pathogen between the infected individual and the susceptible host.

Subsequently, the infected host must transfer the infectious pathogen from the contaminated area (e.g. hands) onto conjunctiva or mucous membranes (Figure 1-4a).

- Indirect contact, which involves transmission throughout direct contact with contaminated objects named “fomites” (e.g. elevator buttons, balls). Specifically, fomites are high-touched surfaces where the pathogens are deposited by an infected individual and then taken by a susceptible host (Figure 1-4b).
- Droplets, which requires the infectious case to generate large droplets by coughing or sneezing that impact onto the mucous membranes or conjunctiva of a susceptible host by following a ballistic trajectory. The droplet spray is traditionally defined as involving droplets bigger than 5 μm in diameter and taking place at close-range distances (< 2m). Current physical distancing guidance is based on the definition of large droplet transmission (Figure 1-4c).
- Aerosol transmission or airborne transmission, which requires a susceptible person to inhale respirable bioaerosols generated by an infected individual (i.e. by talking, coughing, sneezing) directly transmitting the pathogens into the alveolar region. This transmission route typically involves droplets smaller than 5 μm in diameter which can remain suspended in the air for long periods and takes place mainly at long distances between individuals. Importantly, it does not require face-to-face contact between the infected person and the susceptible host (Figure 1-4d). Besides, the resuspension of bioaerosol from solid surfaces due to aerodynamic or mechanical disturbances can lead to the risk of infection once being airborne again.[61,62]

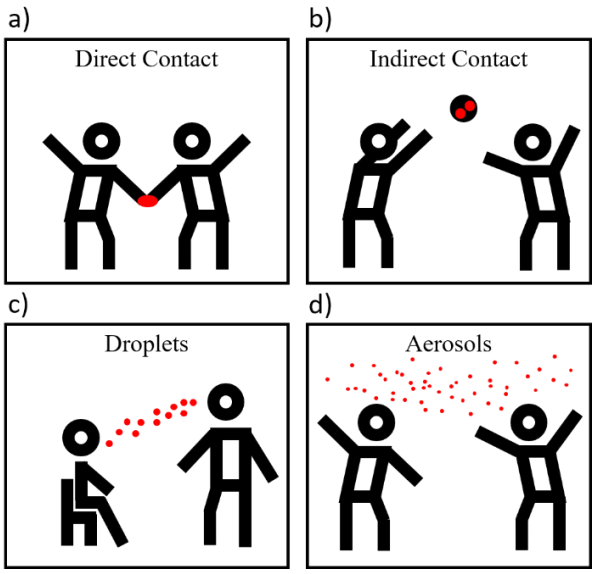

Figure 1-4. Schematic of the different routes of transmission. a) direct contact, b) indirect contact, c) droplets and d) aerosols.

Perhaps surprisingly, the delineation between large and aerosols, in which current social distancing and other infection control strategies are based, dates back to a model of disease transmission developed in 1930 by William F. Wells.[63] This dichotomous classification between respirable and large droplets employs a 5-10 μm diameter boundary, categorizing aerosol routes by the differences in suspension times and deposition regions after inhalation. Thus, and according to Wells, large droplets travel shorter distances since they fall on a shorter timescale than they evaporate while smaller droplets evaporate over a shorter timescale than they fall, even leading to equilibrated droplet nuclei which can be suspended for long periods and travel further.[63] However, this arbitrary delineation of droplet sizes ejecta hampers understanding of disease transmission. Recent studies have demonstrated that exhalation events (e.g. coughing, sneezing, breathing) are composed of a turbulent gas cloud that traps the polydisperse cluster of droplets, allowing them to avoid evaporation and increase their lifetime by a factor of 1000 than if they were emitted individually. Moreover, owing to the high-momentum of the cloud, droplets are propelled longer distances, with large droplets being able to reach up to 8 meters and remain suspended longer than 10 min, depending on atmospheric conditions.[37] The current 1-2 m recommendations for social distancing does not take into account the effect of the turbulent "puff cloud" dynamics and therefore underestimates the

distances and timescales that these emissions can travel, posing important exposure risks for the public and healthcare professionals. Recently, Prather *et al*. have proposed 100 µm diameter as a more appropriate size threshold between droplets and aerosols. This size reflects more accurately the difference in aerodynamic behaviour and the ability to be inhaled of respiratory droplet emissions.[6,64,65]

1.4.4 Parameters Influencing Bioaerosol Survival

A large number of environmental and microbiological factors can affect the survival of microbes during aerosol transport (Table 1-2). The viability of airborne microorganisms is dependent on physical and chemical environmental parameters such as temperature, pressure, ultraviolet light, nutrients composition, pH conditions and pollutant concentrations .[66,67] Many studies have been published in the last decades to investigate the parameters that control the inactivation of airborne pathogens. However, these factors will affect various organisms differently, and the diversity of the methodologies employed for either generation, suspension and sampling, the bioaerosol composition, the microbial species and the environmental conditions lead to results that are challenging to compare.[14,67,68]

Table 1-2. List of environmental and microbiological parameters impacting the survival of airborne microorganisms.

Environmental Factor	**Description**	**References**
Temperature	Wide ranges examined (subzero to above 60°C)	67,69–74
Relative Humidity	Between 0-100% RH	67,69,75–83
UV light	Variability in spectra studied (100-399nm wavelength)	82,84–87
Atmospheric Composition	**Description**	**References**
Gas-phase Atmospheres	N_2, Air, O_2, Helium, Argon, etc.	78–81,84,88–91
Oxygen	Generation of free radicals	78,80,81,84,88,90–92
Atmospheric Gases	OH, NO_3, SO_2, O_3, etc.	19,93–99
Microbiological Factor	**Description**	**References**
Culture Conditions	Various growth phases	33,67,84,90,100–103
Microbial Load	Wide range of concentrations	17
Solute Composition	Proteins, sugars, mucin, etc.	69,78,88,89,91,92,104

Note that the presence of some components such as proteins, mucin, glucose, nutrients, growth conditions and surface-active compounds in the aerosol droplets can influence the impact of these parameters on the viability of microbes, providing some protection against RH, UV light, oxygen toxicity, high salt concentrations and even the droplet surface forces at the air-particle interface.[83,88,102,105–107] The reason for such compositional effects are still unknown. Some hypothesis suggest that these components, such as mucus and proteins, can coat the bacteria and viruses with their highly viscous and hydrophobic properties providing some protection through a viscous layer that limits loss of water on exhalation from the high humidity of the respiratory tract.[69,83,88,89,92]

To fully understand the effect of environmental factors on airborne microbial survival, these parameters need to be further explored under *in vitro* conditions, facilitating data comparison and validation among laboratories by using standardized methodologies, conditions and biological agents.

1.4.4.1 Environmental Factors

The impact of relative humidity (RH) and temperature on the survival of airborne pathogens constitute the greater part of aerobiological studies on the transmission of infectious disease, with the aim of understanding the seasonality of some airborne pathogens.[83,108] The changes in temperature and RH, together with the bioaerosol solute composition, determine the mass flux of water from and to the bioaerosol particles as well as the final particle size at equilibrium with the gas-phase atmosphere.[109] These evaporation and rehydration processes are associated with loss of viability due to osmotic and desiccative stresses.[110]

Briefly, in the case of viruses, the impact of high temperature on survival has been associated with reduction in the integrity of the viral protein and the viral genome (DNA or RNA), reporting an inversely proportional correlation. Thus, the exposure to temperatures above 60 ℃ for short periods is sufficient to ensure the inactivation of most viruses.[67] The effect of RH on the viability of respiratory viruses has been extensively investigated, reporting various contradictory outcomes among studies. A broad concept is that enveloped viruses (e.g. coronavirus, influenza, measles, rubella and varicella) are less stable to the environment than non-enveloped viruses and tend to survive longer under low RHs (20-30%).[67,111] For instance,

the airborne transmission of influenza virus was shown to be more favourable under cold and dry ambient conditions (~6-8℃ and <50% RH).[112] However, some enveloped viruses such as the SARS-CoV reported high stability under a broad range of environmental conditions.[113] In contrast, non-enveloped viruses (e.g. rhinoviruses, adenoviruses) reported longer survival at high RHs (70-90%).[67] A number of studies using different techniques for measurements of airborne survival reported a more complex relationship between RH and survival, a V-shaped curve, for both enveloped and non-enveloped viruses, reporting the lowest virus viability at mid-range RHs (40-70%).[65,102,75,83]

The study of airborne bacteria survival as a function of atmospheric parameters is more complex than with viruses due to their bigger size which is associated with a higher sensitivity to the aerosolization, suspension and collection techniques.[69,115] Besides, bacteria can be structurally different (e.g. gram-negative and gram-positive) and present specific growth requirements (e.g. aerobic and anaerobic). These factors can introduce a great variability in the length of time the microorganisms are capable of surviving in the aerosol phase. Generally, airborne bacteria have been reported to be more resistant to ambient temperature than viruses, showing also a linear inverse relationship between survival and temperature, reporting a reduction in bacterial viability with a temperature increase above 24 ℃ for gram-negative, gram-positive and intracellular bacteria.[70–72,110,116] However, results on the impact of RH on airborne bacterial survival are more complex and highly inconsistent. Thus, the viability of some airborne gram-negative bacteria such as *E. coli*, *Salmonella* sp, and *Serratia marcescens* have been found to decrease at intermediate-to-high RH ranges (~50-90%)[102,117] while another aerosolized gram-negative bacteria, *Pasteurella*, showed great stability at high RH ranges.[118] Besides, some gram-positive bacteria such as *Staphylococcus albus* and vegetative *Bacillus subtilis* are reported to survive poorly at intermediate RHs (50-70%).[102,117,119] Even bacteria with the same structural type (e.g. gram-negative) have reported different survival outcomes under similar ranges of gas-phase RHs and temperature.[67]

In contrast to viruses and bacteria, the study of environmental parameters affecting airborne fungi survival has been relatively limited. Exposure to airborne fungi and their spores can lead to hypersensitive reactions such as sinusitis, asthma and rhinitis and even potentially life-threatening conditions when infecting immunocompromised hosts.[67,116] Generally, fungi and spores are more resilient to environmental parameters than viruses and bacteria, being able to

remain viable even during greater stresses associated with rehydration and desiccation processes as well as UV radiation.[67] Therefore, fungal spores are commonly used as physical traces in bioaerosol studies to determine the physical loss of particles in aerosol systems.[68,69,110]

Another important environmental factor to take into consideration when studying the viability of airborne pathogens is the effect of UV light, which has been generally found to be harmful to both viruses and bacteria.[87,120] The wavelengths of UV light are most commonly used to inactivate microorganisms.[85,86] However, some studies suggested that high values of RH function as a protective thick water coat against UV radiation allowing the survival of *Serratia marcescens* to be increased at high RH levels.[67]

1.4.4.2 Atmospheric Composition and Chemistry

The atmosphere is a very oxidative environment, particularly at low RHs values. The presence of oxygen has been demonstrated to drive one of the main death mechanisms for airborne bacteria, particularly at a RH below 40%.[88] Numerous studies have compared the survival of airborne microorganisms (mostly airborne coliform bacteria) in different gas-phase atmospheres (e.g. nitrogen, air, nitrogen-oxygen mixtures and oxygen), observing similar survival at high RHs (above 70% RH other death mechanisms prevail).[80] On the contrary, the survival in oxygen alone was reported to be the lowest among all the different atmospheres at low RHs,[81] followed by the survival in air when only nitrogen and air atmospheres were compared.[77,79–81,84,88,89,91,92] Besides, small additions of oxygen into a nitrogen atmosphere produced a large reduction in the survival of airborne *E. coli* B and *Serratia marcescens*.[88,91] Hence, this difference in survival was attributed to the lethal action of oxygen dependent on the loss of water from the microorganisms. Bateman *et al.* showed early in 1962 that the exposure to RHs below 70% leads to the loss of strongly bound water from *Serratia marcescens*.[77] Thus, it is hypothesized that the loss of bound water can generate free radicals producing changes in the accessibility and reactivity of macromolecules to oxygen, leading to the inactivation of some enzymes/coenzymes and ultimately to the disturbance of some important metabolic activities.[80,88,92] It is important to note that most of the bioaerosol survival work, including the studies stated above, have been done from wet dissemination. When considering dry dissemination of bioaerosols, where the evaporation of water from the aerosol

does not occur, airborne survival might not depend on the microbial water content since survival decay between dry and wet disseminations were not equivalent in comparative studies.[78,90] Therefore, further work is required to understand the exact mechanisms influencing the survival of airborne pathogens from both types of disseminations.

Moreover, the reactivity of biological aerosols with some atmospheric oxidants such as OH, SO_2, NO_3, and O_3 is largely unknown. Many atmospheric trace gases and SOA (secondary organic aerosols) have been found to significantly reduce the survival of airborne microorganisms. [96–98,110] Many of these atmospheric components constitute the phenomenon known as open-air factors (OAFs), where airborne microorganisms exposed to open atmospheric conditions report a more rapid biological decay than those studied under *in vitro* conditions. The impact of OAFs is not completely understood although it is often associated with the rapid oxidation and degradation of macromolecules such as lipids, nucleic acids, proteins, etc. [93,94,96–99]

The heterogeneous and multiphase chemistry between bioaerosol and atmospheric gases may not only influence the survival of airborne pathogens in the atmosphere but also modify the bioaerosols composition and its physicochemical properties affecting also their roles in atmospheric physics and climate, altering the cloud droplet numbers and the radiative forcing of natural aerosol. Improving our knowledge of how biological aerosols are chemically transformed in the atmosphere at the process level is crucial to predict their impact on health and climate.

1.4.4.3 Microbial Factors

Microbiological properties including the phase of growth, cell line, microbial concentration and culture conditions such as temperature, humidity, aeration, growth media as well as the incubation time may also impact the capability of microorganisms to survive in the aerosol phase.[33,67,100,101] These parameters have the potential to affect the particle size, composition, cell phenotype and, generally, the quality of the sample to be aerosolized which would ultimately impact their survival.[33] Therefore, the detailed characterisation of these species is key for an effective comparison among *in vitro* studies and minimize variability in bioaerosol data.[33]

Various studies have evaluated the effect of culture conditions on the survival of bioaerosols.[90,101–103] For instance, Lever *et al.* performed some comparative studies reporting that plate-grown *Salmonella* species survived longer in the aerosol phase than broth-grown equivalents.[67] Such studies are complicated by potential variation from downstream methods. For example, some studies investigated the effect of using different diluents in the enumeration assay, on the viability of the airborne microorganisms, reporting both lethal and protective data. Interestingly, even the lowest concentration of diluent can exert a significant impact on the decay rate, implying the enumeration method could impact the reported data. [102]

Moreover, some studies have compared the impact of the microbial phase of growth (physiology) on their survival during aerosol transport under the same experimental conditions. Thus, *E. coli* B in the stationary phase (~18hr incubation) has been reported to be more aerosol stable in comparison with the log phase (~4hr incubation).[84] These results agree with subsequent studies performed in the liquid phase where different adaptation mechanisms to osmotic and temperature stresses, through changes in the gene expression pattern, were observed in stationary-phase *E. coli* which were not present during exponential growth.[121–123]

Finally, the effect of microbial load in bioaerosol droplets is another variable to take into consideration when studying bioaerosol survival which has not been yet properly addressed in the literature. Lighthart and Shaffer reported three times higher survival in bacteria-containing particles loaded with higher concentrations of microorganisms. The hypothesized reason for this survival increase is associated with the slower evaporation rates of the larger and more loaded bioaerosol droplets which will eventually acquire a monolayer of microorganisms on the evaporative surface of the droplet. Consequently, the surface monolayer will protect the bacteria located in the deepest interior of the particle from the inactivation processes undergone in the air-particle interface.[17] These mechanisms of surface inactivation are associated with surface forces impacting the infectivity of microorganisms through the extrusion of the hydrophobic part of macromolecules.[106,107]

1.4.5 Difference in Physicochemical Conditions in the Aerosol Phase and Bulk Phase

Understanding the aerosol state is critical since the conditions that a microorganisms experiences in a bioaerosol droplet are dramatically different to those in the bulk liquid phase, representing a challenging environment for the airborne pathogens which can impact their viability and consequently their infectivity potential.[68,124]

For nearly all ambient conditions at RHs below 70%, the evaporation of an aerosol droplet can lead to extremely high solute supersaturation states due to the absence of a solid surface onto which crystallization can occur. Therefore, rapid changes in water content, particle size and solute concentrations during droplet evaporation can vary several orders of magnitude (Figure 1-5),[125] leading to unique physicochemical conditions in the aerosol phase (e.g. supersaturated solute, high salt concentrations, ionic strengths and even ultraviscous and glassy states).[124] Further, these properties enable unique chemical reactions with rates that can be orders of magnitude larger than in the bulk state.[126,127] Moreover, the surface area-to-volume ratios of aerosols are also significantly higher than those for the macroscopic solutions, increasing the importance of reactivity at the air-particle interface.[124]

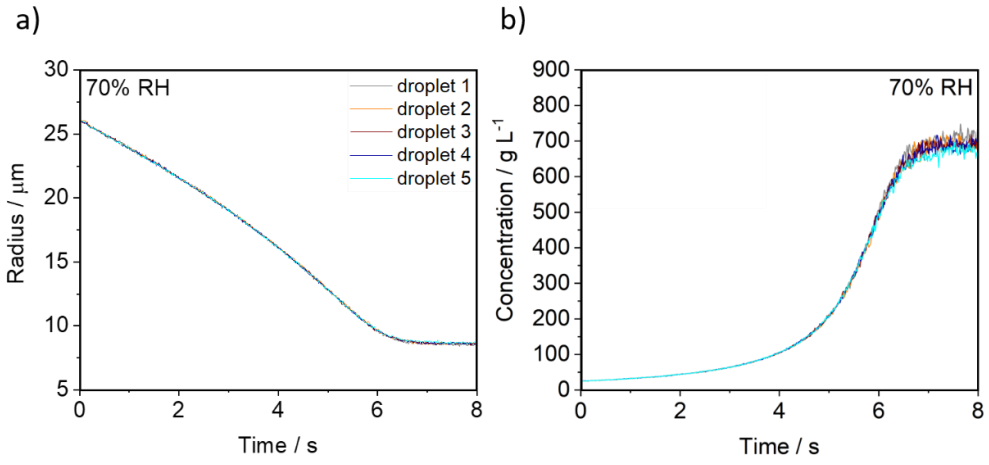

Figure 1-5. Example of evaporation of five Luria-Bertani (LB) broth solution droplets containing 10^9 colony-forming units (CFU) mL^{-1} (~100 CFU droplet -1) into a gas-phase RH of 70%. Figures show changes in a) droplet radius and b) solute concentrations.

Therefore, it is expected that the extreme aerosol conditions impact the microbial physiology of the airborne pathogens, presenting two potential and probably interacting effects: (i) increasing the concentration of toxic compounds (e.g. salts, metabolites) and detrimentally impacting the viability of the microorganisms which are hypothesized to be encased within a 'crust' derived from the droplet fluid or (ii) promoting protective aggregation of micro-organisms where the survival of the microbes located in the deepest core of the particle will be increased. [17]

Moreover, the evaporation and rehydration processes can produce desiccative and osmotic stresses on the microorganisms.[75,128] Both processes are reflective of the water content present in the bioaerosol particles, which is a function of the ambient RH and the droplet solute. Therefore, a detailed understanding of the hygroscopic properties of bioaerosols as a function of solute composition (including the biological components) is critical to understand and predict survival and transmission between hosts.[110]

Consequently, it is critical to take into consideration that the physicochemical properties of an aerosol droplet during bioaerosol survival studies cannot be simulated in the liquid phase sample. Therefore, performing survival measurements in the aerosol phase is crucial to improve our understanding, at the process level, of how these unique chemicals and physical properties impact bioaerosol survival.

1.5 Conventional Techniques for Bioaerosol survival Studies

A variety of techniques can be used in the laboratory to perform bioaerosol studies (Table 1-3). Laboratory studies of bioaerosol survival must consider three fundamental steps to investigate the viability of airborne microbes accurately and produce consistent results:

- Reproducibly simulate the initial droplet size and microbial concentrations generated at source for the natural system being experimentally replicated (e.g. cough, sneeze) whilst minimizing the stresses associated with the aerosolization.
- The prolonged suspension in the true airborne state of the population of bioaerosol droplets in a stable and controllable environment with a wide range of environmental parameters (e.g. temperature, RH, UV light, gaseous species), whilst avoiding the

physical loss of particles and size limitations characteristic of conventional methodologies.

- The collection mechanisms must readily remove the bioaerosol population from the gas phase with a 100% efficiency (e.g. all the bioaerosol particles should be sampled) and deposit it onto an appropriate substrate for further analysis (e.g. enabling a variety of options to test viability and infectivity), whilst reducing the stresses associated with high sampling flow rates, rapid rehydration of the particles, prolonged sampling times, particle bounce, etc which are characteristic of common sampling techniques.

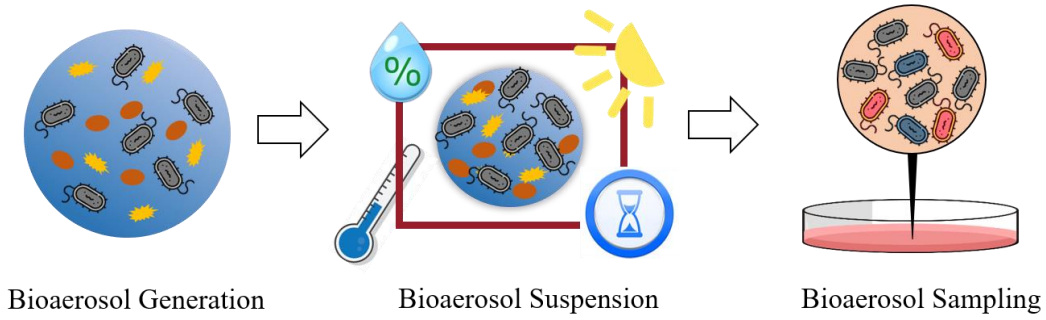

Figure 1-6. Schematic of the three fundamental steps to investigate airborne survival of microorganisms in a laboratory environment.

The reproducible generation of a population of bioaerosol droplets with consistent size and microbial concentration coupled with a 100% efficiency during the sampling process, would enable the quantification of the absolute number of microorganisms probed in each experiment. Therefore, processes for the experimental aerosol generation, suspension and sampling require careful consideration and understanding so that they are representative of the conditions the bioaerosol would experience during the natural transmission mechanism of airborne disease.

Table 1-3. *In vitro* systems used to study the survival of airborne pathogens with a summary of their operational mechanisms.

Generation	Description	References
Refluxing Nebulisers	Recirculation via Venturi effect and wall impaction	70,84,103,115,129–138
Non-refluxing Generators	Atomization avoiding wall impaction	137
Aerosol bubblers	Aerosolization by bursting bubbles	132,137,139
Flow Focusing	Pumping liquid through a capillary needle	137,140,141
Droplet-on-deman (DoD) dispenser	Application of a square waveform to the piezoelectric tip of the DoD	10,68,142
Suspension	**Description**	**References**
Rotating Drum	Suspension by different rotation speeds	9,133,135,138,143–145
Microthread	Capture on ultra-fine spiders'webs	96–98,146,147
Aerosol Chamber	Suspension by mixing air with fans	148
Sphere	Steel sphere with mixing fans	93,97
Greenhouse	No mixing fans	149,150
CELEBS	Electrodynamicbalance (EDB) levitation	10,68
Sampling	**Description**	**References**
Impaction	Inertial collection onto a range of substrates	140,151–153
Filtration and Impaction	Airflow drawn filtration and posterior elution of the sample	140,151,154,155
Impinger	Inertial impaction into liquid	141,151,156–163
Cyclonic Separation	Collection on walls via centrifugal forces into a rotating cylinder	103164
Electrostatic Precipitators	Gentle electrostatic deposition onto collection substrate	165–167
CELEBS	Electrodynamicbalance (EDB) collection	10,68

1.5.1 Generation

The laboratory generation of aerosol containing microorganisms is conducted with a wide range of techniques. In most bioaerosol studies, the refluxing nebuliser is the common aerosol generator normally used in combination with impingers as the sampling method. Collison nebulisers are highly pressurized systems that generate the bioaerosols particles by using a

high-speed airflow through a small orifice to produce a negative pressure that pulls-up the liquid from the reservoir into the jet stream (Venturi effect) and therefore disperse the liquid into thin sheets, ligaments and eventually droplets. The jet flows towards the vessel wall where the impaction produces the settlement of the larger particles back to the liquid reservoir which is in constant recirculation causing accumulated stress to the cell suspension.[168] Besides, pneumatic nebulization has been found to produce the greatest loss of culturability (replication capacity to a detectable level) among aerosol generators as a function of time in both bacteria and viruses.[115,137] The damage is associated to the physical shear, wall impaction and recirculation of microorganisms that do not become fine enough to flow out as the output mist, mainly causing the membrane damage, cell fragmentation and reduction in the ATP activity.[115,137,169] The nebuliser generates high concentrations of small-particle bioaerosols with a size distribution between 1 and 3μm of initial mass median aerodynamic diameter and is commonly used in inhalation studies.[115,137]

Nevertheless, other aerosolization systems have been developed in recent years aiming to reduce damage to microorganisms, including:

- Flow-focusing aerosol generators such as the FFAG (flow-focusing aerosol generator) and the C-Flow nebuliser generate the aerosol particles using the partitioning of microjets which are driven by the aerodynamic suction of an accelerated airflow. These systems reported a significantly lower impact on the cell membrane and respiratory enzymes activities than the Collison nebuliser[115] as well as a good monodisperse size distribution of the bioaerosol plume.[110]

- Aerosol bubbling generators such as the LSA (Liquid Sparging Aerosolizer) are based on the principle of bursting bubbles to generate bioaerosol particles. Some comparative studies with the collison nebulisers also showed that the bubbling generators maintain bacteria culturability at 50% higher after the same aerosolization periods.[137]

- Non-refluxing generators (e.g. single-Pass Aerosolizer) share the same aerosol generation method as the Collison nebuliser (pneumatic nebulization) but avoids the

recirculation of the cell suspension as well as the impaction onto the vessel wall, reducing the stresses associated with both mechanisms.

- DoD microdispersers are recently introduced devices in bioaerosol research based on the application of a small pulse voltage to the piezoelectric tip of the device resulting in the formation of a jet that breaks-up into single micro-droplets, providing a high reproducibility in the initial radii (~20 µm ±0.25 µm).[68] Moreover, the complete chemical and biological composition (e.g absolute number of microorganisms per droplet) can be varied across various orders of magnitude and has shown to not impact the viability of the microorganisms enclosed within the generated droplets.[10,68]

Generally, these alternative systems to refluxing nebulisers have shown better preservation of the physiology of the cells due to the lack of recirculation of the microbial suspension, passing the microbes through the nozzle only once.[115,132,137]

These nebuliser effects may be species dependent and therefore, when selecting a bioaerosol generator, is important to take into consideration not only the performance of the device (e.g. provided droplet size, bioaerosol particle concentration, microbial load in the droplets, monodisperse size distribution) but also its impact on microbial viability. Otherwise, the aerosolized cells can be damaged to a degree that may influence the subsequent aerosol decay and infectivity results and not represent the natural transmission mechanisms involved in the airborne transmission of disease.

1.5.2 Suspension

Techniques for investigating the survival of bioaerosols *in vitro* as a function of time and environmental conditions tend to either suspend the particles in the air (e.g. rotating drum, static chambers, wind-tunnel chambers and electrodynamic levitation) or capture the bioaerosol on a fine substrate assuming to reproduce the physicochemical properties of the true aerosol state (e.g. spider silk threads and hydrophobic surfaces) (Table 1-3). [110,170] The number of viable microorganisms is determined at different time intervals which enable the calculation of the biological decay. Importantly, the viability assays together with the stresses associated with the generation, suspension and sampling process, can impact the number of recovered microorganisms, and therefore, the survival data. The main “dynamic” (e.g. suspended in the

air) and "stationary" (e.g. deposited on a substrate) techniques for bioaerosol survival studies are illustrated in Figure 1-7 and include:

- The rotating drum chamber is probably the standard system used for bioaerosol survival studies since it was designed by Goldberg and colleagues in 1958. In these systems, the competition between centrifugal and gravitational forces maintains the bioaerosol particles airborne. The rotation speed and the suspension periods are a function of the particle size.[171,172] The physical loss of particles is due to the gravitational settling and diffusion of the bioaerosol particles on the walls of the chamber. Various modifications have been implemented in the original design allowing accessibility to a wider range of environmental parameters as well as the suspension of larger particles for longer suspension periods.[9] Unfortunately, limitations such as the physical loss of particles and the uncertainties in the absolute composition of the particles are unavoidable.[171]

- A similar technique for bioaerosol ageing studies is the static aerosol chamber, where the maintenance of the dynamic aerosol is achieved in large chambers by the utilisation of mixing fans, providing shorter suspension periods than the rotating drum. The loss of bioaerosol particles due to gravitational settling is characteristic of these systems.[148,173]

- The wind-tunnel chamber requires a continuous feed of airflow and enables the control of the RH and the temperature in the tunnel. These systems are mostly used to develop and assess the performance of new bioaerosol sampling devices as well as optical sensors.[174,175] The physical loss of particles as a function of size-dependence, gravitational settling and turbulence needs to also been taken into account in data analysis when utilizing these systems.[176]

- The Controlled Electrodynamic Levitation and Extraction of Bio-aerosol onto a Substrate (CELEBS) is a recently developed technology which combined a DoD generator as aerosolization method and the electrodynamic collection and the sampling techniques. The development of this novel approach is the subject of this thesis. This technique uses an electrodynamic field to suspend the bioaerosol particles in a controlled atmosphere. To enable suspension in the electrodynamic field, each

bioaerosol particle holds a small net charge imparted by an induction electrode. After the desired suspension period, the waveform of the electrodynamic field is decreased and the bioaerosol particles extracted onto a substrate with 100% sampling efficiency for subsequent off-line viability/infectivity analysis.[68] Some current limitation of the technique is the range of initial droplet sizes that can be investigated which depends on the diameter of the commercial DoD dispenser available in the market, diameter ranging from 20 to 80 μm. With these devices, it is possible to generate droplets with an initial diameter ranging from <25 μm to >100 μm. This size range encompasses those commonly associated with bioaerosol.

- The microthreads (e.g. spiderwebs or synthetically made) technique was developed in 1967 by May and Driett[147] and used to capture bioaerosol particles and expose them to various environmental conditions for extended periods of time trying to simulate the aerosol state.[147] The utilisation of microthreads avoid the issue related to the physical loss of particles and therefore enables the study of large particles which have high physical loss rates in the static and rotating drums. Limitations related to the stationary state of the bioaerosol particles on the surface of the threads difficulty the complete exposure to the environmental conditions on the adhered side of the aerosols, leading to experimental differences, especially for small size aerosols.[170] Other limitations of this technique are associated with the potential reactivity, toxicity and diameter of the microthreads. However, this technique has shown comparable results to those obtained with the rotating drum when measuring the airborne survival of filoviruses.[146]

- Hydrophobic surfaces have been used to investigate the effect of RH and chemical composition of droplets on the viability of viruses contained in evaporating droplets which are deposited on superhydrophobic surfaces.[104] Observation of the drying process is performed by using optical and fluorescence microscopy.[177] Results derived from this technique can only be extrapolated qualitatively to the real airborne state since it is not known how the surface material may affect the viability of the virus, the

heat conduction and mass transport between the particle and gas phases, and the deposited droplets do not experience airflow. [177]

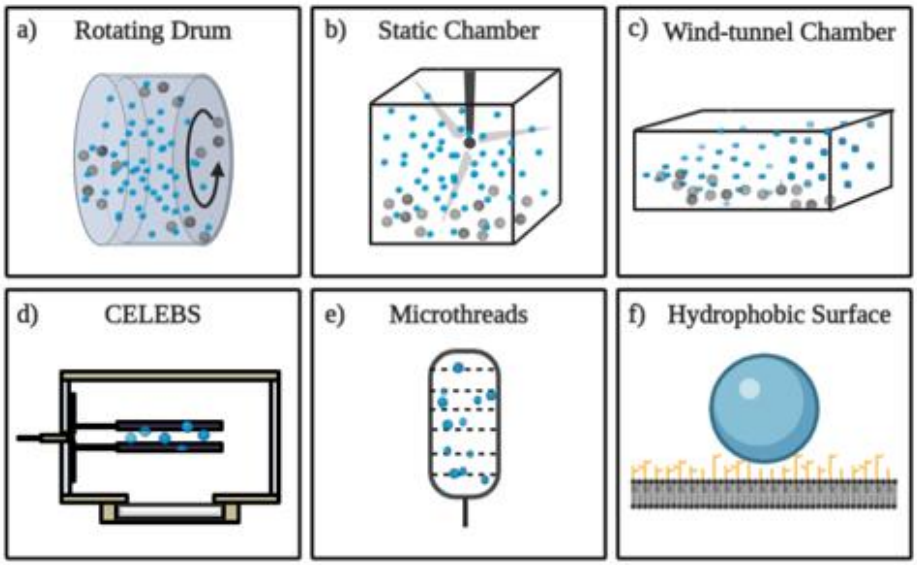

Figure 1-7. Different experimental methods to study bioaerosol survival (both dynamic and stationary) as a function of time and environmental conditions. (a) Rotating Drum, (b) Static Aerosol Chamber, (c) Wind-tunnel Aerosol Chamber, (d) CELEBS, (e) Microthreads and (f) Hydrophobic Surfaces. Note that the particles in grey colour represent the physical loss due to gravitational settling in some conventional systems.

1.5.3 Collection

Methods for sampling airborne microorganisms include impingement, impaction, filtration, cyclonic separation, electrostatic precipitation and electrodynamic collection. A small description of the operational mechanisms for the main collection devices is included in Table 1-3 and further details can be found in the literature.[178] Each sampling technique has advantages and disadvantages for collecting airborne microorganisms, presenting the potential to damage the microbial viability. The stress imparted to the microorganisms depends on the utilized technique, the sampling times (ranging between 1 to 10 min for the determination of decay rates) and the species under study (related to the microbial structure).[110] Stresses imparted by sampling processes include:

- Structural damage normally caused by the utilisation of impingers and impactors due to the inertial deposition and the high collection velocities.
- Rapid rehydration linked to increased osmotic stress in the microbial cells, characteristic of impingers.
- Desiccation stresses commonly observed with filtration methods as air is continuously drawn across the filter.
- Loss of culturability/viability and particle bounce caused by impactors.

The effects of microbial damage related to the above-mentioned stresses can be reduced in several ways: the addition of non-selective media, scavenging enzymes and compatible solutes can increase survival following stresses; the reduction of the sampling times has been reported to promote cell recovery in numerous studies;[151,179] the addition of a thick layer of mineral oil in impactors can significantly reduce particle bounce;[152] and the use of a gelatine membrane during filtration retains moisture and improve bio-efficiency. [137,140] Both the electrostatic precipitation and electrodynamic sampling use similar collection velocities onto the substrates (~ 0.01-0.05 m s^{-1}) which are between two and four orders of magnitude lower than those use by inertial samplers, reducing the detrimental effect on cell physiology while providing excellent collection efficiencies.[68,165,166,180]

In conclusion, the characterisation of the collection device is crucial since previous studies have demonstrated the deleterious effects on microorganisms associated with different sampling processes which significantly affect the variability in the survival of different aerosolized microbes.[140] Moreover, the collection efficiency among sampling systems can vary significantly. This variation has been associated with the destruction of the microbial cells during the sampling processes, the re-aerosolization of microorganisms from the collection media (leading to an underestimation of the sampled material), rapid rehydration and high collection velocities impacting the microbial integrity and, therefore, this variation not being caused by the actual efficiency in the transfer of biological material from the inlet to the collection medium.[140,181] The full understanding of the collector efficiency is critical to develop relationships between biological and physical efficiencies, and to completely understand the losses within the system (decay in viability vs physical loss of particles). Recognizing the impact caused by different collector devices on the viability of microorganisms and the need

of fully characterizing the systems used in *in vitro* studies, will enable an accurate comparison of data among laboratories and the adequate development of the field.

1.6 An Ideal Solution

Conventional techniques for investigating the survival of bioaerosol under laboratory conditions present several limitations that can impact the accurate representation of the natural processes that these particles would experience in the environment, introducing uncertainties at each step of the method. In particular, the *in vitro* study of bioaerosols is challenging and requires careful consideration of various experimental points:

- Quantifying the complete droplet composition, from the individual droplet to the population level, reducing the uncertainties in the number of microbes per droplet associated with bioaerosols of polydispersed size distributions. Conventional techniques normally sample bulk aerosol (the unknown composition of the plume), making it difficult to develop an appreciation of the microenvironment heterogeneity occurring within individual aerosol droplets from the physicochemical and biological perspective. For instance, each individual aerosol droplet may have a different chemical composition, exacerbated by differences in the particle size.
- The complete control and characterisation of the atmospheric variables (e.g. temperature, relative humidity, gas atmosphere, etc) where the droplets are suspended for prolonged periods of time. The detailed characterisation of the experimental environment is critical since these parameters interact with the biological aerosols potentially changing their properties and therefore the outcome of the survival studies. In additions, this environment needs to be constant whilst avoiding the physical loss of the particles.[9,170]
- Minimizing all stresses occurring during the aerosol generation, suspension and sampling processes which cause damage to the microbial cells before the biological decay and infectivity studies are performed. Especially, a reliable and gentle generation and collection of a bioaerosol are essential to produce consistent results since most of these systems have been demonstrated to impart mechanical stresses to

the microbial cell in different degrees affecting their viability. [137] The influence of all these detrimental processes on bioaerosols viability, and subsequently on their infectivity potential, is yet not well characterized.[110,140]

- The distinction among the physical, chemical and biological processes in aerobiological studies. For instance, the particle loss due to gravitational settling of particles in an experimental system must be considered separately from the biological decay.[170]

Moreover, during the past 60 years, there have been many publications whose outcomes are difficult to compare even on the same organisms.[68] This incompatibility is a result of the heterogeneity in experimental approaches used for survival studies together with the variability produced by microbiological analysis. Therefore, the standardization between laboratories is critical for producing reproducible and comparable data between laboratories that relates to the natural aerosol emission being investigated.[170]

The absence of a comprehensive tool capable of making reliable measurements while minimising the amount of damage caused to the microorganism during generation, suspension and sampling has limited the understanding in this field. Therefore, some basic questions about the fundamentals of airborne disease dynamics remain unknown. Consequently, the development of a novel technology was the necessary starting point for this research.

1.7 Aims and Thesis Overview

The transmission of infection via the airborne route has been identified as the major transmission mode in indoor environments in many epidemics. Understanding the parameters that determine the survival of pathogens during atmospheric transport is critical for public health applications, ranging from the development of strategies to mitigate the impact of disease outbreaks, understand the seasonality of infectious diseases, and also improve treatment of respiratory infections. The work described in this thesis aims to investigate the fundamental mechanisms that control the transmission of airborne infection between hosts. Specifically, this thesis aims to:

- Develop a novel instrument for investigating the decay in viability of bioaerosols as a function of atmospheric parameters, bioaerosol compositions and microbiological properties while minimizing the generation and sampling stresses as well as exploring the influence of droplet size, all characteristic of conventional techniques used in bioaerosol research.
- Develop a new approach which combines two complementary experimental tools to explore the complex interconnections between aerosol microphysics and biological decay.
- Elucidate the fundamental mechanisms reducing the viability of airborne respiratory pathogens to identify the parameters that control the transmission of airborne disease.

The structure of this thesis is mostly chronological, providing an account of the development and application of the CELEBS instrument. Following an introductory overview describing the context for these studies, Chapter 2 focuses on the description of the complete methodology developed throughout my studies to interconnect the physicochemical and the biological properties of bioaerosols. Chapter 3 describes the development and validation of a novel instrument to accurately measure bioaerosol survival as a function of a wide range of conditions. This chapter also includes the first survival curve reported with this system a function of the gas-phase RH. Chapter 4 continues the investigation of decay in bacterial viability in the aerosol phase complementing it with measurements for the physicochemical characterisation of the same bioaerosol particles, aiming to determine the mechanisms of inactivation for airborne pathogens. Chapter 5 describes a more complete and representative investigation of the fundamental mechanisms of airborne transmission of respiratory pathogens by including not only a wider range of environmental and compositional parameters, but also different microbiological properties as well as the use of representative respiratory secretions. Finally, a summary of the findings and directions for future work are presented in Chapter 6.

Chapter 2

Novel Experimental Approach to Investigate the Synergistic Interactions Between Physicochemical and Biological Processes Impacting Airborne Microbe Survival

The content of this chapter contains material published in Ref. [10]. I confirm that the published manuscript is all my own work and acknowledge Jonathan P. Reid, Allen E. Haddrell and Richard J. Thomas for project supervision and contributions to instrument development.

Understanding the parameters that determine the survival of airborne microorganisms is crucial to controlling disease outbreaks. The methodologies currently employed are based on techniques often developed in the 1950s and have numerous limitations. Therefore, a new approach to answer the fundamental questions about the interplay of aerosol microphysics and the viability decay of airborne pathogens with the associated impact on disease transmission remains required. The electrodynamic balance has been proved to be a powerful tool for the study of aerosol particles.[182] In this chapter, a summary of the established techniques based on electrodynamic levitation to conduct aerosol research will be discussed. Moreover, the development of the experimental methodology based on electrodynamic levitation for the work presented in this thesis will be also described. Specifically, the TAMBAS (Tandem Approach for Microphysical and Biological Assessment of Airborne Microorganisms Survival) approach allows the investigation of the synergistic interactions between the physicochemical and biological processes that impact the survival of airborne microbes. This innovative method provides a detailed understanding of the processes taking place during aerosol transport, elucidating mechanisms of inactivation not previously described.

2.1 Historical Development of Aerosol Levitation: A Summary of Levitation Techniques

The development of electrodynamic trapping techniques originally started from the motivation to determine the charge of a single electron in the early 20th century. Although providing significant lower values than the current accepted value 1.6021892×10^{-19} C due to various assumptions associated with the charges and monodisperse distribution of the cloud droplet, a series of efforts to measure the value of the elementary charge were first performed in the Cavendish Laboratory at the University of Cambridge. These experiments led to the Wilson cloud chamber and to the Nobel Prize in Physics in 1927, preluding the development of the first electrodynamic trap.[182]

The first successful experiment which provided a remarkable precise value (1.591×10^{-19} C) for the charge of an electron was performed by Millikan at the University of Chicago in 1909.[183] The Millikan Oil Drop Experiment (MODE) was technically an electric-field trap based on a chamber composed of two parallel metal plates connected to a 10000 V battery. Single atomized oil droplets were isolated from the cloud and confined within the electric field (Figure 2-1a). Major limitations of this technique were related to the vertical and lateral stability of the droplets. Although not able to counteract fully the gravitational force by adjusting the Direct Current (DC) field to trap droplets in a stationary position, Millikan was able to use the rate of falling droplets with and without the electric field to determine the mass of the particle to the order of 10 pg. He received the Nobel Prize in Physics for this work in 1923.[182] The addition of a central disk to one electrode, introduced by Fletcher, reduced the horizontal perturbation of the particles, presenting a significant improvement to the Millikan condenser.[184]

In 1953, Paul and Steinwedel developed the first quadrupole ion trap (QIT) for mass spectrometry studies, initially named electric mass filter.[185] The introduction of an Alternate Current (AC) field applied to a hyperbolic electrodes configuration finally enabled the stable trapping of ions along the central axis between the four cylindrical rods (Figure 2-1b) whose trajectories are dictated by the Mathieu's equation. The analytical potential of this technique was not exploited until the 1980s when the design was incorporated into gas chromatography-mass spectrometry. It was in 1989 that Paul and Dehmelt (who used the QIT as an ion storage device by applying radio frequencies)[186] were awarded the Nobel Prize in Physics.[182]

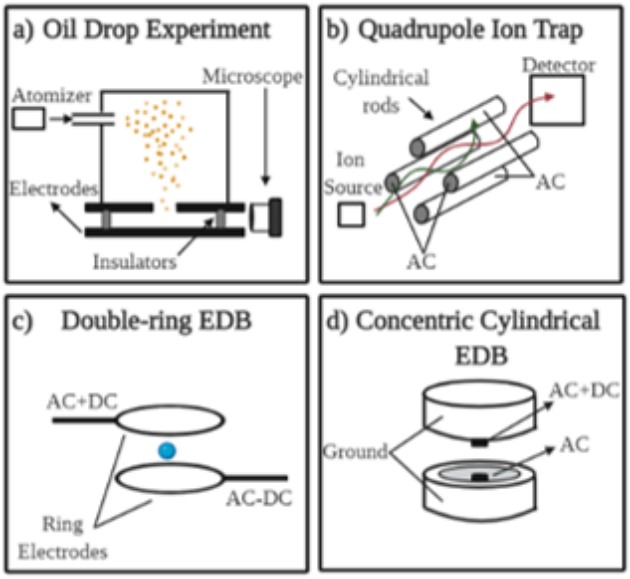

Figure 2-1. Historical development of different electrodynamic balance techniques . (a) set-up of the Millikan's Oil Drop Experiment (MODE),[183] (b) set-up of the Quadrupole Ion Trap,[185] (c) set-up of the double-ring EDB[187] and (d) set-up of the Concentric Cylindrical EDB.[188]

The first electrodynamic balance apparatus (EDB) was presented by Straubel in 1956, who implemented an ac electrode characteristic of the QIT in between the two DC electrodes of a Millikan instrument, ensuring lateral and vertical stabilities.[182] Over the succeeding decades, numerous modifications of the EDB have been developed in the field of aerosol science. A popular adaptation of the Strauble trap was presented by Ray *et al*. in 1989,[187] introducing the double-ring configuration. The elimination of the endcap electrodes and application of superposed AC and DC voltages to two parallel rings electrodes was especially useful to increase the optical accessibility of the levitated particles (Figure 2-1c). This EDB geometry has been adapted to develop the device employed throughout this thesis to study the survival of airborne pathogens: The CELEBS instrument.[68] Finally, a different EDB electrode configuration developed by Heinisch *et al.*, [188] consisting of two concentric cylindrical electrodes, was also employed in this thesis to study the hygroscopic response and dynamic behaviour of bioaerosol droplets.[10,189]

2.2 Comprehensive Methodology for Bioaerosol Survival Studies

The TAMBAS approach was developed to elucidate the fundamental mechanisms responsible for degrading the viability of airborne microorganisms and, thus, identify the parameters that define the transmission of airborne infection. The complementarity of two methodologies is used to resolve the complex interrelationship between the physicochemical and biological processes taking place from the production mechanism such as coughing and sneezing,[55] until the droplet reaches equilibrium with the surrounding environment and through to rehydration during the inhalation process. The CK-EDB (Comparative Kinetics Electrodynamic Balance) method can be used to study the evaporation/condensation processes, the solute hygroscopic properties and the evolving particle morphology during drying of single levitated aerosol particles.[190] These data can be used to develop a detailed understanding of the processes that take place during the evaporation and condensation cycle occurring in a droplet lifespan.

Additionally, the determination of survival of microorganisms in populations of bioaerosol droplets as a function of atmospheric conditions, biological and chemical composition, and other biological factors such as the microbial concentration and cell physiology, can be performed with the novel CELEBS method.[68] An overview of both methodologies is included in Section 2.2.3 (Table 2-1). Some of the key features accessible with the CELEBS technique are the suspension of particles in the true airborne state under a regulated atmosphere for a well-defined and unlimited period (~3 seconds to days) and with high-time resolution (<1s); a quantifiable number of individual microbes containing droplets probed in each experiment; and control over the number of microbial cells hosted within each droplet. Importantly, the main elements of this methodology (e.g. the use of DoD generation to produce droplets of tailored composition, the imposition of low levels of charge on the particles to levitate particles) do not impact the viability of the microorganisms.[68] Details of the set-up, operation and data analysis for both methodologies are detailed in Figure 2-11 and Sections 2.2.1 and 2.2.2, respectively.

Unique to the comprehensive TAMBAS methodology is the ability to combine our understanding of the microphysics and microbiology in the airborne state with time resolutions between 10 ms and 1s, respectively. Not only can this understanding be achieved in the aerosol phase, but the methodology allows us to investigate the repeatability and reproducibility for many droplets with the same desired initial conditions while minimizing stresses affecting

microbial viability during aerosolization, leading to low experimental uncertainties. This valuable alternative to conventional technologies will allow researchers to develop more accurate strategies to control the airborne transmission of disease.

2.2.1 Comparative Kinetics Methodology for Physicochemical Characterisation of Bioaerosols: The CK-EDB Instrument

The ability to measure the dynamic behaviour of single levitated droplets using the cylindrical electrodynamic balance (EDB) has been discussed in the literature.[189] A schematic of the experimental set-up is provided in Figure 2-2. Briefly, a sample solution of known chemical and biological composition is introduced in the reservoir of a DoD micro-dispenser (Microfab MJ-ABP-01, 30 μm orifice). Single droplets are generated with a high level of size reproducibility (Figure 2-3) by applying a pulse voltage to the piezoelectric tip of the DoD. A small net charge is induced during droplet formation employing a high-voltage induction electrode located 2-3 mm from the tip of the DoD, allowing the droplet to be manipulated in the EDB. Approximately 100 ms after generation, the droplet is confined in the null point of the electrodynamic field within the flow from a 200 mL/min gas inlet at a temperature of 20°C which regulates the RH (in a range between 10 and 90%) inside the CK-EDB chamber by altering the mixing ratio of wet and dry nitrogen flows.

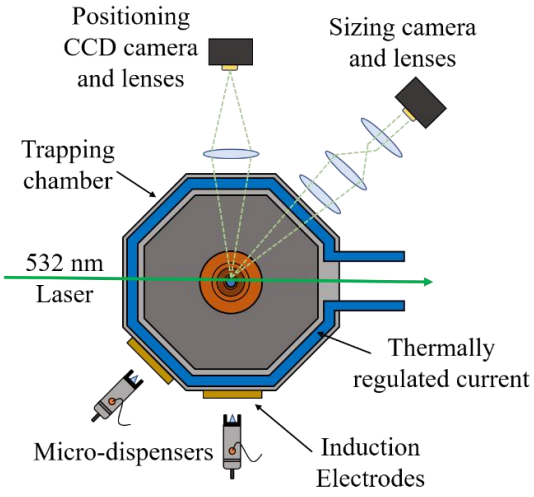

Figure 2-2. Schematic of the CK-EDB system.

The trapped droplet is illuminated with a 532 nm laser beam (Laser Quantum, Ventus continuous wave [CW]) and a CCD camera (Thorlabs) records the light scattering pattern referred to as "phase function" at a central viewing angle of 45° every ~10 ms. By using the Geometrics Optics Approximation, the angular separation between fringes in the phase function pattern is used to determine the absolute radius of the droplet as a function of time. From the droplet evaporation measurements, the hygroscopic growth properties at the thermodynamic equilibrium can be retrieved by using a comparative kinetics approach described in the literature.[191] Besides, the hygroscopicity data derived from the above process can be used to predict the evaporation dynamics for droplets of any size, composition, gas-phase RH, and temperature. Finally, combining the information from the evaporation rates with the diffusion coefficient of *E. coli* cells, it is possible to estimate the subsequent surface enrichment of *E. coli* on the particles as a function of the RH. The methodologies utilized in the determination of the mentioned physicochemical properties are detailed in the sections below.

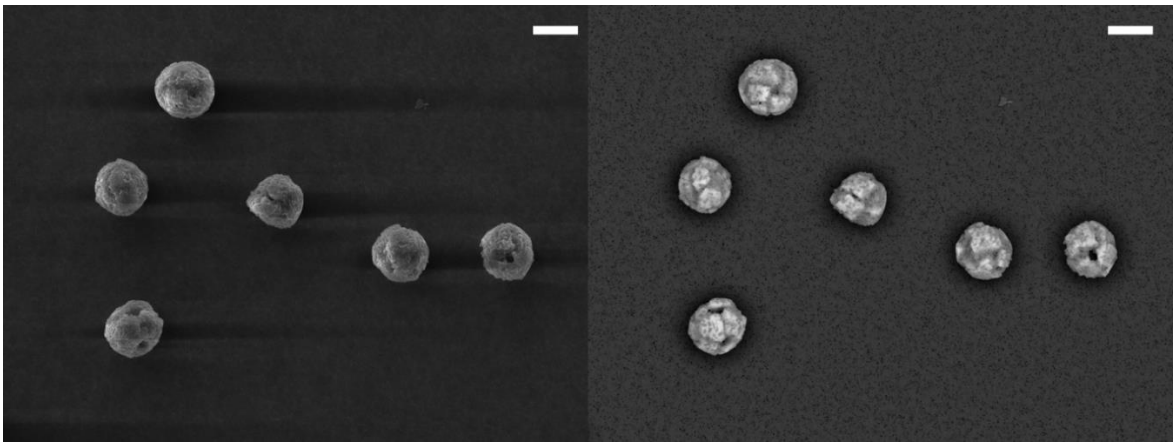

Figure 2-3. An example of the reproducibility in the droplet size of the particles generated with a DoD micro dispenser. SEM images of *E. coli* MRE-162 cells at a concentration of ~10^9 CFU mL^{-1} levitated in Phosphate buffer saline (PBS) droplets at 30% RH. Scale bars represent 10 μm.

2.2.1.1 Determination of Droplet Evaporation Kinetics

Once a droplet is confined, the light scattering pattern is collected every ~10 ms with an angular range from 32° to 58°, centred at 45° to the forward direction of the laser, allowing the

applicability of the Geometrics Optics Approximation for the determination of the particle size with the following equation (Eq.(2-1)).[192]

$$r = \frac{\lambda}{\Delta\vartheta}\left(\cos\left(\frac{\vartheta}{2}\right) + \frac{n\ \sin\left(\frac{\vartheta}{2}\right)}{\sqrt{1+n^2-2n\cos\left(\frac{\vartheta}{2}\right)}}\right)^{-1} \quad \textbf{(2-1)}$$

r is the radius of the droplet, λ is the wavelength of the laser, ϑ is the central viewing angle, n is the real part of the refractive index (RI) of the droplet medium and Δϑ is the average angular difference between the fringes of the scattering pattern for a spherical and homogeneous droplet. This approximation presents an associated accuracy of ±100 nm for droplets <10 μm. [109]

During data acquisition, the estimation of the radius in real-time is performed by using the RI of pure water at a wavelength of 532 nm (1.335) as a constant value, n. In a post-analysis process, firstly the initial droplet size is extrapolated to t=0 s from a linear r^2 vs time relationship to correct for the period between the production of the droplet and the trapping moment, ~ 100 ms from the tip of the DoD to the EDB inside the chamber. Secondly, the variation in the droplet RI with the mass fraction of solute (MFS) is accounted for by applying a solute RI parametrisation generated by using the molar refraction mixing rule (Eq. (2-2)):[193]

$$R = \left(\frac{n^2-1}{n^2+2}\right)\left(\frac{M}{\rho}\right) \quad \textbf{(2-2)}$$

n is the RI of the solution, R is the molar refraction, M is the molecular weight and ρ is the density of the solution at that composition. When working with multi-component solutions, the solution molar refraction, R, is calculated by the sum of the molar refractions of each component (R_i) multiplied by its mole fraction (x_i), assuming the solution is an ideal mixture where the properties of the single constituents are conserved:[194]

$$R = \sum_{i=1}^{N} x_i R_i \quad \textbf{(2-3)}$$

To determine the evolution of the solution RI as the droplet evaporates, a parametrization for the variation of solute density with the MFS is performed according to the solubility of the compound. Bulk measurements of RI and density performed with a density meter and a refractometer respectively need to be extrapolated beyond the compound solubility limit to cover the supersaturated solute concentration regimes achieved in the aerosol state, including an MFS range from 0 to 1 (pure or "melt" component). In the case of solubilities greater than 0.4, the bulk density measurements are preferably fit by plotting density against the square root of MFS and using a third-order polynomial density treatment. However, for solubilities lower than 0.4, the density parametrization is generated by using the ideal mixing density treatment (Eq. (2-4)) which has been demonstrated to minimize uncertainties when MFS approaches 1.[20]

$$\frac{1}{\rho(1-\varphi_s)} = \frac{\varphi_s}{(1-\varphi_s)\rho_s} + \frac{1}{\rho_w} \quad \textbf{(2-4)}$$

Where ρ is the density of the mixture, φ_s is the MFS, ρ_s is the melt density of the pure component and ρ_w is the density of water. From the density treatment, the RI values of the mixture can be corrected as a function of the evolving MFS solving for *n* in Eq. (2-2).

For a first estimation of the changes in droplet size and consequently in solute concentration during evaporation, the light scattering pattern is analyzed by using Eq. (2-1) with n =1.335, then extrapolated to t=0. From the initial droplet radius data, the original MFS of the solution introduced in the DoD is used to determine the variation of solute concentration during evaporation (assuming none of the solutes is volatile)[189] and consequently calculate the corresponding density dependence in order to obtain the corrected RI values calculated as a function of the evolving MFS by using Eq. (2-2). This revision process is repeated over 2-3 iterations until the radii and corresponding refractive indices values converge, providing accurate data for the droplet radius.[109]

Note that surface enrichment and inhomogeneity in the droplet composition are not considered in the estimation of the refractive index values, producing an associated error in the calculation

of the droplet radius. The error resulting from this assumption remains under 5% and only affects the last ~0.1s of the lifetime of the droplet, showing no impact on the estimation of crystallization times.[195] This approach presents a rapid and less computationally demanding alternative than the analysis of light scattering patterns from the trapped particle using the Lorenz-Mie theory,[196] where the radius is estimated by fitting the experimental phase functions with a library of Mie theory simulations.

2.2.1.2 Determination of Droplet Hygroscopicity Properties

A comparative kinetics approach is used to accurately determine the RH of the trapping atmosphere. Measurements are performed with a probe droplet formed by well-known system such as pure water or aqueous NaCl solutions. This is followed by the retrieval of the equilibrium hygroscopicity response of the unknown sample droplet. Specifically, sequences of ten pairs of probe and sample droplets with a different chemical composition are sequentially dispensed by two separate DoD micro-dispensers.

After all the radii data for probe and sample droplets is corrected, the mass and heat transport equation of Kulmala *et al.*[197] Eq. (2-5) is applied to calculate the mass-flux of water, I, during evaporation and condensation kinetics from/to aerosol droplets of different composition under a range of conditions as a function of the concentration gradient of water vapour from the droplet surface to infinitive distance:

$$I = -2Sh\pi r(S_\infty - a_w)\left[\frac{RT_\infty}{M\beta_M D\rho^0 T_\infty A} + \frac{a_w L^2 M}{KR\beta_T T_\infty^2}\right]^{-1} \quad \textbf{(2-5)}$$

The thermophysical terms of this equation and their associated errors have been described in detail in previous work.[109,198,199] Briefly, the main parameters used to define the droplet are the radius, r, and the water activity, a_w. The gas-phase is characterized by S_∞, the equivalent to the RH in the surrounding atmosphere, R represents the ideal gas constant, T_∞ is the gas phase temperature, L is the latent heat of vaporization of water, K represents the gas-phase thermal conductivity, D is the binary diffusion coefficient of water in nitrogen, p^0 is the saturation vapour pressure of water, M is the molecular mass of water and A is the Stefan flow correction

factor. Sh represents the Sherwood number used to account for a mass-flux increment related to the gas-flow surrounding the trapped droplet. Finally, β_M and β_T are the transition correction factors for mass and heat, respectively, which are assumed to be the unity and show an insignificant impact in the uncertainty of the method for the droplet size under study.

The determination of the gas-phase RH is performed by matching simulations generated using Eq. (2-5) and the Extended Aerosol Inorganic Model (E-AIM)[200] thermodynamic model for inorganic salts with the evaporation profile of water probe droplets (when RH > 80%) or the equilibrated size of aqueous NaCl probe droplets (when 45% < RH < 80%). Once the gas-phase RH is known (S_∞), Eq. (2-5) is rearranged to determine the water activity of the measured sample droplet, a_w as shown in Eq. (2-6) at each time-resolved measurement of the droplet size:

$$a_w = S_\infty - \left[\frac{IRT_\infty}{2Sh\pi r M\beta_M D\rho^0 T_\infty A} + \frac{IL^2M}{2Sh\pi rKR\beta_T T_\infty^2}\right]^{-1} \quad \textbf{(2-6)}$$

Thus, it is possible to retrieve the hygroscopic response of the sample droplet by transforming the corrected radius over time data to mass using the density parametrization. From these data, the mass flux as a function of time is calculated and used to determine the water activity at the droplet surface by using Eq. (2-6). Finally, the droplet hygroscopicity is represented as the variation in MFS (calculated from the initial size and droplet composition) against the variation in water activity, providing the whole hygroscopicity curve.

It is important to note that when the droplet evaporates, the mass transfer of water from the droplet to the gas phase is accompanied of a heat transfer, decreasing the droplet temperature proportionally to the evaporation rate due to the associated latent heat absorbed by the droplet. This temperature suppression has an impact on the vapour pressure of water at the droplet surface which affects the evaporation rate. The mass-flux equations of Kulmala and co-workers[197] use an approximation for the temperature dependence of the water pressure of water which is only accurate when the temperature difference between the droplet ($T_{droplet}$) and the surrounding atmosphere (T_{gas}) is less than ~3K (Eq. (2-7)).[191] Therefore, all the data is re-analyzed and only data points where $\Delta T<3$ K in Eq. (2-6) are used to retrieve the final hygroscopicity curve as a relationship between MFS and a_w.

$$T_{droplet} - T_{gas} = -\frac{I\,L}{4\pi\beta_T Kr} \quad \textbf{(2-7)}$$

Measurements of the solute hygroscopicity are limited to a_w between ~0.5 and 0.99 due to the crystallization of solutes al low RH, therefore it is not possible to extract the final equilibrated size from the phase function pattern. The validation of the method for the retrieval of the hygroscopic response of sample droplets has been reported in the literature.[109,191] This approach presents the possibility to accurately measure the hygroscopic growth curve over a wide range of RH within seconds, being the only single particle-based method able to measure hygroscopicity close to saturation states, presenting significant lower uncertainties than conventional techniques.[191]

2.2.1.3 Simulations of Droplet Evaporation Kinetics

Once the hygroscopic properties of the sample droplet are determined, it is possible to generate simulations by using the Kulmala *et al.*[197] model in order to study the evaporation dynamics under a wider range of conditions such as initial solute concentrations, droplet size and gas-phase RH and temperature. The possibility to build models that enable the prediction of evaporation kinetics of aerosol droplets containing microorganisms as a function of the initial droplet radius and composition allows further exploration of the interplay between all the physiochemical parameters affecting airborne bacteria survival (Figure 4-10), assuming a minimal role of the microbe in the dynamics of the aerosol.

The relationship between the relative droplet radius across a broad range of a_w can be estimated from experimental data (evaporation profile of droplets of known composition into an airflow of a known relative humidity) and the equation developed by Kreidenweis *et al* [201] (Eq. (2-8)). This equation is used to generate a solute hygroscopicity parametrization with a_w values between 1 and 0 for aqueous droplets of any composition in terms of radial growth factor (droplet radius at a given water activity divided by the dry radius, GF_r) as a function of the gas-phase RH (equivalent to the a_w assuming thermodynamic equilibrium is established for the droplet composition). Thus, by using Eq. (2-8), the experimental data is fitted across the entire

range of RH, allowing to estimate the continuous hygroscopic behaviour in aqueous aerosol droplets represented by the relative change in particle size (radial growth factor, $GF_{r,}$).

$$GF_r(RH) = \left[1 + (a + bRH + cRH^2)\frac{RH}{1 - RH}\right]^{1/3} \quad \textbf{(2-8)}$$

The coefficients *a, b* and *c* are calculated to minimize the difference between the GF_r experimental data and the GF_r calculated with Eq. (2-8). Finally, the GF_r parametrization together with the density treatment of the specific solution droplet is introduced into Eq. (2-5) to generate the predictions of mass-transfer kinetics. Simulations resulting from this approach have shown an excellent agreement with experimental data. Associated errors with the thermodynamic predictions have been also discussed in previous work.[109] The morphology changes occurring at RHs below 50% are not taken into account when using the model and the modelled particle sizes are hence overestimated.

2.2.1.4 Assignment of Particle Morphology

The same light scattering pattern employed in the calculation of the droplet size has been also used to qualitatively assess and categorise the morphology of single levitated particles.[202,203] Based on qualitative characteristics of the phase function, a new methodology to differentiate among four main particle structures has been recently developed by us.[190] This robust approach relies on over one million experimental observations of individual light scattering patterns to develop an algorithm which categorizes the morphology as particles that are homogeneous, core-shell in structure, droplets containing inclusions or crystal/non-spherical. Specifically, a homogeneous and spherical evaporating droplet produces a regular and smooth structure in its light scattering pattern which is characterized by equally angularly spaced peaks. In the case of droplets containing inclusions, the regularity in the spacing between the peaks is maintained but the intensity pattern can be randomly enhanced or reduced depending on the location of the inclusions within the droplet volume. The sensitivity of this method for the detection of inclusion within a particle was measured by their concentration. The absolute number of inclusions and their size were shown to be irrelevant in the determination of the lower detection limit.[190] The phase function for droplets within a concentration gradient or core-shell structure

is characterized by a repetitive fluctuation in the intensity of the peaks due to the presence of a secondary structure, this time, showing a pattern within the variation in the intensity. Finally, non-spherical or crystalline particles report a highly irregular phase function over time which makes the determination of the particle size near impossible, although the sphere-equivalent size can be inferred from the size and solute concentration of the initial droplet. Fig. (2-4) shows the primary phase functions patterns used to infer the droplets morphology. The ability to detect different morphologies on an individual bioaerosol droplet allows studies of the impact of particle phase and structure on microbial viability.

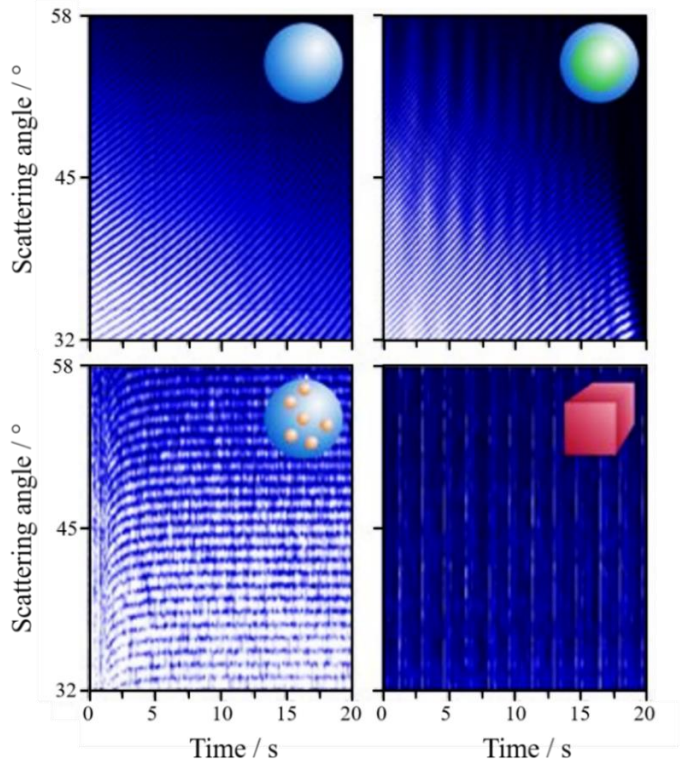

Figure 2-4. Cumulative phase functions over ~20s for single particles with a) homogenous, b) core-shell, c) inclusions and d) non-spherical morphologies. Each cumulative phase function consists of ~2,000 individual phase functions.

2.2.1.5 Estimating Surface Enrichment

The Peclet number (*Pe*) associated with an evaporation rate can be used to assess the likelihood of a surface enrichment in solutes, or microbes, developing during evaporation, providing insight into the different final particle morphologies that form.[204] When the drying rate (inferred from the rate of retraction in the droplet surface boundary) surpasses the diffusional

mixing rate of the microbe (*Pe*>>1), the homogenous composition through the evaporation process is lost leading to a surface enrichment of the droplet with microbes. The diffusion coefficient, D, of E. *coli* bacteria cells was reported in the literature to be 1.2×10^{-12} m^2 s^{-1}.[205] Calculations of the corresponding Peclet numbers were obtained using Eq. (2-9).

$$Pe = \frac{k}{8D} \quad \textbf{(2-9)}$$

The evaporation rate, *k*, is estimated using Eq. (2-10) as the change in surface area over time.[204] In this work, *k* was estimated using a model prediction of the changing diameter (*d(t)*) of an evaporating droplet injected into an airflow of a given RH: [200]

$$k = -\frac{d(d^2)}{dt} \quad \textbf{(2-10)}$$

Thus, combining the information from the evaporation rates with the diffusion coefficient of *E. coli* cells, it was possible to determine the Peclet number and estimate likelihood of surface enrichment of *E. coli* on the particles as a function of the RH. Surface enrichment can be verified offline through SEM analysis of evaporated and collected particles.

2.2.2 Levitation and Sampling Methodology for Biophysical Characterisation of Bioaerosols: The CELEBS Instrument

The ability to determine the biological decay of bioaerosols as a function of time, atmospheric conditions and chemical and biological composition has been recently developed.[68] The CELEBS apparatus is an adaptation of the double-ring electrodynamic trap[182] with important modifications that enable the generation, levitation and sampling of populations of bioaerosol droplets while minimizing the stresses associated with these processes when using conventional techniques for bioaerosol studies.[115,206] All components are enclosed in a 3D printed chamber to avoid the disturbance of the levitated particles in a conditioned environment. CELEBS utilizes the same method of bioaerosol generation used in the CK-EDB with the difference that a population of droplets is generated and levitated in this case. A high-

voltage induction electrode induces a small net charge in each particle allowing the population of droplets to be trapped in the electrodynamic field generated by applying an AC voltage (1000-2700V) to the two parallel ring electrodes located in the centre of the chamber. The like net charge on all particles prevents coalescence among the population of droplets. The particles are confined in a directed flow from a gas inlet, which enables the control of the atmospheric conditions (i.e temperature, RH, gas, etc) inside the chamber. A 580 nm LED light illuminates the population of droplets allowing particle enumeration by using a LabView program developed in-house. A probe connected to the gas inlet registers the % RH and temperature that the droplets are exposed to.

After the desired levitation period, the sampling area and the EDT are connected by removing the safety plate. The particles are extracted from the EDT onto the substrate holder in a smooth fashion by gradually reducing the amplitude of the waveform applied to the electrodes. The CELEBS instrument provides a 100% efficiency in the collection of the levitated particles utilizing similar sampling velocities to the ones used with electrostatic precipitators,[207] consequently reducing the stresses associated with conventional bioaerosol samplers such as impingers.[151,179] Besides, this methodology presents the possibility to probe viability/infectivity when deposited on any type of substrate (i.e lung cells, microbiological media, ATP assays, etc). In this work, the bioaerosol was sampled onto Petri dishes containing a ~3mm layer of LB agar and 300 µL volume of LB broth located in the centre of the plate. Finally, the Petri dishes were removed from the instrument, the LB broth containing the sampled bioaerosol was spread over the agar surface and the plates were incubated during 24h at 37°C. The approach used to calculate the survival of bioaerosol was previously described[68] and is also explained in Section 2.2.2.3.

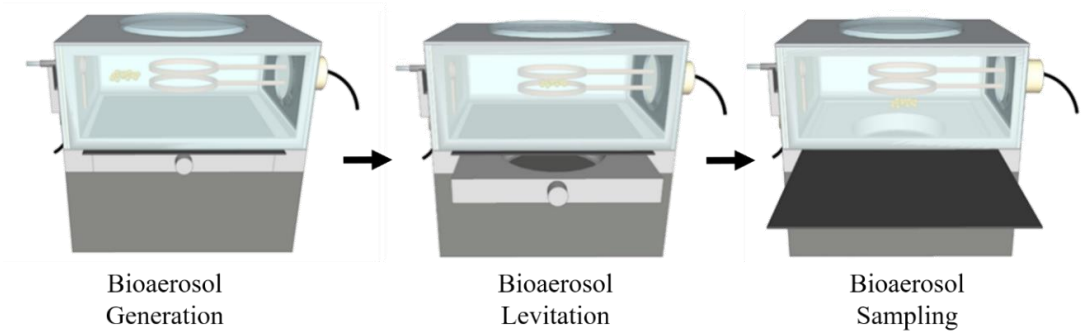

Figure 2-5. Schematic describing the processes involved in the determination of survival decay with the CELEBS system.

2.2.2.1 Development of the CELEBS Methodology

The entire instrument, including the chamber that encases the EDT, the LED light, the DoD dispenser for bioaerosol generation, the CCD camera and the substrate holder for bioaerosol sampling, resides on a small square plate. Its compact design provides high portability across biosafety cabinets.

From the beginning of this research, the design of the system underwent significant modifications to improve the systematization, accuracy and reproducibility of the experiments (Figure 2-6), common challenges encountered in method development projects.

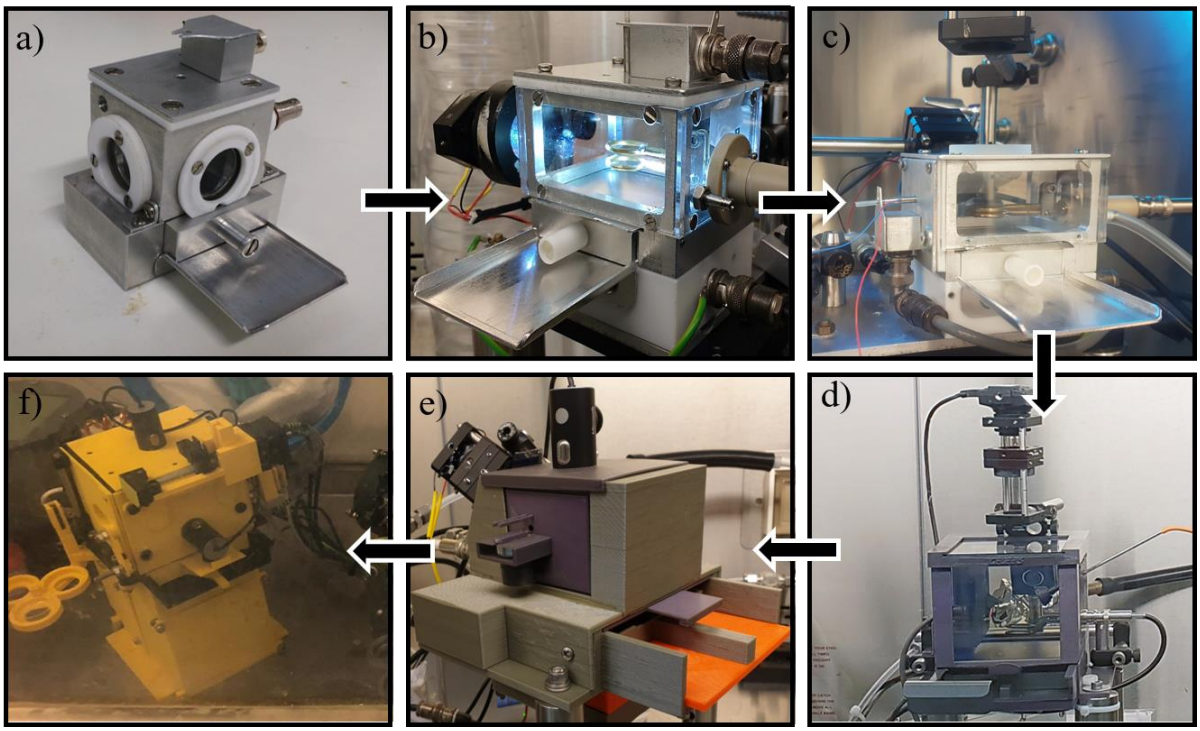

Figure 2-6. Evolution of CELEBS systems during the PhD.

Figure 2-6 shows the evolution of the CELEBS instrument throughout the work described in this thesis. The main breakthroughs in the development of the system include:

- The introduction of the safety plate between the EDT and the substrate holder (modification implemented between Figure 2-6a and Figure 2-6b), ensuring that only the particles levitated are sampled (i.e. avoiding other generated particles, which were not trapped, immediately depositing in the collection media).
- The removal of a ground bottom electrode used to pull the droplets to the centre of the substrate (modification implemented between Figure 2-6a and Figure 2-6b). However, this element raised various issues. Therefore, the sampling process is now controlled by lowering the amplitude of the waveform applied to the ring electrodes, causing the particles to fall onto the substrate.
- The addition of a CCD camera for top-down imaging of the EDT which facilitates the enumeration of the population of bioaerosol droplets throughout an opening in the top wall of the chamber. This feature allows more rapid measurements by avoiding the

manual enumeration of the particles (modification implemented between Figure 2-6b and Figure 2-6c).

- A change in the location of the DoD dispenser from the top wall of the chamber to one sidewall (modification implemented between Figure 2-6b and Figure 2-6c), avoiding the sedimentation of bacteria cells in the DoD reservoir (Figure 2-7). When generated from above, a concentration gradient of bacterial cells within the DOD reservoir developed over time which affected the survival data by reducing the reproducibility of the composition of the droplets and producing clogging problems in the DoD device.
- An increase in the optically open design of the device was introduced to better facilitate the enumeration of the aerosol droplets and ensure the deposition of the particles onto the substrate (modification implemented between Figure 2-6a and Figure 2-6b). In the latest prototypes, the open glass design of the chamber was replaced by an encased plastic chamber (modification implemented between Figure 2-6d and Figure 2-6e). This later modification allowed the collection of sharper images from the CCD camera by avoiding light scattering on the glass walls. To ensure the deposition of the particles, a second CCD camera was positioned sidewise (see both CCD cameras on Figure 2-6f) above the safety plate.

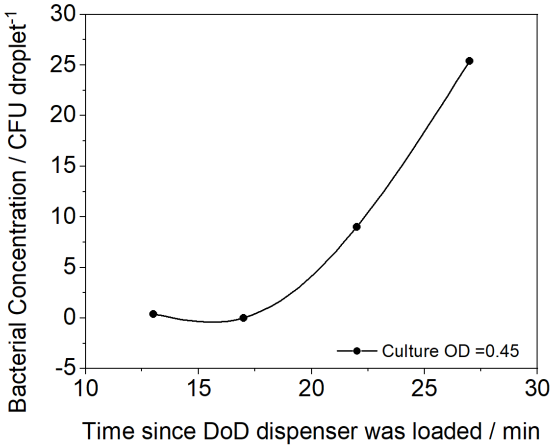

Figure 2-7. Concentration gradient inside DoD due to bacteria sedimentation. Line is to guide the eye.

One of the most recent designs of the CELEBS chamber is shown in Figure 2-8, including a close-up of the main device components and an image from the enumerating CCD camera. This prototype, built-in 2017, already incorporates the main improvements in the development of the instrument. From 2018 onwards, the systems have been built in PLA filament plastic by using a 3D printer instead of the more conventional metal fabrication. This has allowed more rapid response to the growing needs for both the users and the work environments while maintaining a low economic impact on the project. Especially, when performing work under containment, which has created the need of incorporating many new features in a short period of time.

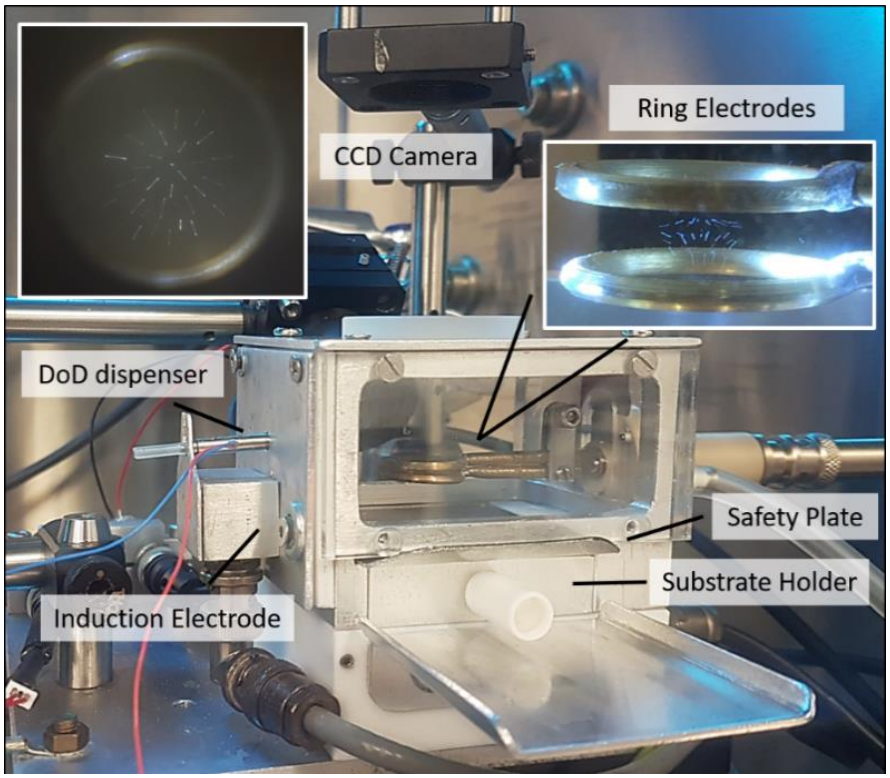

Figure 2-8. CELEBS prototype with a close-up of the device main components.

Other steps in the development of the methodology (e.g harvest technique, sample preparation and off-line viability assessment) were also improved to establish a robust and reproducible technique. For instance, the culture technique was optimized by introducing shaker rotation at 180 rpm while harvesting the bacterial culture, enhancing the availability of oxygen. An increase in the volume of the flask used for cell culturing was included to prevent bacterial

clumps. Finally, the use of glycerol stocks and consistent inoculum concentrations avoid culture contamination and plasmid mutations. A comparison between the initial culturing technique and the improved version is shown in Figure 2-9. The influence of these factors was observed in the growth speed of the bacterial culture (i.e. reaching the stationary phase faster with the new method) and the cell concentration achieved in the stationary phase of growth (i.e. being higher and steadier). Consequently, the optimization of growth conditions led to healthier and more consistent bacterial cultures which achieved higher survival and more consistent results.

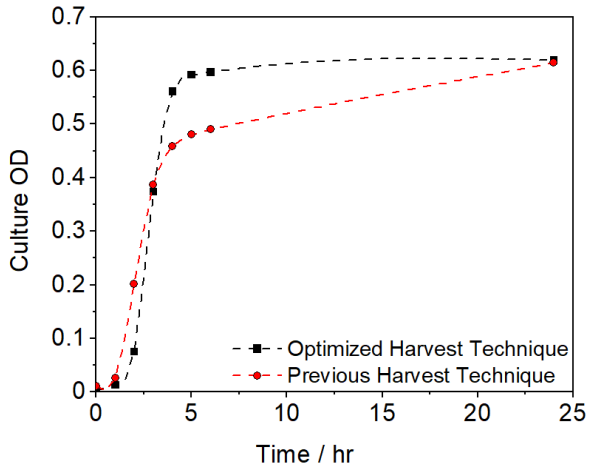

Figure 2-9. Optimization of culture technique and its effect on bacterial growth. Each data point represents a single measurement Optical Density (OD) of the culture. Lines are included as guidance.

In conclusion, the optimal conditions for each step of the methodology were determined and a complete methodology was implemented.

2.2.2.2 Offline Viability Assessment

For the determination of viability, the method developed has been slightly modified during the course of the work described here.

Initially, the population of bioaerosol droplets was collected onto a plastic 35mm Petri dish containing 1 mL of liquid LB broth. Bacterial aggregation was reduced by vigorous pipetting before solidifying the suspension by adding 4 mL of LB agar at a temperature below 45°C to

avoid bacterial inactivation. The mixture of bioaerosol particles, LB broth and LB agar was stirred to ensure blending and solidification. This method enabled the enumeration of colony-forming units (CFU) in the same Petri dish where the bioaerosol sample was collected, without the added risk of transferring to a separate plating media. Plates were air-dried before incubation for 24 h at 37°C. The number of colonies which develop were taken as a measure of the number of viable cells (colony-forming unit, CFU) after specific aerosol suspension times, enabling calculation of the bioaerosol survival. However, this technique presented some limitations related to the suitable solidification of the plates: the formation of a cloudy layer on the agar on some occasions led to non-countable numbers of CFU on the agar.

Therefore, the enumeration method was subsequently changed and the bioaerosol sampling is now performed into a petri dish containing a thin layer (>3 mm) of agar and 300 µL of LB broth positioned in the centre of the plate. The substrate holder is then removed from the EDT chamber and the 300 µL of LB broth containing the bioaerosol particles was gently spread along the agar surface by using an L-shaped spreader. The Petri dishes were then incubated at 37ºC for 24 hrs in a static incubator.

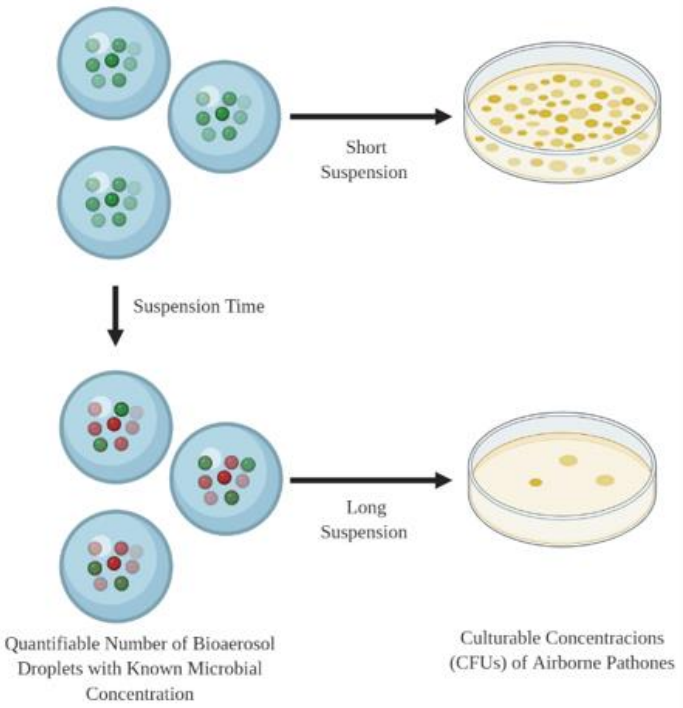

Figure 2-10. Schematic notation of the determination of biological decay in *E. coli* MRE-162 with the CELEBS system.

Figure 2-10 shows a schematic diagram of the off-line viability assessment used in this work to assess biological decay, presenting the relationship between the concentrations of viable bacteria within the droplets over time spent in the aerosol phase. Decline in culturability due to the time spent in the aerosol phase can be determined by comparing recoverable CFU in bioaerosol harvested immediately after production (control-short suspension) and after specific times in aerosol suspension (test-long suspension).

2.2.2.3 Quantitative Characterisation of Survival

Survival in the aerosol phase as a function of time are usually represented by the loss of culturability. [68] Thus, loss of viability of airborne pathogens is represented as a reduction in their ability to form CFU on plating media as a function of time in the aerosol phase by using the following equation:

$$\%\ \text{Survival} = \frac{C_{culturable}(TEST)}{C_{culturable}(CONTROL)} \times 100 \qquad \textbf{(2-11)}$$

$C_{culturable}$ *(TEST)* is the number of CFU obtained after the incubation of the bioaerosol population that was levitated for a set time interval. This measurement is normalized by using a $C_{culturable}$ *(CONTROL)* measurement to facilitate data comparison. Two options are valid as control measurements: one is the absolute number of bacteria cells contained in the droplets calculated from the correlation with the bacterial concentration introduced in the DoD. The second option is the number of culturable cells (CFU /droplet) obtained after a levitation time under 7 s in a preceding measurement. In this case, the levitation period is too brief to impact the viability of the microorganisms and therefore is considered as a non-exposure measurement. The validation of this assumption has been confirmed by comparing a series of CFU/droplet obtained after 5 s "harmless" levitations with the original CFU/droplet estimated by using the concentration of the cell suspension pipetted in the DoD (this comparison will be fully evaluated in Section 3.4.1Figure 3-8).[68]

2.2.3 Overview of Techniques

In this section, a brief overview of the parameters under control during the performance of experiments is presented together with the attainable properties to determine with both techniques (Table 2-1).

Table 2-1. Summary of the parameters controlled during experiments and determinable properties with both the CK-EDB and CELEBS systems.

Controlled Variables	**CELEBS**	**CK-EDB**
Initial droplet size	✓	✓
Temperature	✓	✓
Relative Humidity	✓	✓
Microbial Load	✓	✓
Number of Droplets	✓	✓
Levitation Time	✓	✓
Measurable or Inferred Properties	**CELEBS**	**CK-EDB**
Size Changes		✓
Inferred Droplet Temperature		✓
Inferred Hygroscopicity		✓
Inferred particle morphology	✓	✓
Biological Decay	✓	
Viability / Infectivity	✓	

Figure 2-11 shows images of both set-ups highlighting the main components for the CELEBS system(Figure 2-11a, b and c) and the CK-EDB (Figure 2-11d, e and f).

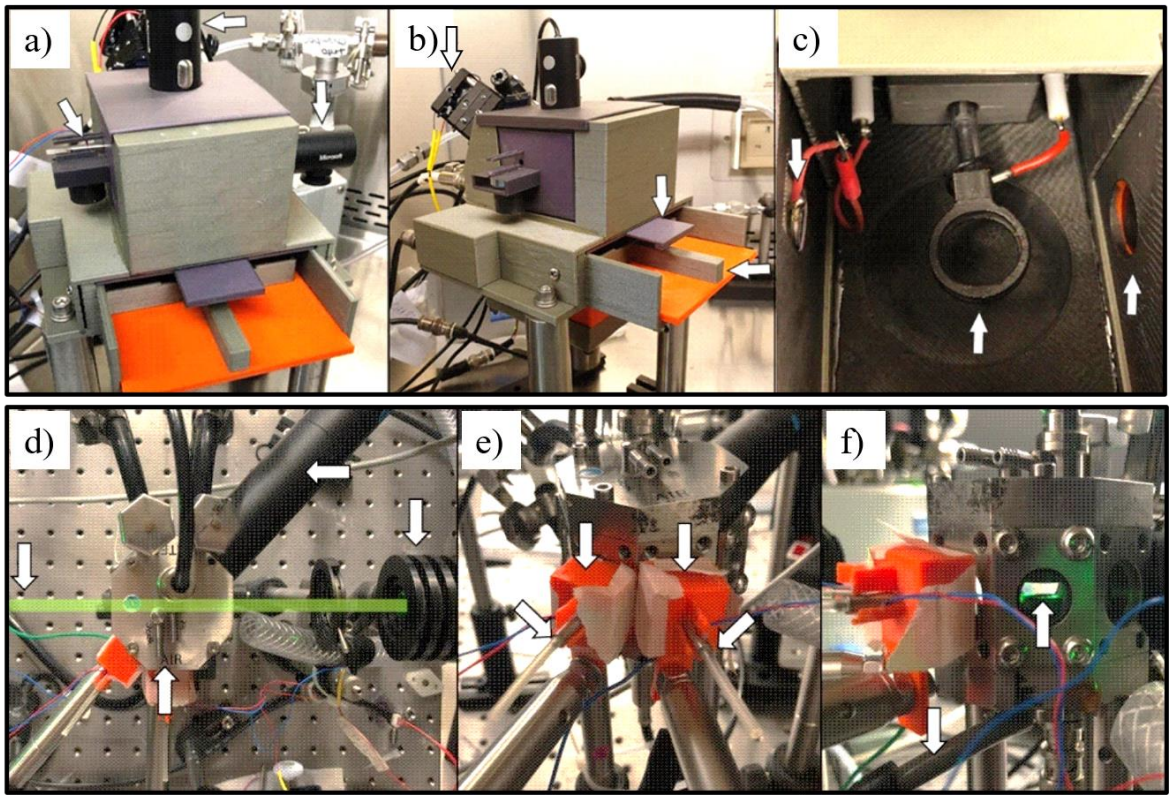

Figure 2-11. Images of the 3D printed CELEBS prototype located in the biosafety cabinet. From left to right, arrows point: (a) DoD, top CCD camera and sidewise CCD camera; (b) L.E.D. light, safety plate and substrate holder; (c) induction electrode, EDT and aperture for the sidewise CCD camera. Images of the CK-EDB. From left to right, arrows point: (d) Laser beam path, trap chamber, CCD camera and laser blocker, (e) DoD (sample), Induction electrode (sample), DoD (probe) and induction electrode (probe) and (f) gas inlet and concentric cylindric electrodes in the centre of the trap chamber.

2.2.4 Generic Materials and Methods for Bioaerosol Survival Studies

2.2.4.1 Microbiological Media

The Luria-Bertani (LB) broth was prepared by dissolving 5 g of yeast extract (Sigma-Aldrich Ltd., UK), 10 g of NaCl (Fisher Scientific, UK) and 10 g of Tryptone (VWR International Ltd, UK) in 1000 mL of sterilized deionized (DI) water and then sterilizing the mixture in an autoclave (Classic, Prestige Medical, UK). Luria agar was prepared by adding 20g L^{-1} of Granulated Agar (BD Difco™ Dehydrated Culture Media, Fisher Scientific, UK) to the previous mixture before sterilization.

The Luria agar was prepared by adding 20 g L^{-1} of Granulated Agar (BD Difco™ Dehydrated Culture Media, Fisher Scientific, UK) to the LB broth solution before autoclaving.

The Phosphate Buffered Saline (PBS) was prepared by dissolving 1 tablet of PBS (Dulbecco A, Thermo Scientific Oxoid, UK) in 100 mL of distilled water and then sterilizing the solution by autoclaving. The formula contains 8 g $L^{-1}$of sodium chloride, 0.2 g $L^{-1}$of potassium chloride, 1.15 g $L^{-1}$of di-sodium hydrogen phosphate and 0.2 g L^{-1} of potassium dihydrogen phosphate. Thus, the mass of solute for PBS is 9.506 g.

The artificial saliva and artificial sputum media were prepared from a ready-to-go powder obtained from the Defence Science & Technology Laboratories (Dstl, Porton Down, Salisbury, United Kingdom) whose compositions are presented in Table 2-2 and Table 2-3, respectively. Both artificial secretions have been reported in the literature as surrogates for *in vitro* simulation studies. [208–210] Specifically, 6.79 g of the artificial saliva powder and 170.36 g of the artificial sputum powder were dissolved in 100 mL of deionized water. From these neat solutions, the 1:10 dilutions for both artificial sputum and saliva were prepared.

Table 2-2. List of components for the artificial saliva media . [209]

Chemical Species	Mol. Wt	Concn (g per 100 mL)
$MgCl_2$	203.21	0.004
$CaCl_2.H_2O$	110.99	0.013
$NaHCO_3$	84.006	0.042
0.2M KH_2PO_4	136.09	2.7218
0.2M K_2HPO_4	174.2	3.484
NH_4Cl	53.49	0.011
KSCN	97.18	0.019
$(NH2)_2CO$	60.06	0.012
NaCl	58.44	0.088
KCl	74.55	0.104
Mucin	N/A	0.3
DMEM	N/A	0.1 mL

Table 2-3. List of components for the artificial sputum media . [208]

Chemical Species	Mol. Wt	Concn (g per 100 mL)
DNA (fish sperm)	N/A	0.4
Mucin	N/A	0.5
L-tyrosine	181.19	0.025
L-cysteine	121.16	0.025
L-alanine	89.09	0.025
L-arginine	174.2	0.025
L-aspartic acid	133.1	0.025
L-glutamic acid	147.1	0.025
L-glutamine	146.1	0.025
L-glycine	75.07	0.025
L-histidine	155.2	0.025
L-isoleucine	131.2	0.025
L-leucine	131.2	0.025
L-lysine.HCl	182.6	0.025
L-methionine	149.2	0.025
L-phenylalanine	165.19	0.025
L-proline	115.1	0.025
L-serine	105.1	0.025
L-threonine	119.1	0.025
L-tryptophan	204.23	0.025
L-ornithine	168.62	0.025
L-valine	117.1	0.025
DTPA	393.55	0.0059
NaCl	58.44	0.5
KCl	74.55	0.22

For the preparation of artificial saliva media containing different concentration of mucin, the mucin powder was added on top of the standard artificial saliva composition. Thus, mucin concentrations of 0.3, 0.5 and 2.5 % w/v in artificial saliva aim to simulate the mucin concentrations in artificial saliva, artificial sputum, and infected artificial sputum, respectively.

2.2.4.2 Bacteria Strains and Cell Culturing

The microorganisms used to evaluate this methodology were *Bacillus atrophaeus* spores and *E. coli* MRE-162. Both strains were kind donations from the in-house culture collection at the Defence Science & Technology Laboratories (Dstl, Porton Down, Salisbury, United Kingdom).

The *B. atrophaeus* stocks in water with a microbial concentration of $6.5 \pm 0.3 \times 10^9$ spores mL^{-1} (triple washed in distilled water).

Stock cultures of *E. coli* MRE-162 with a microbial concentration of $1.4 \pm 0.2 \times 10^9$ (mean ± standard deviation) CFU mL^{-1} were maintained at -20℃ in LB broth containing 20% (w/w) glycerol. Routinely, 200 mL of LB broth was inoculated with 2 μL of *E. coli* MRE-162 stock and cultured at 180 rpm and 37℃ for ~24 h until reaching the stationary phase, producing a concentration of $2.7 \pm 1.7 \times 10^9$ CFU mL^{-1}. Figure 2-12 shows the growth curve for *E. coli* MRE162 over 50h of harvesting.

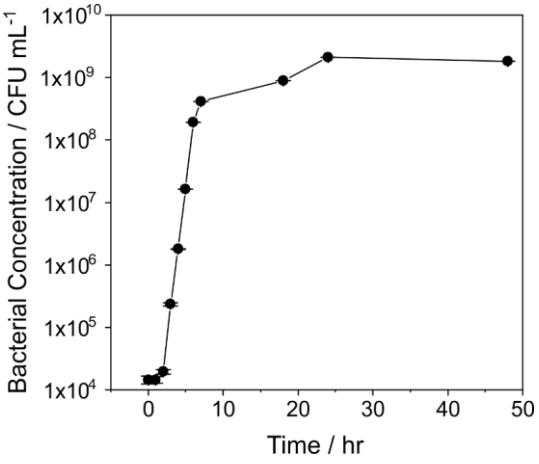

Figure 2-12. Growth curve for *E. coli* MRE-162 showing the different phases of growth: log, exponential, stationary and death phases.

Finally, culture enumeration after 24 h was performed before aerosol experiments by using a serial dilution and plating on agar plates, producing concentrations of $(2.6\pm0.6)\times10^{9}$ CFU mL^{-1}. The number of CFU per droplet estimated from the culture enumeration was used to normalise the survival data as explained in Section 2.2.2.3.

2.2.4.3 Sample Preparation for Determination of Aerosol Dynamics, Aerosol Particle Morphology and Bioaerosol Decay

To perform the viability studies, a *B. atrophaeus* stock culture with a microbial concentration of $6.5 \pm 0.3 \times 10^{9}$ spores mL^{-1} (triple washed in distilled water) was prepared for aerosolization by diluting 50 μL of original water stock in 450 μL of Phosphate-Buffered Saline (PBS). The original LB broth bacterial cultures in stationary phase were used to prepare ten-fold serial dilutions in LB broth and PBS solutions, giving a bacterial concentration of $(2.6\pm0.6) \times10^{8}$ CFU mL^{-1} (28 ± 11 CFU $droplet^{-1}$). For survival experiments with LB broth bacteria solutions, 100 μL from the original culture were directly transferred into 900 μL of non-metabolized LB broth. In the case of PBS bacteria solutions, 1 mL of the original LB broth bacteria culture was centrifuged and resuspended in 1 mL of autoclaved PBS solution, then 100 μL were transferred into 900 μL of the same autoclaved PBS solution. For survival measurements in artificial respiratory secretions, 1 mL of the original culture was resuspended in the specific artificial fluid (artificial saliva, diluted saliva, artificial sputum and diluted sputum) and finally a 10-fold dilution was prepared in the same solution. All samples were vortexed for 10 s before being introduced in the DoD to ensure homogenization.

For hygroscopicity measurements, non-metabolised and metabolized LB broth and also PBS solutions with concentrations of 25, 23 and 9.506 g L^{-1} were diluted to 1% w/w solute in water for evaporation measurements. In the case of spent LB broth, 1 mL of the supernatant of the centrifuged culture was dried out in an oven for 24 hours and the dry weight of solute was measured, obtaining 23 g L^{-1}. In the case of the artificial respiratory secretions, dilutions of 1 and 5% w/w solute and 1 and 2% w/w solute in water were prepared for the hygroscopicity measurements for artificial saliva and artificial sputum, respectively. See Sections 4.2 and 5.2.1 for results and discussion.

For the studies with LB broth bacteria solutions containing surfactants, LB broth solutions were saturated by adding 0.0203 g of heptadecanol (Acros Organics, Fisher Scientific, UK), 0.0100 g of 1,2-dypalmitoyl-rac-glycero-3-phosphocholine (DPPC) (Insight Biotechnology, UK) and 1.5363 g of Tween80 (Acros Organics, Fisher Scientific, UK) to 10 mL, 3 mL and 10 mL of autoclaved LB broth, respectively. Then, the maximum amount of surfactant was dissolved by vortexing the samples for 2 minutes, sonicating for 15 minutes and filtering by using 0.22 μm pore size sterilized filters (JET Biofil, UK). For measurements of evaporation kinetics (Figure 5-14), particle morphology (Figure 5-15) and survival (Figure 5-14d), 1 mL of the original LB broth bacteria culture was centrifuged and resuspended in 1 mL of the corresponding LB broth surfactant solution. For the dynamic measurements with the water solutions saturated with surfactants (Figure 5-17), samples were prepared by saturating 5 mL of DI water samples with the different surfactants followed by vortexing, sonicating and filtering as previously described for the saturated LB broth solutions.

To study the impact of droplet size (Figure 4-8), 1 mL of the original bacteria culture was resuspended in 1 mL of LB broth with the concentration of interest (50, 25 and 12.5 g L^{-1}). Then, the serial dilution was performed in 900 μL of the corresponding LB broth concentration.

To investigate the effect of mucin impacting airborne bacterial viability (Figure 5-10), three different solutions were prepared by adding different amounts of mucin to the standard saliva composition (Table 2-2). The chosen proportions of mucin on the artificial saliva solutions represent the mass fractions of mucin in standard artificial saliva (0.3%), artificial sputum (0.5%) and artificial sputum with higher mucin concentration representative of infection (2.5%). The composition of these artificial respiratory fluids (e.g. artificial saliva, artificial sputum and infected artificial sputum) were obtained from the literature[208–210] and are detailed in Section 2.2.4.1.

Bacterial suspensions to evaluate the effect of cell physiology on airborne survival (Figure 5-6) were prepared by harvesting *E. coli* MRE-162 for 6, 24 and 48 h. Besides, before the aerosol generation, all bacterial suspensions were adjusted to an OD of 0.5 with freshly autoclaved LB broth.

To determine the impact of microbial load in aerosol dynamics, airborne bacterial survival and particle morphology (Figure 5-20 and Figure 5-16), a serial dilution to 10^6 CFU mL^{-1} was

prepared from the original LB broth bacteria culture which presented a concentration in the order of 10^9 CFU mL^{-1}. To prepare the bacteria suspension at a concentration of 10^{10} CFU mL^{-1}, 5 mL of the original bacteria culture in different tubes were centrifuged, the supernatant was removed and the bacterial pellets were resuspended in 200 mL of autoclaved LB broth. Finally, the five bacterial suspensions were transferred to the same vial before aerosolization.

2.2.5 Confocal Microscopic Analysis of Bioaerosols

Bulk suspensions containing three types of particles (i.e. fluorescent beads, 1 mm diameter; *E. coli* MRE612; *B. atrophaeus* spores) at specific concentration ranges were aerosolized by means of a DoD microdispenser. The generated aerosol droplets were collected on gelatine-coated microscope slides for microscopy visualization. All samples were analyzed with a dual-mode (confocal/widefield) imaging system at the Wolfson Bioimaging Facility, University of Bristol (SPE single-channel confocal laser scanning microscope attached to a DMi8 inverted epifluorescence microscope, Leica Microsystems, Germany). Fluorescent samples were excited by the 488nm-spectral line and detected using the green and red channels (590nm LP, 425nm LP). ImageJ software [211] was used to process all images acquired with the confocal/widefield system for both the determination of bacterial viability (proportions of cells exhibiting green fluorescence) after aerosolization and the enumeration of particles encapsulated within the aerosol droplets.

2.2.6 Scanning Electron Microscopy (SEM) Analysis of Bioaerosols

Bioaerosol droplets containing *E. coli* MRE-162 cells at a concentration of 10^9 cell mL^{-1} in water, LB broth and Phosphate buffered saline (PBS) (Figure 2-13), and at a concentration of 10^8 cell mL^{-1} in artificial saliva and artificial sputum, were levitated for 120 s under 10, 30 and 50% RH in the CELEBS apparatus and subsequently sampled on an empty Petri dish containing one polycarbonate filter paper (Whatman® Nucleopore™, 25mm, Sigma-Aldrich, UK). The filters containing the bioaerosol particles were coated with high-purity silver (High-Resolution Sputter Coater, Agar Scientific, UK) to a thickness of approximately 15 nm. A scanning electron microscope (SEM, JSM-IT-300 from JEOL, Japan), with an acceleration

voltage of 15 kV and 10- and 15-mm working distances was used to visualize the bioaerosol particles.

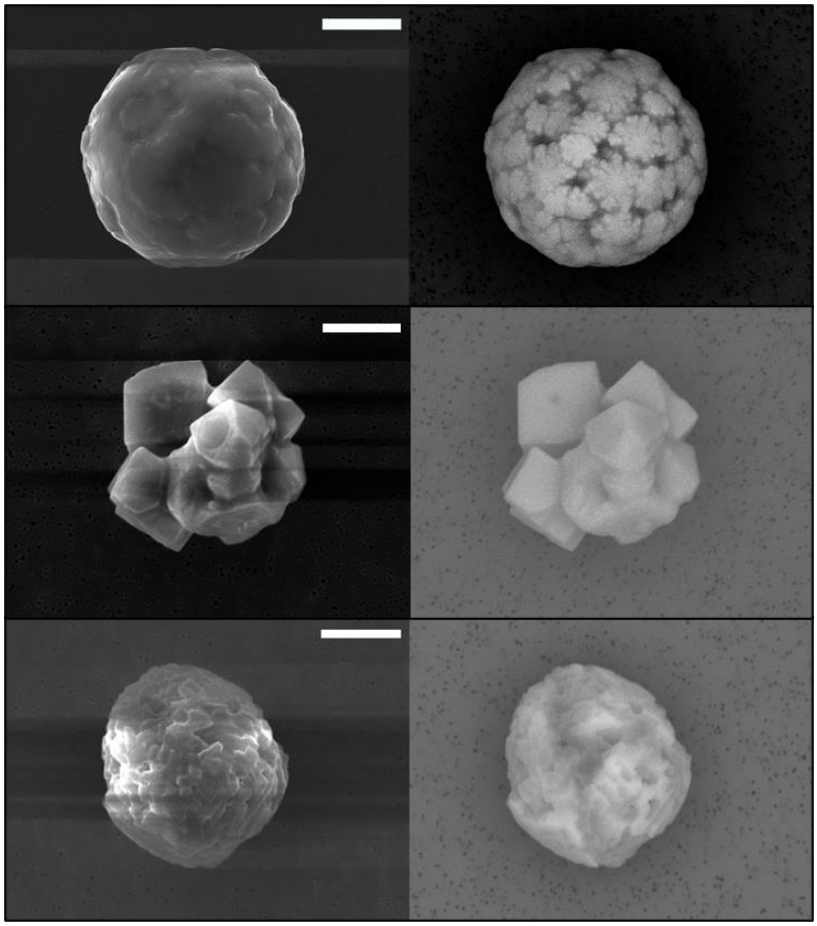

Figure 2-13. An example of SEM and backscattered images of levitated droplets at 30%RH whose composition is a) pure LB broth c) pure PBS and d) *E. coli* MRE-162 cells at a concentration of ~10^9 CFU mL^{-1} in PBS. Scale bars represent 5 μm.

2.3 Summary

The development of the TAMBAS approach as a tool for combining studies on aerosol dynamics and airborne microbial survival has been presented in this chapter. The general principles, instruments operation and interpretation of the experimental data have been described. The methodology described in this chapter sets the foundation for the experimental work performed in the proceeding chapters.

Chapter 3

Developing a Next-Generation Electrodynamic Balance Technique to Assess the Survival of Airborne Pathogens

The content of this chapter is based on a publication, entitled "Assessing the Airborne Survival of Bacteria in Populations of Aerosol Droplets with a Novel Technology", for which I am the first author.[68] *The manuscript was featured on the January 2019 cover of the Journal of the Royal Society Interface (issue 150). The work involved in this publication was reviewed by more than 15 different websites worldwide including Healthline Networks and ScienceDaily as well as aired in the BBC Radio4 Inside Science programme (https://tinyurl.com/u97rf6o). I confirm that the published work is all my own and I performed all data collection, analysis and manuscript writing. I acknowledge Richard J. Thomas from DSTL for providing bimestrial support throughout a collaborative scholarship. I also acknowledge Jonathan P. Reid, Richard J. Thomas and Allen E. Haddrell for contributing to the editing of the manuscript for publication and the design of the study, without their support the results in the manuscript may have not come to be. Finally, I acknowledge Natalie J. Garton and Andrew Hudson from the University of Leicester who provided me with training in basic microbiological techniques.*

Having developed a methodology to study bioaerosols from a physicochemical and biological perspective, chapter 3 focuses on the validation of the novel CELEBS instrument to enable studies of bioaerosol survival as a function of atmospheric conditions and particle compositions to identify the factors that may affect the survival of pathogens. The characterisation of each step of the methodology (generation, levitation and sampling) will demonstrate that CELEBS presents an alternative approach to elucidate the fundamentals of airborne disease dynamics by implementing unique features and several benefits to existing technologies.

3.1 Introduction

Bioaerosols have been studied since the late nineteenth century to determine the sources of epidemic diseases. Interest in bioaerosol has increased in recent decades due in part to a high number of airborne disease outbreaks and concern about the potential roles that airborne microorganisms play in atmospheric processes.[19,212] The multitude of adverse health effects derived from human exposure to bioaerosols particles are not yet fully understood despite their impact in public health and national defence.[213,214] This is mainly due to the present limitations in the current techniques used for bioaerosol studies for exploring aspects of atmospheric transport.[215]

Viability has already been shown to be influenced by aerosol particle size, the presence of air pollutants, solar radiation, ambient temperature and environmental relative humidity, as described in Section 1.4.3 and summarized in Figure 3-1.[17,67] During atmospheric transport, bioaerosol droplets undergo a series of evaporative and rehydration processes which result in changes in their metabolism and physiology. The conditions of atmospheric transport cannot be simulated under bulk conditions in bacterial cultures as aerosol droplets may exist in a state of metastable solute supersaturation not accessible in the bulk phase. [216,217] Further, chemical reaction rates in the aerosol phase can be several orders of magnitude higher than in the bulk state.[126,127,218] It is, therefore, more than conceivable that the microbial physiology is quite different in the aerosol phase (Section 1.4.3). Thus, a “bottom-up” approach to measuring the role of atmospheric process on bioaerosol survival is key to improving the representation of these processes in the true aerosol state extending from the individual cell to the population scale. Understanding the interplay of all the processes that determine microbial responses is key to develop more accurate predictive models of infection transmission and control strategies.

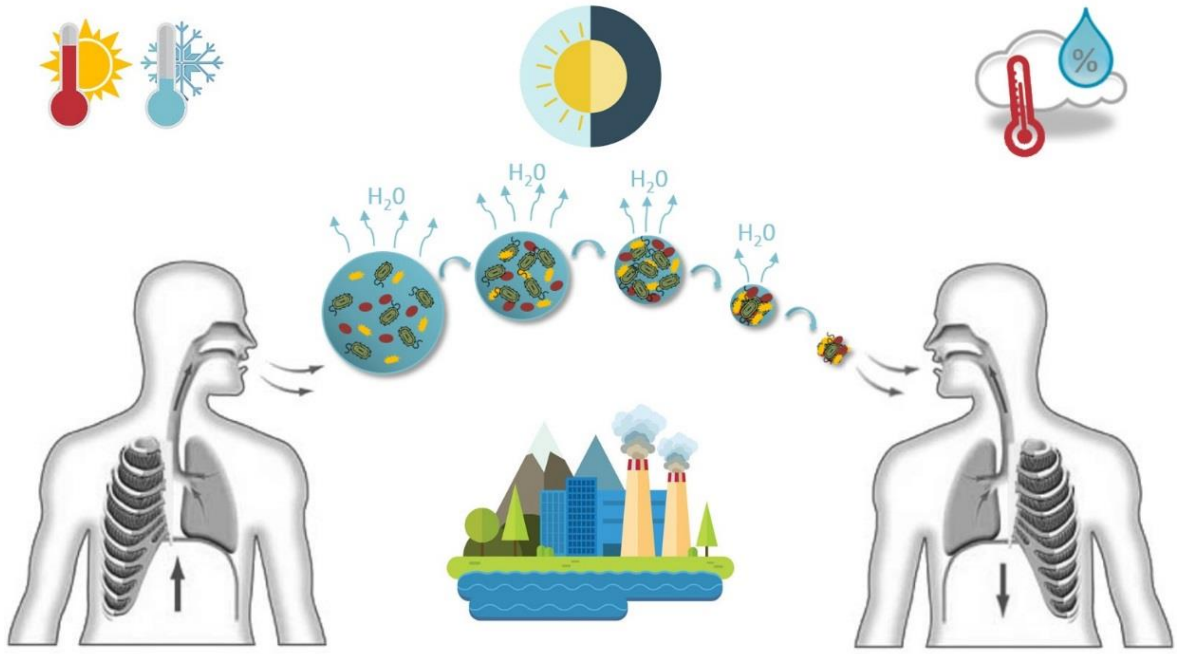

Figure 3-1. Representation of the key areas explored in this thesis , showing the interplay between biological aerosols and atmospheric factors during aerosol transport. Examples of factors include environmental conditions such as the temperature and relative humidity, day and night-time atmospheric chemistry, bioaerosol composition and mixing with anthropogenic and other natural aerosols found in the atmosphere.

Historically, the study of bioaerosol survival *in vitro* has been limited to two main different methodologies: the rotating drum and the use of microthreads. The rotating drum, referred to as an environmental chamber, is the most established approach, based on the aerosol chamber developed by Goldberg *et al.* in 1958.[219] These systems have been used to generate survival decay rates for bacteria and viruses by suspending the bioaerosol using centrifugal forces to counteract gravity.[80,171,172,220,221] Several improvements have allowed the levitation of particles larger than 1-2 μm in diameter for longer suspension periods under a wider range of environmental parameters.[7,19] However, limitations in the suspension times and particle sizes persist due to the gravitational deposition of particles on the walls of the vessel. For instance, the suspension of particles more representative of initial droplet sizes (~360 μm-diameter) produced during coughing and sneezing is difficult in these systems.[222] In the case of microthread techniques, the presence of turbulence can result in a loss of particles on the surfaces of the instrument and antimicrobial compounds on the spider silk can result in a reduction in viability.[110,223] Further disadvantages of these techniques are the stresses to which

the bacteria are subjected during aerosol generation and sampling. Nebulization is typically the preferred method for aerosol generation, but this technique has been proven to cause loss of culturability in some bacterial species[130,132,140] and structural damage.[110,115,137,224] These techniques also lead to polydisperse aerosol droplets, subjecting the contained microorganisms to different surface-to-volume ratios at equilibrium size and potentially produces different biological responses. Hence, the reported results reflect the average behaviour encompassing a range of initial droplet sizes. Finally, the sampling methods used with these techniques involve the use of prolonged sampling periods (i.e. combination of loading, mixing and extraction times) and high collection velocities, a proven cause of reduced viability.[151,158,159,225]

The aim of this work is to adapt an electrodynamic trap (EDT) [226] into a next-generation tool for investigating the decay dynamics of bioaerosols. Utilizing this approach minimizes generation and sampling stresses and reduces the influence of droplet polydispersity. Environmental conditions are readily controlled and timescales of bacteria in the aerosol phase are accurately known and can be varied from seconds to days. Firstly, the new technique is introduced, referred to as Controlled Electrodynamic Levitation and Extraction of Bioaerosol onto a Substrate (CELEBS), before presenting measurements for the validation of each step of the methodology and finalising with contrasting data of the viability of *E. coli* MRE-162 cells and *B. atrophaeus* spores. The results presented in this chapter were obtained during the development of the methodology and represent an indicator of how this technology could be applied in bioaerosol studies to answer some of the fundamental questions regarding the dynamics of bacteria and viruses in the aerosol phase.

3.2 Controlled Electrodynamic Levitation and Extraction of Bioaerosol onto a Substrate (CELEBS) Instrument

The CELEBS instrument is shown in Figure 3-2a and allows routine capture and levitation of single or multiple bioaerosol droplets of monodisperse size in the aerosol phase under controlled environmental conditions for an indefinite time, and subsequent deposition onto a substrate for off-line analysis. A grounded glass-metal chamber confines all the components of the EDT to avoid disturbance of the suspended droplets within a controlled atmosphere. Bioaerosol droplets containing bacterial species are generated on-demand using a commercial

DoD dispenser (Microfab MJ-ABP-01 with 30µm orifice) fixed outside one of the sidewalls of the chamber and facing a small aperture which leads to the EDT. A DC electrode is located 2-3 mm away from the nozzle of the DoD dispenser to induce a charge on bioaerosol particles during formation. The EDT located in the interior of the chamber is composed of two horizontal ring electrodes (30 mm diameter) set in parallel with an intermediate distance of 20 mm where the droplets are suspended. A safety plate separates the EDT volume from the substrate holder to prevent premature exposure of the substrate to the bioaerosol particles. The positional arrangement between a CCD camera, an LED light and the top opening of the chamber facilitates imaging of the EDT from above. The image recorded by the CCD is analyzed to count the number of levitated particles in the EDT using a LabView program developed in-house. The LED light (White LED, 580 nm, RS Components, UK) was tested in the bulk phase to ensure no impact on the viability of bacteria as assessed by CFU determination (Table 3-1). Exposure to the LED light did not show any bactericidal effect. The whole CELEBS instrument resides on a small 20 cm × 20 cm metal plate, allowing its safe operation in a microbiological safety cabinet (MSC) (LabGard model NU-425 Class II Type A2 Biosafety Cabinet, NuAir, UK).

Table 3-1. The impact of LED light on bacterial viability. Comparative studies of recovered CFU between a bacterial culture exposed to the 580nm LED and a non-exposed culture located in a dark area under the same atmospheric conditions. No significant difference in culturability was observed.

Time (hours)	Exposed Culture	Non-Exposed Culture
	Mean value (CFU mL^{-1})	
0	$2.18\pm0.17\times10^{9}$	$2.26\pm0.16\times10^{9}$
1	$2.29\pm0.57\times10^{9}$	$1.92\pm0.26\times10^{9}$
2	$2.68\pm0.29\times10^{9}$	$2.35\pm0.22\times10^{9}$
3	$2.47\pm0.13\times10^{9}$	$2.25\pm0.10\times10^{9}$
4	$2.93\pm0.20\times10^{9}$	$2.75\pm0.24\times10^{9}$
5	$2.59\pm0.22\times10^{9}$	$2.33\pm0.92\times10^{9}$
6	$2.53\pm0.17\times10^{9}$	$2.15\pm0.91\times10^{9}$
24	$2.52\pm0.26\times10^{9}$	$2.14\pm0.21\times10^{9}$

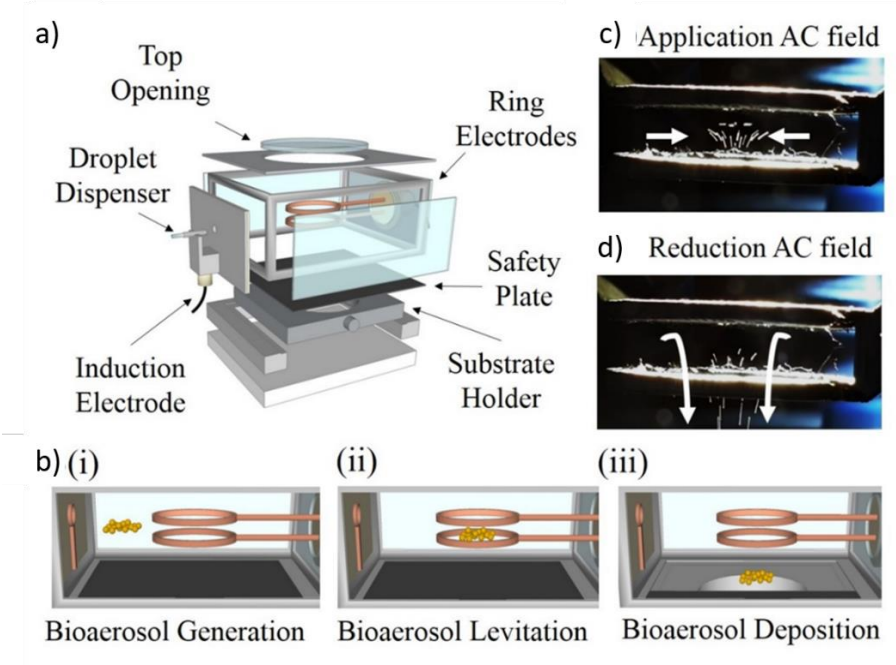

Figure 3-2. Schematic of CELEBS set-up and operation , (a) Expanded view of the main components of the CELEBS apparatus. (b) Schematic diagram of CELEBS operation. (c) and (d) Consecutive close-up images for levitation and initial deposition of the same bioaerosol population. The levitated droplets appear as lines due to the slower shutter speed of the camera compared to the oscillatory motion of the droplets driven by the AC waveform applied to the ring electrodes.

3.3 Bioaerosol Generation

Bacterial culture (10 µL aliquot) is pipetted into the reservoir of the DoD dispenser. A square waveform is applied to the piezoelectric crystal of the micro-dispenser tip, propelling a small volume of fluid out through the dispenser orifice as a jet that divides into an individual micro-droplet with a high reproducible size (27.8±0.08 µm radii). The waveform parameters together with the composition of the loaded suspension determine the characteristics of the drop generation process such as size and speed.[142] A schematic for the whole process of bioaerosol generation is shown in Figure 3-2b(i).

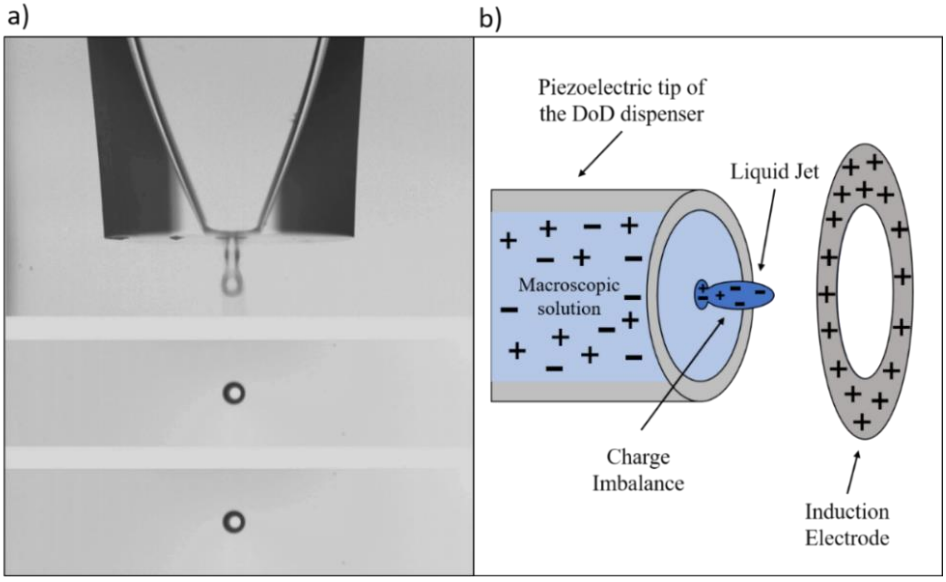

Figure 3-3. Schematic of droplet generation with a DoD . a) A water droplet generated with a commercial DoD micro-dispenser with a 30 µm orifice diameter, b) a schematic of the mechanism used to induce a small net charge in every droplet by means of ion imbalance. Figure 3-3a is reprinted with permission from the author, Dr. Jim Walker.

To enable the suspension of droplets in the EDT, a net charge is induced to every droplet by the DC potential applied to the induction electrode (-100 to -500 V) as shown in Figure 3-3a. During the formation of micro-droplets, the induction electrode produces an ion imbalance in the liquid jet formed at the tip of the DoD dispenser, resulting in a net charge on the droplet of opposed polarity to the induction electrode (Figure 3-3b). The magnitude of the net charge induced to the droplets has been reported previously (<5 fC)[227] producing a chemically insignificant shift in the original ion concentration of the droplets (~ 7×10^{-6} % more sodium than chloride ions), but sufficient for the droplets to be confined by the electrodynamic potential in the centre of the EDT.

3.3.1 Establishing the Number of Bacteria Cells Contained Within Bioaerosol Droplets

Aerosol generation using the DoD dispenser enables the microbial concentration in aerosol droplets to be varied across several orders of magnitude by modifying the concentration of

particulates (i.e. bacteria) in the spray suspension (Figure 3-4). Droplets containing three different types of particles (yellow-green fluorescent beads, 1 µm diameter; E. *coli* MRE162; *B. atrophaeus* spores) were generated from bulk suspensions at specific concentration ranges by using a DoD disperser. Specifically, Yellow-green fluorospheres beads (1 µm diameter; Molecular Probes, United Kingdom) with a commercial concentration of 3.6×10^{10} beads mL^{-1} were used as a surrogate of bacterial cells. Sequential dilutions were prepared in LB broth creating fluorosphere suspensions with concentrations down to 3.6×10^{6} beads mL^{-1}. To cover a similar range of concentration, an *E. coli* MRE162 culture in the stationary phase was concentrated by centrifugation of 4 mL of culture at 2000 RCF for 5 minutes and resuspended in 1 mL of fresh LB broth to a cell suspension of 9.3×10^{9} CFU mL^{-1} following staining with SYTO-9 (Molecular Probes, United Kingdom) by adding 4 µL of 3.34mM SYTO9 to 1mL of a four-times concentrated bacterial culture for 24h at 4°C Ten dilutions were prepared in LB broth with concentrations between 9.3×10^{5} and of 9.3×10^{9} CFU mL^{-1}. A stock of *B. atrophaeus* spores in water with a concentration of 4.0×10^{9} CFU mL^{-1} was stained with 2.56 µM fluorescein isothiocyanate (FITC, Sigma-Aldrich Ltd., UK) for 24h at 4°C and five different dilutions were prepared in water from this stock down to a concentration of 3.0×10^{5} CFU mL^{-1}. In addition, 1% (vol/vol) of aqueous Tween 80 was added to give a final concentration of 0.1% (vol/vol) to promote the separation of cells in all samples. For samples in the order of 10^{7} CFU mL^{-1} or lower, 1% (vol/vol) of a FITC water solution with 0.5% (vol/vol) concentration was added to enhance the visibility of the aerosol droplets under the confocal microscope.

All solutions were aerosolized using a DoD dispenser with aerosol droplets collected on gelatine coated microscope slides and visualized by confocal microscopy (Section 2.2.5).

Independent of particulate type (fluorescent bead, bacteria or spore), the correlational data in Figure 3-4 between the number of particulates in the bulk solution and the number delivered in each aerosol droplet indicate that the droplet composition can be varied reliably over a wide range in concentration. Such a capability makes it possible to explore the role of microbial concentration in bioaerosol droplets plays in the airborne transmission of infection. The effect of droplet size and microbial concentration in bioaerosol droplets have been previously investigated showing a significant impact on airborne survival.[22817] Additionally, the monodispersity (i.e. reproducibility) of the aerosol generated by the DoD dispenser allows

investigation of solute stresses on micro-organisms incorporated in the droplets. Contrary to polydisperse bioaerosols, monodisperse droplets achieve the same microbial concentration and are therefore expected to create a homogeneous biological response whose average represents the behaviour of all aerosolized microorganisms across the population.

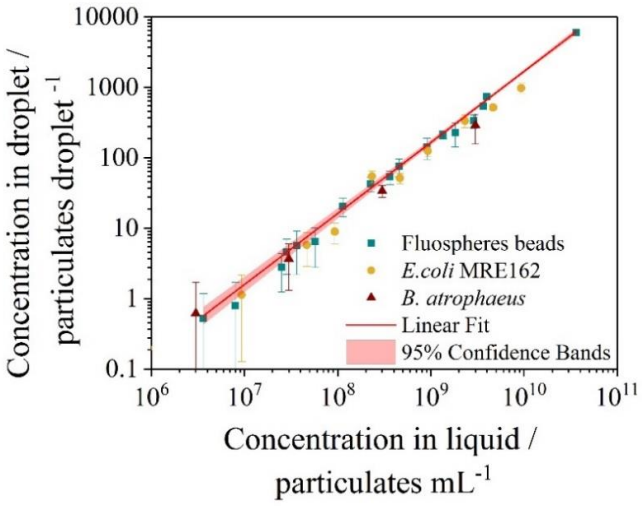

Figure 3-4. Determination of microbial load per droplet by correlating the number of cells per droplet (i.e. fluospheres, bacteria and spores) and the cell concentration of the suspension loaded in the DoD dispenser.

3.3.2 Probability Distribution Function for Low Microbial Cell Concentration in Bioaerosol Droplets

For the statistical analysis of the determination of the number of particles enclosed in the bioaerosol droplets, the particle concentration of at least 20 different droplets was determined. For each concentration of cell suspension pipetted in the DoD, the average and standard deviation values of cells in the droplet were calculated. The Probability Distribution Function (PDF) curves for cell concentration in bioaerosol droplets were produced by using the Poisson Distribution Equation (3-1) where λ represents the Poisson coefficient (average of cells per droplet for the culture concentration loaded in the micro-dispenser) and *k* the number of cells contained in a droplet.

$$PDF = \frac{e^{-\lambda}\,\lambda^{k}}{k!} \qquad \textbf{(3-1)}$$

In this case, the volume fraction of the particulates within a droplet generated by the DoD is very small and, indeed, the presences of cells can even be a rare event at sufficiently low concentrations. As particle concentration increases, the probability that aerosol droplets contain a larger number of particulates increases proportionally, and the PDF curves move towards a Gaussian distribution. We illustrate this transition for the three types of particles (i.e. fluospheres, *E. coli* MRE-162 cells and *B. atrophaeus* spores) in Figure 3-5, with the curves indicating the fitted the Poisson distributions. Therefore, the number of particulates (i.e.1 µm yellow-green fluospheres, *E. coli* MRE-162 cells and *B. atrophaeus* spores) within a bioaerosol droplet must be described by the Poisson distribution for loaded suspensions with particle concentrations less than 10^8 CFU mL^{-1} (Figure 3-5).

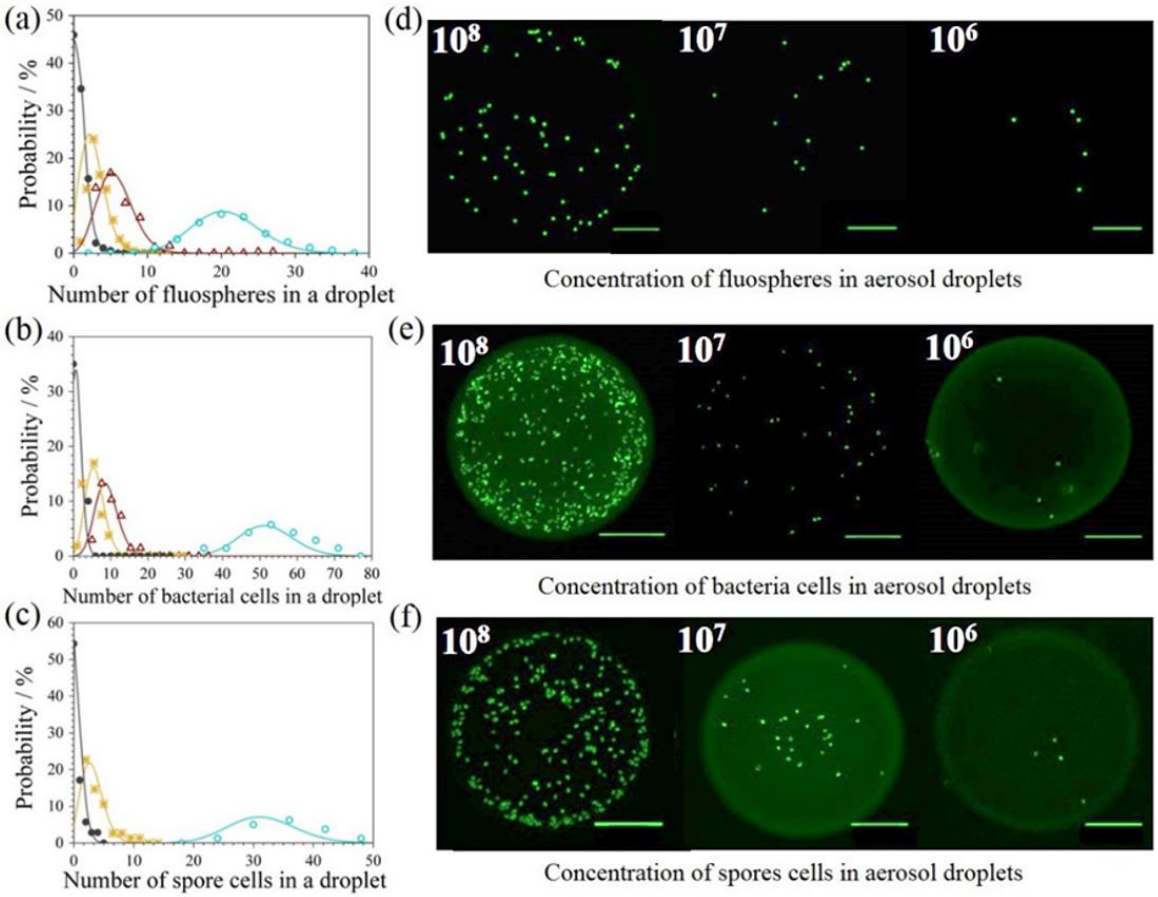

Figure 3-5. PDF curves for microbial concentration in bioaerosol droplets, showing experimental results and confocal microscopy images for particle concentration. Scale bar is 30 µm. Diameters of the deposited droplets are larger than the initial droplet sizes due to impaction on the gelatine used to coat the microscope slides. (a) Modelled curves and experimental results for the number of fluospheres per aerosol droplet. The PDFs for the averages of fluospheres per droplet, λ=0.795, λ= 2.62, λ=5.70 and λ= 20.6, are shown by the black, yellow, maroon and turquoise

curves, respectively. Experimental values for the number of beads per droplet are (●), (✱), (△) and (○) at solution concentrations of 8.0×10^6, 2.5×10^7, 3.64×10^7 and 1.14×10^8 cells mL^{-1}, respectively. (b) Modelled curves and experimental results for the number of *E. coli* MRE-162 cells per aerosol droplet. The PDFs for λ=1.14, λ= 5.83, λ=8.96 and λ= 51.3 are shown by the black, yellow, maroon and turquoise curves, respectively. Experimental values for the number of bacteria cells per droplet are (●), (✱), (△) and (○) at solution concentrations of 9.32×10^6, 4.66×10^7, 9.32×10^7 and 4.66×10^8 CFU mL^{-1}, respectively. (c) Modelled curves and experimental results for the number of *B. atrophaeus* spores per aerosol droplet. The PDFs for λ=0.54, λ= 3.09 and λ=31.49 are shown by the black, yellow and turquoise curves, respectively. Experimental values for the number of spores per droplet (●), (✱) and (○) at solution concentrations of 3.0×10^6, 3.0×10^7 and 3.0×10^8 cells mL^{-1}, respectively. (d), (e) and (f) show confocal microscopy images for different particle concentrations in aerosol droplets containing fluospheres beads, *E. coli* MRE-162 cells and *B. atrophaeus* spores, respectively.

3.3.3 Determining the Effect of Aerosolization on Bacteria Viability

Aerosolization may cause damage to bacterial cell structure.[137] The percentages of *E. coli* MRE-162 cells possessing intact membranes were obtained for cultures subjected to two methods of aerosolization (the DoD and the 1-jet refluxing nebuliser), as well as for the non-aerosolized control sample was measured.

For the evaluation of membrane integrity, samples containing *E. coli* MRE-162 or *B. atrophaeus* spores were subjected to different staining processes to determine the physiological condition of bacteria cells after aerosolization: Live/Dead BacLight bacterial viability and counting kit (Molecular Probes, United Kingdom) was used to determine the aerosolization effect on bacterial viability as measured by a decrease in observed cellular SYTO-9 signal. Bacteria with intact cell membranes fluoresce bright green (SYTO-9) while bacteria with compromised cell membranes fluoresce red (propidium iodide [PI]). Thus, a stationary phase culture of *E. coli* MRE-162 ($1.7\pm 0.7\times10^9$ CFU mL^{-1}), was split into two samples for aerosolization using the two different aerosol generators to demonstrate any effect of aerosolization on bacterial membrane integrity. For 'live' and 'dead' controls, *E. coli* cultures were either untreated (not aerosolized) or treated with 75% (vol/vol) ethanol for one hour at room temperature, respectively. Staining procedures for the samples were performed immediately after collection following the manufacturer's protocol. Specifically, bacterial cells were stained by adding 3 µL of a 10^{-3} dilution of a 1:1 mixture of 8 µL of 3.34 mM SYTO9 with 8 µL of 20 mM PI from the Live/Dead BacLight bacterial viability kit to the 20 µL samples. Subsequently, samples were placed on microscope slides coated with 5% (vol/vol)

porcine gelatine (Sigma-Aldrich Ltd., UK) for microscopic and image analysis (Section 2.2.5). The control showed a high percentage of green-fluorescing viable cells (99 ± 1%).

Firstly, measurements examined the dependence of bacterial viability on the waveform parameters applied to the DoD required to generate droplets (i.e. pulse voltage, frequency and width) and the DC voltage applied to the induction electrode (Figure 3-6). A comparative study was performed by examining the influence of standard (low) and magnified (high) values of all parameters involved in droplet generation. Droplets were collected into an Eppendorf tube containing 10 µL of LB broth and the dye mixture described below for viability analysis. Secondly, bioaerosol droplets were generated from 150 mL of the bacterial culture using a 1-jet refluxing nebuliser for 20 min at 30 psi pressure to assess the effect of nebulization on bacterial viability. Samples were collected from the refluxed bacterial culture remaining in the liquid reservoir of the nebuliser at 5 and 20 min.

For the statistical analysis of the viability of bacterial cells (assessed as those with detected Syto9 fluorescence) enclosed in aerosol droplets, at least 200 cells from five different field of views were analyzed following deposition onto slides. The percentage of viable cells with an intact cell membrane was calculated by dividing the green-stained cells by the total number of cells for each field of view. The average and standard deviations were calculated for each parameter under evaluation. No significant difference between control cells and those aerosolized using the low and high values of the waveform and induction electrode parameters was observed. In contrast, bacteria experiencing conditions within the 1-jet refluxing nebuliser demonstrated significant effects on membrane integrity. Membrane integrity decreased markedly as a function of time, from 100% ± 1% to 33% ± 12% at 5 and 20 min nebulization times respectively. Assuming the aerosol generated with the 1-jet refluxing nebuliser is a direct sample of the culture contained in the reservoir, then the aerosolized bacteria would show the same proportion of adversely affected cells. This difference is a result of fundamental differences between the aerosolization mechanisms. Piezoelectric aerosolization using the DoD dispenser does not involve high pressures or recirculation of the sample contained in the reservoir, reducing stresses associated with shear forces and wall impaction, characteristic of reflux nebulization systems. In addition, the larger volume of the droplets generated by the DoD in comparison with the size of the enclosed bacterial cells may mitigate shear forces providing a greater proportion of bacterial cells assessed as having intact membranes.[229]

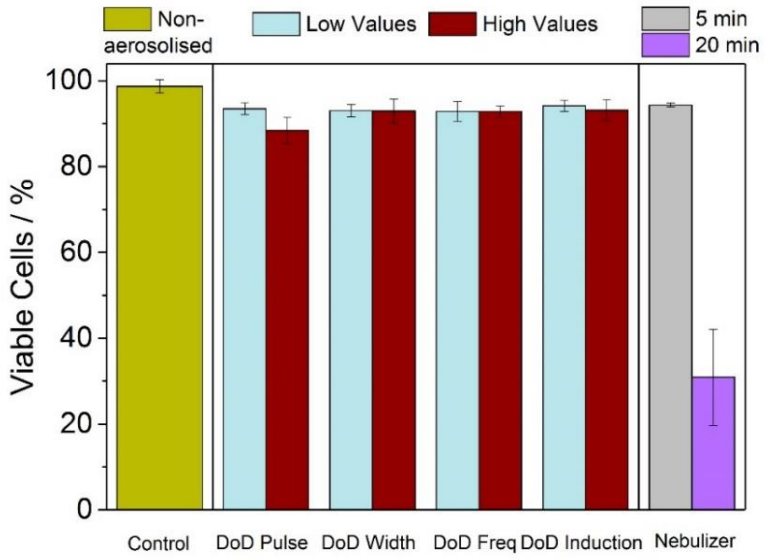

Figure 3-6. Effect of DoD aerosolization on bacterial viability , showing the percentage of cells with intact cell membranes obtained by using different aerosolization devices. In consecutive order, bars represent for each set of values: the non-aerosolized control (green) bacterial culture, the bacterial culture aerosolized by using the DoD with a pulse voltage of 3.5 and 8 V (blue), a frequency of 10 and 1000 Hz (pink), a width of 25 and 45 µsec (yellow) and an induction voltage of 250 and 1050 V (grey), respectively. Finally, the refluxed bacterial culture after 5- and 20-minutes nebulization by using the 1-jet refluxing Nebuliser respectively are shown (maroon). The average and standard deviation for each parameter were calculated by counting at least 200 cells from five different fields of view.

3.4 Bioaerosol Levitation

The fundamentals of micro-particle levitation in the EDT have been previously described.[230–233] The electrodynamic fields used for particle levitation in the EDT is similar to those of the electrodynamic balance[182] or quadrupole ion trap[28]. However, no DC potential is applied directly to the ring electrodes or any of the EDT components in this study.

Dispensed droplets travel horizontally about 30mm towards the interior of the chamber, before getting trapped (Figure 3-2b(ii)). Oscillating forces from the electrodynamic field, created by applying an AC potential (1,000-2,700V) to the ring electrodes, enable the stable confinement of charged particles in the centre of the EDT. Additionally, the electrostatic repulsions among the population of positively charged droplets (up to >200 droplets) prevent their coalescence (Figure 3-2c). The population of trapped droplets reside in or near the null point of the trap.[188]

The glass-metal chamber isolates the trapping region from surrounding air currents and ambient laboratory conditions. The droplets are suspended while a gas inlet enables control of atmospheric conditions in the EDT. The accessible RH range in the system is >10 to <90 % RH and can be readily controlled by adjustment of the ratio of humidified and dry air flows delivered by an air purifier (Precision Air Compressor, Peak Scientific, UK) using two flow valves. The airflow mixture enters the EDT from above the electrodynamic trap where the droplets are levitated. Accurate RH and temperature values are registered by a probe (Humidity and Temperature Meter HMT331, Vaisala, UK) immediately before entering the EDT chamber.

3.4.1 Determining the Effect of Electrodynamic Levitation on Bacteria Viability

The effect of the AC field on the viability of bacteria contained in droplets and suspended in the EDT chamber was investigated. During levitation, the droplets decrease in size by losing water until they reach an equilibrium size of ~5 μm radius, depending on the relative humidity in the cell. Here, bioaerosol particles were initially generated with a size of 27.8 ± 0.08 μm in radius, determined from measurements with the CK-EDB system described in detail in Section 2.2.1.[189] Figure 3-7 shows an example of the variability in the initial droplet size from droplets generated from LB containing *E. coli* cells with a concentration of 6.67×10^{8} cells mL^{-1} until they reach the equilibrium at 33.2% RH.

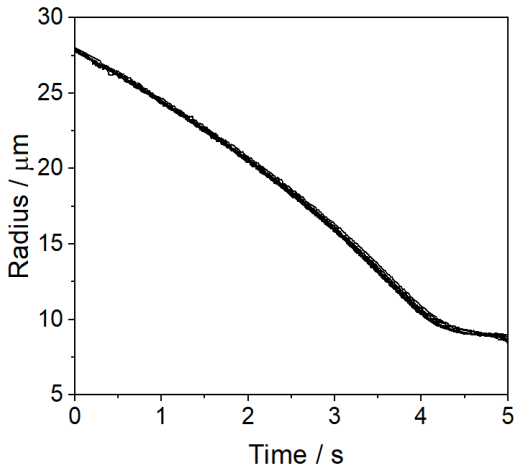

Figure 3-7 Measurements of the initial droplet size and evaporation rate of water using the Comparative Kinetics Electrodynamic Balance for nine droplets generated from LB containing *E. coli* cells with a concentration of 6.67×10^{8} cells mL^{-1} into a gas phase at a RH of 33.2%. The initial droplet size is 27.8±0.08 µm.

The CFU per droplet generated from an *E. coli* culture ($1.7\pm0.9\times10^{8}$ CFU mL^{-1}) aerosolized and levitated for 5 seconds in the AC field were compared with the estimated value of the number of bacteria cells per droplet for that culture concentration (following the linear correlation reported in Figure 3-4). Assuming that aerosol generation, 5-second suspension and sampling would not impact the microbial viability when using the CELEBS system, the experimental and estimated values of bacterial cells/CFU in the droplets should be equivalent. Ten replicates of brief levitation (<5 secs) were performed consecutively under the same conditions (50 ± 2 % RH and 24 ± 1 ºC temperature). The number of CFU per droplet obtained after levitation and incubation (39.2 ± 24.4) compares well with the calculated number of bacterial cells per droplet (43.5 ± 20.8). The concurrence between both bacterial concentrations shows that the culturability of *E. coli* cells in solid media was not significantly affected by short suspension periods in the AC field (2 kV) (Figure 3-8). The impact of electric fields on microbial viability has been previously shown to not reduce the culturability of at least three different bacterial species exposed to an electric field of 4.2 kV as long as 2 hours.[166]

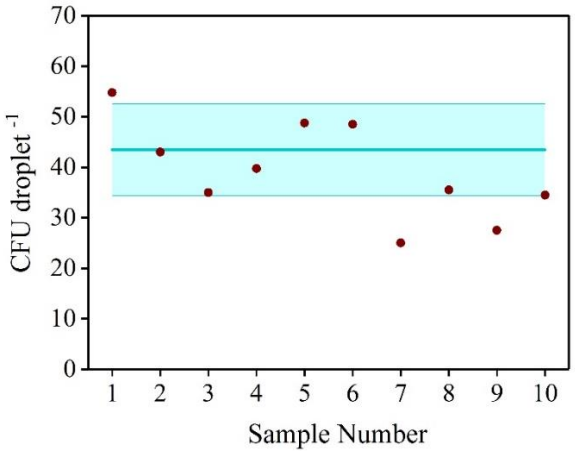

Figure 3-8. Effect of suspension in the AC field on the viability of *E. coli* MRE-162 incorporated in droplets of 27.8± 0.08 µm radii. The graph shows the relationship between the predicted number of CFU per droplet (≡) (mean +/- Std dev) and the number of CFU per droplet formed after the incubation of bioaerosol populations levitated in the EDT for 5 seconds (●).

3.5 Bioaerosol Sampling

After the desired suspension period, the safety plate between the EDT and the substrate holder is removed connecting the trapping and sampling areas. By lowering the amplitude of the waveform applied to the ring electrodes, the levitated droplets are extracted (Figure 3-2b(iii)) from the EDT onto the substrate (i.e. LB broth) in a short period of time (1-3 sec, Figure 3-2d). Collection velocities onto the substrate can be controlled and are typically 0.01 - 0.05 m s^{-1}, avoiding damage to sensitive microorganisms. Calculated velocities (determined by measuring the distance between the EDT and the substrate holder, and the time taken for the droplet to fall at different deposition rates) are equivalent to the velocities of an electrostatic sampler. These sampling methods based on electrostatic precipitation have shown particle velocities between 2 and 4 order of magnitude lower than velocities in inertial samplers reducing the impact on cell viability while providing high collection efficiency.[165–167]

In rotating drums studies, liquid impingers with collection velocities reaching 265 m s^{-1} are used.[166] CELEBS methodology presents 3×10^4 times slower sampling velocities and, consequently, a gentler collection process. A smooth deposition is critical as different sampling techniques have been reported to reduce microbial viability due to high impaction velocities and reduce the sensitivity of measurements to the parameters under study.[110,151,179,234]

Moreover, the CELEBS collection process provides 100% sampling efficiency: every droplet trapped in the electric field is sampled on the collection medium (which can be any substrate, including liquid, gel, glass, and cell culture). This 100% sampling efficiency is unique to CELEBS. Finally, the substrate can be removed from the apparatus and the viability and infectivity of bacteria assessed.

3.5.1 Evaluation of Sampling Efficiency

The correlation between the number of droplets trapped in the EDT and the number of droplets ejected from the AC field and collected in an empty plastic Petri dish was measured (Figure 3-9). The populations of particles collected in each Petri dish were counted with a conventional microscope and compared to the number of droplets levitated. This relationship was determined for four different types of biological and non-biological particles: droplets made of a suspension of 3.6×10^{9} fluospheres mL $^{-1}$ in LB broth; a FITC-labelled *E. coli* MRE-162 culture in stationary phase; a 20% NaCl solution in DI water and a 20% sucrose solution in DI water. The correlation between trapped and collected droplets was excellent reporting an $R^2= 0.999$.

The efficient particle collection of the CELEBS technology, together with the generation of droplets with high reproducibility in size and biological composition (i.e. the number of microorganisms enclosed within the droplets), allows quantification of the absolute number of microorganisms probed in each experiment.

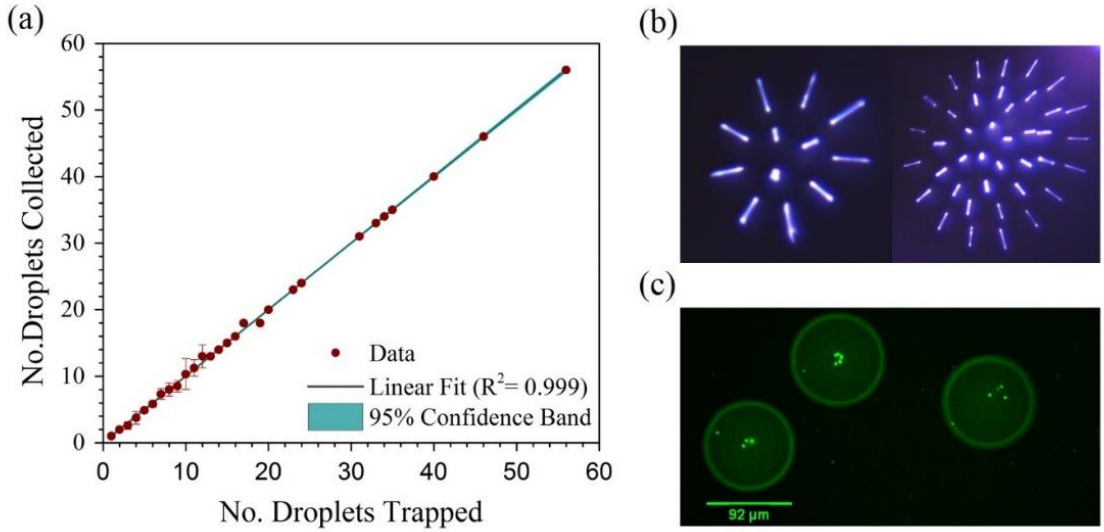

Figure 3-9. Determination of sampling efficiency of the CELEBS instrument (a) The correlation between the number of droplets levitated and the number of droplets collected. Each data point represents a single experiment. (b) Images of different sizes of bioaerosol populations levitated inside the EDT (left image 12 and right image 40 bioaerosol droplets). (c) Representative image of droplets containing fluospheres collected on the substrate immediately after aerosolization. The actual size of the particles at generation was measured with the CK-EDB system (27.8 ± 0.08 µm radii).[189] The enlarged diameter of the impacted droplets provided by the image software is due to droplet spread at impaction on the coated gelatine slide.

3.6 Quantitative Characterisation of Bioaerosol Survival of Bacteria Exposed to 30% RH

To measure the survival, it is important to first confirm that negligible physical loss of particles occurs inside the EDT chamber during particle levitation. *Bacillus* spores are commonly used as physical tracers to distinguish between the biological decay and physical loss in aerosol systems since they remain viable under a wide range of environmental conditions.[90,150,235] Therefore, to evaluate the physical loss of particles during suspension, *B. atrophaeus* spores (triple washed in distilled water) were diluted ten-fold in PBS ($6.5 \pm 2.5 \times 10^8$ spores mL^{-1}), aerosolized and captured in the CELEBS for one hour (33 ± 2 % RH, 23 ± 2 °C). The initial droplet size and spore concentration was 25 ± 0.25 µm radius and 65 ± 12 spore cells per droplet respectively.

In addition, *E. coli* MRE-162 was cultured to stationary phase in LB broth (24 h, 180 rpm, 378C) and diluted ten-fold ($2.1 \pm 0.2\ 10^8$ CFU mL^{-1}). Bioaerosols produced with the DoD and suspended for different time periods (i.e. 2, 5, 10, 15, 20, 30 and 60 min) under similar atmospheric conditions (33 ± 0.91% RH, 24 ± 1℃) to measure airborne bacterial survival as the ability to form a CFU on collection. The initial particle size was 27.8±0.08 μm radius and microbial concentration of 23 ± 11 bacterial cells per droplet.

The survival (Section 2.2.2.3) of *B. atrophaeus* and *E. coli* MRE-162 are referenced to initial control measurements at 2 minutes and 30 seconds (longer than usual due to the early development state of the technique), respectively, as shown in Figure 3-10. The physical loss of particles as a function of time is absent in the CELEBS system over the timescale of an hour since the number of spores does not decay; therefore, only the biological decay needs to be considered when performing ageing experiments which is referred to as survival (Section 2.2.2.3). Consequently, it is possible to directly evaluate the microbial response to specific atmospheric conditions without comparing decay rates between the microorganism of interest and physical tracers.

The interpretation and comparison of data from aerosol survival studies in the literature are complicated due to the diversity of the employed methodologies (generation and sampling), biological species, bioaerosol composition and atmospheric conditions used. Our data shows a 41.5% decrease in recovered *E. coli* MRE-162 cells within the first 2 minutes of aerosol suspension, followed by a less-pronounced decay. The rapid 2-minute decline may be due to evaporative cooling and mass transfer processes experienced within the droplets during the early stages of the aerosol state until equilibrium is reached. Bi-phasic decay has been previously reported in the literature, demonstrating that the majority of decay occurs within the first 1-2 minutes of aerosol suspension.[73,90] Interestingly, previous studies spraying *E. coli* K12 from distilled water have compared survival between nitrogen and air atmospheres. Results reported 10% survival at 35% RH and 26 ℃ after 30 minutes of suspension and collection in PBS.[92] Our methodology reported 24% survival at the same aerosol age. Differences may be due to the presence of dissolved solids in the LB broth together with reduced impact of stresses during generation and sampling. Comparison between these results highlights the value in understanding methodology and validation in bioaerosol research which is critical to facilitate the interpretation of data and standardization between laboratories.

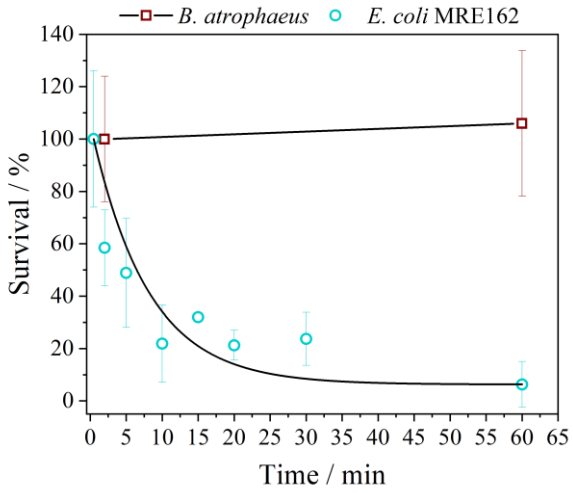

Figure 3-10. Survival percentage for *E. coli* MRE-162 and *B. atrophaeus* spores at 33% RH and 24°C temperature. All the survival data are expressed as the average and standard deviation values for at least three biological replicates (samples from independent *E. coli* cultures) per experiment.

3.7 Summary: Advantages over Conventional Techniques for Bioaerosol Analysis

We have presented a new methodology for measuring microbial survival in aerosol particles as a function of different atmospheric conditions and particle compositions (both biological and chemical). The technology couples a piezoelectric droplet dispenser with an electrodynamic trap to create highly monodisperse bioaerosol droplets with defined composition followed by their suspension in an electric field under controllable atmospheric conditions. CELEBS presents an alternative approach for understanding variables which impact natural transmission mechanisms by more accurately representing initial droplet sizes generated by sneezes/coughs,[236] and minimising stresses involved in the analysis. Ultimately, this will lead to more accurate epidemiological and risk analysis modelling.

The approach we report here presents significant advantages over more conventional approaches used in bioaerosol analysis:

- A quantifiable number of bioaerosol droplets containing bacteria can be generated on-demand with a reproducibility in the initial droplet size of ± 0.25 µm (1 standard deviation)[189] utilizing a DoD micro-dispenser. Moreover, the complete chemical and

biological composition of the bioaerosol droplets can be varied across several orders of magnitude (i.e. number of particulates per droplet). The DoD does not impact cell membrane integrity as measured by Syto9/PI staining and CFU determination, in contrast with a standard methodology of bioaerosol generation.[132,137,138] The technology could be applied to other micro-organisms such as fungi or viruses.

- CELEBS represents a valuable alternative to the rotating drum and micro-thread techniques. Due to using an electric field to levitate droplets, CELEBS does not suffer from the same restrictions on droplet size and hence, airborne suspension times required to avoid physical loss of particles in rotating drums. Furthermore, the CELEBS holds the bioaerosol in the true airborne state in contrast with the micro-thread technique.[9,146,147,171] Short exposures (<5 secs) to the EDT did not impact the ability of levitated microorganisms to form colonies after sampling. Hence, CELEBS incorporates a less physically damaging approach. In addition, the glass design of the EDT chamber enables the visualization and enumeration of the bioaerosol droplets during suspension. Future studies using CELEBS will explore its accessibility to a wider range of atmospheric parameters (i.e. relative humidity, temperature, gaseous species, UV light, etc.).

- High sampling flow rates and long sampling times can reduce the viability of collected microorganisms.[179,237,238] The sampling mechanism in CELEBS based on electrostatic forces uses particle velocities perpendicular to the collection substrate similar to the ones involved in electrostatic precipitation, which are 2-4 orders of magnitude lower than collection velocities used in more standard aerosol samplers (i.e. impactors, filters and impingements).[167] This presents a new “gentle” alternative for microbial collection potentially more representative of the natural mechanisms in the environment. Moreover, the population of bioaerosol droplets can be sampled onto a platform containing any type of substrate (e.g. culture media, lung tissue cells, bacteria cells etc.) enabling numerous options for viability and infectivity analysis.

- The small and open design of the EDT trap offers other advantages in terms of flexibility and easy manipulation of the instrument, particularly for research in microbiological containment. The capability to study multiple types of bioaerosol

concurrently by "daisy-chaining" multiple levitation chambers together is both advantageous and unique to this methodology.

- The small volume of sample required (~10µL) and the small number of the bioaerosol droplets generated, enable safely study airborne micro-organisms in a highly controlled fashion. The likelihood of being exposed to infectious doses of micro-organisms is dramatically reduced.
- We have demonstrated the utility of CELEBS to probe the survival of bioaerosols using *E. coli* MRE-162. Moving forward, the physicochemical properties and dynamic behaviour of the particles produced with a DoD dispenser can be probed via alternative methods, such as a comparative kinetic electrodynamic balance.[52,63] Understanding the processes that drive changes in the physicochemical properties of bioaerosols (i.e. hygroscopicity, surface tension, viscosity, etc.) will enable exploration of the impact of these properties on bioaerosol survival. This will be a fundamentally new and comprehensive approach to studying the transmission of infectious micro-organisms in the aerosol phase.[109,239] Indeed, we also anticipate that this device will be ideally suited to studying the influence of atmospheric oxidants on the viability of bacteria in the aerosol phase.

In conclusion, CELEBS represents a new tool for bioaerosol survival studies with the potential to elucidate the fundamentals of airborne disease dynamics by implementing several benefits to existing technologies.

Chapter 4

Microphysical Factors Influencing the Airborne Transmission of Pathogens

Chapter 4 is based on a publication in Applied and Environmental Microbiology, entitled "Transformative Approach to Investigate the Microphysical Factor Influencing Airborne Transmission of Pathogens", for which I am the first author.[10] *I confirm that I performed the laboratory work, analyzed and interpreted all the experimental data presented in the mentioned manuscript. I acknowledge Richard J. Thomas from DSTL and Henry Oswin for contribution in data acquisition of the hygroscopicity curves and the RH-dependence of the survival for E. coli MRE-162 in LB broth and PBS solution droplets, respectively. I also acknowledge Allen Haddrell and Jonathan P. Reid for their project supervision and advice on the interpretation of experimental results. Finally, I would like to acknowledge Jean-Charles Eloi, who trained me in electron microscopy and contributed to acquiring the SEM images used in this study.*

The development and validation of a comprehensive approach to identifying the physicochemical processes that impact the survival of bacteria in aerosol droplets were introduced in chapters 2 and 3. This chapter will discuss how using this approach can provide an increased mechanistic understanding of how changing the evaporation conditions such as the initial solute concentration, droplet composition and relative humidity can affect the droplet evaporation rates, equilibrium droplet size, and particles morphology. Ultimately, we will discuss how all these intrinsically interrelated changes can impact aerosol survival. Therefore, this new approach will be assessed in this chapter through combined measurements of the dynamics driving the evolving size, composition, morphology, and hygroscopic response with their corresponding biological outcome, using *E. coli* (MRE-162) as a benchmark system.

4.1 Introduction

The substantial impact of the airborne transmission of disease on human health, agricultural productivity, ecosystems stability and livestock has been widely recognized.[240–242] Transmission of respiratory infectious diseases via the airborne route has been identified as the major transmission mode in many epidemics, and a significant mode of transmission in indoor environments including occupational, residential and transportation settings.[215,236,243–245] Nevertheless, little is known about the mechanisms that control the survival of airborne pathogens due to the complex multifactorial processes which are involved and the lack of suitable data for comparison of studies.[67] Therefore, further investigation is critical to determine the fundamental mechanisms of airborne disease transmission, necessary not only to develop strategies to mitigate the impact of disease outbreaks but also to understand the seasonality of infectious diseases,[114] improve treatment of respiratory infections,[246] determine synergistic effects of air pollution on the atmospheric microbial community,[247] and even elucidate the role of bioaerosols on atmospheric processes.[248]

The critical factors that are thought to affect microbial survival in the aerosol phase include relative humidity (RH), temperature, particle size and microbial load.[12,71,75,76,80,117,119,135,228] However, the mechanisms that describe airborne transmission dynamics for most respiratory pathogens remain largely unknown.[241,243] This knowledge gap is mainly due to several challenges involved in undertaking laboratory aerobiological studies. Firstly, the natural transmission mechanisms for the generation (i.e. coughing, sneezing), suspension (i.e. aerosol transport) and deposition in the respiratory tract are not properly represented by the current *in vitro* studies due to the complexity of the interacting physicochemical and biological processes and the technological limitations of conventional methodologies.[116,249] Defining the aerosol ageing timeframe while simultaneously avoiding particle loss (e.g. sedimentation) can be especially challenging since airborne bacteria and viruses require well-defined suspension time intervals to investigate their survival.[250] Secondly, the viability and infectivity of airborne microorganisms are likely dependent on the size, composition and origin of the host droplets and replicating these properties in a laboratory environment is challenging.[236,251] The viability of freshly generated airborne microorganisms can be dependent on the aerosolization method.[33,137] Finally, data comparison between studies is difficult due to the diversity of pathogens, environmental conditions and methodologies employed in survival studies.[68] An

approach that accurately represents, and can clarify, the complex interrelated physicochemical and biological aerosol processes taking place during the generation, atmospheric transport and deposition in the respiratory tract are necessary to fully understand the dynamics of airborne transmission of infection.

To address the fundamental mechanistic questions central to understanding airborne disease transmission, a novel approach that utilises two complementary technologies is applied. First, the aerosol droplet evaporation kinetics, changes in particle morphology during drying and changes in the solute hygroscopicity are fully quantified using a CK-EDB, providing a detailed understanding of the dynamic behaviour of aerosol particles.[109,189] Second, the bioaerosol survival as a function of time, particle composition and environmental conditions, of identical particle types are measured with CELEBS.[68] This next-generation apparatus for bioaerosol survival analysis has the potential to identify the factors that impact the survival of airborne pathogens allowing accurate control and representation of bioaerosol in the atmosphere.[68] When used in combination, these particle levitation technologies can be used to interrogate the true airborne state of airborne microorganisms. Understanding this state is critical since the physicochemical conditions that microorganisms are exposed to within an aerosol host droplet can differ dramatically from those in a bulk phase sample,[216] potentially impacting their viability and consequently, their transmission between hosts (Figure 4-1). Combining the strengths of these complementary methodologies for probing aerosol particles directly, the TAMBAS approach enables an exploration of the complex interconnections between airborne microphysics and biological decay.

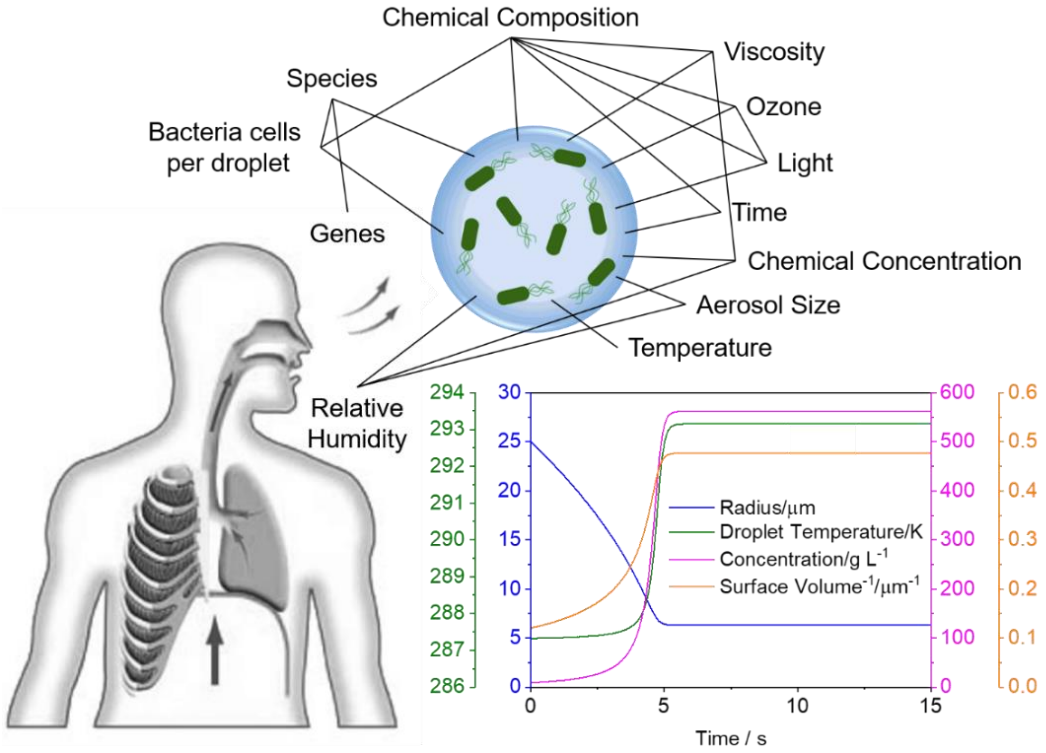

Figure 4-1. Interplay between some biological and physicochemical properties and processes which impact on microorganism viability during aerosol transport. The graph illustrates the typical changes in physicochemical properties that occur during the evaporation of a saline (NaCl, 9 g L^{-1}) droplet injected into ambient RH (50 %). Note that t=0 (time of droplet generation) would represent bulk phase concentrations prior to droplet generation.

In this chapter, these complementary approaches, are used to explore directly for the first-time interconnections between aerosol droplet microphysics and biological decay. The dynamic behaviour and physicochemical properties of the bioaerosol determined with the CK-EDB are used to inform the biological responses measured with CELEBS. The aim of this study is to use this complementarity to elucidate the mechanisms responsible for degrading the viability of airborne bacteria and identify parameters that define their survival.

4.2 The Water Content of Microbiological Media: Bacterial Processing of Growth Media Affects Aerosol Hygroscopicity

The retrieval of equilibrium hygroscopic properties of microbial media from mass-transfer kinetics measurements was performed in the CK-EDB,[109,191] utilizing a comparative

evaporation kinetics approach previously described in Section 2.2. The relationship between water activity and aerosol composition for common microbial media are compared to thermodynamic model predictions for NaCl (E-AIM,[252], Figure 4-2). The hygroscopic responses of the typical culture media used in microorganism survival measurements are crucial to the exploration of the relationship between hygroscopicity and airborne bacterial survival in later sections. The composition and concentrations of the different media solutions are described in Section 2.2.4. Freshly autoclaved LB broth and LB broth previously used to culture bacteria over 24h with subsequent withdraw of *E. coli* MRE-162 cells, are referred to as non-metabolized and metabolized, respectively. The hygroscopic growth as a function of water activity (equivalent to RH) is shown in Figure 4-2 in three different forms, typical of this type of measurement: as a mass fraction of solute (MFS, represented by the mass of solute divided by the combined mass of the solute and water), and as both mass and radial growth factors (GF_m and GF_r), the ratio between the wet and dry masses of the particle, and the wet and dry radii, respectively.

The hygroscopic growth curves in Figure 4-2 show that PBS has similar hygroscopicity to NaCl alone (NaCl makes up 83% of the mass of PBS), examples of high hygroscopic growth. However, both LB broth solutions, with 60% of the solute mass arising from organic components, are much less hygroscopic. Interestingly, non-metabolized and metabolized LB broth display different hygroscopicity, suggesting that the metabolization of LB broth by bacteria alters the solute composition and, thus, the water content of aerosol droplets at a particular RH. Although it is well known that bacteria alter the composition of media through metabolism, the effect that this has on aerosol hygroscopicity is a novel observation. Ostensibly, microbes affect the physicochemical properties of bioaerosol altering the initial solute composition.

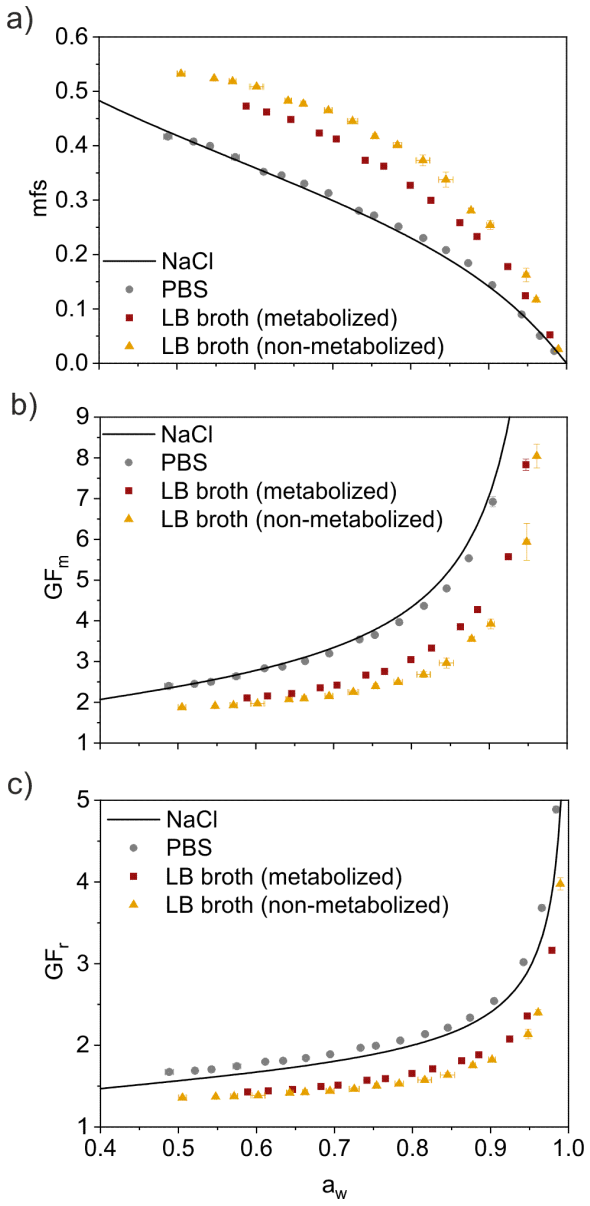

Figure 4-2. Hygroscopic response of different culture media with variation in solution water activity (a_w), equivalent to RH, presented in terms of (a) mass fraction of solute (MFS), (b) radial growth factor (*GFr*) and (c) and mass growth factor (GF_m). Predicted curves for NaCl hygroscopicity (line) from the Extended Aerosol Inorganic model (E-AIM) (for reference purposes) are also shown. Uncertainties on the hygroscopicity measurements corresponding to an error in a_w of ±0.002 at a_w >0.9 and ±0.001 at a_w <0.9. [109,253]

The estimation of the original dry mass of solute for droplets composed of metabolized LB broth was performed after removing the bacteria cells from the suspension using a micro-centrifuge. Then, 1 mL of the supernatant solution was dried out in an oven for 24 hours and the dry weight of solute was measured. Figure 4-3 shows the slight difference in the evaporation

kinetics of LB broth solution droplets containing ~10^9 CFU mL^{-1} produced by the variation in composition between metabolized and non-metabolized LB broth in.

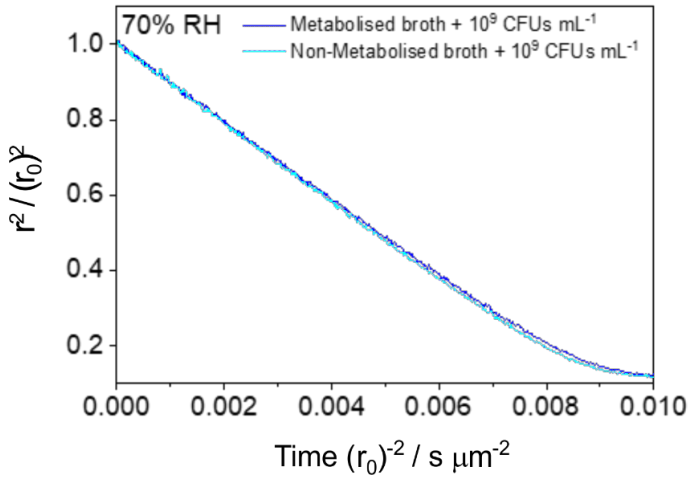

Figure 4-3. Effect of bacterial metabolization of media on aerosol dynamics. Comparison of the dynamics between droplets composed of non-metabolized LB broth (cyan, 5 droplets) and metabolized LB broth (dark blue, 5 droplets) containing ~10^9 CFU mL^{-1}.

4.3 Modelling Dynamics of Evaporating LB broth and PBS Solution Droplets into a Wide Range of RHs

The condensation and evaporation of water from bioaerosol particles are dictated by the conditions in the surrounding atmosphere.[254] The equilibration of the water content of aerosol droplets with the moisture content of the gas-phase environment can lead to unique conditions that are not accessible in macroscopic solutions, reaching significantly higher solute concentration, reactivity and even singular phase behaviour.[124] Therefore, understanding the dependence of airborne survival with ambient parameters is critical to control the spread of airborne disease.

The simulations of droplet evaporation kinetics were performed for LB broth and PBS droplet compositions at different RHs by using an approach previously described in Section 2.2.1.3. Briefly, predictions of mass transfer kinetics were generated by using the Kulmala equation[197] together with the density treatment and hygroscopicity parametrization of the solution droplet. The kinetic simulations reported in Figure 4-4 and Figure 4-5 provide information about the rapid changes in particle size, solute concentration, surface-to-volume ratio and evaporative

cooling undergone during drying of LB broth and PBS droplets, respectively, under a wide range of RHs (30-90%) in short periods (<30 s) after droplet generation. Additionally, the size distribution of the generated droplets in this study is representative to some of the droplet sizes found in a cough or a sneeze.[55] Importantly, different droplet size distributions would experience different dynamics.

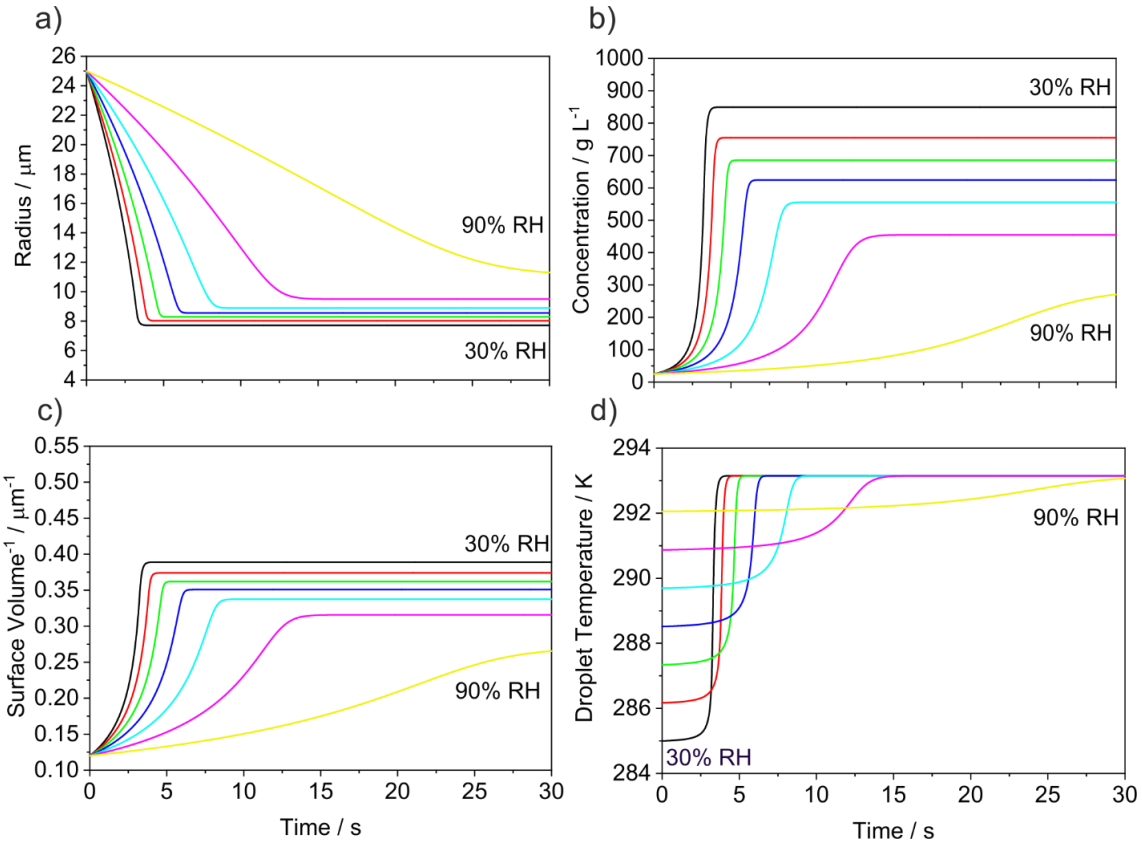

Figure 4-4. Modelled dynamics for LB broth solution droplets . Specifically, model results of the time-dependent (a) evaporation profiles, (c) droplets concentration, (c) surface/volume ratio and (d) droplets temperature for droplets equilibrating over a range of gas-phase RHs values between 30 and 90% at 20℃. Simulations were obtained using the mass and heat transport equations from the Kulmala model.[109,197]

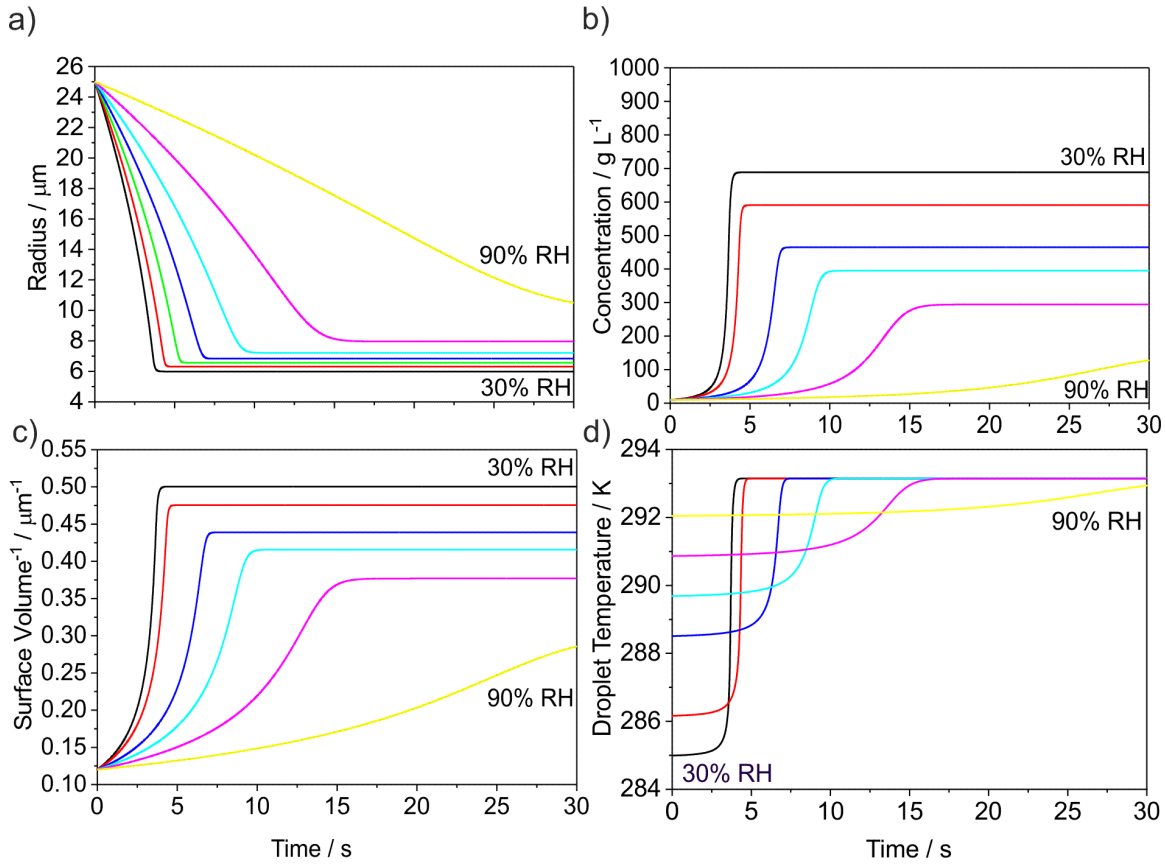

Figure 4-5. Modelled dynamics for PBS solution droplets . Specifically, model results of the time-dependent (a) evaporation profiles, (b) droplets concentration, (c) surface/volume ratio and (d) droplets temperature for droplets equilibrating over a range of gas-phase RHs values between 30 and 90% at 20℃. Simulations were obtained using the mass and heat transport equations from the Kulmala model.

These dramatic changes in the physicochemical properties of the aerosol droplets can affect not only the viability of the airborne microorganisms but also the droplet lifetime in the aerosol phase (e.g. loss rates dues to sedimentation) as well as their deposition in the respiratory system.[254–256] Therefore, it is critical to understand the impact that aerosol dynamics have on the transmission of airborne pathogens.

4.4 Changes in Phase/Morphology and Solute Concentration During Droplet Evaporation at Varying RH Affect Microorganism Viability

The evaporation kinetics (including changes in morphology) of non-metabolized individual LB broth droplets (Figure 4-6a) and PBS droplets (Figure 4-6b) into RHs of 30%, 50% and 70% have been investigated. For evaporating LB broth solution droplets, the light scattering analysis[190] suggests the formation of NaCl inclusions (NaCl makes up 40% of the mass of LB broth) during evaporation into RHs of 30 and 50% while complete homogeneity is sustained when evaporating at 70% RH (Figure 4-6a). The PBS solution droplets remain homogenous during evaporation into RHs of 50 % and above, but crystal formation is observed when evaporating at an RH of 30% (red point in Figure 4-6b); at this RH, the determination of the size of the crystallized non-spherical particle is not possible.[189] As expected, the efflorescence of PBS was observed to occur at an RH between 30 and 50% which agrees with the known efflorescence RH for NaCl (45-50%).[198] In both Figure 4-6a and Figure 4-6b, the morphology analysis is most certain after the droplets reach equilibrium with their environment, i.e. once the cumulative phase functions become consistent making the phase identification more robust.

To further explore the morphologies formed from the drying of PBS and LB broth droplets at 30% RH, particles were captured for SEM (scanning electron microscopy) analysis (Figure 4-6c and Figure 4-6d). The morphologies are as expected from the light scattering analysis performed in the CK-EDB measurements. Briefly, LB broth particles are broadly spherical in shape (Figure 4-6c and Figure 2-13a) with clear evidence of dendritic salt inclusions, reflecting the likely diffusional limitation due to elevated particle viscosity of these organic-rich droplets formed on rapid drying as inclusions form (60% MFS of organic compounds).[257,258] By contrast, PBS droplets form multiple crystals (Figure 4-6d and Figure 2-13c) as the droplet rapidly dries with multiple nucleation events occurring as the solute concentration surpasses critical supersaturation for efflorescence.[195]

The rapid changes in particle size and water content during drying lead to conditions in the aerosol phase that are not accessible in the bulk liquid (e.g. supersaturated solute, high salt concentrations, ultra-viscous and even glassy states) for nearly all ambient conditions when the RH falls below 70%, potentially impacting the survival of enclosed microorganisms.[126,216,217,259,260] In Figure 4-6e and Figure 4-6f, the time-dependent changes in solute

concentrations accompanying evaporation of non-metabolized LB broth and PBS droplets into gas-phases of 30, 50, 70 and 90% RHs are compared. The dynamics for these solution droplets are simulated using a quasi-steady evaporation model that accounts for the interplay of mass and heat transport during drying and is benchmarked against the experimental measurements.[197]

The impacts on *E. coli* MRE-162 survival of the interconnected changes in size, particle morphology and solute concentrations taking place during evaporation of PBS and LB broth droplets at 300 s are reported in Figure 4-6g and Figure 4-6h. Bacterial survival is reported as the ability of a bacterium to form a colony (colony-forming unit, CFU) after suspension, collection and 24 hr incubation. Overall, an inverse correlation between the final equilibrated solute concentration and *E. coli* MRE-162 survival is observed.

At high RH (90-70%), where all droplets remain homogeneous during evaporation for both droplet compositions, bacteria survival shows a significant decrease in LB broth droplets with a decrease in RH, potentially due to the high solute concentration at 70%. In the case of PBS droplet composition, the reduction in survival with RH is moderate. When comparing LB broth and PBS compositions, there was not a significant difference between survival over this range of RHs. A higher survival at 70% RH (Figure 4-6h) is reported in PBS droplets, possibly due to the higher mass of water, larger droplet size and lower solute concentration when achieving equilibrium with the gas-phase composition (c.f. Figure 4-4 and Figure 4-5).

Under the driest conditions (50 to 30% RH), a significant decline in *E. coli* MRE-162 survival is observed in PBS droplets (Figure 4-6h) compared with a smaller decrease for LB broth droplets (Figure 4-6g). This sudden reduction in survival in PBS coincides with a transition in particle phase, in this case from homogenous droplets to salt crystals (Figure 4-6b and Figure 4-6d). Comparing droplet compositions, a statistically significant difference survival was observed at 50% RH, also matching a difference in droplet morphologies between composition, showing lower survival in LB broth droplets where inclusions where observed in contrast with the homogeneity of the PBS droplets (c.f. Figure 4-6a and Figure 4-6b). Conversely, the survival reported in LB broth droplets at 30% RH is marginally higher than for PBS, likely due to the presence of organic components in LB broth which potentially enhances survival (compare Figure 4-6g and Figure 4-6h).

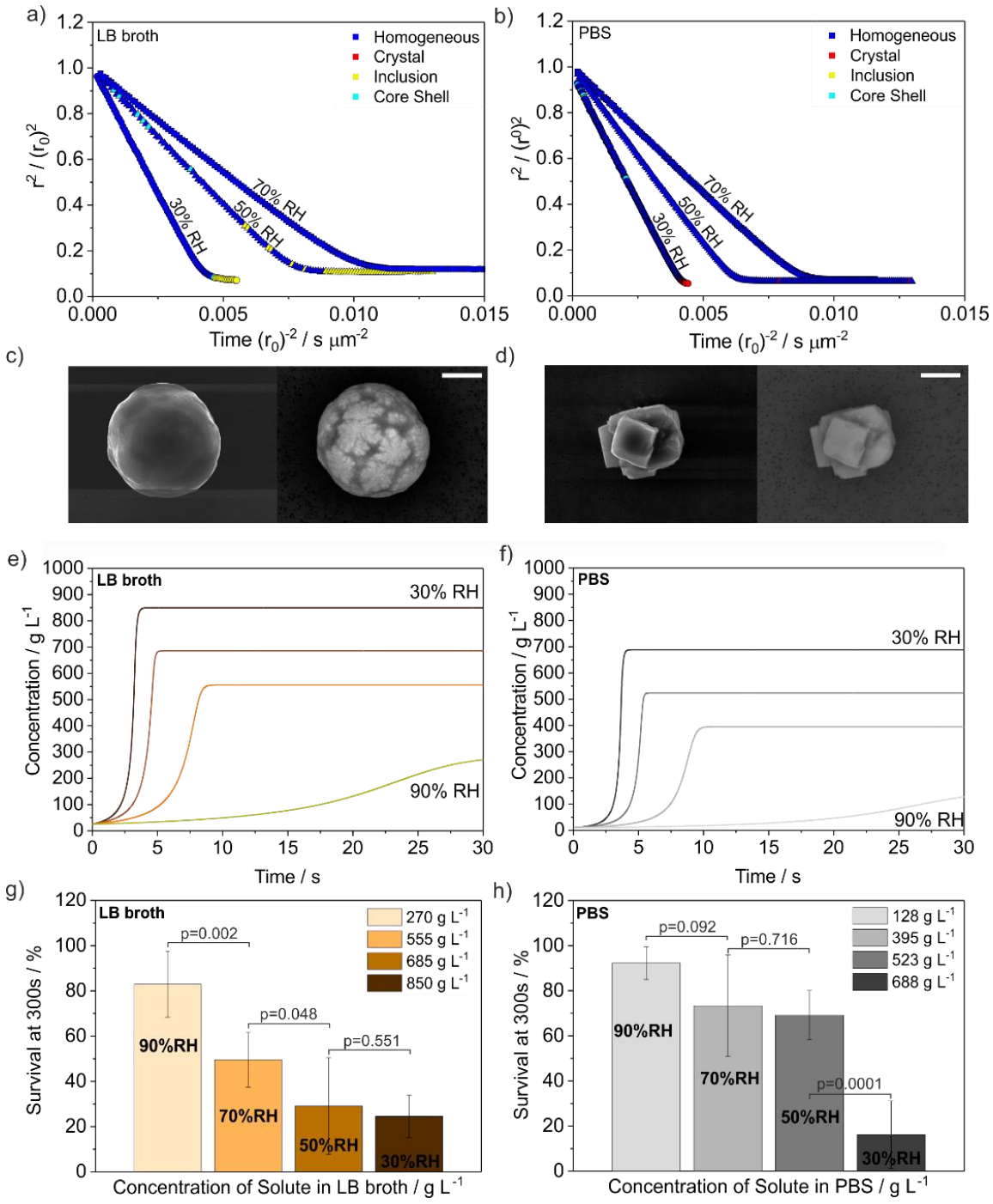

Figure 4-6. Evolution of size and morphology for evaporating droplets of (a) non-metabolized LB broth, (b) PBS into 30%, 50% and 70% gas-phase RHs. Slopes for the linear trend in the radius-squared are -216.7, -118.1 and -90.4 in the case of LB broth droplets and -221.9, -153.4 and -108.7 for PBS droplet composition, each at 30, 50 and 70% RHs, respectively. SEM and backscattered electron images for particles formed from (c) non-metabolized LB broth and (d) PBS at 30% RH are shown. Predicted time-dependent solute concentrations for evaporation of droplets into RHs spanning from 30 to 90% RHs and 20 ℃ for droplets solutions of (e) non-metabolized LB broth and (f) PBS are shown. To simulate the evaporation profiles, a starting radius of 25 μm and concentration of 25 g L-

[1] and 9.5 g L^{-1} for LB broth and PBS were used, respectively. The impact of morphology and solute concentration on airborne bacteria viability at 300 s from droplet generation under RHs of 30 to 90% RH are shown for (g) LB broth and (h) PBS droplets containing *E. coli* MRE-162 (starting concentration of (2.6±0.6)×10^8 CFU mL^{-1}, 28±11 CFU $droplet^{-1}$). *p*-values obtained when comparing LB broth and PBS compositions at 90, 70, 50 and 30% RHs by applying a two-sample t-test are 0.137, 0.079, 0.00 and 0.22, respectively, showing only a significant difference on survival between compositions at 50% RH.

4.5 No loss of Viability is Observed during the Rapid Drying Phase of Bioaerosol Droplets; Bacteria Act as a Crystallization Nuclei

Time-dependent measurements of the viability for *E. coli* MRE-162 ((2.6±0.6) ×10^8 CFU mL^{-1}, 28±11 CFU $droplet^{-1}$) enclosed in LB broth and PBS droplets equilibrated at 30, 50, 70 and 90% RH were performed over 1h, as shown in

Figure 4-7. Due to the gentle aerosolization processes and high-resolution sampling achieved with CELEBS, the CFU observed for the shortest survival measurements (<5s suspension time) agree with the estimated microbial concentrations in the droplets. This expected concentration is estimated from the cell concentration in the suspension loaded into the DoD dispenser, described with a Gaussian distribution when cell concentrations are in the order of 10^8 cells mL^{-1} (Figure 3-4 and Figure 3-5). The efficiency of the sequence of processes (biological sample solution to aerosol droplet creation to aerosol droplet sampling/recovery) has been discussed in detail in Chapter 3. [68] Thus, only the biological decay processes occurring in the aerosol phase need be considered.

Little decline in biological viability over a timescale of 5 s is observed at any of the droplet compositions and RHs (Figure 4-7a and Figure 4-7b). This holds even for the very rapid evaporation and equilibration time at the lowest RHs where the evaporative cooling and rise in solute concentration at the droplet surface can be expected to be most severe (e.g. Figure 4-4 and Figure 4-5). Thus, the dynamic processes taking place (e.g. water evaporation, surface cooling, rapid changes in size and solute composition) seem to not immediately impact *E. coli* MRE-162 survival. The lack of impact of the dynamics occurring during evaporation can be contrasted with current assumptions whereby two different decay constants have been reported, suggested as arising from a rapid initial decay attributed to the drying process and subsequent slower secondary phase associated with oxidative stress and the effect of environmental

conditions. [80,117,119,261–264] These studies were performed by using reflux atomization for aerosol generation and various methodologies for particle suspension such as the rotating drum and the static and dynamic storage chambers. [117,119,261,262,264].

The marginal decay observed up to 5 s suggests that previous reports of a rapid initial loss of viability (with decay constants of 1 sec) [117,262] are likely not occurring in the aerosol phase, but may be a systematic artefact of the aerosolization process used since many aerosol generators impact the structural integrity of microorganisms when nebulized.[33,137] Further, the disturbance in gas-phase conditions produced by the cumulative mass of water introduced to the system by the cloud of droplets from nebulisers is often not contemplated and, therefore, the conditions studied are not often precisely reported during droplet evaporation (tens of minutes may be necessary for the droplet cloud to reach equilibrium).[265] The ability to determine microbial decay during dynamic microphysical processes in the aerosol phase is unique to TAMBAS approach.

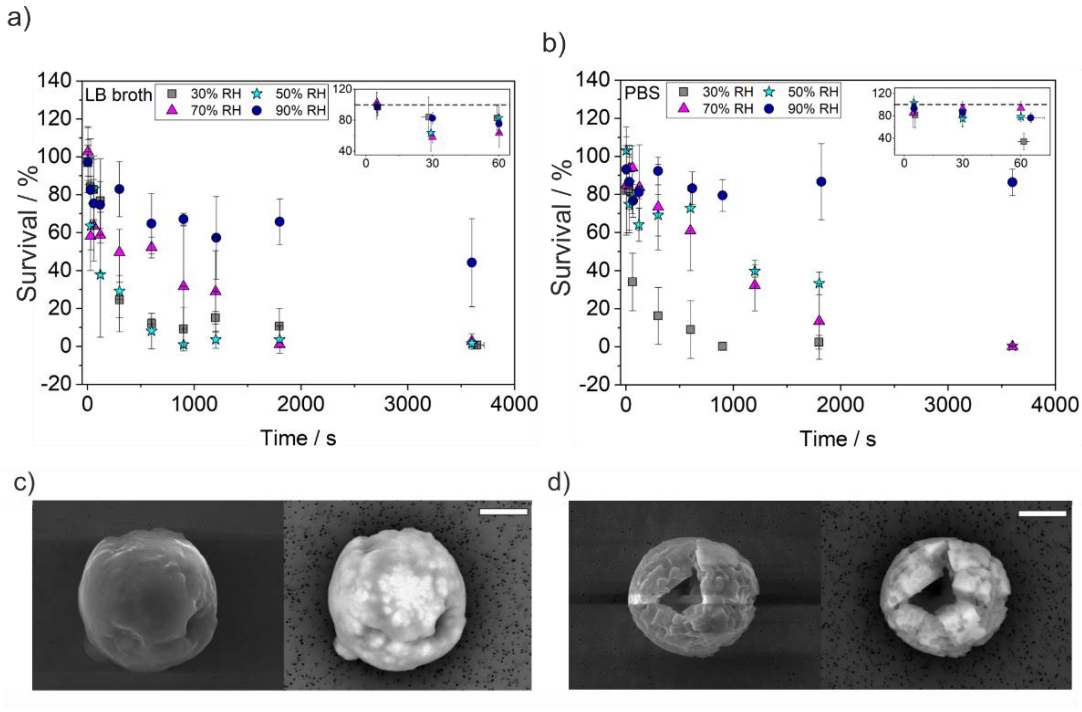

Figure 4-7. Relationship between solute compositions and survival for *E. coli* MRE-162 (2.6±0.6 10^8 CFU mL^{-1}) as a function of RH in (a) LB broth and (b) PBS droplets. Note that in (b), the data points for 50% and 70%RH at 3600s overlap. Insets show the survival during a timeframe of 60 s levitation. SEM and backscattered electron images for (c) LB broth and (d) PBS droplets containing *E. coli* MRE-162 at (2.6±0.6) ×10^9 CFU mL^{-1} at 30% RH. Scale bars represent 5 μm.

The time for the first decay is apparent in Figure 4-7 and is considerably longer that the time required for the droplets to reach thermodynamic equilibrium, a time that is dependent on RH (Figure 4-4 and Figure 4-5). Interestingly, a significant decrease in airborne bacteria viability (compared to 5s measurement) is observed only at the lowest RHs (30 and 50%) for droplets composed of PBS during the first 60 s of suspension (*p-values* of 0.00004 and 0.00015 respectively). In contrast, the loss of viability was significant only at the highest RHs (70 and 90%) (*p-values* of 0.0013 and 0.0001 respectively) in the case of LB broth droplets. This general trend describing greater survival in PBS droplet composition at high RHs is maintained at longer timescales. Thus, no significant decay is observed at 90% RH after 1h suspensions for droplets composed of PBS (*p-values* of 0.2) while the reduction on viability is significant for droplets with LB broth composition (*p-values* of 0.00005). This divergence in survival in droplets of different compositions may be a result of the higher solute hygroscopicity of PBS, linked to greater water content in the droplets and lower solute concentrations (Figure 4-4b and Figure 4-5b).

Interestingly, the structure of bacteria containing PBS particles dried at 30% RH observed in the SEM analysis show *E. coli* MRE-162 cells embedded in the salt crystals, coinciding with a considerable increase in the overall number of crystals when compared with pure PBS droplets (compare Figure 4-6d with Figure 4-7d and Figure 2-13c with Figure 2-13d), consistent with bacteria acting as crystallization nuclei. Conversely, little change in the phase behaviour of LB broth is observed when containing bacteria (compare Figure 4-6c with Figure 4-7c and Figure 2-13a with Figure 2-13b).

4.6 Droplet Size Affects Airborne Bacterial Viability

To isolate the effects of different factors (such as solute concentration and droplet size) impacting airborne bacterial survival, the viability response of *E. coli* MRE-162 levitated for 300s in droplets of LB broth with different initial solute concentrations equilibrating at 50%RH are compared in Figure 4-8c.

The evaporation profiles of three different starting concentrations of non-metabolized LB broth are reported in Figure 4-8a. The different initial concentrations lead to different equilibrated sizes although each achieves the same concentration of LB broth and moisture content when reaching an equilibrium at a specific RH (Figure 4-8b), thereby having the same density. Thus, evaluation of solely the effect of different particle sizes containing the same solute concentration at equilibrium is possible. This is a unique and important element of this approach. The data in Figure 4-8c suggests that either particle size and/or the dynamic processes during evaporation plays a crucial role in the survival response of *E. coli* MRE-162.

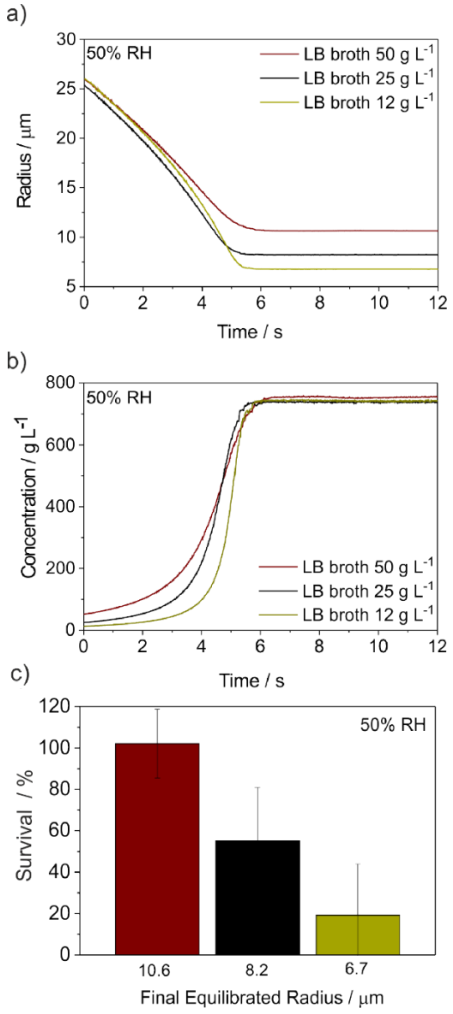

Figure 4-8. Effect of droplet size on airborne bacterial survival . (a) Comparison of the measured (a) particle size and (b) changes in solute concentration (g L^{-1}) of LB broth droplets with different initial solute concentrations evaporating into 50% RH and 20 ℃. (c) The effect of the equilibrium particle size on bacteria viability. All the survival data are expressed as the average and standard deviation for three replicates per experiment were populations from 2 to 6 droplets were levitated.

4.7 Outline of the Relationships Between Aerosol Microphysics and Bacteria Viability

The relationship between ambient RH and airborne *E. coli* bacteria viability can be summarized in three different regimes for LB and PBS particle compositions:

- *Dry conditions (< 50 % RH).* Most of the water is rapidly lost during evaporation, producing important changes in particle size, solute concentration, phase and particle morphology. In this humidity regime, salt concentrations reach supersaturated states which are not accessible in the bulk liquid phase and usually crystallize. A reduction in the viability of *E. coli* MRE-162 was observed in this region, but this reduction was not directly a function of the phase change itself. The survival of bacteria in LB broth droplets at 30% RH is slightly higher than in PBS droplets, likely due to 60% of organic solute content contained in the LB broth solution, mostly amino acids and long-chained fatty acid which lead to fundamentally different phase behaviour. The differences in survival trends for both compositions in this RH regime might be due to the different solute hygroscopicity producing different changes in the particle size, solute concentration and the relative mass of water intake when increasing the RH. The relative change between wet and dry particle size for PBS and LB broth particles (i.e. change in the radial growth factor) at RHs below 50% is estimated by a using a correlation between GF_r and RH (Figure 4-9),[201] observing a steeper change in the relative particle size for PBS droplets, undergoing a higher increase in volume. A detailed comparison of the hygroscopic properties for LB broth and PBS droplet solutions are also presented in Figure 4-2.

- *Intermediate conditions (~50 to 70% RH).* Here, the difference in survival is not significant for both LB and PBS compositions in this range of RH. There are no significant changes taking place in the morphology of the droplets, with little change in water content with RH and little variation in the ratio of wet and dry particle mass (mass growth factor) for both PBS and LB broth droplets (Figure 4-2). For RHs above 50%, the higher solute hygroscopicity of PBS promotes greater water retention (and hence larger droplet size) than for LB broth particles at the same RH and for particles

containing the same dry solute mass. Thus, lower solute concentrations exist in PBS droplets perhaps explaining the observed greater survival.

- *Wet conditions (>70%).* Greater retention of water mass takes place for both compositions, particularly in the case of PBS due to its higher hygroscopicity (Figure 4-2) coupled with a reduction in evaporation rate (Figure 4-5a). The size of the particles at 90% RH is much larger than at lower RHs and hence the salt concentration is at levels that are not harmful to the microorganisms. In this regime, the *E.* coli MRE-162 survival in PBS droplets seems to be independent of RH up to one hour in the aerosol phase (Figure 4-7).

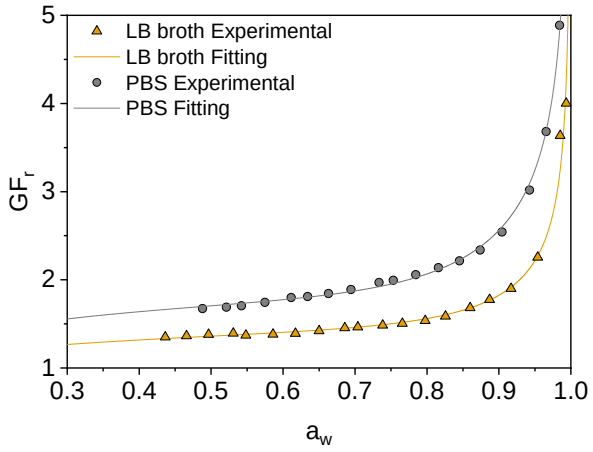

Figure 4-9. Comparison of the *GFr* for LB broth (orange) and PBS (grey) droplets . The fitting does not account for the change in morphology therefore the real equilibrium size is smaller than that obtained by using the model. The morphology change leads to the formation of inclusions and crystals in the case of LB broth and PBS respectively (Fig. 4); this event takes place in a water activity (equivalent to RH) interval between 0 and 0.4 where the estimated equilibrium size is not accurate. Thus, the relative change in the size of the particle during water intake is steeper than estimated for both droplets' compositions.

The capability of this approach to further explore the connection between aerosol microphysics and the survival of airborne microbes is shown in Figure 4-10. Here, three physicochemical properties (e.g. salt concentration, volume reduction and temperature suppression) are correlated with the viability decay of *E. coli* MRE-162 at different suspension time intervals in the aerosol phase (i.e 120, 600 and 1800). Generally, the more stochastic correlations shown in the shortest suspension times (i.e. 120 s) are notably sharped as a function of time in the

aerosol phase for the properties related to the evaporative process (Figure 4-10b and Figure 4-10c).

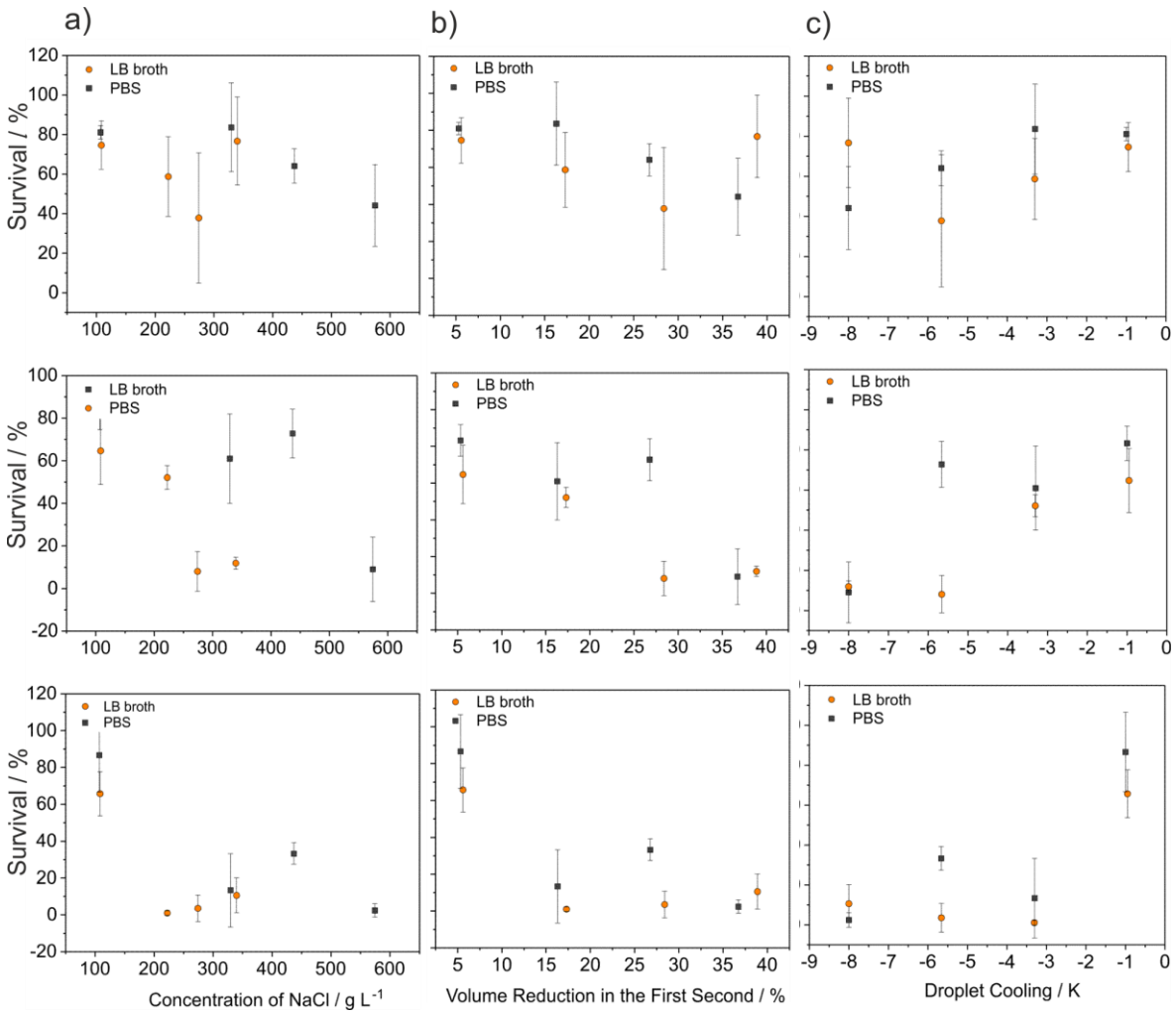

Figure 4-10. Relationship between physicochemical and biological properties . Specifically, the effect of (a) NaCl concentration (b) evaporation rates and (c) droplet cooling on the viability of *E. coli* MRE-162 contained in LB broth and PBS solution droplets at 120, 600 and 1800 seconds (from top to bottom) of suspension in the aerosol phase is reported.

Figure 4-11 shows *E. coli* MRE-162 viability at 300 s of suspension as a function of six different parameters (droplet cooling, volume reduction, surface-to-volume ratio, concentration of NaCl, concentration of solute and droplet volume) where only three (Figure 4-11b and Figure 4-11e) demonstrate a large collective correlation for both particle types (e.g. PBS and LB broth) reporting R^2 values of 0.78, 0.80 and 0.87 for droplet cooling, volume

reduction and solute concentration, respectively. These correlations of viability with droplet cooling, volume reduction and solute concentration, are all associated with the initial water mass flux from the droplet at the point of generation. Thus, although there is no apparent loss in viability during the drying phase (first 5-10 seconds), the impact of the initial mass flux from the droplet on microbe longevity, and overall change in size (Figure 4-8), is consistent with an impact on viability over longer timescales. Put simply, the data suggest that the initial evaporation dynamics of the bioaerosol have a pronounced and predictable delayed effect on bioaerosol survival and should be further explored.

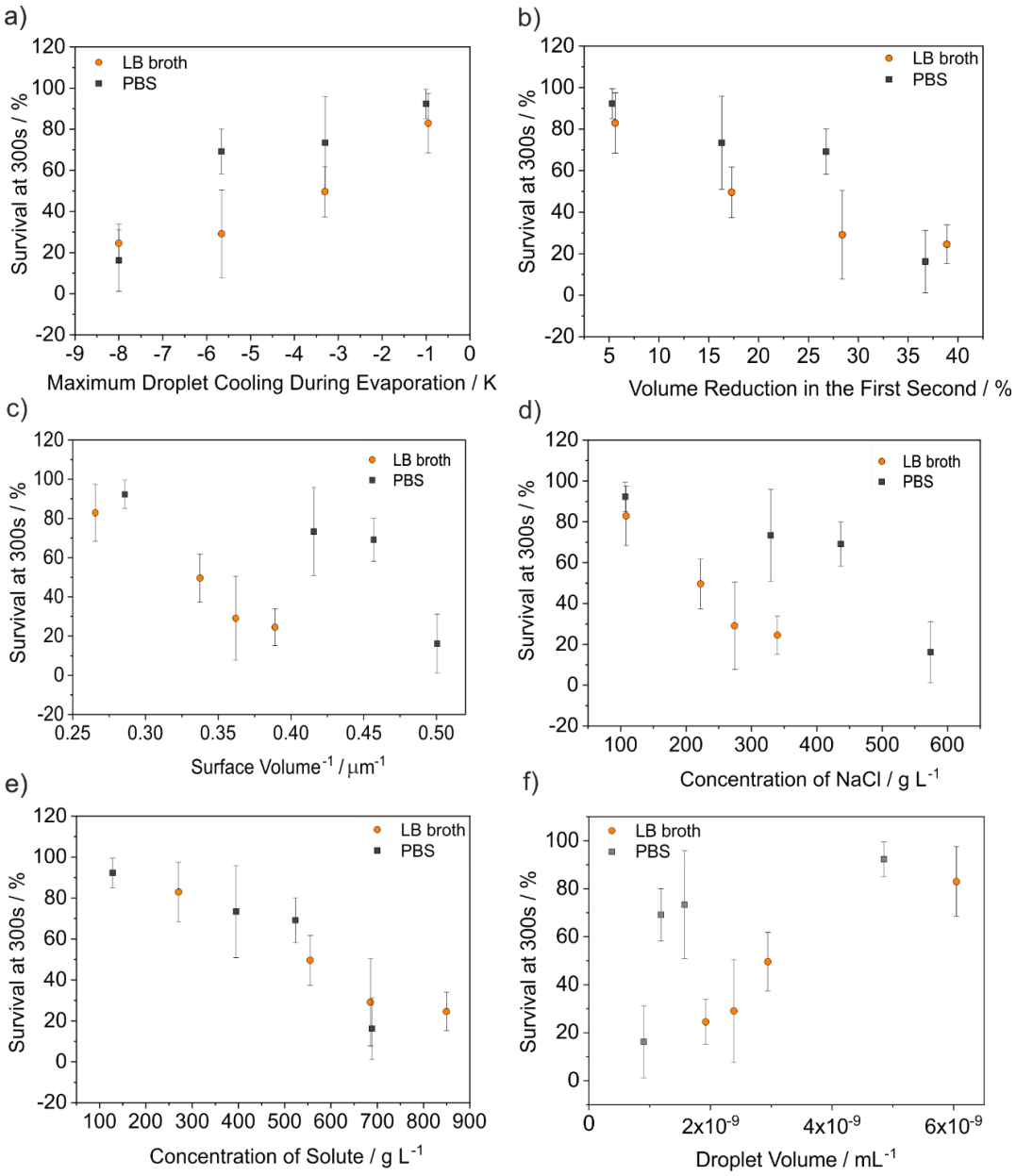

Figure 4-11. Correlation between changes in physicochemical properties and survival of *E. coli* MRE-162. Specifically, (a) Maximum droplet cooling, (b) Evaporation rates in terms of change of droplet volume within the first second after aerosolization, (c) Surface-to-volume ratio, (d) NaCl concentration in the droplets at the thermodynamic equilibrium, (e) Total solute concentrations (organic and inorganic compounds) and (f) Droplet volume when evaporating at 30, 50, 70 and 90% RH. Note that the values for the physicochemical properties were estimated using the kinetic model for a droplet of 25 µm initial radius and concentration of 25 and 9.5 g L^{-1} for LB broth (orange circles) and PBS respectively (grey squares).

4.8 Summary and Conclusions

The novel TAMBAS approach presented provides the opportunity to explore the effect of individual parameters on airborne survival which could be crucial for fully understanding the fundamental mechanisms that control the transmission of airborne diseases. The ability to measure the impact of aerosol dynamics on the survival of microorganisms in the aerosol phase while reducing stresses involved in the generation, suspension and sampling processes is unique to this technique. Previous studies performed with evaporating sessile droplets (i.e. droplets deposited on surfaces) [177] or conventional technologies [116,266] are often not representative of the natural mechanisms involved in the airborne transmission of disease. Therefore, data comparison becomes challenging due to the wide variety of methodologies, bioaerosol compositions and environmental conditions employed in survival studies.

Ultimately this transformative approach will contribute to a more complete understanding of the fundamental factors influencing the airborne transmission of pathogens enabling the development of refined hazard mitigation strategies.

Chapter 5

Inactivation Mechanisms of Airborne Pathogens in Biologically Representative Respiratory Droplets

The results presented in this chapter are subject of two manuscripts in preparation for publication. I confirm that the presented work is all my own and I acknowledge Jonathan P. Reid, Allen E. Haddrell and Richard J. Thomas for their supervision and advice on the interpretation of experimental data.

The preceding chapters discuss the methodology developed to investigate the survival of airborne pathogens. In Chapters 2 and 3, the theory and validation of this approach were introduced. The experimental data provided in Chapter 4 consolidated the methodology as well as elucidated some of the key microphysical parameters impacting the viability of airborne pathogens. In this chapter, aerosol microphysics and microbiological properties are correlated with the survival of airborne bacteria contained in biologically representative solutions in aerosol droplets. First, experimental measurements of the physicochemical properties of these complex mixtures (e.g. hygroscopicity, evaporation dynamics and droplet morphology) will be presented. This work aims to fully understand the equilibrium, dynamic and surface properties of artificial respiratory secretions in aerosol droplets. Secondly, the biological response of airborne bacteria as a function of time and RH in the same droplet compositions will be studied. The chapter also reports the experimental measurement of the impact of relevant physicochemical and microbiological properties (e.g. presence of surfactants, microbial concentration, cell physiology, changes in the droplet chemical composition, surface enrichment, etc) on airborne survival, allowing the determination of the main mechanisms of death for airborne respiratory pathogens.

5.1 Introduction

The current SARS-CoV-2 pandemic presents an enormous health and economic challenge for the entire world. To develop public health strategies, epidemiological models are used to predict the progression of infectious diseases and the success of mitigation measures such as non-pharmaceutical interventions, reporting a range of potential outcomes which can be conflicting. These models are dependent on numerous parameters which, in the case of a novel pathogen, are unknown and in turn limits their performance. With the on-going pandemic and recurrent cases of new outbreaks in the last decades,[267,268] there is an emerging need to fully and rapidly understand the underlying complexity and interconnectivity among the different mechanisms that drive the transmission of airborne pathogens. This deeper understanding would enable prediction of the longevity of pathogens across a wide range of conditions eluding the need to measure the impact of every single parameter independently. The ability to measure bioaerosol survival at the detail which enables one to characterize these processes individually in the aerosol phase has not been possible until recently.[10,68]

We propose here a comprehensive and robust *in vitro* approach to predict pathogen longevity as a function of specific mechanisms that can be grouped into 5 contributing and competing rates (Figure 5-1). The overall microbial death rate is a result of the cumulative effect of each one of these processes, where each impacts the viability of the airborne microorganisms through different processes. The overall aim of this approach is to be able to predict longevity through a better understanding of the underlying mechanisms of pathogen inactivation. The effect that each of these subcategories has on *E. coli* MRE-162 longevity within the TAMBAS approach has been explored independently.[10] For example, consider the impact of the aerosolization device on the viability of the microorganisms: the effect of conventional aerosolization devices on viability has been assessed in the literature, reporting a loss of physiological function which is linked to mechanical stress caused by high aerosolization pressures and shear forces.[130,137,250] In addition, a comparative study to examine the effect of two aerosolization methods (using the 1-jet refluxing nebuliser and the DoD dispenser) on membrane integrity of *E. coli* MRE-162 was previously published.[68] Results showed that the waveform and induction electrode parameters used with the DoD dispenser caused no structural damage to bacteria cells, on the contrary, membrane integrity was reduced 67% after 20 min of nebulization when using the 1-jet refluxing nebuliser, demonstrating that both

mechanisms are fundamentally different. Thus, an extensive body of evidence about the impact of different aerosolization devices on airborne microbial viability has been reported.[115,130,137,250] However, while it is clear that the aerosolization process itself affects microbe health, what is unclear is the knock-on effect that this damage has over time, and across conditions. For example, the effect of solute concentration, droplet size, temperature, microbial concentration, and surface to volume ratio has on bacterial longevity needs to be considered.

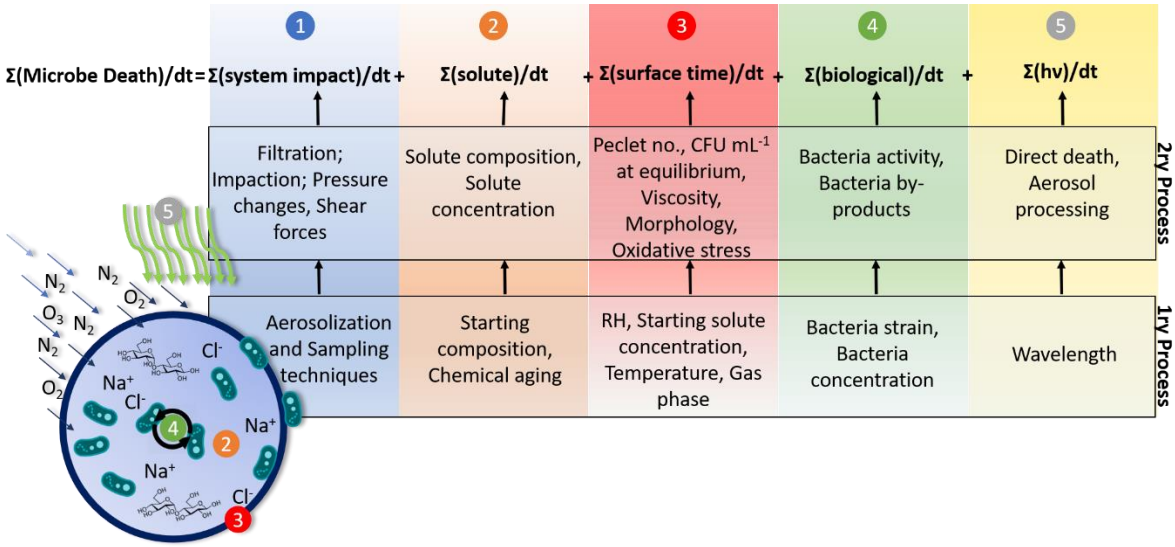

Figure 5-1. Novel *in vitro* approach to predict the death rate of airborne pathogens as a cumulative effect of different mechanism impacting the viability of microbe's viability. Note that aerosol generation and sampling effects will occur at either end of the experimental system. The primary effect is the driving parameter (e.g. RH) while the secondary effect is the property of the aerosol affected by the primary parameter (e.g. viscosity).

The paradigm illustrated in Figure 5-1 describes a sequence of mechanistic steps by which one can systematically accumulate individual effects on longevity through an understanding of the underlying mechanisms of microbial harm/death. With this more complete comprehension, one should be able to accurately predict microbe survival in various environments/aerosol compositions/timescales without needing to make numerous measurements and enable extrapolation between laboratory datasets by understanding some fundamental aspects of the aerosol system.

In this work, the effect of drying kinetics, surface enrichment, particle morphology, solute composition, microbial concentration, and bacterial physiology on airborne bacterial survival are reported. With this approach, it is possible to explore the role of each of the various

categories (specifically 1 to 4) described in Figure 5-1 and obtained the combined impact of the main parameters affecting the survival of bioaerosols by using the proposed equation (Figure 5-1). This is a comprehensive approach to describe the real-world airborne disease transmission whose outcomes will potentially enable more impactful control strategies.

5.2 Physicochemical Properties of Representative Respiratory Aerosol Droplets

5.2.1 At Equilibrium: The Water Content (Hygroscopicity) of Artificial Respiratory Secretions

The hygroscopic properties of artificial respiratory droplets (i.e. artificial saliva and artificial sputum) were characterized for the first time by using the comparative kinetics technique with the CK-EDB (Section 2.2.1). In Figure 5-2, the relationships between solute composition with the ambient RH for droplets made of representative respiratory secretions are compared with previously published hygroscopicity measurements for common microbiological media (i.e. LB broth and PBS solution droplets)[10] and the E-AIM (extended aerosol inorganics model) model predictions for NaCl.[200]

In general, aerosol droplets containing a large solute fraction of inorganic compounds, such as phosphate-buffered saline (PBS) and NaCl, have higher hygroscopicity than droplets containing a significant organic solute fraction. Both LB broth (60% of the mass arising from organic components) and artificial sputum (80% of organics by mass) report similar hygroscopic responses. Unexpectedly, the artificial saliva droplets were the least hygroscopic of the series despite high salt content (approximately 95% of salts by mass). Once the hygroscopicity is determined, it is possible to assess the impact of solute concentration changes on the survival of the microbial components of the aerosol. For instance, considering an artificial saliva droplet, its solute weight percent will change from 15% to 50% when the ambient RH decreases from 90% to 50%. This dramatic change in concentration will be expected to influence microbial health. Developing these interconnections between physicochemical parameters and microbial viability is crucial to fully understand the inactivation of microorganisms in the aerosol phase.

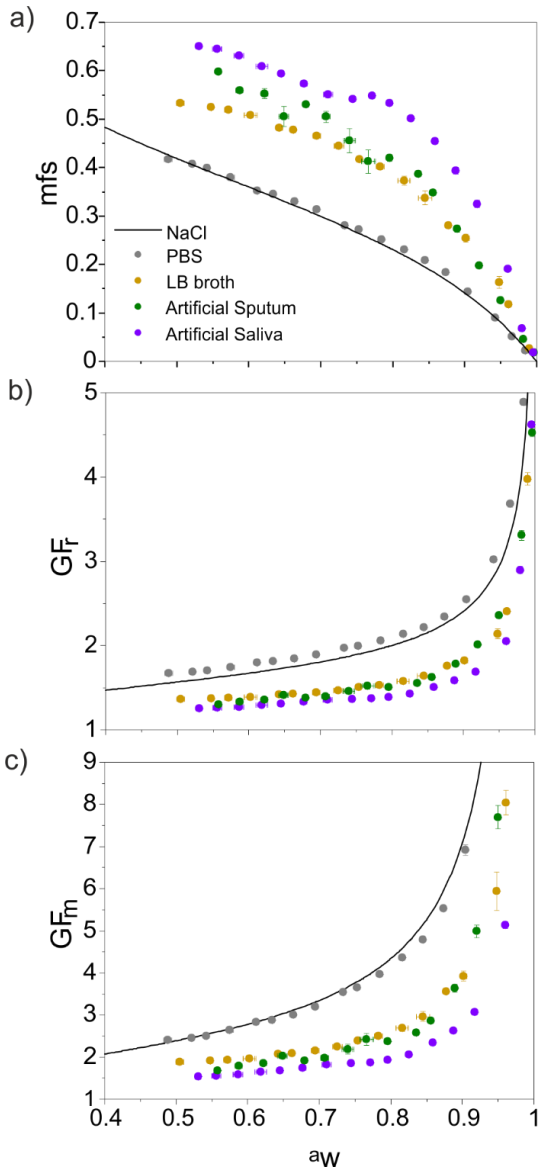

Figure 5-2. Hygroscopic response of various droplet solutions (e.g. PBS, LB broth, artificial saliva and artificial sputum) as a function of droplet water activity (a_w), equivalent to the gas-phase RH, presented in terms of (a) mass fraction of solute (MFS), (b) mass growth factor (GF_m) and (c) and radial growth factor (GF_r). The predicted curve for the hygroscopicity properties of NaCl (line) from the Extended Aerosol Inorganic model (E-AIM) is shown for reference purposes.

Changes in equilibrium composition of aerosol droplets, principally changes in water content, as a function of atmospheric conditions are likely to impact on airborne transmission mechanisms. Linking equilibrium solution compositions with airborne survival data enables determination of the key physicochemical parameters of airborne particles (e.g. water mass,

solute concentration, particle size) impacting bioaerosol survival. This capacity to predict the important parameters for survival/infectivity/viability in the aerosol phase will support a faster implementation of mitigations (i.e. tailor the RH and temperature in indoor environments, identify the risk factor that enhance the spread of disease, etc)

5.2.2 Mass Transport During Evaporation: Modelling Aerosol Droplets Composed of Artificial Respiratory Secretions

An accurate understanding of the mass and heat transport accompanying the evaporation or condensation of water from aerosol droplets composed of respiratory fluids is increasingly recognized to be critical to predict the risks in the airborne transmission of disease.[10,110,124,269] Aerosol droplets expelled when speaking, coughing and sneezing will evaporate to equilibrate with the surrounding atmosphere. The rate of mass and heat transfer to and from respiratory droplets is determined by the conditions of the gas-phase and the droplet composition, specifically the water activity of the solution phase. Evaporation on exhalation frequently leads to rapid and dramatic changes in solute concentration, droplet size and even droplet temperature. Thus, aerosol particles can exhibit supersaturated states with solute concentrations higher than the solubility limit for macroscopic solutions, enhanced reactivity rates[270,271] and even unique phase behaviour[255] due to their chemical and physical characteristics. The kinetics of mass and heat transfer will not only impact the viability of the microorganisms enclosed in a respiratory droplet but also the lifetime of the droplets during aerosol transport and even their deposition in the respiratory system when droplets are inhaled by an exposed individual.[35,63,254,256] These unique attributes highlight the need to understand the effect that the microphysical properties of aerosols play in airborne disease transmission.

Our model predictions of evaporating artificial respiratory droplets into a wide range of RHs (Figure 5-3, Figure 5-4, Figure 5-5 and Figure 5-6) yield the time-dependent changes in size, solute concentration, surface-to-volume ratio and temperature suppression experienced by aerosol droplets as a function of the gas-phase RH. The kinetic simulations reported here were obtained using the mass and heat transport equations from the Kulmala model[197] and the parametrization of density for each droplet solute. Specifically, the model predictions included in Figure 5-3, Figure 5-4, Figure 5-5 and Figure 5-6 are for droplets composed of artificial

saliva, artificial diluted (1:10) saliva, artificial sputum and artificial diluted (1:10) sputum, respectively. All the dynamic changes take place over a time period of less than 30 s regardless of the ambient RH. Note that the simulations presented in this section are for relatively large droplets (similar to those in a sneeze).

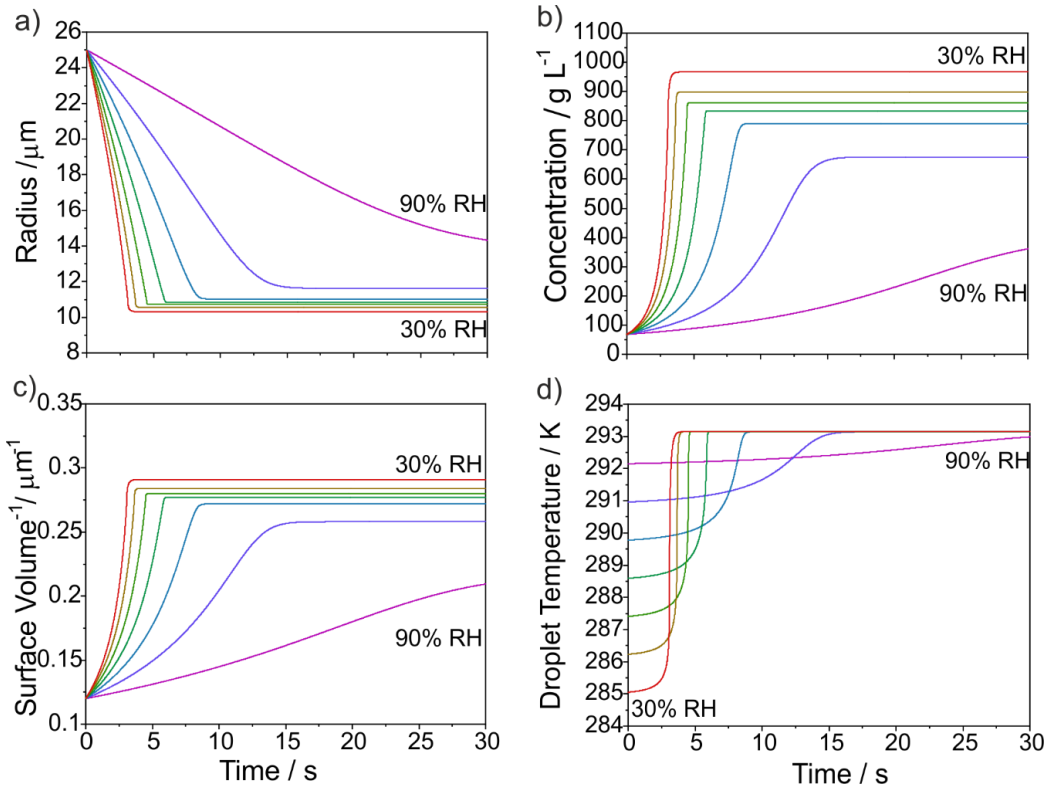

Figure 5-3. Modelled dynamics for artificial saliva droplets (neat concentration). Specifically, model results of the time-dependent (a) evaporating radius, (c) solute concentration, (c) surface-to-volume ratio and (d) temperature suppression for droplets equilibrating over a RH interval between 30 and 90% at 20℃.

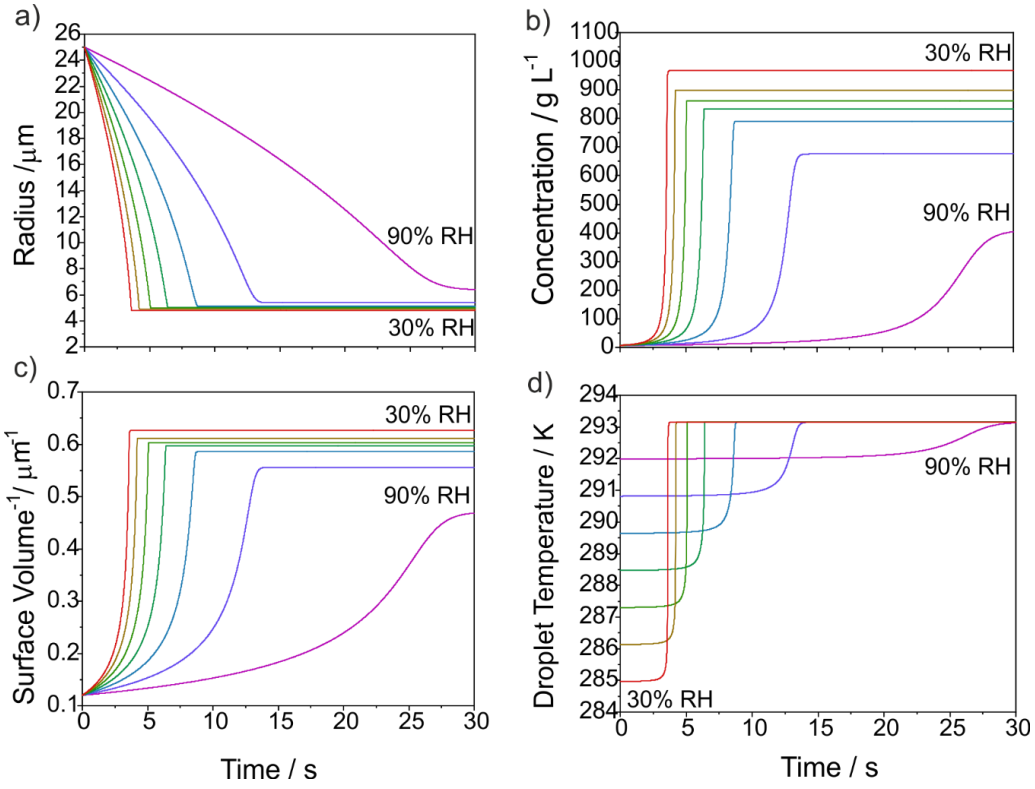

Figure 5-4. Modelled dynamics for diluted artificial saliva droplets . Specifically, model results of the time-dependent (a) evaporating radius, (c) solute concentration, (c) surface to volume ratio and (d) temperature suppression for droplets equilibrating over a RH interval between 30 and 90% at 20℃.

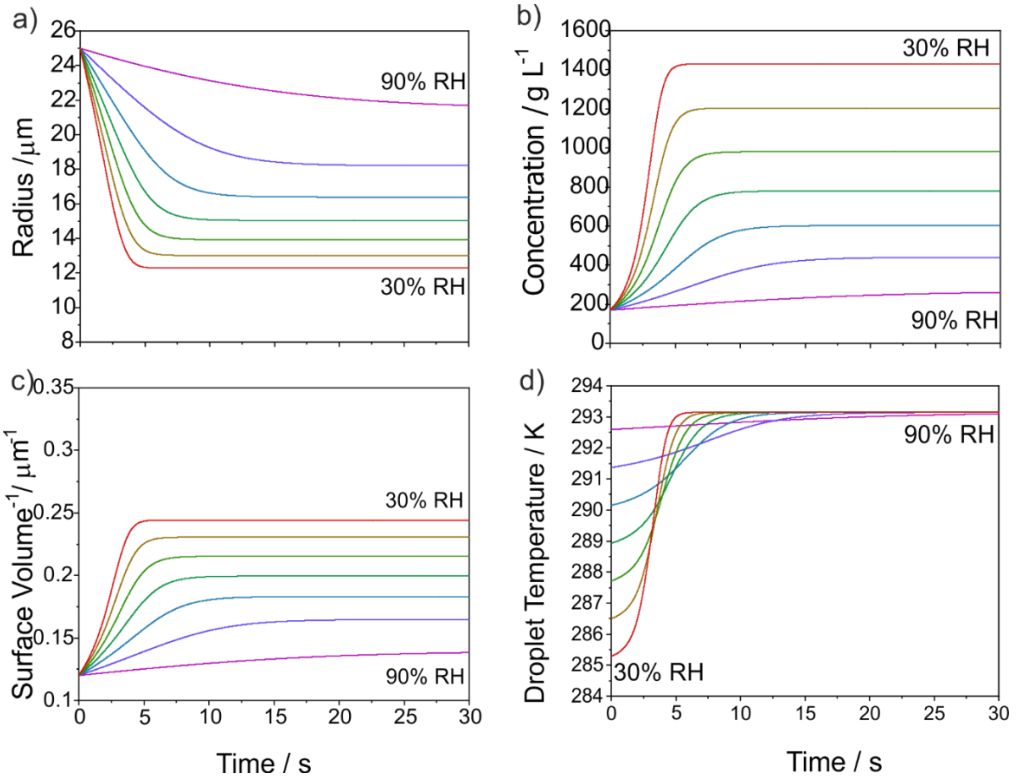

Figure 5-5. Modelled dynamics for artificial sputum droplets. Specifically, model results of the time-dependent (a) evaporating radius, (c) solute concentration, (c) surface to volume ratio and (d) temperature suppression for droplets equilibrating over a RH interval between 30 and 90% at 20℃.

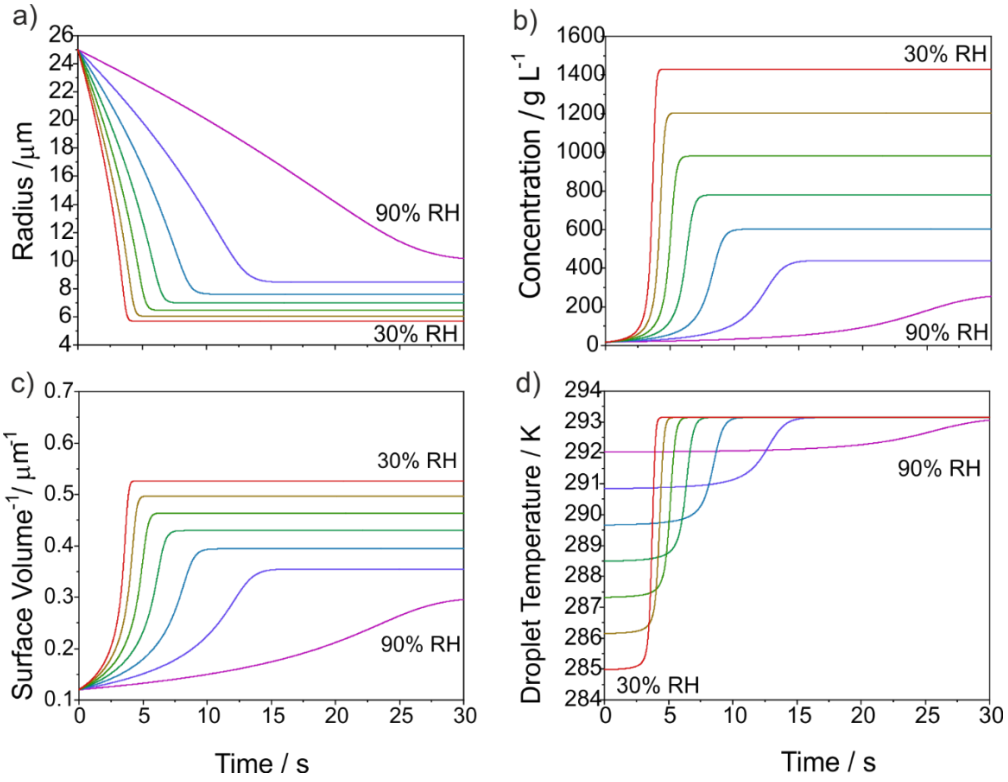

Figure 5-6. Modelled dynamics for diluted artificial sputum droplets. Specifically, model results of the time-dependent (a) evaporating radius, (c) solute concentration, (c) surface to volume ratio and (d) temperature suppression for droplets equilibrating over a RH interval between 30 and 90% at 20℃.

5.2.3 Surface Properties and Morphologies of Bioaerosol Droplets/Particles with Different Respiratory Fluids

The TAMBAS approach[10] presents the unique possibility of connecting microphysics with bioaerosol survival measurements made in the aerosol phase by combining the CK-EDB and CELEBS instruments, while allowing subsequent extraction of the aerosol particles from the gas-phase atmosphere for analysis off-line. To compare the particle morphology of dried bioaerosol particles with different compositions, we generated populations of bioaerosol particles and levitated them for 120 s in varying gas-phase RHs in the CELEBS system. The micro-dispenser parameters have similar values to the ones used during the evaporation measurements in the CK-EDB system, aiming to correlate the particle morphologies observed under SEM microscopy with the corresponding Peclet values (Pe) characteristic of the dynamic drying process studied in the CK-EDB (Section 2.2.1.5). Once dried, the particles were

collected onto a nitrocellulose membrane filter placed in a Petri dish located in the substrate holder of the CELEBS instrument and analyzed offline using an SEM microscope as described in the Section 2.2.6. Figure 5-7 shows the SEM and backscattered micrographs of different bioaerosol particle compositions obtained after evaporation under 10 and 30% RH.

Under 30% RH, an agglomerate of *E. coli* cells is obtained as a result of levitating the bacteria at a concentration of ~10^8 cells mL^{-1} in water solution droplets (Figure 5-7a). Under 10% RH, the evaporation of LB broth solution droplets containing ~10^9 cells mL^{-1} leads to the formation of spherical microparticles with dendritic salt inclusions more noticeable in the backscattered images (Figure 5-7b). The complex mixture of salts and nutrients (40% and 60% by mass respectively) in the LB broth solution appears to form a surface shell surrounding the bacteria cells in the interior of the particle. The organic components of LB broth, when dried become more viscous[125] and are likely to produce a diffusional limitation in the evaporation of droplets with this composition.

Under the same drying conditions, the PBS solution droplets containing bacteria at a concentration of 10^9 cells mL^{-1} show the formation of multiple crystals (Figure 5-7c). The backscattered images show the bacteria cells confined on the surface of the salt crystals, reflecting the location of the bacteria when the crystallization event occurs. Finally, the droplets composed of artificial saliva and *E. coli* cells at a concentration of 10^9 cells mL^{-1} show clear surface deformations resembling buckled morphologies typical of drying at high Pe number when dried at 30% RH. The changes in particle structure of PBS droplets containing *E. coli* MRE-162 cells transitioning across 10, 30 and 50 % RH are presented in Figure 5-8 where a clear diffusion of bacteria cells from the crystal-particles surface is observed as a function of the increasing RH due to the longer crystallization times, increasing the chances of bacteria to diffuse towards the centre of the bioaerosol droplets.

The interplay between Peclet number, droplet viscosity and microbe location will be discussed in great detail in Section 5.4.2.2.

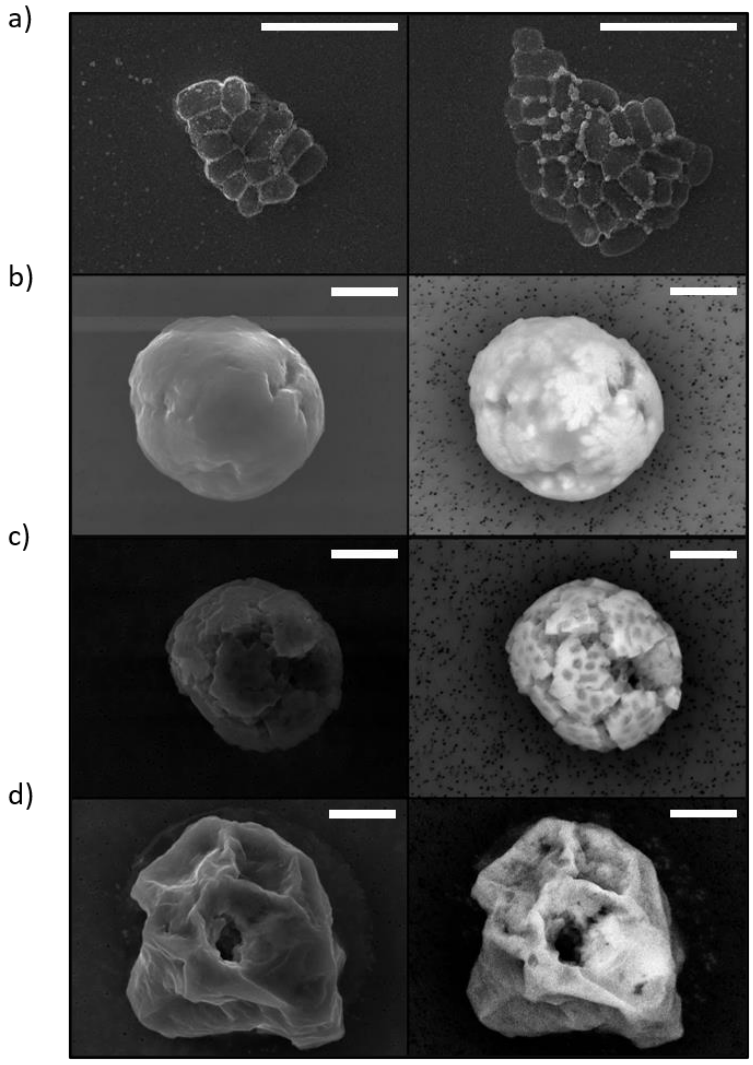

Figure 5-7. SEM images of the particle morphology for various droplet compositions containing *E. coli* MRE-162 cells. Specifically, a) both SEM images of bacteria at a concentration of ~10^{-8} CFU mL^{-1} sprayed in water at 30% RH; b) SEM and backscattered images of bacteria at a concentration of ~10^{-9} CFU mL^{-1} in LB broth droplets at 10% RH, c) SEM and backscattered images of bacteria at a concentration of ~10^{-9} CFU mL^{-1} in PBS droplets at 10% RH and d) SEM and backscattered images of bacteria at a concentration of ~10^{-8} CFU mL^{-1} in artificial saliva droplets at 30% RH. Scale bars represent 5 μm.

The impact of particle morphology in bioaerosol survival is largely unknown. Previous studies have linked changes in particle morphology with sudden reductions in the survival of airborne bacteria. [10] The effect of particle morphology and surface properties of aerosols has been demonstrated to play an important role in the optical properties of aerosols affecting radiative forcing and climate,[272,273] the atmospheric chemistry underwent at the surface of aerosol

particles[274] and even the spray-drying industrial processes of pharmaceuticals and food products.[275] Inherently, different surface composition/chemistry will have a fundamentally different impact on the biological properties of the particles.

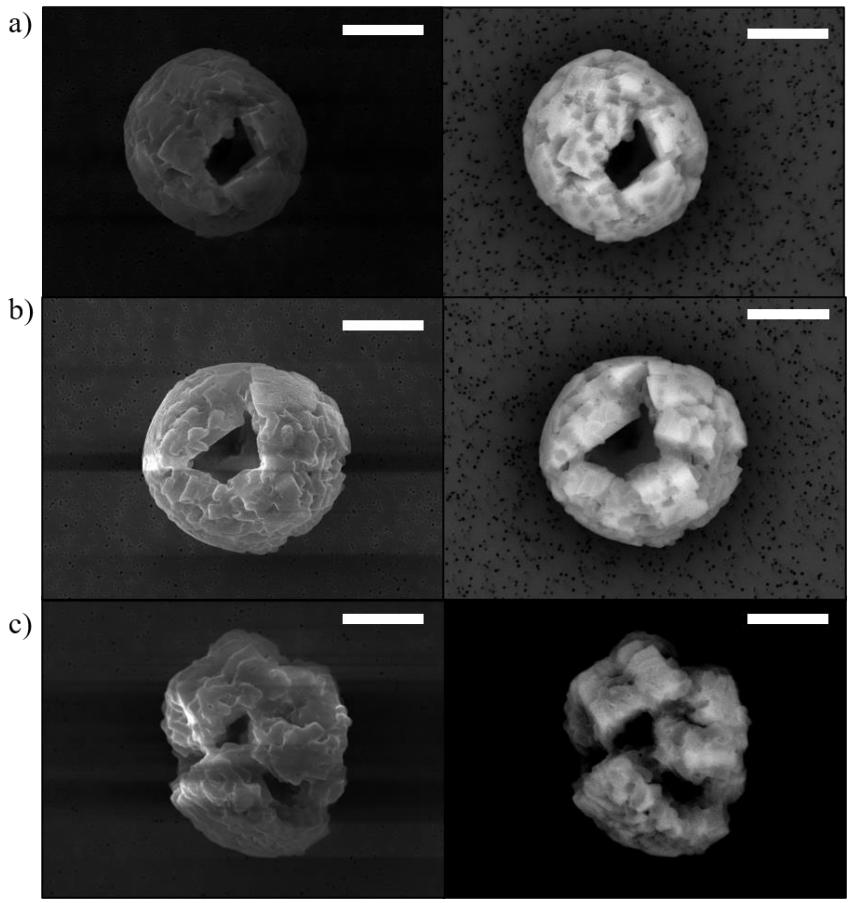

Figure 5-8. SEM images of *E. coli* MRE-162 cells at a concentration of ~10^9 CFU mL^{-1} levitated in PBS droplets at (a) 10%RH, (b) 30% RH and (c) 50% RH. Scale bars represent 5 μm.

5.3 Biological Response of Airborne Bacteria in Representative Respiratory Aerosol Droplets as a Function of Time and RH

5.3.1 Time-Dependent Measurements of the Viability of Bacterial Survival in Artificial Respiratory Secretions as a Function of the RH

Bioaerosol survival studies are normally conducted as a function of time, RH and temperature to understand the seasonality of infectious diseases.[114,276] When measuring airborne survival,

commonly used techniques such as the rotating drum need to take into consideration the particle loss during suspension[172] and the impact of the aerosolization device on the microbial viability.[137] Other techniques use evaporating droplets on hydrophobic surfaces[177] or spider webs[146] that are assumed to reproduce the physicochemical properties of the true aerosol state. The CELEBS instrument has been designed to only consider the biological decay as a function of time and environmental conditions while suspending the particles airborne in an atmosphere. Damage to microorganisms by both aerosol generation and sampling process has been minimized. Further, the conditions the microorganisms experience are not complicated by the cloud of droplets generated by nebulisers.[265] The detailed methodology has been discussed in Chapter 2 (Section 2.2.2) and previous publications.[10,68]

In this study, *E. coli* MRE-162 at a concentration of $2.32\pm0.6 \times 10^8$ CFU mL^{-1} was aerosolized in different artificial respiratory fluids (i.e. artificial saliva, diluted artificial saliva and diluted sputum) and suspended under 30, 50 and 90% RHs for 5, 120 and 600s (extra data points at 60 and 300s were included in the graphs for some of the droplet compositions). As shown in Figure 5-9, the resulting viability percentages are compared to previously reported *E. coli* MRE-162 survival in PBS droplets for reference.[10] Note that the new survival data presented here have been normalized by using the number of CFU per droplet after a suspension time under 5 s as the control measurement. For all droplet compositions, the impact of this short suspension period is negligible on the bacteria viability, therefore, it is used as a non-exposure reference measurement.

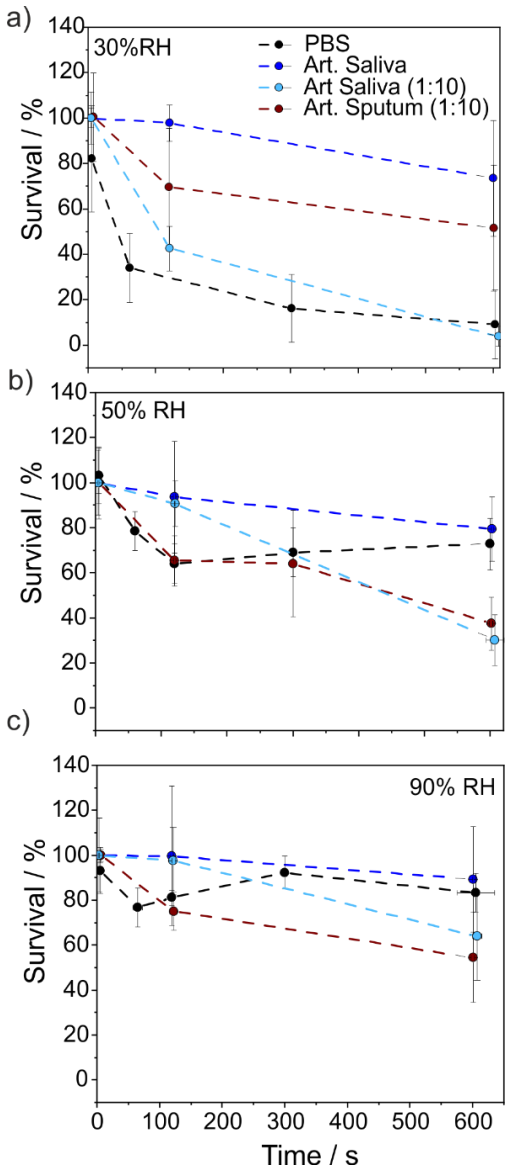

Figure 5-9. Survival percentages for *E. coli* MRE-162 ($2.32\pm0.6 \times 10^8$ CFU mL^{-1}) over time in: artificial saliva (blue), diluted artificial saliva (light blue), diluted artificial sputum (green) and PBS (grey) droplets compositions at a) 30, b) 50 and c) 90% RH. Each data point is expressed as the average and standard deviation of at least three replicates.

Under the driest conditions (30% RH), the most significant decrease at early time, regarding the survival at <7 s, was observed for *E. coli* MRE-162 at 120s levitations in droplets composed of diluted artificial saliva (p, 4.4×10^{-3}). After 600s, the decay in airborne bacteria viability becomes also significant in both diluted saliva and diluted sputum compositions (p values 1.6×10^{-4} and 1.1×10^{-2} respectively).

As an RH of 50 or 90%, *E. coli* MRE-162 viability in droplets of diluted sputum experiences a significant (p<0.05) decrease after all the suspensions times performed on this study (p values 1.6×10^{-4} and 3.40×10^{-7} for 120 s and 600 s respectively at 50% RH and 1.4×10^{-4} and 6.1×10^{-4} for 120s and 600s respectively at 90% RH) while only the longest levitation periods significantly impact the survival of airborne *E. coli* MRE-162 in diluted artificial saliva droplets (P values 2.6×10^{-5} and 2.9×10^{-2} at 600s for 50 and 90% RH respectively).

Interestingly, no significant decay is observed for E. *coli* MRE-162 in artificial saliva droplets at any of the RH and suspension times over 10 minutes. This may be a result of the low hygroscopicity coupled with the high initial mass fraction of solute presented in this respiratory fluid, leading to smaller changes in solute concentration and size when equilibrating with the gas-phase RH. In summary, *E. coli* MRE-162 has reported greater survival in droplets composed of artificial saliva than in droplets made of PBS and diluted respiratory fluids (sputum 1:10 and saliva 1:10). To understand why this relationship exists, the data from Sections 5.2 and 5.3 must now be considered in conjunction.

5.4 Correlation Between Airborne Bacterial Survival and Physicochemical Properties of Bioaerosols

5.4.1 The Effect of Aerosol Droplet Chemical Composition on Airborne Viability

In order to more accurately study the risk of airborne disease transmission in natural conditions, the use of respiratory secretions should be used. In this section, the role that droplet solute alone plays on airborne bacterial survival will be explored.

5.4.1.1 The effect of Mucin on Airborne Bacterial Survival

Mucin glycoproteins are the main constituents of respiratory mucus, a viscous biological compound that protects and lubricates portions of the human respiratory airways.[277] The biophysical properties of respiratory secretions depend on the concentration of mucus which is a function of the type of disease (e.g. sinusitis, pneumonia), disease state (e.g. healthy,

asymptomatic and infected individuals) and the anatomical location (e.g. nasal, bronchial) in the respiratory airways.[250,278] Different viscoelastic properties of respiratory mucin have been reported to affect the size distribution and concentration of droplets generated during coughing or breathing.[279] It is, therefore, expected that these varied rheological properties will affect the evaporation rates, settling velocities and even the biological processes dictating the airborne survival of pathogens enclosed in these droplets.

The evaporation profiles of artificial saliva droplets with different mucin concentrations (0.3, 0.5 and 2.5% mass to volume ratio (m/v)) into a gas-phase RH of 30% are shown in Figure 5-10a. The data are presented in the form of a normalized change in the radius-squared at normalized time *t* relative to the initial droplet radius r_0^2 (Eq. (5-1), (5-2)),

$$r^2 = r_0^2 - kt \quad \textbf{(5-1)}$$

or

$$\frac{r^2}{r_0^2} = 1 - k\frac{t}{r_0^2} \quad \textbf{(5-2)}$$

where *k* is the gradient of the resulting straight-line and is the rate of evaporation (units of m^2 s^{-1}) until equilibration in the composition is approached. The normalization of data is performed to remove the effect of slight variations in the initial size of the droplets at generation and is consistent with the use of the often applied radius-squared rule for steady droplet evaporation.[217] Despite the potentially different physical properties among droplet compositions, the changes in mucin concentrations do not significantly affect aerosol dynamics, reporting similar linear trends in the radius-squared than pure water droplets (Figure 5-10a).

The same artificial saliva compositions were used to resuspend an *E. coli* MRE-162 culture at a concentration of $(2.3\pm0.3)\times10^8$ CFU mL^{-1}. The bacterial suspension was aerosolized and levitated for 120 and 1800 s at 30% RH. The impact of different simulant mucin concentrations on the survival of *E. coli* MRE-162 is reported in Figure 5-10b, showing no significant change on the survival of *E. coli* MRE-162 (corresponding *p-values* in

Table 5-1). Despite reported studies showing that the presence of respiratory mucus provides a protective effect that remarkably increases the survival of human influenza viruses under dry conditions, the reasons for this previous observation are not completely clear.[83,105,111,280] The relationship between airborne bacterial viability and mucin concentrations in aerosol droplets has yet not been investigated in detail in the literature and needs to be further explored, but our results here suggest that mucin does not play a significant role for droplets of the size considered here.

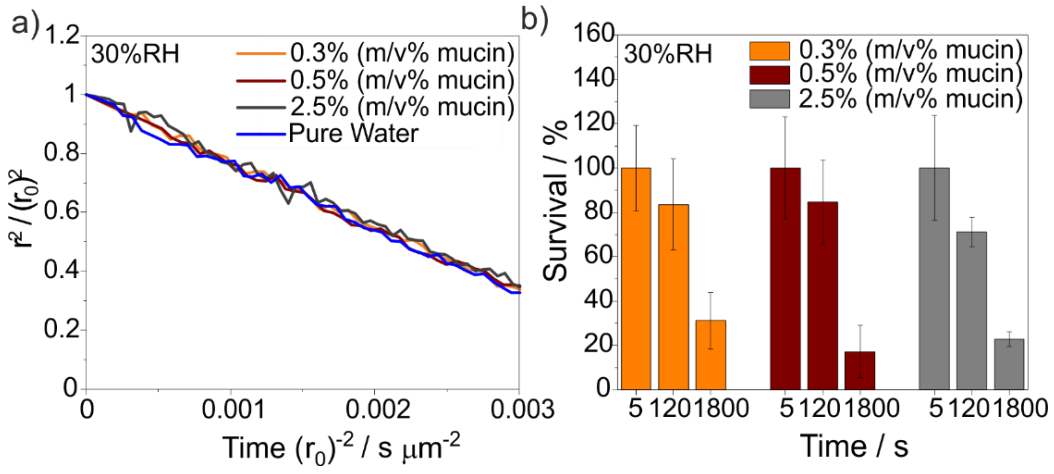

Figure 5-10. Effect of mucin concentrations on evaporation and survival of *E. coli* MRE-162. a) normalized evaporation rates of artificial saliva droplets composition containing three different mucin concentrations and pure water droplets and b) Survival of *E. coli* MRE-162 in artificial saliva droplets containing the same three different mucin concentrations, both at 30% RH. The mass fractions of mucin in artificial saliva represent the mucin concentrations in standard artificial saliva (0.3%), artificial sputum (0.5%) and artificial sputum with higher mucin concentration representative of infection (2.5%).

Table 5-1. Calculated *p-values* comparing the impact of different mucin concentration on the survival percentages of *E. coli* MRE-162 after levitation periods of 120 and 1800 s.

m/v mucin / %	*p-values* for survival at 120 s	*p-values* for survival 1800 s
Between 0.3 and 0.5	0.938	0.111
Between 0.3 and 2.5	0.161	0.196
Between 0.5 and 2.5	0.216	0.337

5.4.1.2 The effect of Gas-to-Particle Partitioning of Pyruvic Acid on Airborne Bacterial Survival

Little is known about the reactivity of bacteria with trace gases present in the atmosphere, such as atmospheric oxidants (e.g. OH, NO_3, and O_3). This relationship is further complicated by both the oxidants and the microbes potentially modifying the composition and physicochemical properties of the droplet itself through heterogeneous and multiphase reactions,[19] and biological processing. Incorporating this information to improve our quantitative understanding at the process level of how bioaerosols interact with atmospherically relevant species and how these reactions impact their survival, lifetime and physicochemical properties (e.g. hygroscopicity) is crucial to develop a complete understanding of the mechanisms determining the airborne transmission of disease and should be considered when building infection models.

In this section, pyruvic acid is used as a surrogate representation of a secondary organic aerosol (SOA) component to investigate the effect of gas/aqueous-phase partitioning and reactions on airborne bacterial survival. In the atmosphere, pyruvic acid is generated as an isoprene oxidation product, characterized by its high solubility and strong dissociation constant (pK_a) which enhances its partitioning potential into the aqueous aerosol phase. [281] In this work, a bubbler containing aqueous solutions with different volume fractions of pyruvic acid was connected to the gas inlet; this sets the gas-phase RH to 30% while simultaneously introducing pyruvic acid to the levitated droplets (Figure 5-11).

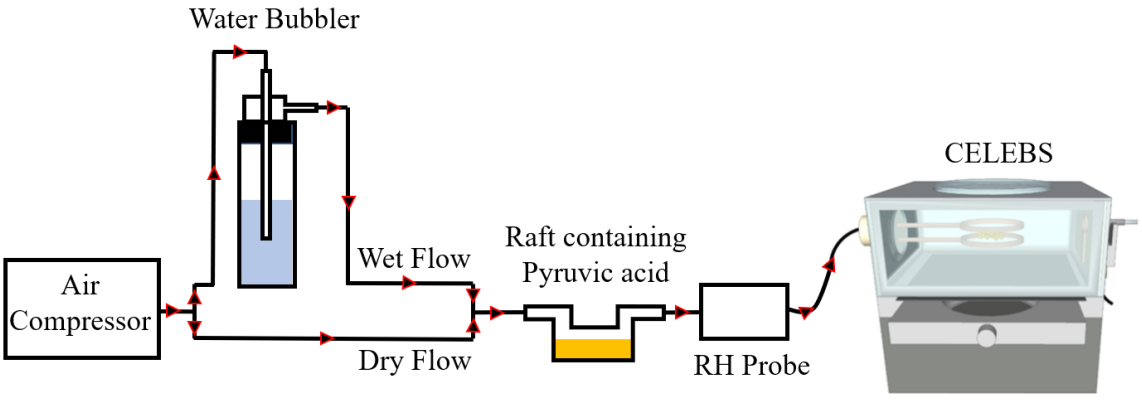

Figure 5-11. Diagram of the gas flow set-up for pyruvic acid studies on bacterial viability.

Estimated saturation concentrations of pyruvate compounds as a function of its gas-phase partial pressures (which were calculated with the Raoult's law) are shown in Table 5-2; these estimates assume a gas/aqueous-phase equilibria within the dilute limit, evading the dependence of the low RH in the particle phase to avoid large uncertainties arising from various non-idealities when using Henry's law. For these calculations, a Henry-constant value of $(3.1\pm0.8)\times10^{5}$ mol kg^{-1} atm^{-1} was used to estimate the concentration of pyruvate compounds in the aqueous phase.[281] Both, the partial pressures, and concentrations of condensed pyruvic acid were found to be increased by the addition of pyruvic acid into the bubbler (Table 5-2).

Table 5-2. Equilibrium saturation concentrations of pyruvic acid in the aqueous phase as a function of the volume fraction of pyruvic acid introduced in the gas inlet at 30% RH.

Volume percentage of Pyruvic Acid in bubbler as aqueous solution (% v/v)	Vapour pressure of pyruvic acid above equilirated solution (atm)	Solution phase concentration of Pyruvic acid in bubbler and equilibrated in droplet (mol kg^{-1})
0	0.00	0.00
0.01	4.34×10^{-08}	0.01
0.1	4.34×10^{-07}	0.13
100	1.70×10^{-03}	527.55

The survival of the airborne bacteria is only affected when pure pyruvic acid is added to the bubbler (not representative of real atmospheric conditions), which increases the concentrations of condensed pyruvate compounds by 4×10^{3} times when compared to the 0.1% v/v of pyruvic acid in the bubbler, reporting an immediate lethal effect on airborne bacteria (Figure 5-12).

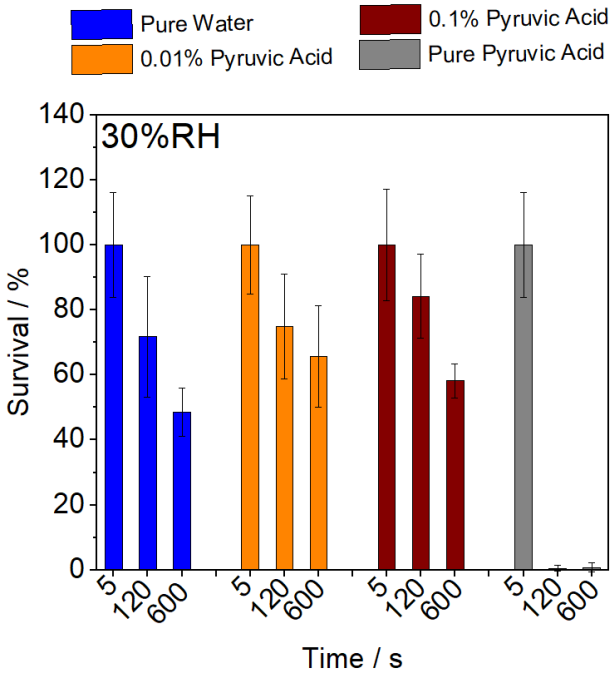

Figure 5-12. Effect of different volume fractions of pyruvic acid on survival of *E. coli* MRE-162 at a concentration of (2.8±0.3)×10^{8} CFU mL^{-1}in droplets composed of artificial saliva at 30% RH. Survival was obtained by introducing pure water in the bubbler are shown for reference purpose.

One potential explanation is that the high concentration of pyruvic acid produces a change in the pH of the droplet decreasing the bacterial survival after 120 s of levitation. Pyruvic acid exists as its keto and diol forms when dissolved, maintaining a naturally acidic pH (~2.3) in diluted solutions.[282] However, the extent of hydration to the diol form is pH-dependent, which is also likely to vary as the droplet evaporates and the solution concentration evolves. Note that the gas-particle equilibration time for the pyruvic acid partitioning is likely to be shorter than the drying time/loss of water to achieve equilibrium. Although the effect of pH on pathogens suspended in the aerosol phase has not yet been documented in the literature, previous studies on evaporating droplets deposited onto polystyrene surfaces investigated the impact of this parameter on microbial viability. They show a significant inactivation of enveloped viruses generally more noticeable than in non-enveloped ones under acidic and basic conditions due to the denaturing of the membrane proteins and the hydrolysis of the viral genome caused by extreme pHs.[104] Concerning *E. coli* bacteria, a study in the liquid phase has reported the pH-dependent inhibitory effect of anionic products of sulphur dioxide (SO_2) on bacteria viability,

increasing their toxicity as the pH of the environment decreases. However, the stress generated by hydrogen ion concentrations (pH) differs widely among microbes, some being able to grow under acidic (acidophilic bacteria), neutral (neutralophilic bacteria) and basic (alkalophilic bacteria) conditions while others being able to regulate their internal pH by producing enzymes (pH homeostasis).[283] Therefore, extrapolation of results from laboratory experiments between different microorganisms needs to be considered with caution. Moreover, determining the real-time pH in evaporating aerosol droplets, and therefore explain the impact of pH and photochemistry on the viability of airborne pathogens, is challenging and needs the implementation of new tools.[104] Certainly, given the known pH sensitivity of some virus since spike, these tools would be extremely useful.

5.4.2 The Effect of Evaporation Rates on Airborne Bacterial Viability

The dynamic processes occurring within single aerosol particles during evaporation and drying can drive changes in physicochemical properties and reaction rates across several orders of magnitude.[125,195,216] For example, aerosol particles commonly reach supersaturated solute, ultra-viscous and even glassy states, [126,216,217,260] and this can potentially influence the survival of microorganisms in aerosol particles.[259] To what extent are any biological processes taking place in an aerosol droplet governed by these physicochemical changes?

In previous work[10] (Chapter 4), the effect of solute concentration as a function of the ambient RH, on airborne bacterial survival was explored. An inverse correlation between survival and the equilibrated solute concentration for both LB broth and PBS solution droplets was obtained. Also, the impact of droplet size alone on survival was investigated, showing a significant increase in bacterial survival directly proportional to the equilibrated droplet size when the solute concentrations and moisture content achieved at equilibrium were the same.[10] Moreover, if the effect of particle size alone determines survival, all viability decay data would be highly dependent on the generation techniques (e.g. nebulisers, micro-dispensers, atomizers, etc). However, some studies in the literature explore changes in viability with smaller droplets than the ones used in our work (initial radius of ~25 µm with the DoD dispenser[68] and final radius ~ 1-3µm with the nebuliser),[284] reporting longer survival,[10,68,73,94,117,261,285] suggesting that size does not solely drive microbe death.

Thus, at a glance, relationships between physicochemical properties (e.g. equilibrated solute concentration and droplet size) and airborne bacterial death (e.g. smaller droplets die quicker) that when taken together, they all seem to contradict each other; for example, higher solute concentrations lead to lower bacterial survival but bigger droplet sizes with same solute concentrations lead to higher survival. However, when the dynamics are considered all of the apparent contradictions clarify: size and solute concentration are interlinked predictably. Proposed here is that it is not the size or solute concentration at equilibrium affecting microbe health, rather it's the rate and extent of size change from the generation to equilibrium. Regardless of the source, the evaporation profile of a given aerosol of an identical starting formulation/generation technique will follow a similar trend. This hypothesis will be explored in the following sections.

5.4.2.1 The Presence of Surfactants in LB broth Droplets Has No Effect on Bioaerosol Dynamics or Airborne Bacterial Survival

Previous studies have reviewed the effect of monolayers of surface-active species on mass transfer of water in aerosols, limiting the rate of water transport from and to the droplet, and impacting atmospheric processes.[198,257,286–291] The inhalation of surfactants with the aim of modifying the surface tension properties of the lung airway has been shown to impact the concentrations of exhaled bioaerosol providing a simple way to reduce the spread of potential airborne outbreaks.[292] More importantly, and related to this work, recent studies have investigated the role of pulmonary surfactants on the activation of virulence pathways and survival of *Staphylococcus aureus* in host lung tissue.[293]

The influence of three commercially available surfactants (Tween80, dipalmitoylphosphatidylcholine and heptadecanol, Figure 5-13) on the normalized evaporation profiles of LB broth droplets containing *E. coli* MRE-162 at concentration of ~ 10^8 CFU mL^{-1} drying under 30, 50 and 70% gas-phase RHs, is reported in Figure 5-14. Dipalmitoylphosphatidylcholine (DPPC) was included as an example of a component naturally occurring in lung epithelial lining fluid.[294] Tween80 is a common surfactant used in biological studies, while heptadecanol is a more well understood aerosol surfactant. The preparation of LB broth solutions containing surfactants and *E. coli* MRE-162 bacteria cells is described in the Generic Materials and Methods for Bioaerosol Survival Studies section 2.2.4.

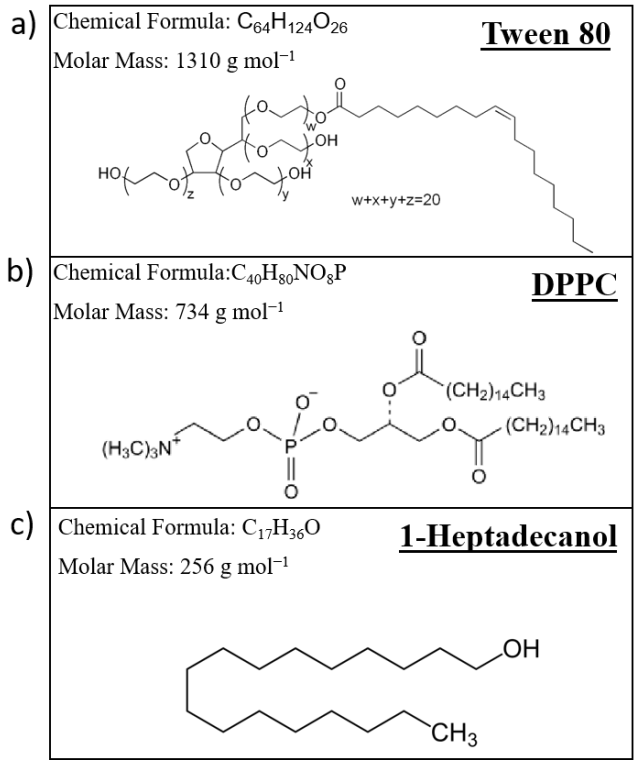

Figure 5-13. Chemical formulas, structures and molar masses of surfactants a) Tween 80, b) DPPC and c) 1-Heptadecanol.

The data indicates that the mass transfer of water from the droplet is not limited by the addition of surfactants, reporting similar evaporation rates to the ones observed for pure LB broth droplets (black and magenta lines in Figure 5-14). Figure 5-14 shows that the starting (saturated) concentrations of surfactants in LB broth are far too low, due to their insolubility in water, to play a significant role in the evaporation kinetics of the droplets. The presence of Tween80, which has the highest water solubility (5-10 g per 100 mL), shows a larger equilibrium size due to the higher solute concentration present in the droplet, but no kinetic limitation is imposed on the mass transfer of water. This is consistent with earlier work on long-chain alcohols which suggests that limitations to mass transfer rates only occur for droplets larger than 1 μm diameter once a solid condensed film form at the droplet surface.[289] Tween80 is a water soluble surfactant, as such appears to not limit mass transfer of water across the surface of the droplet during evaporation.

The effect of the presence of surfactants on the viability of *E. coli* MRE-162 cells at a concentration of (2.6±0.6) $\times 10^8$ CFU mL^{-1} after being suspended at 50% RH for 300 s in surfactant saturated LB broth droplets is reported in Figure 5-14d. No significant difference in *E. coli* MRE-162 survival among bioaerosols containing saturated levels of surfactants and non-metabolized LB broth droplets was observed. This was consistent with the hypothesis that dynamics are affecting survival; the concentration of the surfactants was too low to affect the aerosol dynamics in any way.

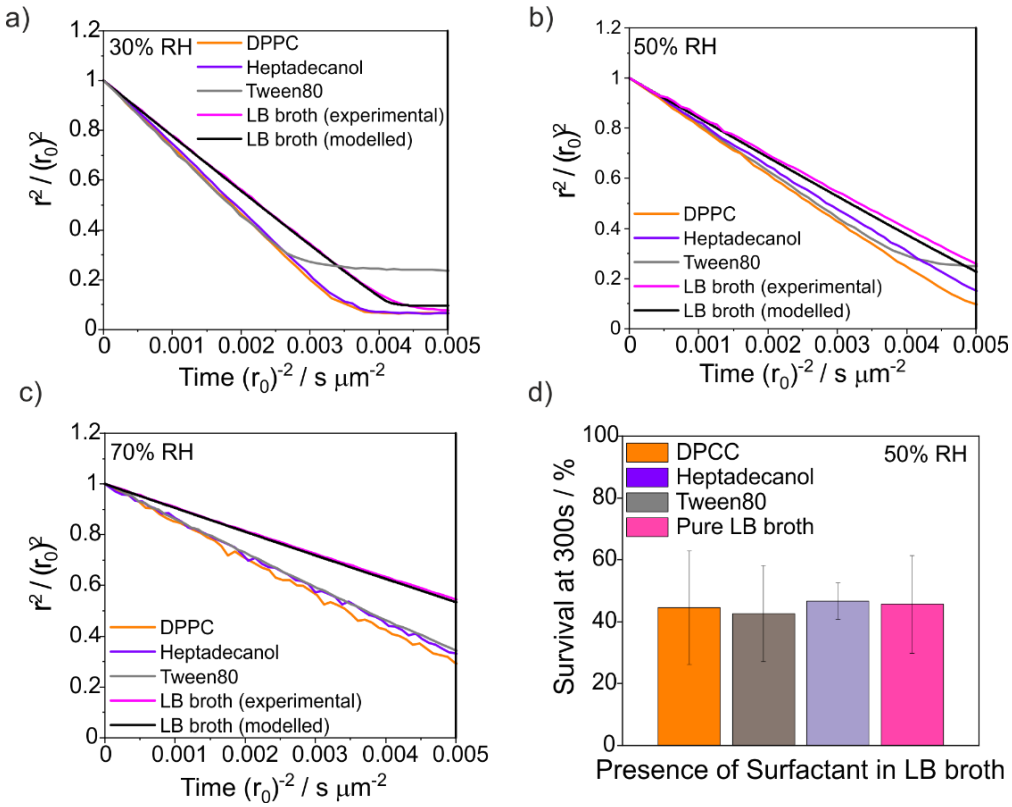

Figure 5-14. Effect of surfactants on aerosol dynamics and bacterial survival a) Comparison of evaporation kinetics among droplets composed of autoclaved LB broth (magenta), LB broth saturated with DPPC and containing (4.5±2.4)×10^8 CFU mL^{-1} *E. coli* MRE-162 bacteria mL^{-1}(orange), LB broth saturated with heptadecanol and containing (3.6±2.1)×10^8 CFU mL^{-1} *E. coli* MRE-162 bacteria mL^{-1} (grey) and LB broth saturated with Tween80 and containing (3.0±0.8)×10^8 CFU mL^{-1} *E. coli* MRE-162 bacteria mL^{-1} (violet) into a gas-phase RH of a) 30%, b) 50% and c) 70% RH. Experimental measurements are compared with simulations for pure LB broth droplets obtained using the evaporation/condensation kinetics model (black lines). Model predictions agree with the experimental measurements of LB broth particles without surfactants for all gas-phase RHs. Small variations on the evaporation profiles are due to minor fluctuation in the gas-phase RH. (d) For the same particles, comparison of *E. coli* MRE-162 survival to evaluate the impact of the presence of surfactants on airborne bacteria viability at 50% RH.

To further explore the effect of surfactants on bioaerosol droplets containing airborne bacteria, a more extensive investigation on the particle morphology, evaporation kinetics and droplet composition was performed:

a) The Presence of Surfactants in LB broth Droplets Has No Effect on the Particle Morphology during Evaporation

A comparison of the changes in morphology that occur during the evaporation of the same LB broth solutions droplets saturated with Tween90, DPPC and heptadecanol and containing *E. coli* MRE-162 at a concentration of ~ 10^8 CFU mL^{-1} when drying at 30, 50 and 70% RH are reported in Figure 5-15. Morphology changes during water evaporation are identified from the temporal changes in angular light scattering pattern (the phase function) observed in CK-EDB measurements, an approach recently reported[190] and detailed in Section 2.2.1.4

Figure 5-15 reports that the LB broth solution droplets that contain surfactants show an appreciable departure from homogeneity immediately after aerosolization before the equilibrium is reached, reporting the formation of inclusions (potentially micelles). This suggests that the solubility of the low surfactant concentration could lead to the formation of an emulsion inside the droplets, rather than forming a complete surfactant monolayer or shell on the surface of the droplet which could lead to a limitation on the evaporation rate. However, the emergence of inclusions could be also due to the presence of bacterial cells reaching a sufficient concentration during evaporation to be detected as inclusions. Specifically, saturated solution droplets present an initial concentration of $(4.5\pm2.4)\times10^8$, $(3.6\pm2.1)\times10^8$ and $(3.0\pm0.8)\times10^8$ CFU mL^{-1} when saturated with DPPC, heptadecanol and Tween80, respectively. What is unclear is the source of the inclusions: is it bacteria or micelles?

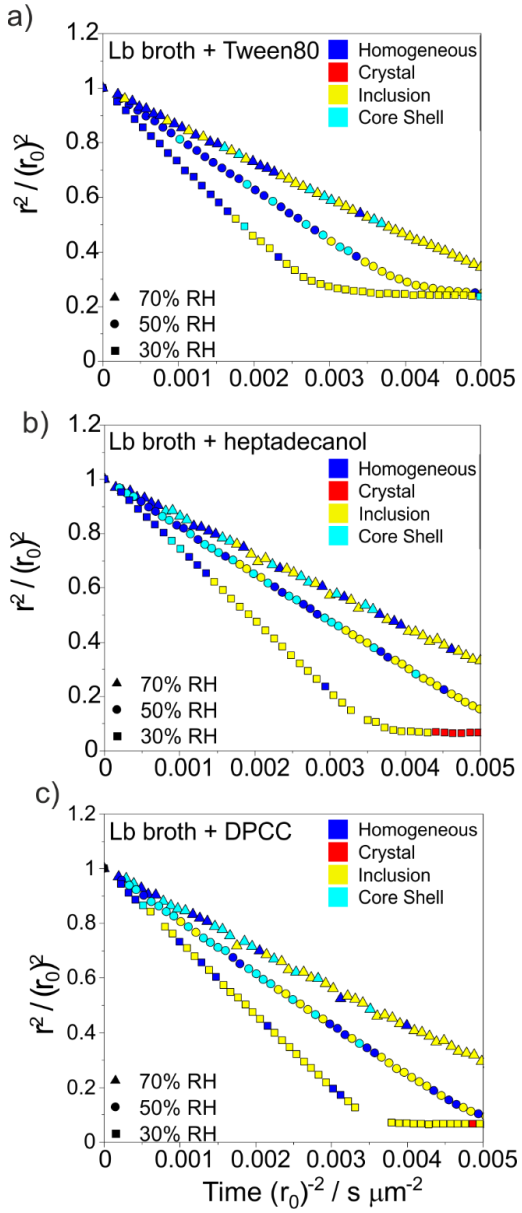

Figure 5-15. Phase function analysis for LB broth solution droplets containing surfactants (e.g. Tween80, DPPC and heptadecanol) while evaporating into gas-phase RHS of 30%, 50% and 70 % RH. Symbols: ▲ –70% RH, ● – 50% RH and ■ – 30% RH. a) Comparison of the evolving particle morphology of drying droplets composed of LB broth containing Tween80, b) Comparison of the evolving particle morphology of drying droplets composed of LB broth containing helptadecanol and c) Comparison of the evolving particle morphology of drying droplets composed of LB broth containing DPCC.

A comparison of the general trends observed in the particle morphology of single LB broth droplets containing initial bacteria cell concentrations ranging from 10^6 to 10^9 cell mL^{-1} (~1±1 to 1000±150 CFU per droplet) was performed (Figure 5-16b). The phase function analysis for

droplets composed of pure LB broth evaporating into 30, 50 and 70% RHs (Figure 5-16a) are included for comparison in order to evaluate the impact of the presence of bacteria cells on the particle morphology. Figure 5-16a shows that the pure LB broth droplets are completely homogeneous during the early evaporation independent of the RH, only forming inclusions when reaching the equilibrium size at gas-phase RHs of 30 and 50%, likely due to the formation of NaCl inclusions (efflorescence of NaCl takes place between 45-50% RH).[198]

The changes in morphology during evaporation at 50% RH for LB broth droplets containing varying numbers of bacteria at 10^6, 10^7, 10^8 10^9 and 10^{10} CFU mL^{-1} is reported in Figure 5-16b. Inclusions can be detected from the phase function at a limit of only ~0.04% volume fraction of the droplet (for 450 nm polystyrene spheres).[190] For the first time (Figure 5-16b), the minimum detectable total percentage volume of bacteria in the droplet as inclusions is determined to be at a volume fraction of ~ 0.14 % of *E. coli* MRE-162 cells for evaporating droplets containing an initial number of ~45 CFU per droplet with an estimated cell volume of 0.7 μm^3 (0.25-1.0 μm diameter). Therefore, the reported inclusion in Figure 5-15 is likely due to the presence of bacteria cells since the concentration of bacteria used in this figure is in the order of the detection limit of bacteria cells in the phase function analysis. However, the impact of surfactants and bacteria cells on the droplet's morphology should be further investigated.

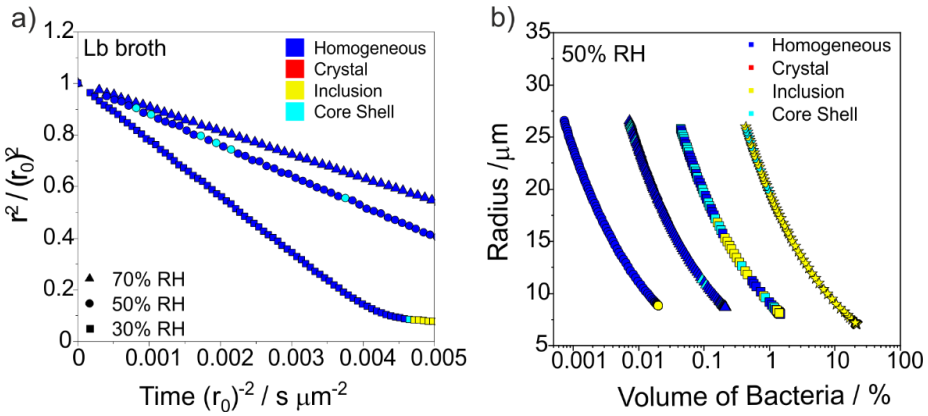

Figure 5-16.Phase function analysis of LB broth droplets with different microbial loads a) Comparison of the phase functions for LB broth solution droplets while evaporating into gas-phase RHS of 30%, 50% and 70 % RH. Symbols: ▲ –70% RH, ● – 50% RH and ■ – 30% RH. b) Changes in morphology in terms of radii as a function of % volume of bacteria for droplets composed of LB broth containing 10^6 *E. coli* MRE-162 cells mL^{-1} (spheres), LB broth containing 10^7 *E. coli* MRE-162 cells mL^{-1} (triangle), LB broth containing 10^8 *E. coli* MRE-162 cells mL^{-1} (squares) and LB broth containing 10^9 *E. coli* MRE-162 cells mL^{-1} (stars), evaporating into a 50% gas-phase RH.

Note that the difference in the phase function between a droplet containing inclusions and a core-shell structured droplet is sometimes subtle and misidentified by the algorithm. It is, therefore, necessary to analyse several droplets to determine the dominant morphology. In this case, the analysis concludes that the droplets all contain inclusions.

b) The Presence of Surfactants Has No Effect on the Evaporation of Saturated Water Droplets

To more fully explore the role of surfactants on the evaporation profile of droplets under biologically relevant (e.g. ethanol free) conditions, the effect of the presence of different types of surfactants (Tween80, DPPC, heptanol, heptadecanol, decanol, octadecanol, pentadecanol and tetradecanol) on the evaporation dynamics of saturated pure water solution droplets is reported in Figure 5-17. No impact on the mass transfer rates due to their low solubility was observed. A comparison with droplets containing heptanol in a 1:1 water-ethanol mixture is included to show the clearly discernible effect that a surfactant can have on the evaporation rate when at sufficient concentration to form a complete and cohrenet solid film on the surface of the evaporating droplet. Here, the ethanol is added as a solubilising component that aids the dissolution of sufficient surfactant to generate a condensed organic film that impedes the kinetics of water transport through the surface layer.[289]

Thus, it can be concluded that for many surfactants, their concentrations in aerosolized droplets of 10's micrometres size were insufficient to impact on mass transfer rates and consequently bacteria viability. This is a consequence of their often-low solubility in water (Figure 5-17) and the continuum-dominated gas-diffusion limited kinetics for mass transport in such large droplets. Besides, it is highly unlikely in the natural environment to have a starting solute concentration low enough such that the droplet can be reduced in size to the point that the surfactant will be able to form a monolayer on the droplet surface. To put it succinctly, surfactants will probably not affect airborne bacterial survival through altering particle evaporation kinetics (e.g. evaporation rate). However, biologically generated surfactants required further investigation.

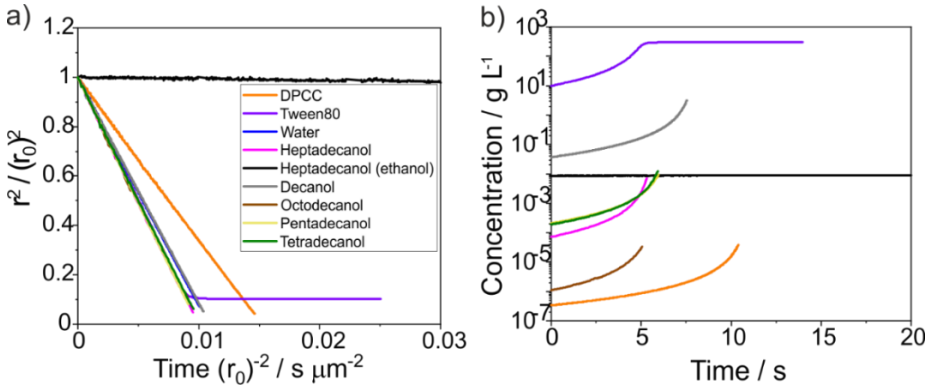

Figure 5-17. Physicochemical changes of water droplets containing various surfactants (a) Measured radii of a series of 7 saturated water solutions droplets containing different surfactants compared to that of pure water solution (light blue) and to that of heptadecanol dissolved in a 1:1 water-ethanol mixture (black) into the same conditions. (b) For the same droplets, change in the volume-average concentration as a function of time inferred from the experimental measurements of radii. Colours for the different water solution compositions under study: Orange, violet, magenta, green, navy blue, grey and brown – saturated water solutions with DPPC, Tween80, heltadecanol, decanol, octadecanol, pentadecanol and tetradecanol, respectively.

5.4.2.2 The Effect of Surface Enrichment on Airborne Bacteria Survival

The surface-to-volume ratios of aerosols (<100 microns) is several orders of magnitude higher than those of macroscopic solutions.[124] As a result, microorganisms enclosed in aerosol droplets will spend a larger fraction of their time at the air-particle interface when compared to the bulk phase. The interface is a unique microenvironment in comparison with the droplet core; mechanisms of loss of viability, such as exposure to gaseous oxygen and ozone, direct solar radiation, surface tension and open-air factors (OAF),[94,295] will occur only at the interface. This makes the surface-to-volume ratio an important property of aerosols to consider when studying microbe survival. Biological decay of microorganisms due to surface inactivation has been reported in various studies performed in shaking solutions and in aerosol droplets. [106] The rate of inactivation seems to be dependent on the RH, salt concentrations, the protective effect of surface-active amino acids and the presence of air, and has been attributed to the extrusion of hydrophobic parts of the microorganisms into the air phase.[106,295,296] Benbough *et al.* demonstrated the toxicity of oxygen on airborne bacteria at low RH which was connected to the loss of bound structural water from the microorganism, producing changes in the reactivity of macromolecules (throughout free-radical formation) and, consequently, the inactivation of oxidative enzymes.[80,88] All these studies suggest that the occupation of the droplet surface is

potentially more hazardous to the microorganisms than residence at the core. However, little is known about the processes governing the inactivation of pathogens in airborne particle interface.

Figure 5-18a and Figure 5-18b show that both rapid evaporation (linked to high Peclet numbers) coupled with large volume change ($1-V_f/V_i$) is required for *E. coli* MRE-162 to significantly decay in a short time period. The initial solute concentration dictates the degree to which the droplet will shrink followed aerosolization and the gas-phase RH determines its evaporation rate. Thus, both factors control the percentage of microorganisms that are subject to the conditions in the droplet surface for at least some period of time, which also depends on the diffusivity of the microbes within the droplet. This hypothesis is supported when evaluating the survival data of airborne bacteria in both saliva and diluted 1:10 saliva. The same solute compositions but at different initial solute concentrations yield dramatically different dynamics; when the concentration of solute is low, the total volume change during evaporation is greater than when the initial higher solute concentrations are high (resulting in larger particle size at equilibrium). The survival data for bacteria in these droplets are extremely different, showing a pronounced decay for the diluted saliva due to the greatest change in volume immediately on droplet generation, leading to a survival of 4% against the 73% for the standard saliva droplets at 30% RH.

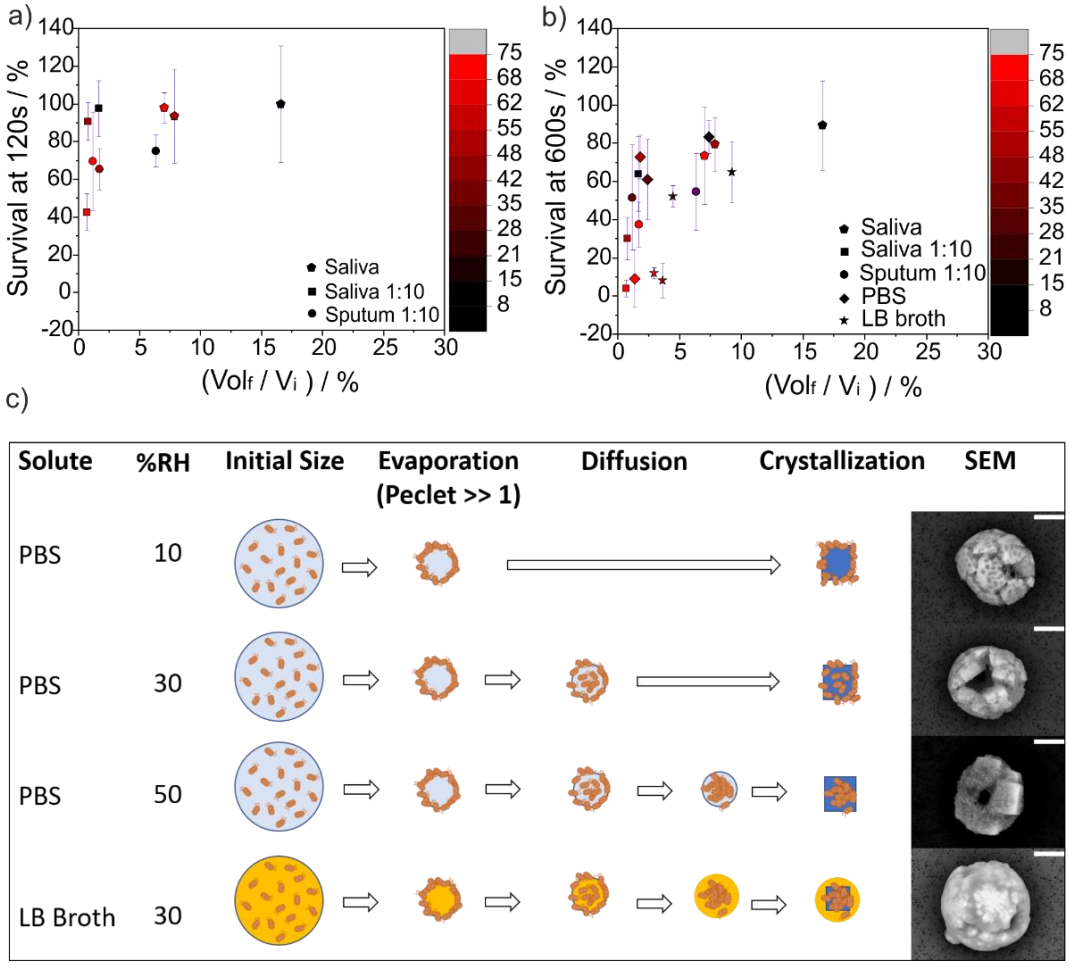

Figure 5-18. The effect of the size change rate on airborne bacterial survival after (a) 120s levitation for 3 different particle composition, (b) 600s levitation for 5 different particle composition. (c) The effect of different drying kinetics as a function of the gas-phase RH resulting in subsequent particle morphologies. The impact of phase/morphology changes on airborne bacteria viability occurring when decreasing the gas-phase RH for LB broth and PBS droplets.

The only condition measured where the bacterial cells are immobile on the surface of the particle (and not just near the surface) due to the formation of NaCl crystals is for PBS droplets at 30% RH (see Figure 5-8). In all other cases, the bacterial cells can diffuse in some degree to the interior of the droplet before or after nucleation (see also Figure 5-7). This rapid crystallization and the capture of bacteria cells on the droplet surface produce significant harm to the microbes as they are exposed at the surface, resulting in a dramatic death rate after 600 s of suspension (only 9% survival at 30% RH). Hence, the degree of volume change coupled with the information of the Peclet numbers are excellent predictors of the survival of airborne bacteria.

The evaluation of the different drying kinetics and crystallization processes of bioaerosol droplets with different compositions as a function of the gas-phase RH is shown as a schematic in Figure 5-18c and is presented in more detail in Table 5-3. The evaporation rates (*k*) were obtained as described in the Estimating Surface Enrichment section, resulting in drying rates of 9.4×10^{-10}, 6.6×10^{-10} and 4.7×10^{-10} m^2 s^{-1} for PBS particles at 10, 30, and 50% RH, respectively, and 7.0×10^{-10} for LB broth droplets at 30% RH (Figure 5-18c). To determine the degree of surface enrichment during evaporation, Peclet numbers for the different droplet compositions and RHs were calculated by using Eq.(2-9) and a diffusion coefficient value of 1.2×10^{-12} m^2 s^{-1} for *E. coli* bacteria cells (in water) (Table 5-3).[205] The evaporation kinetics during the first second was used to determine the Peclet numbers; during this same short time period the viscosity of the solution was expected to be similar to that of water. For PBS solution droplets evaporating at 10, 30, and 50% RH, Peclet numbers of 98, 68 and 49 were obtained, respectively. For LB broth solution droplets drying at 30% RH, the calculated Peclet number is 73 (Figure 11c). Given these values are >>1 and a 93-99% reduction of volume occurs during droplets evaporation between 90 and 30% RH, the majority of the bacteria cells are expected to be located on the surface of the droplets during evaporation.

Table 5-3. Dynamic processes taking place during droplet drying for different droplet compositions and RHs.

PBS droplets	**10% RH**	**30% RH**	**40% RH**	**50% RH**	**70% RH**	**90% RH**
Evaporation Rate / m^2 s^{-1}	9.4×10^{-10}	6.6×10^{-10}	5.6×10^{-10}	4.7×10^{-10}	2.8×10^{-10}	8.9×10^{-11}
Peclet Numbers	98.1	68.3	58.5	48.8	29.1	9.3
Eq. Solute Concentration/ gL^{-1}	1068.7	688.4	590.4	523.5	395.0	128.3
Eq. Radius / μm	5.2	6.0	6.3	6.6	7.2	10.5
V_f/V_i / %	0.9	1.4	1.6	1.8	2.4	7.4
Total Volume Change/ %	99.1	98.6	98.4	98.2	97.6	92.6
Survival at 600 s / %	-	16.2	-	69.1	73.4	92.3
LB broth droplets	**10% RH**	**30% RH**	**40% RH**	**50% RH**	**70% RH**	**90% RH**
Evaporation Rate / m^2 s^{-1}	9.0×10^{-10}	7.0×10^{-10}	6.0×10^{-10}	5.0×10^{-10}	3.0×10^{-10}	9.4×10^{-11}
Peclet Numbers	93.5	72.8	62.3	51.9	30.8	9.8
Eq. Concentration/ g L^{-1}	1106.8	849.6	755.2	685.5	555.4	270.5
Eq. Radius / μm	7.1	7.7	8.0	8.3	8.9	12.1

V_f/V_i / %	2.3	2.9	3.3	3.6	4.5	9.2
Total Volume Change/ %	97.7	97.1	96.7	96.4	95.5	90.8
Survival at 600 s / %	-	11.9	-	8.1	52.2	64.7
Saliva droplets	**10% RH**	**30% RH**	**40% RH**	**50% RH**	**70% RH**	**90% RH**
Evaporation Rate / $m^2\ s^{-1}$	8.7×10^{-10}	6.8×10^{-10}	5.8×10^{-10}	4.8×10^{-10}	7.0×10^{-10}	7.0×10^{-10}
Peclet Numbers	90.9	70.4	60.2	49.9	29.4	8.7
Eq. Concentration/ g L^{-1}	1254.3	922.6	857.8	821.5	754.2	390.5
Eq. Radius / μm	9.3	10.3	10.6	10.7	11.0	13.7
V_f/V_i / %	5.2	7.0	7.6	7.9	8.6	16.6
Total Volume Change/ %	94.8	93.0	92.4	92.1	91.4	83.4
Survival at 600 s / %	-	73.4	-	79.4	-	89.2
1:10 Saliva droplets	**10% RH**	**30% RH**	**40% RH**	**50% RH**	**70% RH**	**90% RH**
Evaporation Rate / $m^2\ s^{-1}$	8.7×10^{-10}	8.7×10^{-10}	8.7×10^{-10}	8.7×10^{-10}	8.7×10^{-10}	8.7×10^{-10}
Peclet Numbers	91.3	71.3	61.1	50.9	30.5	10.1
Eq. Concentration/ g L^{-1}	1314.7	967.0	899.1	861.0	790.5	409.6
Eq. Radius / μm	4.3	4.8	4.9	5.0	5.1	6.4
V_f/V_i / %	0.5	0.7	0.8	0.8	0.9	1.7
Total Volume Change/ %	99.5	99.3	99.2	99.2	99.1	98.3
Survival at 600 s / %	-	3.8	-	30.1	-	63.9
1:10 Sputum droplets	**10% RH**	**30% RH**	**40% RH**	**50% RH**	**70% RH**	**90% RH**
Evaporation Rate / $m^2\ s^{-1}$	8.4×10^{-10}	6.6×10^{-10}	5.6×10^{-10}	4.7×10^{-10}	2.8×10^{-10}	9.1×10^{-10}
Peclet Numbers	87.9	68.4	58.6	48.9	29.2	9.5
Eq. Concentration/ g L^{-1}	1732.2	1430.1	1203.2	980.6	602.4	268.1
Eq. Radius / μm	5.3	5.7	6.0	6.5	7.6	9.96
V_f/V_i / %	1.0	1.2	1.4	1.7	2.8	6.3
Total Volume Change/ %	99.0	98.8	98.6	98.3	97.2	93.7
Survival at 600 s / %	-	51.5	-	37.4	-	54.6

While the bacteria may be on the surface during the evaporation process, the length of time the bacteria remain on the surface at equilibrium will be dependent on the *efflorescence time*, the bacterial cells diffusion coefficient and the viscosity of the droplet. At equilibrium, for more complex solutions, such as artificial saliva, the diffusion coefficient will be much lower which

will in turn further limit the diffusivity of the microbe from the surface. Based on the viscosity of PBS at 70% RH 4.38 mPa s^{-1} (data collected by Young Song, private communication), the expected diffusion coefficient would be $6.0x10^{-14}$ m^2s^{-1}. This reduction in the diffusion coefficient would result in the bacteria remaining on the surface for a longer period of time.

The time that the concentrations surpass a threshold for the water activity at which efflorescence has previously been seen in measurements to occur abruptly is simplified here to the term *efflorescence time*. The *efflorescence times* for PBS droplets were estimated from when the evaporating droplet reached a GF_r of 1.673; at a water activity (*aw*) of 0.45 NaCl [198] which makes up 83% of the mass of PBS is expected to effloresce.[10] *Efflorescence times* of 2.8, 3.7, 4.3 and 5.3 s were obtained for PBS at RHs of 10, 30, 40 and 50% respectively. If the volume of the droplet deemed to be the surface contains solely the outer 0.1 μm layer, we speculate that these periods of over a second are long enough for the bacteria cells to diffuse (whose diffusion coefficient is <0.6 $\mu m^2/s$) from the droplet surface prior to crystallization at medium-high RHs; the majority of cells are locked at the droplet surface inside NaCl crystals at 10% RH, as observed in the SEM images included in Figure 5-18c.

The presence of organic components coupled with higher overall solute concentrations in the LB broth droplets results in the retention of water mass which increases the evaporation times and allows a further diffusion of the bacteria from the surface during the evaporation process (where the diffusion rate is nearer to that of water) without reaching a complete crystallization of the salts.[10] Thus, the survival reported for LB broth droplets at 30% RH is slightly higher than for PBS (24% vs 16% in PBS and LB broth respectively), supporting the theory that greater diffusivity of bacteria cells from the surface enhances airborne bacteria survival by reducing their exposure to droplet surface. These findings were supported by SEM images collected of the dried PBS and LB broth particles, wherein various degrees of bacteria were observed at the surface of the particle as a function of RH and solute composition (Figure 5-18c), increasing the visible bacteria cells at the droplet surface when decreasing the RH.

These results suggest that the time for crystallization to occur rather than the phase change itself (crystallization) could affect airborne bacteria survival; the crystallization time determines the final location of the microorganisms within the particle and their degree of exposure to the air-particle interface. These findings suggest that the mechanisms of death could be more related to the evaporation of cellular water from the bacterial cells on the droplet

surface than to the water and heat transfer between the droplet surface and the gas-phase environment. Further study is necessary to identify mechanistically what is driving bacteria death.

5.4.3 The Effect of Microbiological Properties on Airborne Survival

The fate of airborne pathogens is likely to be dependent on the microbiological conditions, including the cell physiology and the microbial load in the aerosol droplets. Culture conditions such as incubation time, temperature and growth media can influence the phenotype of the cells and therefore their airborne survival.[84,101] The microbial concentration contained in the aerosol droplets used in experimental systems can impact the droplets composition, size, dynamics and even their microphysical properties. Besides, the biological component in aerosol survival studies can impact the quality of the sample to be aerosolized and introduce variability in the outcome of the study. A detailed characterisation of these variables should be taken into consideration to successfully compare bioaerosol research between laboratories.[33,250]

5.4.3.1 The effect of Bacteria Physiology on Airborne Survival.

To investigate the effect of cell physiology on the survival of *E. coli* MRE-162 suspended in LB broth droplets after 5, 120 and 600s at 30% RH (Figure 5-19), the bacteria were cultured for 6, 12, 24 and 48 hours in LB broth before aerosolization and adjusted to an OD=0.5, as detailed in the Generic Materials and Methods for Bioaerosol Survival Studies section. The calculation of survival is described in Section 2.2.2.3. Interestingly, a significant biological decay after 120 s suspension was observed for all the aerosolized bacterial cultures (*P* values 0.035, 0.005 and 0.036 for 6, 24 and 48 hours respectively) except for the bacterial suspension incubated for 12 hours (*P*, 0.871) which reports no impact on the airborne bacteria viability (Figure 5-19). For longer suspension times (600s), the highest survival was also reported for the culture incubated for 12 hs and no significant decay in survival was observed (*P*, 0.097) in comparison with the survival at 120 s.

Generally, the doubling rate of *E. coli* is 20 min when cultured in a nutrient-rich medium. In this case, the 12 hours incubation period corresponds to the early stationary phase for this

particular strain. The growth curve of *E. coli* MRE-162 is included in Section 2.2.4.2. It has been reported that the bacterial response to starvation when cells enter into the stationary phase can trigger different adaptation mechanisms altering gene expression through alternative RpoS sigma factors and regulators which prepare the cells to survive under difficult conditions,[122,123,297] in some cases protecting against osmotic stress[121] and temperature stress.[298] Besides, the cell wall (peptidoglycam layer) thickens upon entry in the stationary phase providing greater tolerance to stresses. The results presented in Figure 5-19 agree with a comparative study of *E. coli* aerosol survival between the log and resting phases of growth which was performed by Cox *et al*. in air and nitrogen atmospheres at 20% RH, reporting higher aerosol stability in bacteria in the stationary phase.[84]

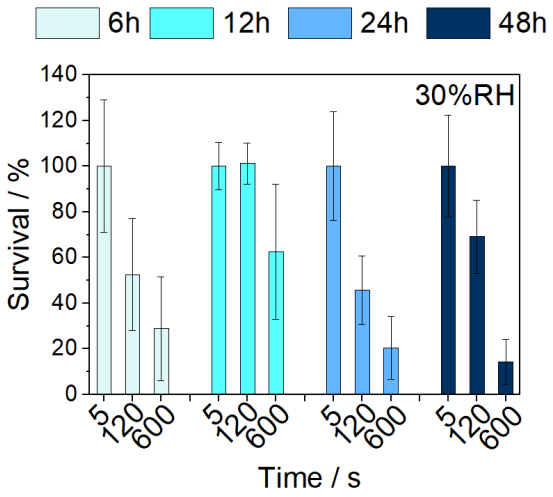

Figure 5-19. The effect of incubation times on airborne bacterial survival . Colours represent cell age being 6h (grey), 12h (cyan), 24h (light blue) and 48h (dark blue). Each data point represents the mean and standard deviation of at least three replicates.

5.4.3.2 The Effect of Microbial Load on Airborne Bacterial Survival.

The evaporation dynamics of LB broth droplets containing different bacterial concentrations ranging over five orders of magnitude (from 10^5 to 10^{10} cells mL^{-1}) into a gas-phase RH of 30% are shown in Figure 5-20. Each evaporation curve represents the average of 6, 15, 4, 2, 4 and 11 droplets for 10^5, 10^6, 10^7, 10^8, 10^9 and 10^{10} cells mL^{-1}, respectively. Increased *E. coli*-MRE-162 counts showed no impact on the evaporation rates of the aerosol droplets, reporting only a subtle effect on the kinetics for the droplets generated with cell suspension containing

the highest bacterial concentration (10^{10} cells mL^{-1}). The faster evaporation of this droplet composition is possibly due to the elevated number of bacteria cells on the surface of the droplets affecting the surface tension. Under low RHs, the rate of evaporation can surpass the diffusion rate of the *E. coli* cells, leading to the enrichment of the droplet surface (Figure 5-20b). Thus, the surface of the droplets generated with the 10^{10} cells mL^{-1} suspension is covered by a monolayer of bacteria cells 3 s after generation (black dotted lines in Figure 5-20b) which prevent the rest of cells to reach the droplet surface. Although the formation of a monolayer is not achieved for droplets with lower microbial load, a percentage of the droplet surface will be also filled with the bacteria cells after complete evaporation (28% and 3% for droplets containing 10^8 and 10^9 cells mL^{-1} respectively) which also prevent, to a smaller extent, additional bacterial cells from reaching the droplet surface. Even though the enrichment of bacteria at the droplet surface has no relevant impact on the evaporation dynamics (Figure 5-20a), it inhibits a significant percentage of the bacteria cells from reaching the surface of the droplet which in turn appears to increase overall airborne bacterial survival (Figure 5-20c). The inactivation of *E. coli* MRE-162 due to surface processes shows a time-lag effect, reporting a pronounced decay after 600 s and not immediately after evaporation at 120s.

Perhaps the reason for enhanced survival of bacteria in aerosol particles with higher bacterial load is that a greater fraction of bacteria remain in the droplet core where they are more resilient to processes that occur rapidly at the surface (e.g. oxidative stress, dehydration). Previous studies have also shown bacteria survive up to three times better in droplets when containing larger proportions of bacterial spores to vegetative cells (the aerosolized bacteria suspension were composed of different cell to spore ratios).[228] Interestingly, in the case of viruses, several studies have shown the effect of surface processes in the inactivation of viruses at high RH in both aerosol droplets and shaking solutions.[106,111,280] The mechanisms of inactivation are proposed to be due to the denaturation of the hydrophobic lipid bilayer contained in some viruses due to surface forces, removing the property of infectivity. [106,107] Saturation of the gas-liquid interface with proteins has been reported to lead to protection over viral inactivation by reducing access of the virus to the air-liquid interface and therefore preventing the loss of infectivity.[296] Also, surface inactivation of viruses increases with increasing acidity and salt concentrations.[106,111,296]

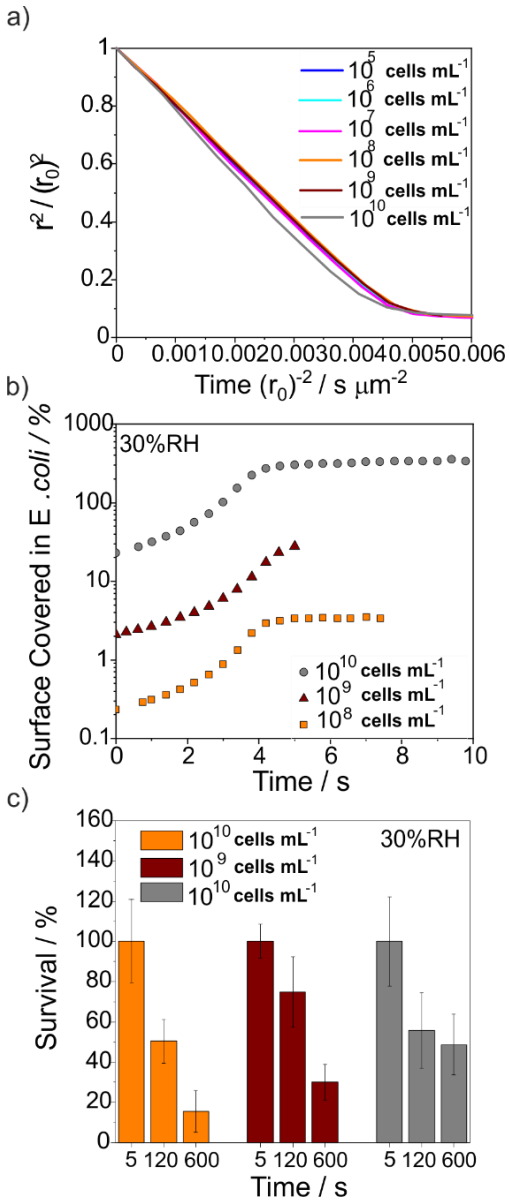

Figure 5-20.Impact of microbial load on aerosol dynamics and bacterial survival a) Evaporation dynamics for droplets composed of LB broth with different bacterial cell concentrations ranging from 10^5 cells mL^{-1} to 10^{10} cells mL^{-1}. b) Percentage of droplet surface covered by bacteria cells as a function of the microbial concentration introduced in the DoD. Note that these calculations assume that the surface area for a bacteria cell is 0.5 μm^2, considering 1 μm length and 0.5 μm width as the section of the surface area of bacteria covering the droplet surface, and c) Effect of the microbial cell concentration in the droplets on the survival of *E. coli* MRE-162 bacteria, all at a gas-phase RH of 30%. Colours: grey (10^{10} cells mL^{-1}), brown (10^9 cells mL^{-1}), orange (10^8 cells mL^{-1}), magenta (10^7 cells mL^{-1}), turquoise (10^6 cells mL^{-1}) and blue (10^5 cells mL^{-1}).

The data presented in Figure 5-20 show the importance not only of the microbial content of aerosol particles but the precise location of the microorganisms after the evaporation process is complete which will determine their disposition to a variety of phenomena at the air-droplet interface. These results support the interpretation of data shown in the previous section (Figure 5-18). The importance of surface processes driving the inactivation of pathogens in the air-droplet interface is critical to understand airborne survival and should be explored further.

5.5 Connecting the Outcomes

To understand the impact of particle morphology on airborne bacteria viability, the survival percentages of *E. coli* MRE-162 levitated for 600s in aerosol droplets with three different initial NaCl concentrations (5, 10 and 20 g L^{-1}) equilibrating at 30 and 70% RH are compared in Figure 5-21. The evaporation dynamics of LB broth droplets containing different initial NaCl concentrations are reported in Figure 5-21a and Figure 5-21b. The higher initial NaCl concentrations lead to higher particle sizes at the equilibrium in both RHs. Due to the different overall compositions in the LB broth droplets (25, 40 and 57% w/w of initial NaCl leading to 75, 60 and 43% w/w of organic content), the NaCl concentrations at the equilibrium also increase with the initial NaCl concentrations, presenting different moisture contents at the same RH (same a_w) Figure 5-21c shows the effect of the equilibrated NaCl concentrations on airborne bacterial survival, reporting opposite trends between RHs. Figure 5-21d shows the same trends as a function of RHs in bacteria survival as a function of the initial NaCl concentrations.

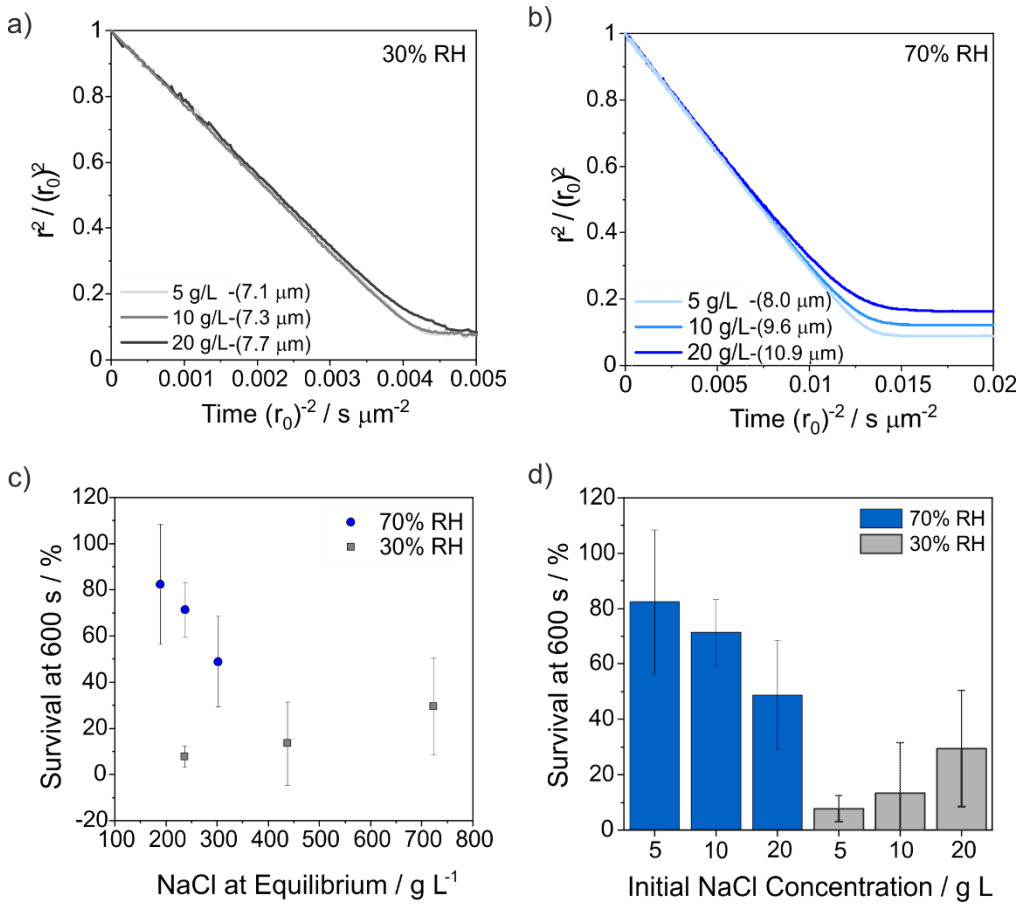

Figure 5-21. Connecting the dots. Comparison of the measured particle size for droplets composed of LB broth with three different initial NaCl concentrations into gas-phases of a) 30% and b) 70% RH, showing the corresponding particle sizes at equilibrium. c) The effect of the equilibrium NaCl concentrations on the survival of airborne *E. coli* MRE-162. d) RH dependence of the survival of *E. coli* MRE-162 at 600s as a function of the initial NaCl concentration in LB broth droplets.

The data indicate that the overall viability of airborne bacteria is higher in solution droplets (above the efflorescence RH) at 70% than in dry particles at 30% RH. Specifically, at 70% RH, airborne survival decreases with the increase in salt concentrations on the droplet composition, possibly due to osmotic stress caused on the microorganisms.[250] Interestingly, the equilibrated particle size seems to have minimal effect on the viability response (Figure 5-21b and Figure 5-21d). Rather, higher survival was observed in droplets with smaller equilibrated particle sizes whose salt concentrations at equilibrium were lower (Figure 5-21c). In our previous work,[10] when particles were larger at equilibrium the higher survival was reported for droplets with the same equilibrated solute concentrations at 50% RH. On the contrary, at 30% RH, the survival

of airborne bacteria increases proportionally to the NaCl concentrations at the equilibrium which also leads to bigger equilibrated particles sizes (shown as insets in Figure 5-21a and Figure 5-21b). In this case, the bioaerosol particles present higher solute concentrations than at 70% RH and lower water activity than the efflorescence point for NaCl (44-45 % RH).[195] Therefore, the salts contained in the bioaerosols present a different particle morphology than in the previous aqueous solution droplets, forming salt crystals with numerous nucleation events (Figure 5-7 and Figure 5-8). The higher survival is likely due to a smaller shrinkage in the droplets containing higher salt concentrations. Consequently, the equilibrium size and the surface area of these droplets will be bigger, leading to a smaller percentage of bacteria cells exposed on the surface of the droplets. In addition, higher salt concentrations allow further diffusivity of the bacteria cells from the particle surface before the efflorescence takes place (longer crystallization times for higher solute concentrations).

5.6 Summary of the Interconnections Between Aerosol Microphysics and Bacteria Viability

Figure 5-22 summarises the relationship between aerosol dynamics and airborne bacteria viability. The viability of airborne *E. coli* MRE-162 at 600s of suspension is shown as a function of six different physicochemical variables: equilibrated droplet volume, the surface to volume ratio, equilibrate solute concentration, the concentration of salts at equilibrium, the equilibrated concentration of Na^+ and temperature suppression of the droplet when equilibrating with the gas-phase atmosphere. From all correlations, only three (Figure 5-22a, Figure 5-22b and Figure 5-22f) report a significant collective correlation (with α=0.05) for the five different particle compositions (e.g. diluted sputum, saliva, diluted saliva, LB broth and PBS) reporting R values of 0.631 for droplet volume, -0.626 for surface to volume ratio and 0.595 for droplet cooling with corresponding p-values of 0.006, 0.007 and 0.011 respectively. Besides, correlation coefficients were also calculated for other parameters not included in Figure 5-22, obtaining significant collective correlations also for evaporation rates, Peclet numbers, RH, final to initial volume ratio and surface area with R values of -0.607, -0.607, 0.589, 0.631 and 0.595 and p-values of 0.010, 0.010, 0.013 and 0.007, 0.012 respectively. The majority of these correlations are related to the evaporation dynamics (e.g. evaporation rates,

temperature cooling, etc) undergone by the aerosol particles immediately after generation, reflecting a delayed impact in survival over longer times in the aerosol phase (e.g. 600s) instead of after few seconds of suspension (e.g. 5 or 120 s). It is important to note that these processes will dictate the final phase and morphology of the bioaerosol particles, determining the location of the microorganisms in the particles once equilibrated with the gas-phase and, therefore, dictate the different degrees of exposure to open-air and other toxic factors they will experience.

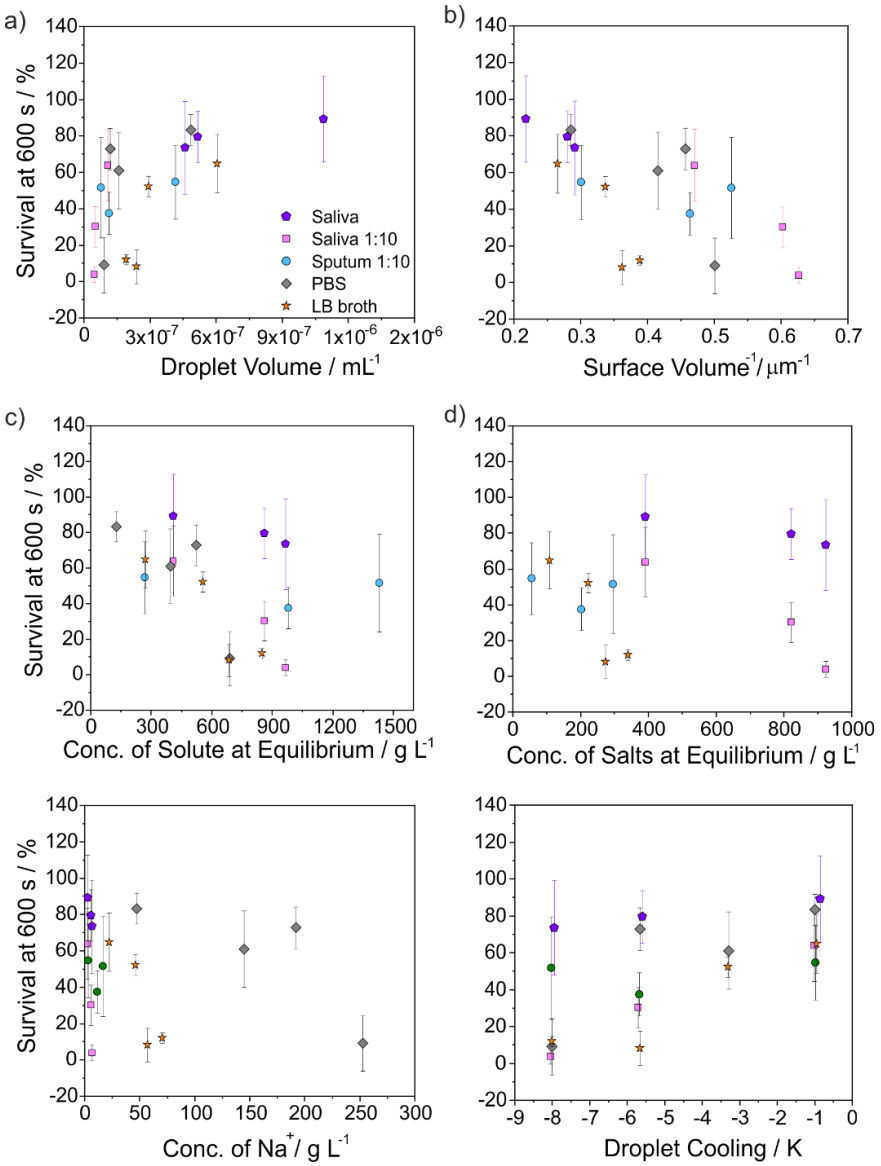

Figure 5-22. Correlations between bacterial survival and physicochemical changes in a) droplet volume at equilibrium, b) surface area to volume ratio, c) solute concentration at equilibrium, d) concentration of salts at equilibrium, e) concentration of Na+ at equilibrium and f) maximum droplet cooling for droplets of 5 different

compositions evaporating into RHs of 30, 50, 70 and 90%. Note that in the case of Saliva, 1:10 Saliva and 1:10 Sputum the correlations at 70% RH are not reported. The droplet dynamics for all droplet composition were calculated using the mass-transfer kinetic model for droplets with an initial size of 25 μm and an initial solute concentration of 25 g L-1 for LB broth, 9.59 g L-1 for PBS, 67.99 g L-1 for Saliva, 6.79 g L-1 for 1:10 Saliva and 17.04 g L^{-1} for 1:10 Sputum.

This innovative approach to study bioaerosol survival enables a detailed understanding of the synergistic interaction between the physicochemical and the biological processes that occur from droplet generation to the equilibrium with the surrounding atmosphere. Expending the knowledge of the dynamics of real respiratory fluids and across respiratory pathogens such as SARS-CoV2, *Neisseria meningitisdis*, *Streptococcus pneumoniae* and *Mycobacterium tuberculosis*, will enable the development of effective prevention policies.

5.7 Summary and Future Work

This chapter aims to identify the main mechanisms of inactivation of airborne bacteria to predict survival as a function of the physicochemical properties of the aerosol and the microorganisms. Thus, a phenomenological model (Figure 5-1) to quantify bioaerosol survival is formulated as the sum of the effect of predictable processes based on experimental measurements. The degree at which each of the processes included in the equation drive microbial death is dependent on the environmental conditions, the strain of microorganisms, compositional parameters of the aerosol particles, etc.

With this approach, it is possible to some degree of certainty predict the survival one would expect for *E. coli* MRE-162 in a solution droplet where the starting formulation is known (e.g. very diluted solution droplets) and it is injected into a known gas-phase RH. For example, considering saliva as a solute, we should be able to predict the combination of the initial saliva concentration needed to equilibrate in a specific RH to produce a significant biological decay in the microorganisms. In this particular case, the dynamic processes required include an overall reduction in the volume of >95% coupled with a Peclet number greater than 50 (Figure 5-18). These dynamics trends suggest that microbes with similar behaviour to *E. coli* MRE-162 injected into the same atmosphere from a freshwater lagoon would die faster than those produced from a WWTP (wastewater treatment plant) due to the higher concentration of

suspended solids. Thus, it is critical to consider the source and how it impacts on droplet composition when predicting microbe survival in the aerosol phase. This could explain common diseases such as the "sewage worker's syndrome" and the high infection risk via bioaerosols associated with WWTP.[11,299] Briefly, considering a microbe which appears to be sensitive to the surface of the droplet (like *E. coli* MRE-162), its survival will be dependent on the difference in water activity between the starting droplet solution and the gas-phase instead of on the gas-phase RH itself. These type of detailed predictions (e.g. predict the evaporation dynamics for different concentrations of the starting solute compositions) are not possible by using the standard survival curves (e.g. time-dependent bioaerosol survival as a function of environmental conditions) reported in the literature. Importantly, when probing a microorganism which is not sensitive to the processes included in one of the subcategories (e.g. 1 to 5), the equation (Figure 5-1) becomes simplified. For instance, in the case of spore-forming bacteria such as *B. atrophaeus* spores; in general spores are much more resistant than vegetative bacterial cells.

Previously, it was reported that the concentration of solute was altered through the manipulation of the gas-phase RH where the droplets were levitated, also impacting the physicochemical properties.[10] Subsequently, here we cover the effect of surface enrichment which is described by a competition between the evaporation and diffusion processes taking place within the droplet. This drying process determines the enrichment of microbes at the droplet surface together with the morphology of the final particles. The data establish that both parameters are correlated to the degree of harm inflicted on the *E. coli* MRE-162 during the droplet evaporation. The degree and rate of volume reduction in the droplets as they equilibrate with the gas-phase is a function of the RH and the solute concentration. This evaporation rate is independent on the generation device, and droplet generated with both nebulisers and micro-dispensers will experience the same dynamic changes, therefore the same survival response is expected although the final particle sizes are orders of magnitude different. [10,68,73,94,117,261,285] However, the impact of the aerosol generator and sampling system on microbes viability are factors that differ between experimental systems (Figure 5-1) affecting the survival of airborne microbes. Also, the effect of biological factors, such as the microbial concentration in the particles and the bacterial physiology, on survival were explored. These physicochemical and

biological processes are included in the subcategories 3 and 4 of the proposed equation (Figure 5-1), respectively.

Finally, the effect of solar irradiation on airborne viability has been studied by using conventional techniques for bioaerosol ageing such as the rotating drum and spider webs.[82,147,300] Results have shown that microbial death rates are proportional to the exposure time and the intensity of the light. Besides, the lethal effect of sunlight irradiance appears to decrease with increase in particle size, with smaller particles reporting a higher sensitivity to solar exposure.[250] Several studies in the bulk phase have reported microbial eradication under high-intensity visible light while the low-intensity stimulates bacterial growth, consistent with results from the aerosol phase.[301,302] The investigation of the effect of sunlight by using CELEBS will be a focus of investigation in the near future.

Chapter 6

Summary and Future Directions

The principal aim of this thesis was to develop, characterise and utilize a novel technique based on the electrodynamic levitation of populations of bioaerosol droplets (with particle diameter varying from ~50 to < 5 μm) within a controlled environment to investigate the main parameters (i.e. RH, temperature, droplet composition, etc) impacting the survival of airborne pathogens enclosed as a function of time. As a result, most of the nature of the work undertaken throughout this thesis was related to method development. This aim was achieved and reported in Chapter 3, with the development and characterisation of the next-generation EDT for aerobiological applications, named CELEBS. Furthermore, this work also aimed to investigate the complex interconnections between aerosol dynamics (e.g. changes in size, solute concentration and temperature during the evaporative process), aerosol physicochemical properties at the equilibrium (e.g. hygroscopicity, particle size and particle morphology), microbiological factors (e.g. microbial load and cell physiology) and the biological response of the microorganisms enclosed in aerosol droplets. Therefore, a comprehensive approach that combines the CELEBS instrument with the CK-EDB was developed. A detailed study of the effect of aerosol microphysics on airborne bacterial survival was presented in Chapter 4. The complexity of the solution droplets was increased towards more representative biological secretions in Chapter 5, where the studies were also extended to evaluate the impact of microbiological factors on airborne survival.

The following chapter will summarise the different stages of this research work, describing the starting point of this technique and how it was developed to gain insight at the interface between aerobiology, aerosol physics and atmospheric chemistry. Then, a description of the current experiments employing the developed approach will be introduced. Finally, some potential experiments and future applications for this new technique will be also discussed.

6.1 Initial Work

Conventional techniques for bioaerosol analysis present experimental limitations to disentangle the interconnections between the processes taking place during aerosol transport and bioaerosol survival, mainly due to the bulk analysis of polydisperse aerosols. Briefly, the dynamics occurring during processes of aerosol generation, transport and inhalation impart a series of stressful conditions (e.g. evaporative stress, osmotic stress, high salt and solute concentrations, etc) on the microbes that can alter their physiology, viability and ultimately their infection capacity. Thus, this thesis aimed to elucidate these synergistic interactions between physicochemical and biological properties of aerosol by developing a novel experimental system to be initially used with low hazard bacteria falling into the Hazard Group 1 (HG1).

At the starting point of this project, the only capability of the original EDT prototype was to provide qualitative data on the survival of airborne *E. coli* BL21 at gas-phase RHs under 50% for periods up to 90 min. After the desired suspension time, the bioaerosol particles were collected into 1 mL of LB broth and the survival of the airborne bacteria was determined by the cloudiness of the broth where the bioaerosol was collected after 24 hs incubation (Figure 6-1).

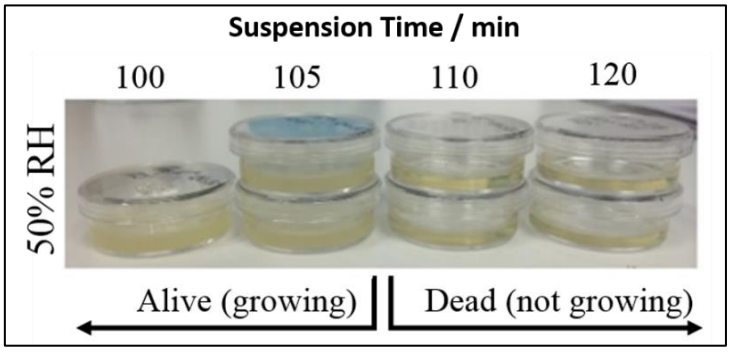

Figure 6-1. Petri dishes showing the initial qualitative survival data generated in CELEBS . The survival of airborne *E. coli* BL21 was based on the turbidity of the incubated LB broth containing levitated populations (< 200 droplets) of bioaerosols which were suspended for different time intervals. Note that broth turbidity is observed up to 110 min levitations when all the bacteria is assumed to have died in the aerosol phase under these conditions.

During this thesis, important advancements included the development of the technique and the first steps in using this novel capability to understand how a wide variety of parameters (e.g. biological, environmental, compositional) dictate the length of time microorganisms remain viable in the aerosol phase.

Initially, the main focus of this work was to completely characterize the experimental system as well as its impact on the viability of the microorganisms, aiming to generate robust quantitative survival data. Thus, some of the main findings achieved during the first half of the PhD are described in Chapter 3 and include: the incorporation of key modifications in the experimental system to improve the overall operation and reproducibility in the results; the development of an off-line viability assay to calculate airborne survival; the determination of the effect of aerosolization with the DoD micro-dispenser and suspension in the electrodynamic field on bacteria viability; the characterisation of the microbial load in the generated aerosol droplets; the determination of the sampling efficiency of CELEBS and the initial characterisation of survival for airborne bacteria as a function of the atmospheric RH and time.

During the last years of this work, the focus turned into increasing the complexity of the experimental systems and extending the parameters being proved to impact airborne survival. These results are included in Chapters 4 and 5 and investigate how the particle size, spray fluid, particle morphology, presence of atmospheric gases and other relevant parameters, affect the viability of airborne bacteria contained in more representative biological droplet compositions (i.e using artificial respiratory secretions).

6.2 Current Applications

The outbreak of the current SARS-CoV-2 pandemic has catalyzed the integration of CELEBS into high-level microbiological containment to investigate the environmental parameters impacting SARS-CoV-2 and, therefore, generate important information to reduce the risk of infection during the current pandemic by integrating this data in risk infection models. The transitioning and development of the CELEBS instrument for use with HG2, 3 and 4 pathogens has been carried out since March of 2020. Currently, two different instruments are located in a biosafety cabinet at containment level 3 and another CELEBS system is located at containment level 2 to enable experimental work with the novel SARS-CoV-2 and its proxy, the Mouse

Hepatitis Virus (MHV). An important number of instrumental adaptations have been incorporated into the previous CELEBS prototype to enable the manipulation of the instrument under high containment, including for example the automatic load/unload of the DoD dispenser using an in-house developed LabView programme combined with a vacuum system which prevents the manual manipulation of the DoD and thus reducing the risk of infection, the implementation of wider control of the chamber atmosphere (i.e. combining both temperature and RH control) and the systematic operation of several instruments by using a single PC and a single programme.

Importantly, the development of novel assays for the determination of viral infectivity rates have been also performed. This has presented some challenges associated with the low viral concentrations in the aerosol droplets (~1 virus per droplet) which are distributed across a droplet population according to Poisson statistics, and therefore impact the reproducibility of the data. Therefore, efforts have been made to increase the viral concentration by generating larger aerosol droplets able to contain a higher number of viral particles (i.e. modifying the DoD parameters during generation, decreasing the viscosity of the viral suspension before aerosolization and even increasing the titre of the original stocks). These limitations required the tailoring of conventional microbiological techniques to determine the virus infectivity rates to fit the requirements of this novel methodology. Specifically, the number of viral particles per droplet is calculated by plating the media containing the levitated droplets into a 96-well plate containing VERO E6 TMPRSS 2 cells by using a Poisson distribution equation.

In addition to the experimental adaptations of the instrument and the methodology, a large number of control and containment procedures have been developed to reduce the risk of exposure to the viruses via inhalation or direct contact and ensure the safety of the laboratory workers. To mention a few: the whole lab is maintained under negative pressure and all direct work with the viruses is undertaken either in a class three biosafety cabinet (i.e. for experiments with SARS-CoV-2) or in a class two biosafety cabinet (i.e. for experiments with MHV); the adequate pressure inside the cabinets is checked daily before the performance of experiments and all the equipment used to protect the workers, including the PPE, HEPA filters, autoclave and biosafety cabinets are regularly maintained following COSHH regulations. Moreover, emergency procedures for spillages and personal contamination have been also implemented as well as specific procedures for waste disposal. Importantly, extensive and suitable training

has been provided in both the theoretical and practical aspects of the work before performing any type of laboratory work.

6.3 Future Work

Other than the past and current applications already addressed, there are a few other studies I believe could be performed by using the methodology developed during this thesis. Firstly, I believe it is important to perform comparative studies of CELEBS with standard experimental systems such as the rotating drum and micro-threads to provide a full characterisation of the experimental techniques and enable the comparison of airborne survival data across laboratories. Secondly, to enable the complete development of a robust predictive tool based on the main mechanisms of inactivation of airborne microorganisms, studies should be extended across a wider number of infectious respiratory pathogens, both bacterial and viral microorganisms (e.g. SARS-CoV-1, Ebola virus, Influenza virus, *Yersinia Pestis*, *Neisseria meningitis*, *Mycobacterium tuberculosis*, etc). Importantly, the study of the molecular response of airborne microorganisms to the processes taking place in the aerosol phase, by comparing the response of genetically modified strains of a pathogen to the wild type, enabling the identification of genes influencing the microbe airborne survival. Finally, investigating the impact of atmospheric pollutant, Secondary Organic Aerosols (SOA), the interplay between RH and temperature, sunlight and Open-Air Factors (OAF) on bioaerosol survival would be crucial to fully understand all the atmospheric processes occurring in the natural environment. These factors have been previously reported to have a deleterious effect on airborne survival.[97,98]

Besides, future work should be carried out to improve some experimental limitations currently presented in this methodology. For instance, the use of very viscous materials such as the artificial sputum becomes a tedious work by using the current DoD micro-dispensers. Although attainable, the continuous clogging of the DoD system with this type of solutions results in a time-consuming data acquisition process in comparison with the use of other loading suspensions. Additionally, the use of a DoD systems with a broader range of initial droplet sizes would be useful to further explore this parameter and generate more representative bioaerosols. This may require the development of an improved dispensing system that allows

the ready generation of aerosol droplets from solutions with a wider range of viscosities. Thus, ideally, it would be possible to further investigate the microphysical properties and bioaerosol survival in real respiratory fluids. Finally, the incorporation of UV light and increased accessibility to different gas atmospheres would enable to investigate the reactivity of bioaerosol particles and study its impact on the survival of airborne pathogens. Finally, linking aerosol survival with infectivity as well as investigating the effect of rehydration on evaporated droplets to mimic inhalation would provide valuable information to better understand the whole picture of airborne disease transmission.

6.4 Closing Remarks

Summarizing, we have developed a useful methodology to answer fundamental questions about the mechanisms dictating airborne disease transmission. A better understanding of the interactions between processes taking place during aerosol transport and biological survival at the empirical level will provide critical data for epidemiological and risk models together with additional confidence in the development of operational policies. Moreover, the predictive potential of this approach to determine what are the important factors affecting the viability of airborne pathogens could lead to quicker implementation of mitigation strategies (e.g. conditioning indoor environments such as hospitals to reduce the risk of infection). Therefore, the information provided by this methodology can be of high utility to both Public Health, epidemiology, ecology, agriculture, biosecurity, climate and atmospheric processes.

References

1 R. Pung, C. J. Chiew, B. E. Young, S. Chin, M. I. C. Chen, H. E. Clapham, A. R. Cook, S. Maurer-Stroh, M. P. H. S. Toh, C. Poh, M. Low, J. Lum, V. T. J. Koh, T. M. Mak, L. Cui, R. V. T. P. Lin, D. Heng, Y. S. Leo, D. C. Lye, V. J. M. Lee, K. qian Kam, S. Kalimuddin, S. Y. Tan, J. Loh, K. C. Thoon, S. Vasoo, W. X. Khong, N. A. Suhaimi, S. J. Chan, E. Zhang, O. Oh, A. Ty, C. Tow, Y. X. Chua, W. L. Chaw, Y. Ng, F. Abdul-Rahman, S. Sahib, Z. Zhao, C. Tang, C. Low, E. H. Goh, G. Lim, Y. Hou, I. Roshan, J. Tan, K. Foo, K. Nandar, L. Kurupatham, P. P. Chan, P. Raj, Y. Lin, Z. Said, A. Lee, C. See, J. Markose, J. Tan, G. Chan, W. See, X. Peh, V. Cai, W. K. Chen, Z. Li, R. Soo, A. L. Chow, W. Wei, A. Farwin and L. W. Ang, Investigation of three clusters of COVID-19 in Singapore: implications for surveillance and response measures, *Lancet*, 2020, **395**, 1039–1046.

2 A. C. Fears, W. B. Klimstra, P. Duprex, A. Hartman, S. C. Weaver, K. S. Plante, D. Mirchandani, J. Plante, P. V. Aguilar, D. Fernandez, A. Nalca, A. Totura, D. Dyer, B. Kearney, M. Lackemeyer, J. K. Bohannon, R. Johnson, R. F. Garry, D. S. Reed and C. J. Roy, Comparative dynamic aerosol efficiencies of three emergent coronaviruses and the unusual persistence of SARS-CoV-2 in aerosol suspensions, *medRxiv*, 2020, **2**, 2020.04.13.20063784.

3 Y. Li, X. Huang, I. T. S. Yu, T. W. Wong and H. Qian, Role of air distribution in SARS transmission during the largest nosocomial outbreak in Hong Kong, *Indoor Air*, 2005, **15**, 83–95.

4 L. Morawska, J. W. Tang, W. Bahnfleth, P. M. Bluyssen, A. Boerstra, G. Buonanno, J. Cao, S. Dancer, A. Floto, F. Franchimon, C. Haworth, J. Hogeling, C. Isaxon, J. L. Jimenez, J. Kurnitski, Y. Li, M. Loomans, G. Marks, L. C. Marr, L. Mazzarella, A. K. Melikov, S. Miller, D. K. Milton, W. Nazaroff, P. V. Nielsen, C. Noakes, J. Peccia, X. Querol, C. Sekhar, O. Seppänen, S. ichi Tanabe, R. Tellier, K. W. Tham, P. Wargocki, A. Wierzbicka and M. Yao, How can airborne transmission of COVID-19 indoors be

minimised?, *Environ. Int.*, , DOI:10.1016/j.envint.2020.105832.

5 S. J. Olsen, H. L. Chang, T. Y. Y. Cheung, A. F. Y. Tang, T. L. Fisk, S. P. L. Ooi, H. W. Kuo, D. D. S. Jiang, K. T. Chen, J. Lando, K. H. Hsu, T. J. Chen and S. F. Dowell, Transmission of the Severe Acute Respiratory Syndrome on Aircraft, *N. Engl. J. Med.*, 2003, **349**, 2416–2422.

6 L. Morawska and J. Cao, Airborne transmission of SARS-CoV-2 : The world should face the reality, *Environ. Int.*, 2020, **139**, 105730.

7 Q. J. Leclerc, N. M. Fuller, L. E. Knight, S. Funk and G. M. Knight, What settings have been linked to SARS-CoV-2 transmission clusters?, *Wellcome Open Res.*, , DOI:10.12688/wellcomeopenres.15889.2.

8 T. F. Booth, B. Kournikakis, N. Bastien, J. Ho, D. Kobasa, L. Stadnyk, Y. Li, M. Spence, S. Paton, B. Henry, B. Mederski, D. White, D. E. Low, A. McGeer, A. Simor, M. Vearncombe, J. Downey, F. B. Jamieson, P. Tang and F. Plummer, Detection of airborne severe acute respiratory syndrome (SARS) coronavirus and environmental contamination in SARS outbreak units, *J. Infect. Dis.*, 2005, **191**, 1472–1477.

9 D. Verreault, C. Duchaine, M. Marcoux-Voiselle, N. Turgeon and C. J. Roy, Design of an environmentally controlled rotating chamber for bioaerosol aging studies, *Inhal. Toxicol.*, 2014, **26**, 554–558.

10 M. Otero Fernandez, R. J. Thomas, H. Oswin, A. E. Haddrell and J. P. Reid, Transformative Approach to Investigate the Microphysical Factors Influencing the Airborne Transmission of Pathogens, *Appl. Environ. Microbiol.*, 2020, **86**, 1–13.

11 M. Lou, S. Liu, C. Gu, H. Hu, Z. Tang, Y. Zhang, C. Xu and F. Li, The bioaerosols emitted from toilet and wastewater treatment plant: a literature review, *Environ. Sci. Pollut. Res.*, , DOI:10.1007/s11356-020-11297-8.

12 A. M. Jones and R. M. Harrison, The effects of meteorological factors on atmospheric bioaerosol concentrations - A review, *Sci. Total Environ.*, 2004, **326**, 151–180.

13 J. Fröhlich-Nowoisky, C. J. Kampf, B. Weber, J. A. Huffman, C. Pï¿½hlker, M. O. Andreae, N. Lang-Yona, S. M. Burrows, S. S. Gunthe, W. Elbert, H. Su, P. Hoor, E. Thines, T. Hoffmann, V. R. Desprï¿½s, U. Pï¿½schl, C. Pöhlker, M. O. Andreae, N.

Lang-Yona, S. M. Burrows, S. S. Gunthe, W. Elbert, H. Su, P. Hoor, E. Thines, T. Hoffmann, V. R. Després and U. Pöschl, Bioaerosols in the Earth system: Climate, health, and ecosystem interactions, *Atmos. Res.*, 2016, **182**, 346–376.

14 V. R. et al Despres, Primary biological aerosol particles in the atmosphere: A review, *Tellus, Ser. B Chem. Phys. Meteorol.*, , DOI:10.3402/tellusb.v64i0.15598.

15 M. Yao, Bioaerosol: A bridge and opportunity for many scientific research fields, *J. Aerosol Sci.*, 2017, **115**, 108–112.

16 R. Thomas, C. Davies, A. Nunez, S. Hibbs, H. Flick-Smith, L. Eastaugh, S. Smither, A. Gates, P. Oyston, T. Atkins and S. Eley, Influence of particle size on the pathology and efficacy of vaccination in a murine model of inhalational anthrax, *J. Med. Microbiol.*, 2010, **59**, 1415–1427.

17 B. Lighthart and B. T. Shaffer, Increased Airborne Bacterial Survival as a Function of Particle Content and Size, , DOI:10.1080/02786829708965483.

18 Z. Xu, Y. Wu, F. Shen, Q. Chen, M. Tan and M. Yao, Bioaerosol science, technology, and engineering: Past, present, and future, *Aerosol Sci. Technol.*, 2011, **45**, 1337–1349.

19 A. D. Estillore, J. V. Trueblood and V. H. Grassian, Atmospheric chemistry of bioaerosols: heterogeneous and multiphase reactions with atmospheric oxidants and other trace gases, *Chem. Sci.*, 2016, **7**, 6604–6616.

20 D. Ivanov, The great leveler: violence and the history of inequality from the stone age to the twenty-first century, *Eur. Soc.*, 2020, **22**, 149–151.

21 D. Huremović, in *Psychiatry of Pandemics*, Springer International Publishing, 2019, pp. 7–35.

22 O. J. Benedictow, *The Black Death and Later Plague Epidemics in the Scandinavian Countries:*, De Gruyter Open Poland, 2016.

23 S. Pruitt, Medieval 'Black Death' Was Airborne, Scientists Say - HISTORY, https://www.history.com/news/medieval-black-death-was-airborne-scientists-say, (accessed 16 April 2021).

24 New findings rewrite the story of the Black Death in Britain | Channel 4,

https://www.channel4.com/press/news/new-findings-rewrite-story-black-death-britain?journey=sign-in, (accessed 16 April 2021).

25 S. Ochmann, Smallpox, https://ourworldindata.org/smallpox#citation, (accessed 8 February 2021).

26 J. M. Elwood, Smallpox and its eradication, *J. Epidemiol. Community Heal.*, 1989, **43**, 92–92.

27 S. Riedel, Edward Jenner and the History of Smallpox and Vaccination, *Baylor Univ. Med. Cent. Proc.*, 2005, **18**, 21–25.

28 H. P. Lambert, The Conquest of Smallpox: The Impact of Inoculation on Smallpox Mortality in Eighteenth Century Britain. Peter Razzel. London: Caliban Books, 2nd (edn) 2003, pp. 288, 40.00. ISBN: 1-85066-045-X, *Int. J. Epidemiol.*, 2004, **34**, 230–231.

29 J. K. Taubenberger and D. M. Morens, 1918 Influenza: the Mother of All Pandemics, *Emerg. Infect. Dis.*, 2006, **12**, 15–22.

30 E. D. Kilbourne, Influenza pandemics of the 20th century, *Emerg. Infect. Dis.*, 2006, **12**, 9–14.

31 W. P. Glezen, Emerging infections: Pandemic influenza, *Epidemiol. Rev.*, 1996, **18**, 64–76.

32 L. Piroth, J. Cottenet, A. S. Mariet, P. Bonniaud, M. Blot, P. Tubert-Bitter and C. Quantin, Comparison of the characteristics, morbidity, and mortality of COVID-19 and seasonal influenza: a nationwide, population-based retrospective cohort study, *Lancet Respir. Med.*, 2021, **2600**, 1–9.

33 M. Alsved, L. Bourouiba, C. Duchaine, J. Löndahl, L. C. Marr, S. T. Parker, A. J. Prussin and R. J. Thomas, Natural sources and experimental generation of bioaerosols: Challenges and perspectives, *Aerosol Sci. Technol.*, 2019, **0**, 1–25.

34 R. Dhand and J. Li, Coughs and Sneezes: Their Role in Transmission of Respiratory Viral Infections, including SARS-CoV-2, *Am. J. Respir. Crit. Care Med.*, 2020, **202**, 651–659.

35 L. Bourouiba, E. Dehandschoewercker and J. W. M. Bush, Violent expiratory events: On coughing and sneezing, *J. Fluid Mech.*, 2014, **745**, 537–563.

36 B. E. Scharfman, A. H. Techet, J. W. M. M. Bush and L. Bourouiba, Visualization of sneeze ejecta: steps of fluid fragmentation leading to respiratory droplets, *Exp. Fluids*, 2016, **57**, 1–9.

37 M. L. Bourouiba, Where Sneezes Go, *Nature*.

38 L. Liu, J. Wei, Y. Li and A. Ooi, Evaporation and dispersion of respiratory droplets from coughing, *Indoor Air*, 2017, **27**, 179–190.

39 S. Asadi, A. S. Wexler, C. D. Cappa, S. Barreda, N. M. Bouvier and W. D. Ristenpart, Aerosol emission and superemission during human speech increase with voice loudness, *Sci. Rep.*, , DOI:10.1038/s41598-019-38808-z.

40 F. K. A. Gregson, N. A. Watson, C. M. Orton, A. E. Haddrell, L. P. McCarthy, T. J. R. Finnie, N. Gent, G. C. Donaldson, P. L. Shah, J. D. Calder, B. R. Bzdek, D. Costello and J. P. Reid, Comparing the Respirable Aerosol Concentrations and Particle Size Distributions Generated by Singing, Speaking and Breathing, *ChemRxiv*, 2020, **0**, 000.

41 L. Morawska, G. R. Johnson, Z. D. Ristovski, M. Hargreaves, K. Mengersen, S. Corbett, C. Y. H. Chao, Y. Li and D. Katoshevski, Size distribution and sites of origin of droplets expelled from the human respiratory tract during expiratory activities, *J. Aerosol Sci.*, 2009, **40**, 256–269.

42 G. Traverso, S. Laken, C. Lu, R. Maa, R. Langer and L. Bourouiba, Fluid fragmentation from hospital toilets, 2014, 2–4.

43 H. M. Darlow and W. R. Bale, Infective Hazards of Water-Closets, *Lancet*, 1959, **273**, 1196–1200.

44 E. L. Best, J. A. T. Sandoe and M. H. Wilcox, Potential for aerosolization of Clostridium difficile after flushing toilets: The role of toilet lids in reducing environmental contamination risk, *J. Hosp. Infect.*, 2012, **80**, 1–5.

45 S. Poulain and L. Bourouiba, Disease transmission via drops and bubbles, *Phys. Today*, 2019, **72**, 70–71.

46 S. Poulain, E. Villermaux and L. Bourouiba, Ageing and burst of surface bubbles, 2018, 636–671.

47 T. Gilet and L. Bourouiba, Fluid fragmentation shapes rain-induced foliar disease transmission, *J. R. Soc. Interface*, , DOI:10.1098/rsif.2014.1092.

48 Y. Wang and L. Bourouiba, Non-isolated drop impact on surfaces, *J. Fluid Mech.*, 2018, **835**, 24–44.

49 T. Gilet and L. Bourouiba, Rain-induced ejection of pathogens from leaves: Revisiting the hypothesis of splash-on-film using high-speed visualization, *Integr. Comp. Biol.*, 2014, **54**, 974–984.

50 The Aerobiology Pathway, *Air Spora*, 2006, 15–34.

51 R. J. Thomas, Particle size and pathogenicity in the respiratory tract., *Virulence*, 2013, **4**, 847–58.

52 J. P. Duguid, The size and the duration of air-carriage of respiratory droplets and droplet-nuclei, *J. Hyg. (Lond).*, 1946, **44**, 471–479.

53 R. S. Papineni and F. S. Rosenthal, The size distribution of droplets in the exhaled breath of healthy human subjects, *J. Aerosol Med. Depos. Clear. Eff. Lung*, 1997, **10**, 105–116.

54 G. Zayas, M. C. Chiang, E. Wong, F. MacDonald, C. F. Lange, A. Senthilselvan and M. King, Cough aerosol in healthy participants: Fundamental knowledge to optimize droplet-spread infectious respiratory disease management, *BMC Pulm. Med.*, 2012, **12**, 11.

55 G. R. Johnson, L. Morawska, Z. D. Ristovski, M. Hargreaves, K. Mengersen, C. Y. H. Chao, M. P. Wan, Y. Li, X. Xie, D. Katoshevski and S. Corbett, Modality of human expired aerosol size distributions, *J. Aerosol Sci.*, 2011, **42**, 839–851.

56 S. Yang, G. W. M. Lee, C. M. Chen, C. C. Wu and K. P. Yu, The size and concentration of droplets generated by coughing in human subjects, *J. Aerosol Med. Depos. Clear. Eff. Lung*, 2007, **20**, 484–494.

57 F. L. Lederer, T. J. Günther, J. Raff and K. Pollmann, E. coli filament formation induced by heterologous S-layer expression, *Bioeng. Bugs*, 2011, **2**, 178–181.

58 T. Je, D. M. Cb, L. Dooley, E. Ferroni, A. La, B. Ga, V. D. Ml, J. Ma, S. Thorning, B. Em, J. Clark, H. Tc, G. Pp, C. Jm, T. Je, D. M. Cb, L. Dooley, E. Ferroni, A. La, B. Ga, V. D. Ml, J. Ma, S. Thorning, B. Em and J. Clark, Je erson T, Del Mar CB, Dooley L, Ferroni E, Al-Ansary LA, Bawazeer GA, van Driel ML, Jones MA, Thorning S, Beller EM, Clark J, Ho mann TC, Glasziou PP, Conly JM, , DOI:10.1002/14651858.CD006207.pub5.www.cochranelibrary.com.

59 S. Asadi, N. Bouvier, A. S. Wexler and W. D. Ristenpart, The coronavirus pandemic and aerosols: Does COVID-19 transmit via expiratory particles?, *Aerosol Sci. Technol.*, 2020, **54**, 635–638.

60 R. Tellier, Y. Li, B. J. Cowling and J. W. Tang, Recognition of aerosol transmission of infectious agents: A commentary, *BMC Infect. Dis.*, 2019, **19**, 1–9.

61 W. T. Leung, S. C. Fu, G. N. Sze To and C. Y. H. Chao, Comparison of the resuspension behavior between liquid and solid aerosols, *Aerosol Sci. Technol.*, 2013, **47**, 1239–1247.

62 M. Z. Bazant and J. W. M. Bush, Beyond six feet: A guideline to limit indoor airborne transmission of COVID-19, *medRxiv*, 2020, 1–13.

63 L. Bourouiba, Turbulent Gas Clouds and Respiratory Pathogen Emissions: Potential Implications for Reducing Transmission of COVID-19, *JAMA - J. Am. Med. Assoc.*, 2020, **323**, 1837–1838.

64 M. . W. Prather, K.; Marr, L.; Schooley, R.; McDiarmid and D. M.; Milton, Airborne Transmission of SARS-CoV-2, *Science (80-.).*, 2020, **370**, 303–305.

65 B. K. A. Prather, C. C. Wang and R. T. Schooley, Reducing transmission of SARS-CoV-2, *Science (80-.).*, 2020, **368**, 1422–1424.

66 L. Deguillaume, M. Leriche, P. Amato, P. a. Ariya, A. M. Delort, U. Pöschl, N. Chaumerliac, H. Bauer, a. I. Flossmann and C. E. Morris, Microbiology and atmospheric processes: chemical interactions of Primary Biological Aerosols, *Biogeosciences Discuss.*, 2008, **5**, 841–870.

67 J. W. Tang, The effect of environmental parameters on the survival of airborne infectious agents, *J. R. Soc. Interface*, 2009, **6**, S737–S746.

68 M. Otero-Fernandez, R. J. Thomas, N. J. Garton, A. Hudson, A. Haddrell and J. P. Reid,

Assessing the airborne survival of bacteria in populations of aerosol droplets with a novel technology, *J. R. Soc. Interface*, 2019, **16**, 20180779.

69 C. S. Cox, Airborne bacteria and viruses, *Sci. Prog.*, 1989, **73**, 469–500.

70 R. Ehrlich and S. Miller, Survival of airborne Pasteurella tularensis at different atmospheric temperatures, *Appl Microbiol*, 1973, **25**, 369–372.

71 R. Ehrlich, S. Miller and R. L. Walker, Relationship between atmospheric temperature and survival of airborne bacteria, *Appl. Microbiol.*, 1970, **19**, 245–249.

72 R. Ehrlich and S. Miller, Effect of relative humidity and temperature on airborne Venezuelan equine encephalitis virus, *Appl Microbiol*, 1971, **22**, 194–199.

73 C. M. Wathes, K. Howard and A. J. F. Webster, The survival of Escherichia coli in an aerosol at air temperatures of 15 and 30 °C and a range of humidities, *J. Hyg. (Lond).*, 1986, **97**, 489–496.

74 K. A. Thompson, A. M. Bennett and J. T. Walker, Aerosol survival of Staphylococcus epidermidis, *J. Hosp. Infect.*, 2011, **78**, 216–220.

75 J. E. Benbough, Some Factors Affecting the Survival of Airborne Viruses, *J. gen. Virol.*, 1971, **10**, 209–220.

76 M. S. Davis and J. B. Bateman, Relative humidity and the killing of bacteria. I. Observations on Escherichia coli and Micrococcus lysodeikticus., *J. Bacteriol.*, 1960, **80**, 577–579.

77 J. B. Bateman, C. L. Stevens, W. B. Mercer and E. L. Carstenses, Relative humidity and the killing of bacteria: the variation of cellular water content with external relative humidity or osmolality., *J. Gen. Microbiol.*, 1962, **29**, 207–219.

78 C. S. Cox, Aerosol survival of Escherichia coli B disseminated from the dry state., *Appl Microbiol*, 1970, **19**, 604–7.

79 C. S. Cox, The aerosol survival of Escherichia coli B in nitrogen, argon and helium atmospheres and the influence of relative humidity., *J Gen Microbiol*, 1968, **50**, 139–47.

80 J. E. Benbough, Death mechanisms in airborne Escherichia coli., *J. Gen. Microbiol.*,

1967, **47**, 325–333.

81 M. F. R. Kets, The toxic effect of oxygen upon the aerosol survival of Escherichia coli B, *J. gen. Microbiol*, 1967, **49**, 115–117.

82 J. M. BEEBE, Stability of disseminated aerosols of Pasteurella tularensis subjected to simulated solar radiations at various humidities, *J. Bacteriol.*, 1959, **78**, 18–24.

83 W. Yang, S. Elankumaran and L. C. Marr, Relationship between Humidity and Influenza A Viability in Droplets and Implications for Influenza's Seasonality, *PLoS One*, 2012, **7**, 1–8.

84 C. S. Cox, M. C. Bondurant and M. T. Hatch, Effects of oxygen on aerosol survival of radiation sensitive and resistant strains of Escherichia coli B, *J. Hyg. (Lond).*, 1971, **69**, 661–672.

85 B. Lighthart and Y. Tong, Effect of simulated solar radiation on mixed outdoor atmospheric bacterial\npopulations, *FEMS Microbiol. Ecol.*, 1998, **26**, 311–316.

86 Y. Tong and B. Lighthart, Solar radiation has a lethal effect on natural populations of culturable outdoor atmospheric bacteria, *Atmos. Environ.*, 1997, **31**, 897–900.

87 C. M. Walker and G. Ko, Effect of ultraviolet germicidal irradiation on viral aerosols, *Environ. Sci. Technol.*, 2007, **41**, 5460–5465.

88 J. E. Benbough, Factors affecting the toxicity of oxygen towards airborne coliform bacteria., *J. Gen. Microbiol.*, 1969, **56**, 241–250.

89 C. S. Cox, The Survival od Escherichia coli sprayed into Air and into Nitrogen from Distilled Water and from Solutions of Protecting Agents, as a function of Relative Humidity, *J. Gen. Microbiol.*, 1966, **43**, 383–399.

90 C. S. Cox, Aerosol survival of Pasteurella tularensis disseminated from the wet and dry states., *Appl. Microbiol.*, 1971, **21**, 482–486.

91 G. E. Hess, Effects of oxygen on aerosolized Serratia marcescens, *Appl. Environ. Microbiol.*, 1965, **13**, 781.

92 C. S. COX, The Aerosol Survival and Cause of Death of Escherichia coli K12, *Microbiology*, 1968, **54**, 169–175.

93 P. Down, Open-air factors in enclosed systems, 1974, 53–60.

94 G. de Mik and I. de Groot, The germicidal effect of the open air in different parts of The Netherlands, 1977, **78**, 175–187.

95 R. Ehrlich and S. Miller, Effect of NO 2 on airborne Venezuelan equine encephalomyelitis virus, *Appl Microbiol*, 1972, **23**, 481–484.

96 A. I. Donaldson and N. P. Ferris, The Survival of Foot-and-Mouth Disease Virus in Open Air Conditions, *J. Hyg. (Lond).*, 1975, **74**, 409–416.

97 a. M. Hood, An indoor system for the study of biological aerosols in open air conditions, *J. Hyg. (Lond).*, 2009, **69**, 607.

98 F. A. Dark and T. Nash, Comparative Toxicity of Various Ozonized Olefins to Bacteria Suspended in Air, *J. Hyg.*, 1970, **68**, 245-.

99 G. De Mik and I. De Groot, Breaks induced in the deoxyribonucleic acid of aerosolized Escherichia coli by ozonized cyclohexene, *Appl. Environ. Microbiol.*, 1978, **35**, 6–10.

100 C. S. Cox and S. J. Gagen, Aerosol survival of Sevvatia marcescens as a function of oxygen concentration, relative humidity, and time, 1974, **20**, 1529–1534.

101 S. a Faith, L. P. Smith, A. S. Swatland and D. S. Reed, Growth conditions and environmental factors impact aerosolization but not virulence of Francisella tularensis infection in mice., *Front. Cell. Infect. Microbiol.*, 2012, **2**, 126.

102 W. D. Won and H. Ross, Effect of diluent and relative humidity on apparent viability of airborne Pasteurella pestis, *Appl Microbiol*, 1966, **14**, 742–745.

103 N. Turgeon, M. J. Toulouse, B. Martel, S. Moineau and C. Duchaine, Comparison of five bacteriophages as models for viral aerosol studies, *Appl. Environ. Microbiol.*, 2014, **80**, 4242–4250.

104 K. L. Id, C. R. Schulte and L. C. M. Id, Survival of MS2 and Φ 6 viruses in droplets as a function of relative humidity , pH , and salt , protein , and surfactant concentrations, 2020, 1–18.

105 K. A. Kormuth, K. Lin, J. P. Ii, E. P. Vejerano, A. J. Tiwari, S. S. Cox, M. M. Myerburg, S. S. Lakdawala, L. C. Marr, A. J. Prussin, E. P. Vejerano, A. J. Tiwari, S. S. Cox, M.

M. Myerburg, S. S. Lakdawala and L. C. Marr, Influenza virus infectivity is retained in aerosols and droplets independent of relative humidity, *J. Infect. Dis.*, 2018, **218**, 739–747.

106 T. Trouwborst, S. Kuyper, J. C. De Jong and A. D. Plantinga, Inactivation of some bacterial and animal viruses by exposure to liquid air interfaces, *J. Gen. Virol.*, 1974, **24**, 155–165.

107 T. Trouwborst and J. C. De Jong, Interaction of Some Factors in the Mechanism of Inactivation of Bacteriophage MS2 in Aerosols, *Appl. Microbiol.*, 1973, **26**, 252–257.

108 I. Hayakawa and C. P. Poon, Short Storage Studies on the Effect of Temperature and Relative Humidity on the Viability of Airborne Bacteria, *Am. Ind. Hyg. Assoc. J.*, 1965, **26**, 150–160.

109 J. F. Davies, A. E. Haddrell, A. M. J. Rickards and J. P. Reid, Simultaneous analysis of the equilibrium hygroscopicity and water transport kinetics of liquid aerosol, *Anal. Chem.*, 2013, **85**, 5819–5826.

110 A. E. Haddrell and R. J. Thomas, Aerobiology: Experimental considerations, observations, and future tools, *Appl. Environ. Microbiol.*, 2017, **83**, 1–17.

111 T. P. Weber and N. I. Stilianakis, Inactivation of influenza A viruses in the environment and modes of transmission: A critical review, *J. Infect.*, 2008, **57**, 361–373.

112 A. C. Lowen, S. Mubareka, J. Steel and P. Palese, Influenza virus transmission is dependent on relative humidity and temperature, *PLoS Pathog.*, 2007, **3**, 1470–1476.

113 M. H. Wolff, S. A. Sattar, O. Adegbunrin and J. Tetro, Environmental survival and microbicide inactivation of coronaviruses, *Coronaviruses with Spec. Emphas. First Insights Concern. SARS*, 2005, 201–212.

114 L. C. Marr, J. W. Tang, J. Van Mullekom and S. S. Lakdawala, Mechanistic insights into the effect of humidity on airborne influenza virus survival, transmission and incidence, *J. R. Soc. Interface*, 2019, **16**, 20180298.

115 R. J. Thomas, D. Webber, R. Hopkins, A. Frost, T. Laws, P. N. Jayasekera and T. Atkins, The cell membrane as a major site of damage during aerosolization of Escherichia coli, *Appl. Environ. Microbiol.*, 2011, **77**, 920–925.

116 A. Fernstrom and M. Goldblatt, Aerobiology and its role in the transmission of infectious diseases., *J. Pathog.*, 2013, **2013**, 493960.

117 S. J. Webb, Factors affecting the viability of air-borne bacteria, *Can. J. Microbiol.*, 1959, **14**, 742–745.

118 K. W. F. Jericho, E. V. Langford and J. Pantekoek, Recovery of Pasteurella hemolytica from aerosols at differing temperature and humidity, *Can. J. Comp. Med.*, 1977, **41**, 211–214.

119 E. W. Dunklin and T. T. Puck, The lethal effect of relative humidity on air-borne bacteria, *Public Health*, 1948, **87,2**, 87–101.

120 T. A. Myatt, S. L. Johnston, S. Rudnick and D. K. Milton, Airborne rhinovirus detection and effect of ultraviolet irradiation on detection by a semi-nested RT-PCR assay, *BMC Public Health*, 2003, **3**, 1–7.

121 D. E. Jenkins, S. A. Chaisson and A. Matin, Starvation-induced cross protection against osmotic challenge in Escherichia coli, *J. Bacteriol.*, 1990, **172**, 2779–2781.

122 J. Mar, N. Llorens, A. Tormo and E. Mart, Stationary phase in gram-negative bacteria, 2010, **34**, 476–495.

123 S. Lacour and P. Landini, σS-dependent gene expression at the onset of stationary phase in Escherichia coli: Function of σS-dependent genes and identification of their promoter sequences, *J. Bacteriol.*, 2004, **186**, 7186–7195.

124 B. R. Bzdek, J. P. Reid and M. I. Cotterell, Open questions on the physical properties of aerosols, *Commun. Chem.*, 2020, **3**, 10–13.

125 Y. C. Song, A. E. Haddrell, B. R. Bzdek, J. P. Reid, T. Bannan, D. O. Topping, C. Percival and C. Cai, Measurements and Predictions of Binary Component Aerosol Particle Viscosity, *J. Phys. Chem. A*, 2016, **120**, 8123–8137.

126 M. Girod, E. Moyano, D. I. Campbell and R. G. Cooks, Accelerated bimolecular reactions in microdroplets studied by desorption electrospray ionization mass spectrometry, *Chem. Sci.*, 2011, **2**, 501–510.

127 R. M. Bain, C. J. Pulliam and R. G. Cooks, Accelerated Hantzsch electrospray synthesis

with temporal control of reaction intermediates, *Chem. Sci.*, 2015, **6**, 397–401.

128 E. Lang, F. Zoz, C. Iaconelli, S. Guyot, P. Alvarez-Martin, L. Beney, J. M. Perrier-Cornet and P. Gervais, Recovery estimation of dried foodborne pathogens is directly related to rehydration kinetics, *PLoS One*, 2016, **11**, 1–10.

129 Z. Zuo, T. H. Kuehn, A. Z. Bekele, S. K. Mor, H. Verma, S. M. Goyal, P. C. Raynor and D. Y. H. Pui, Survival of airborne MS2 bacteriophage generated from human saliva, artificial saliva, and cell culture medium, *Appl. Environ. Microbiol.*, 2014, **80**, 2796–2803.

130 H. Zhen, T. Han, D. E. Fennell and G. Mainelis, Release of free DNA by membrane-impaired bacterial aerosols due to aerosolization and air sampling, *Appl. Environ. Microbiol.*, 2013, **79**, 7780–7789.

131 J. F. Young-Jae; Frank, Biological Aerosols: A Review of Airborne Contamination and its Measurement in Dairy Processing Plant, *J. Food Prot.*, 1989, **7**, 512–524.

132 T. Reponen, K. Willeke, V. Ulevicius, S. A. Grinshpun and J. Donnelly, Techniques for Dispersion of Microorganisms into Air, *Aerosol Sci. Technol.*, 1997, **27**, 405–421.

133 T. J. Piercy, S. J. Smither, J. A. Steward, L. Eastaugh and M. S. Lever, The survival of filoviruses in liquids, on solid substrates and in a dynamic aerosol, *J. Appl. Microbiol.*, 2010, **109**, 1531–1539.

134 M. H. Woo, A. Grippin, D. Anwar, T. Smith, C. Y. Wu and J. D. Wander, Effects of relative humidity and spraying medium on UV decontamination of filters loaded with viral aerosols, *Appl. Environ. Microbiol.*, 2012, **78**, 5781–5787.

135 C. S. Cox and L. J. Goldberg, Aerosol survival of Pasteurella tularensis and the influence of relative humidity, *Appl Microbiol*, 1972, **23**, 1–3.

136 K. R. May, The collison nebulizer: Description, performance and application, *J. Aerosol Sci.*, , DOI:10.1016/0021-8502(73)90006-2.

137 H. Zhen, T. Han, D. E. Fennell and G. Mainelis, A systematic comparison of four bioaerosol generators: Affect on culturability and cell membrane integrity when aerosolizing Escherichia coli bacteria, *J. Aerosol Sci.*, 2014, **70**, 67–79.

138 D. J. Adams, J. C. Spendlove, R. S. Spendlove and B. B. Barnett, Aerosol stability of infectious and potentially infectious reovirus particles, *Appl. Environ. Microbiol.*, 1982, **44**, 903–908.

139 K. P. Fennelly, M. D. Tribby, C. Y. Wu, G. L. Heil, L. J. Radonovich, J. C. Loeb and J. A. Lednicky, Collection and measurement of aerosols of viable influenza virus in liquid media in an Andersen cascade impactor, *Virus Adapt. Treat.*, 2014, **7**, 1–9.

140 P. Dabisch, J. Yeager, J. Kline, K. Klinedinst, A. Welsch and M. L. Pitt, Comparison of the efficiency of sampling devices for aerosolized Burkholderia pseudomallei., *Inhal. Toxicol.*, 2012, **24**, 247–54.

141 R. J. Thomas, D. Webber, W. Sellors, A. Collinge, A. Frost, A. J. Stagg, S. C. Bailey, P. N. Jayasekera, R. R. Taylor, S. Eley and R. W. Titball, Characterization and deposition of respirable large- and small-particle bioaerosols, *Appl. Environ. Microbiol.*, 2008, **74**, 6437–6443.

142 K.-C. Fan, J.-Y. Chen, C.-H. Wang and W.-C. Pan, Development of a drop-on-demand droplet generator for one-drop-fill technology, *Sensors Actuators A Phys.*, 2008, **147**, 649–655.

143 F. Rabey, R. J. Janssen and L. M. Kelley, Stability of St. Louis encephalitis virus in the airborne state, *Appl Microbiol*, 1969, **18**, 880–882.

144 B. Lighthart, Survival of airborne bacteria in a high urban concentration of carbon monoxide., *Appl Microbiol*, 1973, **25**, 86–91.

145 V. Krumins, E. K. Son, G. Mainelis and D. E. Fennell, Retention of inactivated bioaerosols and ethene in a rotating bioreactor constructed for bioaerosol activity studies, *Clean - Soil, Air, Water*, 2008, **36**, 593–600.

146 S. J. Smither, T. J. Piercy, L. Eastaugh, J. A. Steward and M. S. Lever, An alternative method of measuring aerosol survival using spiders' webs and its use for the filoviruses, *J. Virol. Methods*, 2011, **177**, 123–127.

147 K. R. May and H. a. Druett, A Microthread Technique for Studying the Viability of Microbes in a Simulated Airborne State, *J. Gen. Microbiol.*, 1968, **51**, 353–366.

148 R. Bailey, L. Fielding, A. Young and C. Griffith, Effect of Ozone and Open Air Factor

against Aerosolized Micrococcus luteus, 2007, **70**, 2769–2773.

149 M. V. Walter, B. Marthi, V. P. Fieland and L. M. Ganio, Effect of aerosolization on subsequent bacterial survival, *Appl. Environ. Microbiol.*, 1990, **56**, 3468–3472.

150 B. Marthi, V. P. Fieland, M. Walter and R. J. Seidler, Survival of bacteria during aerosolization, *Appl. Environ. Microbiol.*, 1990, **56**, 3463–3467.

151 P. Dabisch, K. Bower, B. Dorsey and L. Wronka, Recovery efficiencies for *Burkholderia thailandensis* from various aerosol sampling media., *Front. Cell. Infect. Microbiol.*, 2012, **2**, 78.

152 Z. Xu, K. Wei, Y. Wu, F. Shen, Q. Chen, M. Li and M. Yao, Enhancing Bioaerosol Sampling by Andersen Impactors Using Mineral-Oil-Spread Agar Plate, *PLoS One*, , DOI:10.1371/journal.pone.0056896.

153 C.-S. Li, Sampling Performance of Impactors for Bacterial Bioaerosols, *Aerosol Sci. Technol.*, 1999, **30**, 280–287.

154 C. S. Li and Y. C. Lin, Storage effects on bacterial concentration: Determination of impinger and filter samples, *Sci. Total Environ.*, 2001, **278**, 231–237.

155 M. Dybwad, G. Skogan and J. M. Blatny, Comparative Testing and Evaluation of Nine Different Air Samplers: End-to-End Sampling Efficiencies as Specific Performance Measurements for Bioaerosol Applications, *Aerosol Sci. Technol.*, 2014, **48**, 282–295.

156 J. R. Hermann and J. J. Zimmerman, Analytical sensitivity of air samplers based on uniform point-source exposure to airborne Porcine reproductive and respiratory syndrome virus and swine influenza virus, *Can. J. Vet. Res.*, 2008, **72**, 440–443.

157 A. M. Rule, J. Kesavan, K. J. Schwab and T. J. Buckley, Application of flow cytometry for the assessment of preservation and recovery efficiency of bioaerosol samplers spiked with Pantoea agglomerans, *Environ. Sci. Technol.*, 2007, **41**, 2467–2472.

158 S. A. Grinshpun, K. Willeke, V. Ulevicius, A. Juozaitis, S. Terzieva, J. Donnelly, G. N. Stelma and K. P. Brenner, Effect of impaction, bounce and reaerosolization on the collection efficiency of impingers, *Aerosol Sci. Technol.*, 1997, **26**, 326–342.

159 C.-S. Li, Evaluation of Microbial Samplers for Bacterial Microorganisms, *Aerosol Sci.*

Technol., 1999, **30**, 100–108.

160 X. Lin, T. A. Reponen, K. Willeke, S. A. Grinshpun, K. K. Foarde and D. S. Ensor, Long-term sampling of airborne bacteria and fungi into a non-evaporating liquid, *Atmos. Environ.*, 1999, **33**, 4291–4298.

161 X. Lin, T. Reponen, K. Willeke, Z. Wang, S. a. Grinshpun and M. Trunov, Survival of Airborne Microorganisms During Swirling Aerosol Collection, *Aerosol Sci. Technol.*, 2000, **32**, 184–196.

162 L. Riemenschneider, M. H. Woo, C. Y. Wu, D. Lundgren, J. Wander, J. H. Lee, H. W. Li and B. Heimbuch, Characterization of reaerosolization from impingers in an effort to improve airborne virus sampling, *J. Appl. Microbiol.*, 2010, **108**, 315–324.

163 K. R. MAY and G. J. HARPER, The efficiency of various liquid impinger samplers in bacterial aerosols., *Br. J. Ind. Med.*, 1957, **14**, 287–297.

164 G. Cao, J. D. Noti, F. M. Blachere, W. G. Lindsley and D. H. Beezhold, Development of an improved methodology to detect infectious airborne influenza virus using the NIOSH bioaerosol sampler, *J. Environ. Monit.*, 2011, **13**, 3321.

165 G. Mainelis, K. Willeke, P. Baron, T. Reponen, S. A. Grinshpun, R. L. Górny and S. Trakumas, Electrical charges on airborne microorganisms, *J. Aerosol Sci.*, 2001, **32**, 1087–1110.

166 G. Mainelis, S. A. Grinshpun, K. Willeke, T. Reponen, V. Ulevicius and P. J. Hintz, Collection of airborne microorganisms by electrostatic precipitation, *Aerosol Sci. Technol.*, 1999, **30**, 127–144.

167 G. Mainelis, K. Willeke, A. Adhikari, T. Reponen and S. a Grinshpun, Design and Collection Efficiency of a New Electrostatic Precipitator for Bioaerosol Collection, *Aerosol Sci. Technol.*, 2002, **36**, 1073–1085.

168 J. Q. Feng, L. S. Go, J. Calubayan and R. Tomaska, Working mechanism and behavior of collison nebulizer, *arXiv*.

169 T. Han, M. Wren, K. DuBois, J. Therkorn and G. Mainelis, Application of ATP-based bioluminescence for bioaerosol quantification: Effect of sampling method, *J. Aerosol Sci.*, 2015, **90**, 114–123.

170 J. L. Santarpia, S. Ratnesar-Shumate and A. Haddrell, Laboratory study of bioaerosols: Traditional test systems, modern approaches, and environmental control, *Aerosol Sci. Technol.*, 2020, **54**, 585–600.

171 R. L. Gruel, C. R. Reid and R. T. Allemann, The optimum rate of drum rotation for aerosol aging, *J. Aerosol Sci.*, 1987, **18**, 17–22.

172 B. Asgharian and O. R. Moss, Particle Suspension in a Rotating Drum Chamber When the Influence of Gravity and Rotation are Both Significant, *Aerosol Sci. Technol.*, 1992, **17**, 263–277.

173 M. Dybwad, G. Skogan, S. G. Bacteria, M. Dybwad and G. Skogan, Aerobiological Stabilities of Different Cell Clusters of Different Compositions, 2017, **83**, 1–12.

174 A. R. McFarland, J. S. Haglund, M. D. King, S. Hu, M. S. Phull, B. W. Moncla and Y. Seo, Wetted wall cyclones for bioaerosol sampling, *Aerosol Sci. Technol.*, 2010, **44**, 241–252.

175 S. Ratnesar-Shumate, M. L. Wagner, C. Kerechanin, G. House, K. M. Brinkley, C. Bare, N. A. Baker, R. Quizon, J. Quizon, A. Proescher, E. Van Gieson and J. L. Santarpia, Improved method for the evaluation of real-time biological aerosol detection technologies, *Aerosol Sci. Technol.*, 2011, **45**, 635–644.

176 T. L. Montgomery and M. Corn, Aerosol deposition in a pipe with turbulent airflow, *J. Aerosol Sci.*, , DOI:10.1016/0021-8502(70)90034-0.

177 E. P. Vejerano and L. C. Marr, Physico-chemical characteristics of evaporating respiratory fluid droplets, *J. R. Soc. Interface*, 2018, **15**, 1–10.

178 J. Kesavan and J.-L. Sagripanti, Evaluation criteria for bioaerosol samplers, *Environ. Sci. Process. Impacts*, 2015, **17**, 638–645.

179 A. Juozaitis, K. Willeke, S. A. Grinshpun and J. Donnelly, Impaction onto a glass slide or agar versus impingement into a liquid for the collection and recovery of airborne microorganisms, *Appl. Environ. Microbiol.*, 1994, **60**, 861–870.

180 G. Mainelis, K. Willeke, A. Adhikari, T. Reponen and S. A. Grinshpun, Design and Collection Efficiency of a New Electrostatic Precipitator for Bioaerosol Collection, *Aerosol Sci. Technol.*, 2002, **36**, 1073–1085.

181 P. A. Jensen, W. F. Todd, G. N. Davis and P. V Scarpino, Evaluation of eight bioaeorosol samplers challenged with aerosols of free bacteria, *Am. Ind. Hyg. Assoc. J.*, 1992, **53**, 660–667.

182 E. J. Davis, A history of single aerosol particle levitation, *Aerosol Sci. Technol.*, 1997, **26**, 212–254.

183 R. A. Millikan, The isolation of an ion, a precision measurement of its charge, and the correction of Stokes's law, *Phys. Rev. (Series I)*, 1911, **32**, 349–397.

184 M. Sapti, A verification of the theory of the brownian movements and a direct determination of the value of the NE for gaseous ionization, *Phys. Rev.*, 1911, **33**, 81–110.

185 W. Paul and M. Raether, Das elektrische Massenfilter, *Zeitschrift für Phys.*, 1955, **140**, 262–273.

186 H. G. Dehmelt and F. G. Major, Orientation of (He4)+ ions by exchange collisions with cesium atoms, *Phys. Rev. Lett.*, 1962, **8**, 213–214.

187 A. K. Ray, R. D. Johnson and A. Souyri, Dynamic Behavior of Single Glycerol Droplets in Humid Air Streams, *Langmuir*, 1989, **5**, 133–140.

188 C. Heinisch, J. B. Wills, J. P. Reid, T. Tschudi and C. Tropea, Temperature measurement of single evaporating water droplets in a nitrogen flow using spontaneous raman scattering, *Phys. Chem. Chem. Phys.*, 2009, **11**, 9720–9728.

189 J. F. Davies, A. E. Haddrell and J. P. Reid, Time-resolved measurements of the evaporation of volatile components from single aerosol droplets, *Aerosol Sci. Technol.*, 2012, **46**, 666–677.

190 A. Haddrell, G. Rovelli, D. Lewis, T. Church, J. Reid, A. Haddrell, G. Rovelli, D. Lewis and T. Church, Identifying time-dependent changes in the morphology of an individual aerosol particle from its light scattering pattern, *Aerosol Sci. Technol.*, 2019, **0**, 1–18.

191 G. Rovelli, R. E. H. Miles, J. P. Reid and S. L. Clegg, Accurate Measurements of Aerosol Hygroscopic Growth over a Wide Range in Relative Humidity, *J. Phys. Chem. A*, 2016, **120**, 4376–4388.

192 W. J. Glantschnig and S.-H. Chen, Light scattering from water droplets in the geometrical optics approximation, *Appl. Opt.*, 1981, **20**, 2499.

193 C. Cai, R. E. H. H. Miles, M. I. Cotterell, A. Marsh, G. Rovelli, A. M. J. J. Rickards, Y. H. Zhang and J. P. Reid, Comparison of methods for predicting the compositional dependence of the density and refractive index of organic-aqueous aerosols, *J. Phys. Chem. A*, 2016, **120**, 6604–6617.

194 Y. Liu and P. H. Daum, Relationship of refractive index to mass density and self-consistency of mixing rules for multicomponent mixtures like ambient aerosols, *J. Aerosol Sci.*, 2008, **39**, 974–986.

195 F. K. A. Gregson, J. F. Robinson, R. E. H. Miles, C. P. Royall and J. P. Reid, Drying Kinetics of Salt Solution Droplets: Water Evaporation Rates and Crystallization, *J. Phys. Chem. B*, 2019, **123**, 266–276.

196 T. C. Preston and J. P. Reid, Angular scattering of light by a homogeneous spherical particle in a zeroth-order Bessel beam and its relationship to plane wave scattering, *J. Opt. Soc. Am. A*, 2015, **32**, 1053.

197 M. Kulmala, T. Vesala and P. E. Wagner, An Analytical Expression For the Rate of Binary Condensational Particle Growth, *Proc. R. Soc. A Math. Phys. Eng. Sci.*, 1993, **441**, 589–605.

198 J. F. Davies, A. E. Haddrell, R. E. H. Miles, C. R. Bull and J. P. Reid, Bulk, surface, and gas-phase limited water transport in aerosol, *J. Phys. Chem. A*, 2012, **116**, 10987–10998.

199 R. E. H. Miles, K. J. Knox, J. P. Reid, A. M. C. Laurain and L. Mitchem, Measurements of mass and heat transfer at a liquid water surface during condensation or evaporation of a subnanometer thickness layer of water, *Phys. Rev. Lett.*, 2010, **105**, 1–4.

200 S. L. Clegg, P. Brimblecombe and A. S. Wexler, Thermodynamic Model of the System $H^+ - NH_4^+ - Na^+ - SO_4^{2-} - NO_3^- - Cl^- - H_2O$ at 298.15 K, *J. Phys. Chem. A*, 1998, **102**, 2155–2171.

201 J. R. Butler, L. Mitchem, K. L. Hanford, L. Treuel and J. P. Reid, In situ comparative measurements of the properties of aerosol droplets of different chemical composition, *Faraday Discuss.*, 2007, **137**, 351–366.

202 J. Archer, M. Kolwas, D. Jakubczyk, G. Derkachov, M. Woźniak and K. Kolwas, Evolution of radius and light scattering properties of single drying microdroplets of colloidal suspension, *J. Quant. Spectrosc. Radiat. Transf.*, 2017, **202**, 168–175.

203 U. K. Krieger and P. Meier, Observations and calculations of two-dimensional angular optical scattering (TAOS) patterns of a single levitated cluster of two and four microspheres, *J. Quant. Spectrosc. Radiat. Transf.*, 2011, **112**, 1761–1765.

204 A. Baldelli, M. A. Boraey, D. S. Nobes and R. Vehring, Analysis of the Particle Formation Process of Structured Microparticles, *Mol. Pharm.*, 2015, **12**, 2562–2573.

205 A. Nenninger, G. Mastroianni, A. Robson, T. Lenn, Q. Xue, M. C. Leake and C. W. Mullineaux, Independent mobility of proteins and lipids in the plasma membrane of Escherichia coli, *Mol. Microbiol.*, 2014, **92**, 1142–1153.

206 S. Terzieva, J. Donnelly, V. Ulevicius, S. A. Grinshpun, K. Willeke, G. N. Stelma and K. P. Brenner, Comparison of methods for detection and enumeration of airborne microorganisms collected by liquid impingement, *Appl. Environ. Microbiol.*, 1996, **62**, 2264–2272.

207 G. Mainelis, A. Adhikari, K. Willeke, S. A. Lee, T. Reponen and S. A. Grinshpun, Collection of airborne microorganisms by a new electrostatic precipitator, *J. Aerosol Sci.*, 2002, **33**, 1417–1432.

208 S. Kirchner, J. L. Fothergill, E. A. Wright, C. E. James, E. Mowat and C. Winstanley, Use of Artificial Sputum Medium to Test Antibiotic Efficacy Against Pseudomonas aeruginosa in Conditions More Relevant to the Cystic Fibrosis Lung, *J. Vis. Exp.*, 2012, e3857.

209 M. H. Woo, Y. M. Hsu, C. Y. Wu, B. Heimbuch and J. Wander, Method for contamination of filtering facepiece respirators by deposition of MS2 viral aerosols, *J. Aerosol Sci.*, 2010, **41**, 944–952.

210 B. Krismer, M. Liebeke, D. Janek, M. Nega, M. Rautenberg, G. Hornig, C. Unger, C. Weidenmaier, M. Lalk and A. Peschel, Nutrient Limitation Governs Staphylococcus aureus Metabolism and Niche Adaptation in the Human Nose, *PLoS Pathog.*, , DOI:10.1371/journal.ppat.1003862.

211 J. Schindelin, I. Arganda-Carreras, E. Frise, V. Kaynig, M. Longair, T. Pietzsch, S. Preibisch, C. Rueden, S. Saalfeld, B. Schmid, J. Y. Tinevez, D. J. White, V. Hartenstein, K. Eliceiri, P. Tomancak and A. Cardona, Fiji: An open-source platform for biological-image analysis, *Nat. Methods*, 2012, **9**, 676–682.

212 C. E. Morris, D. C. Sands, M. Bardin, R. Jaenicke, B. Vogel, C. Leyronas, P. A. Ariya, R. Psenner, P. Sciences and O. Sciences, Microbiology and atmospheric processes: Research challenges concerning the impact of airborne micro-organisms on the atmosphere and climate, *Biogeosciences*, 2011, **8**, 17–25.

213 J. Douwes, P. S. Thorne and D. Heederik, Monitoring and Evaluation of Bioaerosol Exposure, 2003, 39–42.

214 S. M. Walser, D. G. Gerstner, B. Brenner, J. Bünger, T. Eikmann, B. Janssen, S. Kolb, A. Kolk, D. Nowak, M. Raulf, H. Sagunski, N. Sedlmaier, R. Suchenwirth, G. Wiesmüller, K. M. Wollin, I. Tesseraux and C. E. W. Herr, Evaluation of exposure-response relationships for health effects of microbial bioaerosols - A systematic review, *Int. J. Hyg. Environ. Health*, 2015, **218**, 577–589.

215 J. Douwes, P. Thorne, N. Pearce and D. Heederik, Bioaerosol health effects and exposure assessment: Progress and prospects, *Ann. Occup. Hyg.*, 2003, **47**, 187–200.

216 R. M. Power, S. H. Simpson, J. P. Reid and A. J. Hudson, The transition from liquid to solid-like behaviour in ultrahigh viscosity aerosol particles, *Chem. Sci.*, 2013, **4**, 2597.

217 A. E. Haddrell, G. Hargreaves, J. F. Davies and J. P. Reid, Control over hygroscopic growth of saline aqueous aerosol using Pluronic polymer additives, *Int. J. Pharm.*, 2013, **443**, 183–192.

218 J. K. Lee, S. Kim, H. G. Nam and R. N. Zare, Microdroplet fusion mass spectrometry for fast reaction kinetics, *Proc. Natl. Acad. Sci.*, 2015, **112**, 3898–3903.

219 L. J. Goldberg, H. M. S. Watkins, E. E. Boeeke, E. E. Boerke and M. A. Chatigny, The use of a rotating drum for the study of aerosols over extended periods of time, *Am. J. Hyg.*, 1958, **68**, 85–93.

220 M. S. Lever, A. Williams and A. M. Bennett, Survival of mycobacterial species in aerosols generated from artificial saliva, *Lett. Appl. Microbiol.*, 2000, **31**, 238–241.

221 R. G. LOUDON, L. R. Bumgarner, J. LACY and G. K. COFFMAN, Aerial transmission of mycobacteria., *Am. Rev. Respir. Dis.*, 1969, **100**, 165–171.

222 Z. Y. Han, W. G. Weng and Q. Y. Huang, Characterizations of particle size distribution of the droplets exhaled by sneeze Characterizations of particle size distribution of the droplets exhaled by sneeze, *J. R. Soc. Interface*, 2013, **10**, 20130560.

223 S. Wright and S. L. Goodacre, Evidence for antimicrobial activity associated with common house spider silk, *BMC Res. Notes*, 2012, **5**, 1–6.

224 P. Hambleton, Repair of wall damage in Escherichia coli recovered from an aerosol., *J. Gen. Microbiol.*, 1971, **69**, 81–88.

225 J. Kesavan, D. Schepers and A. R. McFarland, Sampling and Retention Efficiencies of Batch-Type Liquid-Based Bioaerosol Samplers, *Aerosol Sci. Technol.*, 2010, **44**, 817–829.

226 W. Paul, Electromagnetic Traps for Charged and Neutral Particles(Nobel Lecture), *Angew. Chemie Int. Ed. English*, 1990, **29**, 739–748.

227 A. E. Haddrell, J. F. Davies, A. Yabushita and J. P. Reid, Accounting for changes in particle charge, dry mass and composition occurring during studies of single levitated particles, *J. Phys. Chem. A*, 2012, **116**, 9941–9953.

228 B. Lighthart, B. T. Shaffer, B. Lighthart*, B. T. Shaffer, B. Lighthart, B. T. Shaffer, B. Lighthart* and B. T. Shaffer, Increased Airborne Bacterial Survival as a Function of Particle Content and Size, *Aerosol Sci. Technol.*, 1997, **27**, 439–446.

229 S. Moon, E. Ceyhan, U. A. Gurkan and U. Demirci, Statistical modeling of single target cell encapsulation, *PLoS One*, , DOI:10.1371/journal.pone.0021580.

230 E. J. Davis, M. F. Buehler and T. L. Ward, The double-ring electrodynamic balance for microparticle characterization, *Rev. Sci. Instrum.*, 1990, **61**, 1281–1288.

231 M. J. Bogan and G. R. Agnes, MALDI-TOF-MS Analysis of Droplets Prepared in an Electrodynamic Balance: "Wall-less" Sample Preparation, *Anal. Chem.*, 2002, **74**, 489–496.

232 A. E. Haddrell, H. Ishii, S. F. van Eeden and G. R. Agnes, Apparatus for Preparing

Mimics of Suspended Particles in the Troposphere and Their Controlled Deposition onto Individual Lung Cells in Culture with Measurement of Downstream Biological Response, *Anal. Chem.*, 2005, **77**, 3623–3628.

233 M. J. Bogan and G. R. Agnes, Wall-less sample preparation of μm-sized sample spots for femtomole detection limits of proteins from liquid based UV-MALDI matrices, *J. Am. Soc. Mass Spectrom.*, 2004, **15**, 486–495.

234 P. Hambleton, The sensitivity of gram-negative bacteria, recovered from aerosols, to lysozyme and other hydrolytic enzymes., *J. Gen. Microbiol.*, 1970, **61**, 197–204.

235 C. S. Cox, J. S. Derr, E. G. Flurie and R. C. Roderick, Experimental technique for studying aerosols of lyophilized bacteria., *Appl Microbiol*, 1970, **20**, 927–34.

236 Z. Y. Han, W. G. Weng and Q. Y. Huang, Characterizations of particle size distribution of the droplets exhaled by sneeze, *J. R. Soc. Interface*, 2013, **10**, 20130560.

237 G. A. McFeters, S. C. Cameron and M. W. LeChevallier, Influence of diluents, media, and membrane filters on detection of injured waterborne coliform bacteria, *Appl. Environ. Microbiol.*, 1982, **43**, 97–103.

238 M. P. Buttner and L. D. Stetzenbach, Evaluation of 4 Aerobiological Sampling Methods for the Retrieval of Aerosolized Pseudomonas-Syringae, *Appl. Environ. Microbiol.*, 1991, **57**, 1268–1270.

239 J. F. Davies, R. E. H. Miles, A. E. Haddrell and J. P. Reid, Temperature dependence of the vapor pressure and evaporation coefficient of supercooled water, *J. Geophys. Res. Atmos.*, 2014, **119**, 10931–10940.

240 B. Spikes, This Week in The Journal, *J. Neurosci.*, 2004, **24**, 49.

241 J. Zhou, J. Wei, K.-T. Choy, S. F. Sia, D. K. Rowlands, D. Yu, C.-Y. Wu, W. G. Lindsley, B. J. Cowling, J. McDevitt, M. Peiris, Y. Li and H.-L. Yen, Defining the sizes of airborne particles that mediate influenza transmission in ferrets, *Proc. Natl. Acad. Sci.*, 2018, **115**, 201716771.

242 E. L. Brodie, T. Z. DeSantis, J. P. M. Parker, I. X. Zubietta, Y. M. Piceno and G. L. Andersen, Urban aerosols harbor diverse and dynamic bacterial populations, *Proc. Natl. Acad. Sci.*, 2007, **104**, 299–304.

243 N. I. Stilianakis and Y. Drossinos, Dynamics of infectious disease transmission by inhalable respiratory droplets, *J. R. Soc. Interface*, 2010, **7**, 1355–1366.

244 G. N. Sze To, M. P. Wan, C. Y. H. Chao, L. Fang and A. Melikov, Experimental study of dispersion and deposition of expiratory aerosols in aircraft cabins and impact on infectious disease transmission, *Aerosol Sci. Technol.*, 2009, **43**, 466–485.

245 M. P. Wan, G. N. Sze To, C. Y. H. Chao, M. P. Wan, L. Fang and A. Melikov, Modeling the fate of expiratory aerosols and the associated infection risk in an aircraft cabin environment, *Aerosol Sci. Technol.*, 2009, **43**, 322–343.

246 I. Kukavica-Ibrulj and R. C. Levesque, Animal models of chronic lung infection with Pseudomonas aeruginosa: useful tools for cystic fibrosis studies., *Lab. Anim.*, 2008, **42**, 389–412.

247 P. Du, R. Du, W. Ren, Z. Lu and P. Fu, Seasonal variation characteristic of inhalable microbial communities in PM 2.5 in Beijing city, China, *Sci. Total Environ.*, 2018, **610**–**611**, 308–315.

248 P. a. Ariya, J. Sun, N. a. Eltouny, E. D. Hudson, C. T. Hayes and G. Kos, *Physical and chemical characterization of bioaerosols – Implications for nucleation processes*, 2009, vol. 28.

249 J. Gralton, E. Tovey, M. L. McLaws and W. D. Rawlinson, The role of particle size in aerosolised pathogen transmission: A review, *J. Infect.*, 2011, **62**, 1–13.

250 A. H. Haddrell and R. J. Thomas, Aerobiology: Experimental Consideration, Observations and Future Tools, *Appl. Environ. Microbiol.*, 2017, **83**, 1–15.

251 G. R. Johnson, L. D. Knibbs, T. J. Kidd, C. E. Wainwright, M. E. Wood, K. A. Ramsay, S. C. Bell and L. Morawska, A novel method and its application to measuring pathogen decay in bioaerosols from patients with respiratory disease, *PLoS One*, 2016, **11**, 1–20.

252 K. S. Carslaw, S. L. Clegg and P. Brimblecombe, A Thermodynamic Model of the System HCl-HNO3-H2SO4-H2O, Including Solubilities of HBr, from <200 to 328 K, *J. Phys. Chem.*, 1995, **99**, 11557–11574.

253 G. Rovelli, E. H. R. Miles, P. J. Reid and L. S. Clegg, Hygroscopic properties of aminium sulfate aerosols, *Atmos. Chem. Phys.*, 2017, **17**, 4369–4385.

254 C. S. Ng, K. L. Chong, R. Yang, M. Li, R. Verzicco and D. Lohse, Growth of respiratory droplets in cold and humid air, *medRxiv*, 2020, **XXX**, 2020.10.30.20222604.

255 J. P. Reid, A. K. Bertram, D. O. Topping, A. Laskin, S. T. Martin, M. D. Petters, F. D. Pope and G. Rovelli, The viscosity of atmospherically relevant organic particles, *Nat. Commun.*, 2018, **9**, 1–14.

256 Y. S. Cheng, Mechanisms of Pharmaceutical Aerosol Deposition in the Respiratory Tract, *AAPS PharmSciTech*, 2014, **15**, 630–640.

257 D. L. Bones, J. P. Reid, D. M. Lienhard and U. K. Krieger, Comparing the mechanism of water condensation and evaporation in glassy aerosol, *Proc. Natl. Acad. Sci. U. S. A.*, 2012, **109**, 11613–11618.

258 M. Goto, Y. Oaki and H. Imai, Dendritic growth of NaCl crystals in a gel matrix: Variation of branching and control of bending, *Cryst. Growth Des.*, 2016, **16**, 4278–4284.

259 W. Yang and L. C. Marr, Mechanisms by which ambient humidity may affect viruses in aerosols, *Appl. Environ. Microbiol.*, 2012, **78**, 6781–6788.

260 R. M. Power and J. P. Reid, Probing the micro-rheological properties of aerosol particles using optical tweezers, *Reports Prog. Phys.*, 2014, **77**, 074601.

261 R. M. Ferry, W. F. Brown and E. B. Damon, Studies of the loss of viability of bacterial aerosols: III. Factors affecting death rates of certain Non-Pathogens, *J. Hyg. (Lond).*, 1958, **56**, 389–403.

262 R. M. Ferry, W. F. Brown and E. B. Damon, Studies of the loss of viability of stored bacterial aerosols. II. Death rates of several non-pathogenic organisms in relation to biological and structural characteristics, *J. Hyg. (Lond).*, 1958, **56**, 125–150.

263 W. J. Scott, The effect of residual water on the survival of dried bacteria during storage., *J. Gen. Microbiol.*, 1958, **19**, 624–633.

264 R. M. Ferry and T. G. Maple, Studies of the loss of viability of stored bacterial aerosols. I. Micrococcus candidus., *J. Infect. Dis.*, 1954, **95**, 142–159.

265 C. Cai, D. J. Stewart, J. P. Reid, Y. H. Zhang, P. Ohm, C. S. Dutcher and S. L. Clegg,

Organic component vapor pressures and hygroscopicities of aqueous aerosol measured by optical tweezers, *J. Phys. Chem. A*, 2015, **119**, 704–718.

266 L. Willem, K. van Kerckhove, D. L. Chao, N. Hens and P. Beutels, A Nice Day for an Infection? Weather Conditions and Social Contact Patterns Relevant to Influenza Transmission, *PLoS One*, , DOI:10.1371/journal.pone.0048695.

267 Y. Hu, H. Cheng and S. Tao, Environmental and human health challenges of industrial livestock and poultry farming in China and their mitigation, *Environ. Int.*, 2017, **107**, 111–130.

268 B. Ghosh, H. Lal and A. Srivastava, Review of bioaerosols in indoor environment with special reference to sampling, analysis and control mechanisms, *Environ. Int.*, 2015, **85**, 254–272.

269 M. Nicas, W. W. Nazaroff and A. Hubbard, Toward understanding the risk of secondary airborne infection: Emission of respirable pathogens, *J. Occup. Environ. Hyg.*, 2005, **2**, 143–154.

270 X. Yan, R. M. Bain and R. G. Cooks, Organic Reactions in Microdroplets: Reaction Acceleration Revealed by Mass Spectrometry, *Angew. Chemie - Int. Ed.*, 2016, **55**, 12960–12972.

271 S. Banerjee, E. Gnanamani, X. Yan and R. N. Zare, Can all bulk-phase reactions be accelerated in microdroplets?, *Analyst*, 2017, **142**, 1399–1402.

272 R. K. Chakrabarty and W. R. Heinson, Scaling Laws for Light Absorption Enhancement Due to Nonrefractory Coating of Atmospheric Black Carbon Aerosol, *Phys. Rev. Lett.*, 2018, **121**, 218701.

273 R. F. Service, Climate change: Study fingers soot as a major player in global warming, *Science (80-.).*, 2008, **319**, 1745.

274 A. K. Y. Lee, R. Zhao, R. Li, J. Liggio, S. M. Li and J. P. D. Abbatt, Formation of light absorbing organo-nitrogen species from evaporation of droplets containing glyoxal and ammonium sulfate, *Environ. Sci. Technol.*, 2013, **47**, 12819–12826.

275 E. Amstad, M. Gopinadhan, C. Holtze, C. O. Osuji, M. P. Brenner, F. Spaepen and D. A. Weitz, Production of amorphous nanoparticles by supersonic spray-drying with a

microfluidic nebulator, *Science (80-.).*, 2015, **349**, 956–960.

276 E. Lofgren, N. H. Fefferman, Y. N. Naumov, J. Gorski and E. N. Naumova, Influenza Seasonality: Underlying Causes and Modeling Theories, *J. Virol.*, 2007, **81**, 5429–5436.

277 G. Lamblin, J. P. Aubert, J. M. Perini, A. Klein, N. Porchet, P. Degand and P. Roussel, Human respiratory mucins, *Eur. Respir. J.*, 1992, **5**, 247–256.

278 G. Hersen, S. Moularat, E. Robine, E. Géhin, S. Corbet, A. Vabret and F. Freymuth, Impact of health on particle size of exhaled respiratory aerosols: Case-control study, *Clean - Soil, Air, Water*, 2008, **36**, 572–577.

279 M. D. Anwarul Hasan, C. F. Lange and M. L. King, Effect of artificial mucus properties on the characteristics of airborne bioaerosol droplets generated during simulated coughing, *J. Nonnewton. Fluid Mech.*, 2010, **165**, 1431–1441.

280 Y. Thomas, G. Vogel, W. Wunderli, P. Suter, M. Witschi, D. Koch, C. Tapparel and L. Kaiser, Survival of influenza virus on banknotes, *Appl. Environ. Microbiol.*, 2008, **74**, 3002–3007.

281 I. Khan, P. Brimblecombe and S. L. Clegg, The henry's law constants of pyruvic and methacrylic acids, *Environ. Technol. (United Kingdom)*, 1992, **13**, 587–593.

282 R. J. Rapf, M. R. Dooley, K. Kappes, R. J. Perkins and V. Vaida, PH Dependence of the Aqueous Photochemistry of α-Keto Acids, *J. Phys. Chem. A*, 2017, **121**, 8368–8379.

283 H. Babich and G. Stotzky, Influence of pH on inhibition of bacteria, fungi, and coliphages by bisulfite and sulfite, *Environ. Res.*, 1978, **15**, 405–417.

284 R. J. Thomas, D. Webber, W. Sellors, A. Collinge, A. Frost, A. J. Stagg, S. C. Bailey, P. N. Jayasekera, R. R. Taylor, S. Eley and R. W. Titball, Generation of large droplet aerosols within microbiological containment using a novel flow-focussing technique, *Aerobiologia (Bologna).*, 2009, **25**, 75–84.

285 D. Anderson, of Escherichia coli, 1966, 303–313.

286 Z. Ha and C. K. Chan, The Water Activities of MgCl2, Mg(NO3)2, MgSO4, and Their Mixtures, *Aerosol Sci. Technol.*, 1999, **31**, 154–169.

287 D. J. Donaldson and V. Vaida, The influence of organic films at the air-aqueous

boundary on atmospheric processes, *Chem. Rev.*, 2006, **106**, 1445–1461.

288 P. S. Gill, T. E. Graedel and C. J. Weschler, Organic Films on Atmospheric Aerosol Particles, Fog Droplets, Cloud Droplets, Raindrops, and Snowflakes, *Rev. Geogr. Sp. Phys.*, 1983, **21**, 903–920.

289 J. F. Davies, R. E. H. H. Miles, A. E. Haddrell and J. P. Reid, Influence of organic films on the evaporation and condensation of water in aerosol., *Proc. Natl. Acad. Sci. U. S. A.*, 2013, **110**, 8807–12.

290 P. Davidovits, C. E. Kolb, L. R. Williams, J. T. Jayne and D. R. Worsnop, Mass accommodation and chemical reactions at gas-liquid interfaces, *Chem. Rev.*, 2006, **106**, 1323–1354.

291 J. Ovadnevaite, A. Zuend, A. Laaksonen, K. J. Sanchez, G. Roberts, D. Ceburnis, S. Decesari, M. Rinaldi, N. Hodas, M. C. Facchini, J. H. Seinfeld and C. O' Dowd, Surface tension prevails over solute effect in organic-influenced cloud droplet activation, *Nature*, 2017, **546**, 637–641.

292 S. Obradović, B. Gligić and V. Orozović, Reperfuziona terapija akutnog infarkta miokarda., *Vojnosanit. Pregl.*, 2002, **59**, 281–292.

293 M. S. Lopez, I. S. Tan, D. Yan, J. Kang, M. McCreary, Z. Modrusan, C. D. Austin, M. Xu and E. J. Brown, Host-derived fatty acids activate type VII secretion in Staphylococcus aureus, *Proc. Natl. Acad. Sci.*, 2017, **114**, 201700627.

294 H. Hamm, C. Kroegel and J. Hohlfeld, Surfactant: A review of its functions and relevance in adult respiratory disorders, *Respir. Med.*, 1996, **90**, 251–270.

295 T. Trouwborst, J. C. de Jong and K. C. Winkler, Mechanism of inactivation in aerosols of bacteriophage T 1 ., *J. Gen. Virol.*, 1972, **15**, 235–242.

296 M. H. ADAMS, Surface inactivation of bacterial viruses and of proteins, *J. Gen. Physiol.*, 1948, **31**, 417–431.

297 H. Weber, T. Polen, J. Heuveling, V. F. Wendisch and R. Hengge, Genome-wide analysis of the general stress response network in Escherichia coli: σS-dependent genes, promoters, and sigma factor selectivity, *J. Bacteriol.*, 2005, **187**, 1591–1603.

298 M. Givskov, L. Eberl, S. Moller, L. K. Poulsen and S. Molin, Responses to nutrient starvation in Pseudomonas putida KT2442: Analysis of general cross-protection, cell shape, and macromolecular content, *J. Bacteriol.*, 1994, **176**, 7–14.

299 J. W. Zabinski, K. J. Pieper and J. M. D. Gibson, A Bayesian Belief Network Model Assessing the Risk to Wastewater Workers of Contracting Ebola Virus Disease During an Outbreak, *Risk Anal.*, 2018, **38**, 376–391.

300 M. Schuit, S. Gardner, S. Wood, K. Bower, G. Williams, D. Freeburger and P. Dabisch, The Influence of Simulated Sunlight on the Inactivation of Influenza Virus in Aerosols, , DOI:10.1093/infdis/jiz582.

301 A. Lipovsky, Y. Nitzan, A. Gedanken and R. Lubart, Visible light-induced killing of bacteria as a function of wavelength: Implication for wound healing, *Lasers Surg. Med.*, 2010, **42**, 467–472.

302 E. L. Nussbaum and O. N. Mg, Effects of low intensity laser irradiation during healing of infected skin wounds in the rat, 2015, **3**, 23–36.